

ROLE OF CALPASTATIN ISOFORMS IN BREAST CANCER LYMPHOVASCULAR INVASION

BHUDSABAN SUKKARN

B Pharm, MSc (Medical science)

Thesis submitted to the University of Nottingham

for the degree of Doctor of Philosophy

September 2020

Abstract

Expression of calpastatin protein or exon3-containing variant (CASTexon3 mRNA) is negatively associated with various clinicopathological features of the high-risk group for breast cancer recurrence, including the presence of lymphatic invasion, a predominant form of lymphovascular invasion (LVI). It is mostly unknown how individual calpastatin isoforms originated from a single gene regulate such processes. This study, therefore, aimed to assess the role that individual calpastatin isoforms, encoded by CASTexon3 mRNA, play in regulating calpain activity as well as breast cancer progression and LVI *in vitro*.

Stably transfected monoclonal cells overexpressing calpastatin Type 1 (231CAST1 and T47DCAST1), Type 2 (231CAST2), Type 3 (T47DCAST3) and the mock-transfected controls (231Ctrl and T47DCtrl) were generated from MDA-MB-231 and T47D lines using DNA transfection and single-cell selection techniques. By immunofluorescence confocal microscopy, Type 1 and 3 were expressed mainly in the cytoplasm and partially in the nuclei. Type 2 uniquely showed a predominant perinuclear expression. This suggested to select Type 1 and 2 to fully examine and compare their roles in regulating breast cancer progression and LVI due to the differences between their intracellular localisation and mRNA sequences by only one exon. The cell models overexpressing Type 1 and 2 were examined for calpain activity using the t-BOC assay. Growth curve and clonogenic survival assays were used to assess the effect of calpastatin isoform overexpression on cancer progression-related phenotypic endpoints, i.e., cell proliferation and clonogenicity, respectively. For LVI-related phenotypic features, the cell models were assessed for cell migration and interactions to blood vascular hMEC-1 vs lymphatic hTERT-LEC endothelial cells (BECs vs LECs) using scratch-wound migration and static adhesion assays, respectively.

While calpain inhibitor calpeptin significantly suppressed calpain activity, cell proliferation, migration, and interactions to hMEC-1 model in MDA-MB-231 cells, upregulation of both Type 1 and 2 unexpectedly contributed to a significant increase of calpain activity (39.82 and 70.78 %increase respectively) and promotion of cancer progression- and LVI-related phenotypic endpoints of the

cells. Type 1 overexpression seemed to shorten the doubling time of MDA-MB-231 and T47D cells relative to controls (29.13 vs 38.41 hours and 33.11 vs 41.97 hours, respectively), although a significant difference was not observed. MDA-MB-231 doubling time was not affected by Type 2 overexpression (35.63 hours), while MDA-MB-231 clonogenic survival was not altered by both Type 1 and 2 overexpression (survival fraction = 1.04 and 0.96 respectively). Type 1 overexpression significantly enhanced MDA-MB-231 and T47D cell migration by 42.61% and 93.30%, respectively, at 24 hours post-scratch, with a similar increase in migration observed at other time-points. Type 2-overexpressing MDA-MB-231 migration was also enhanced with statistical significance observed at 2 hours after wounding (37.44% increase). Type 1 and 2 overexpression showed differential effects on tumour cell adhesion to both EC models - inducing and suppressing effects, respectively. However, a significantly increased adhesiveness of 231CAST1 cells was only observed with hTERT-LEC cells (41.47% increase), while a significantly reduced adhesion of 231CAST2 cells was only detected with the hMEC-1 model (49.80% decrease). T47D cells did not adhere firmly to either EC model limiting the ability to study the role of Type 1 in regulating cell adhesion. With limited upregulation of calpain activity by a 24-hour treatment with 0.5 µM A23187 in both 231CAST1 (35.39% increase) and 231CAST2 cells (10.12% increase), A23187 significantly inhibited the interactions previously observed between hMEC-1 and tumour cells, including 231CAST1 (42.83% inhibition), 231CAST2 (12.86% inhibition), and the mock-transfected cells (35.42% inhibition), but did not affect other phenotypic endpoints.

This study presented the opposing role of calpastatin to what has been published before in regulating calpain activity and cancer progression. Type 1 may induce tumour cell proliferation, migration, and endothelial interactions, in particular to LECs. Type 2 may enhance breast cancer cell migration but suppress tumour cell adhesion, specifically to BECs. These differential effects of Type 1 and 2 probably related to their distinct subcellular localisation.

Dedicated to the memory of my mother, Nipa Sukkarn,

who is the first thing that comes to my mind every morning

and the last thing that stays on my mind every night.

To my father, Wiruth Sukkarn,

for his unconditional, timeless love and support.

Acknowledgements

First and foremost, I would like to express my greatest gratitude to my supervisors, Professor Stewart Martin, for all guidance, support, and encouragement throughout this project. Without his assistance, this PhD would not have been achievable.

My sincerest appreciation to the Royal Thai Government, Thailand, for financial support, while doing my PhD at the University of Nottingham.

Special thanks to the group of Prof Tim Parr and Dr Kirsty Jewell, School of Biosciences, for designing and producing calpastatin primers and DNA constructs of calpastatin isoforms. I am deeply grateful to Dr Sarah Storr and Dr Aula Ammar for sharing techniques, knowledge, expertise as well as their kind help and guidance. To my labmates, Dr Pu Xuan, Dr Zhang Siwei, Dr Khaled Al-Hadyan (our Bang), Dr Nurul Abdullah, Dr Yao Anqi, Radhika Aiyappa, and Richa Vasan, thank you all for your support, fun, and optimistic attitudes. I will miss our good old time we have spent together here in Nottingham. My gratefulness is also to all members of the Academic Unit of Oncology who have always been helpful, especially Christopher Norman and Mohamed Gijon (our Mo).

I would like to send my sincere appreciation message to my friends - Amornpan Thaemngoen, Rungarun Anupansupsai, Sinee Thongmee, Supapun Kangkasuwan, and Panita Chuayiam, for their encouragement, support, and helps. Without all of you, it seems impossible to pass through all difficulties or hardships.

I am deeply indebted to Dr Aula Ammar and Dr Poonsit Hiransai, my sister and brother. Because of you both, my thesis has eventually been nicely done. I owe you a lot and will never forget the valuable time you have dedicated to me.

Lastly, my deepest and heartfelt appreciation goes to my parents, Wiruth and Nipa Sukkarn, who always believe and never doubt in my ability. I would thank you from the bottom of my heart for your timeless, unconditional love and support.

Conference and Awards

Conference Presentation

Poster presentation. “The role of calpastatin isoforms in breast cancer progression”. AACR Annual Meeting 2017, Cancer Research 77 (13 Supplement): 890. April 5-10, 2017, Washington DC, USA.

Awards

2017 BACR/CRUK Student Travel Awards.

2017 University of Nottingham Graduate School Travel Prize.

2017 University of Nottingham School of Medicine Travel Prize.

Abbreviation

κ	Kappa
2D	two dimensional
3D	three dimensional
AIF	apoptosis-inducing factor
AJCC	American Joint Committee on Cancer
aka	also known as
Akt	protein kinase B or PKB
ALLN	N-Acetyl-Leu-Leu-Met-al
AP	alkaline phosphatase
AP1	activator protein 1
APAF1	apoptotic protease-activating factor 1
ASCs	adipose-derived stromal/stem cells
AT(1)R	angiotensin II (Ang II) type 1 receptor
ATCC	American Type Culture Collection
ATM	ataxia telangiectasia mutated
BAECs	bovine aortic ECs
BAX	Bcl-2 Associated X, aka Bcl-2-like protein 4
Bcl-2	B-cell lymphoma 2
BECs	blood endothelial cells
bFGF	basic fibroblast growth factor
BMI	body mass index
bp	base pair
BRCA	breast cancer gene
BRCA1	breast cancer 1, early onset
BRCA2	breast cancer 2, early onset
BRIP1	BRCA1-interacting protein 1
BVI	blood vascular invasion
C2L	C2 domain-like
CaM	calmodulin
CaMKII	calmodulin-dependent protein kinase II
CaSR	calcium-sensing receptor
CAST	calpastatin gene
CCL21	chemokine (C-C motif) ligand 21
CCNB1	cyclin B1
CCNE1	the gene endcoding for cyclin E1

CCR7	chemokine (C-C motif) receptor 7
CDH1	cadherin-1
CDK5	cyclin-dependent kinase 5
cDNA	complementary deoxyribonucleic acid
CHEK2	checkpoint kinase 2
CLL	chronic lymphocytic leukaemia
C_t	cycle threshold
CTGF	connective tissue growth factor, aka CCN2
CXCL1	chemokine (C-X-C motif) ligand 1
CXCL12	chemokine (C-X-C motif) ligand 12
CXCR4	C-X-C chemokine receptor type 4
CysPc	the calpain-like cysteine protease sequence motif domain
Da	dalton
DBCG	Danish Breast Cancer Cooperative Group
DBS	donor bovine serum
DCIS	ductal carcinoma *in situ*
DFI	disease-free interval
DFS	disease-free survival
DG	dentate gyrus
DM	distant metastasis
DMSO	dimethyl sulfoxide
DNA	deoxyribonucleic acid
DSMZ	Deutsch Sammlung von Mikroorganismen und Zellkulturen Gmbh
DT	doubling time
E	efficiency of the PCR reaction
ECL	enhanced chemiluminescent
ECM	extracellular matrix
EDTA	ethylenediaminetetraacetic acid
EGF	epidermal growth factor
EGFR	epidermal growth factor receptor
EMT	epithelial-mesenchymal transition
ER	endoplasmic reticulum
ER	estrogen receptor
FA	focal adhesion
FAK	focal adhesion kinase
FMLP	n-formyl-methionyl-leucine-phenylalanine

FOXC1	forkhead box C1
FOXO3a	forkhead box O3
G418	Geneticin
Gas2	growth arrest-specific protein 2
Gas2DN	Gas2 dominant negative
gDNA	genomic deoxyribonucleic acid
GFP	green fluorescent protein
GI	gastrointestinal
GPI	glycosylphosphatidylinositol
GR	glycine-rich hydrophobic
H&E	haematoxylin and eosin
HA	human influenza hemagglutinin
HER2	human epidermal growth factor receptor 2
h-GIP	human gastric inhibitory peptide
hMEC-1	immortalised human microvascular endothelial cell line
HMVEC dLy Neo	neonatal dermal lymphatic microvascular endothelial cells
HPRT	Hypoxanthine-guanine phosphoribosyltransferase
HR	hazard ratio
hr	hour
HRP	horseradish peroxidase
HRT	hormone replacement therapy
hTERT-LEC	human telomerase reverse transcriptase lymphatic endothelial cell
HUVEC	human umbilical vein endothelial cells
IC50	half-maximal inhibitory concentration
ICAM-1	intercellular Adhesion Molecule 1
IDC	invasive ductal carcinoma
IF	immunofluorescence
IGF1R	insulin-like growth factor receptor 1
IHC	Immunohistochemistry
IL	interleukins
IL-1	Interlukin-1
ILC	invasive lobular carcinoma
IκBα	inhibitor of nuclear factor kappa-B kinase subunit alpha
JNK	c-Jun N-terminal kinase

K	kilo
kDa	kilodalton
LCIS	lobular carcinoma *in situ*
LECs	lymphatic endothelial cells
LI	lymphatic invasion
LN	lymph node
LVD	lymph vessel density
LVI	lymphovascular invasion
M	molar
MARCKS	Myristoylated alanine-rich C kinase substrate
MKI67	marker of proliferation Ki-67
mL	millilitre
mm	millimetre
mM	millimolar
MMP(s)	matrix metalloproteinase(s)
mRNA	messenger RNA
MT-MMP1	membrane-type matrix metalloproteinase 1 or MMP14
MYBL2	V-myb avian myeloblastosis viral oncogene homolog-like 2
NCI-DTP	National Cancer Institute - Developmental Therapeutics Program
ND	not determined
NFAT	nuclear factor of activated T-cells
NFIs	hypophosphorylated nuclear factor I
NF-κB	nuclear factor-kappa B
NF-*κ*B	nuclear factor-*κ*B
NHS	National Health Service
nM	nanomolar
NPI	Nottingham Prognostic Index
NPI+	Nottingham Prognostic Index Plus
NSC	neural stem cells
NTC	no template control
OS	overall survival
P	passage number
p53	tumour protein p53 (TP53), also known as cellular tumour antigen p53 (UniProt name), phosphoprotein

	p53, tumour suppressor p53, antigen NY-CO-13, or transformation-related protein 53 (TRP53)
PA	plasminogen activation
PAGE	polyacrylamide gel electrophoresis
PALB2	partner and localiser of BRCA2
PAM50	Prediction Analysis of Microarray
PAR1	protease-activated receptor 1
PARP1	poly(ADP-ribose) polymerase 1
PASMCs	pulmonary artery smooth muscle cells
PBCF	Physical Sciences-Oncology Center Network Bioresource Core Facility
PBMCs	peripheral blood mononuclear cells
PBS	phosphate-buffered saline
PCR	polymerase chain reaction
PDCD4	programmed cell death 4
PDGF	platelet-derived growth factor
PDGF-R	*platelet-derived growth factor receptors*
PE	plating efficiency
PEF	penta EF-hand
PI3K	phosphoinositide 3-kinase or phosphatidylinositol 3-kinase
PKA	protein kinase A, also known as Akt
PMA	phorbol myristate acetate
PP2A	protein phosphatase 2A
PR	progesterone receptor
pRb	retinoblastoma protein
PTEN	phosphatase and tensin homolog
PTGS2	prostaglandin-endoperoxide synthase 2, aka cyclooxygenase-2, or COX-2
PTP1B	protein tyrosine phosphatase 1B
RH	relative hazard
rpm	round per minute
RR	relative risk
RT	reverse transcription
RT-qPCR	reserve transcription-quantitative polymerase chain reaction
SD	standard deviation
SDS	sodium dodecyl sulfate

SDS-PAGE	sodium dodecyl sulfate polyacrylamide gel electrophoresis
SF	surviving fraction
shRNA	short hairpin RNA
siRNA	small interference RNA
Src	proto-oncogene tyrosine-protein kinase Src
STAT3	signal transducer and activator of transcription 3
STK11	serine/threonine kinase 11
STR	short tandem repeating
t-BOC	fluorescent substrate CMAC, t-BOC-Leu-Met, 7-Amino-4-chloromethylcoumarin, t-BOC-L-Leucyl-L-Methionine amide
TNBC	triple-negative breast cancer
TNF-α	tumour necrosis factor-α
TP53	tumour protein 53
TRPM7	transient receptor potential-melastatin-like 7
uPAs	urokinase plasminogen-type activators
V	volt
v/v	volume by volume
VCAM-1	Vascular cell adhesion protein 1
VEGF	vascular endothelial growth factor
WHO	World Health Organization
µg	microgram
µg/mL	microgram per millilitre
µL	microlitre
µM	micromolar
χ^2	Pearson Chi-Square test of association

Table of content

ABSTRACT ..... **I**

ACKNOWLEDGEMENTS ..... **IV**

CONFERENCE AND AWARDS ..... **V**

ABBREVIATION ..... **VI**

TABLE OF CONTENT ..... **XII**

LIST OF TABLES ..... **XV**

LIST OF FIGURES ..... **XVII**

CHAPTER 1 INTRODUCTION **1**

1.1 Breast cancer 1

1.1.1 Epidemiology 1
1.1.2 Risk factors 2
1.1.3 Breast cancer classification 6

1.2 Cancer metastasis and lymphovascular invasion 12

1.2.1 Metastatic dissemination of cancer 12
1.2.2 Lymphovascular invasion 17
1.2.3 Metastasis and lymphovascular invasion in breast cancer 23

1.3 Calpains and calpastatin 30

1.3.1 Calpain family 31
1.3.2 Calpastatin 36
1.3.3 Calpain and calpastatin distribution in subcellular and tissue levels 39
1.3.4 Calpain activation and calpain-calpastatin interaction 40
1.3.5 Roles of calpains and calpastatin in cancer 43

1.4 Hypothesis, aim, and objectives 58

CHAPTER 2 MATERIALS AND METHODS **60**

2.1 Cell culture 60

2.1.1 Cell lines and growth medium 60
2.1.2 Subculture of adherent cell lines 61
2.1.3 Cryopreservation and recovery from cryopreservation 61

2.2 Chemicals and drug preparation 62
2.3 Cell growth curve analysis and evaluation of cell proliferation 63
2.4 Western blotting 64

2.4.1 Cell treatment and preparation of cell lysate 64
2.4.2 SDS-polyacrylamide gel electrophoresis (SDS-PAGE) 65
2.4.3 Immunoblotting 66

2.5 Measurement of mRNAs expression 69

2.5.1 Purification of total RNA from cultured cells 69
2.5.2 cDNA synthesis by reverse transcription 71
2.5.3 Real-time quantitative polymerase chain reaction analysis 74

2.6 Establishment of stably transfected breast cancer cell lines overexpressing calpastatin isoforms 76
2.6.1 Optimisation of G418 concentration in the selection medium 76
2.6.2 DNA transfection 77
2.6.3 Selection of monoclonal cell populations expressing the highest level of HA-tagged calpastatin isoforms 80
2.7 Immunofluorescence microscopy 80
2.8 t-Boc calpain activity assay 81
2.9 Clonogenic survival 83
2.10 Haptotaxis scratch-wound migration assay 84
2.11 Endothelial adhesion assays 87
2.11.1 Peripheral blood mononuclear cell isolation 87
2.11.2 Static adhesion assays 88
2.12 Statistical analysis 89

CHAPTER 3 CALPASTATIN ISOFORM OVEREXPRESSION AND INTRACELLULAR LOCALISATION 91

3.1 Hypotheses and aims 91
3.2 Establishment of stably transfected breast cancer cell lines overexpressing calpastatin isoforms 93
3.2.1 Selection of breast cancer cell lines to overexpress calpastatin isoforms 93
3.2.2 Calpastatin DNA transfection and selection of transfected monoclonal cells 102
3.3 Expression of the calpain-calpastatin system proteins and CAST mRNA in the cells overexpressing calpastatin isoforms 110
3.3.1 Expression levels of the calpain-calpastatin system proteins 110
3.3.2 Expression levels of CAST mRNA 113
3.4 Effects of cell culture factors on calpastatin expression and migration of transfected cells 116
3.4.1 Effects of serial cell passaging on calpastatin expression in transfected cells 116
3.4.2 Effects of G418-free culture medium on calpastatin expression and cell migration in transfected cells 118
3.5 Intracellular localisation of calpastatin isoforms 121
3.6 Summary 126

CHAPTER 4 ROLES OF CALPASTATIN ISOFORM OVEREXPRESSION IN BREAST CANCER PROGRESSION AND LVI 128

4.1 Hypotheses and aims 128
4.2 Role of calpastatin isoform overexpression in regulating calpain activity *in vitro* 130
4.2.1 Effects of calpeptin on cell proliferation 130
4.2.2 Inhibitory effect of calpeptin on calpain activity 134
4.2.3 Inductive effect of A23187 calcium ionophore on calpain activity 137
4.2.4 Effects of calpastatin isoform overexpression on calpain activity 139

4.3 Role of calpastatin isoform overexpression on *in vitro* models of breast cancer progression (proliferation and clonogenic survival) 142
4.3.1 Cell proliferation 142
4.3.2 Clonogenicity 146
4.4 Role of calpastatin isoform overexpression in breast cancer LVI *in vitro* 149
4.4.1 Cell migration 150
4.4.2 Endothelial cell interactions 163
4.5 Summary 170
CHAPTER 5 DISCUSSION, LIMITATIONS AND CONCLUSION 172
5.1 Discussion 172
5.1.1 Expression of calpain and calpastatin system proteins and CAST mRNA in different breast cancer phenotypes *in vitro* 174
5.1.2 Establishment of stably transfected breast cancer cells overexpressing calpastatin isoforms 177
5.1.3 Expression of the calpain-calpastatin system proteins and CAST mRNA in transfected cells models 179
5.1.4 Effects of cell culture factors on calpastatin expression and migration of transfected cells models 184
5.1.5 Intracellular localisation of calpastatin isoforms 186
5.1.6 Role of calpastatin isoform overexpression in regulating calpain activity *in vitro* 190
5.1.7 Role of calpastatin isoform overexpression in *in vitro* models of breast cancer progression (cell proliferation and clonogenicity) 193
5.1.8 Role of calpastatin isoform overexpression on *in vitro* models of breast cancer LVI (cell migration and endothelial interactions) 198
5.1.9 Effects of A23187 calcium ionophore on calpain activity and phenotypic characteristics 207
5.2 Limitations and suggestions for future work 214
5.2.1 Cell lines, other models and related phenotypic assays 214
5.2.2 Regulation of calpain activity 217
5.2.3 Expression of calpastatin mRNA and proteins 220
5.3 Conclusion 221
REFERENCES 222
APPENDIX 260
Appendix A: Permission for republishing or display content 260
Appendix B 266
Appendix C 275
Appendix D 279

List of tables

Chapter 1

Table 1.1 Subtypes of breast carcinomas 7
Table 1.2 NPI prognostic groups and prognosis.....11
Table 1.3 Seven core breast cancer NPI+ biological classes 11
Table 1.4 The calpain family.....33
Table 1.5 Summary of calpastatin isoforms identified in tissues.....38

Chapter 2

Table 2.1 Materials for determination of protein expression by Western blotting 66
Table 2.2 Sources and dilutions of primary antibodies used in Western blotting.....67
Table 2.3 Components of RNA sample preparation and reverse-transcription reaction mix.....72
Table 2.4 Components of gDNA elimination mix and reverse-transcription reaction mix 73
Table 2.5 Sequences of specific oligonucleotide forward and reverse primers 75
Table 2.6 Confocal laser scanning microscope settings.....81

Chapter 3

Table 3.1 Doubling times of breast cancer cell lines calculated from current data and reviewed from publications 94
Table 3.2 Linear equations of standard curves and amplification efficiencies of PCR reactions for evaluating CAST and HPRT mRNA expression in seven breast cancer cell lines.....99
Table 3.3 Calpain-calpastatin system protein expression in MDA-MB-231 cells overexpressing calpastatin isoforms assessed by Western blotting.....111
Table 3.4 Linear equations of standard curves and amplification efficiencies of PCR reactions for evaluating CAST and HPRT mRNA expression.....114

Chapter 4

Table 4.1 IC50 values of doxorubicin on breast cancer cells proliferation (n = 3). 131
Table 4.2 Cell doubling times of parental and stably transfected breast cancer cell lines. 143
Table 4.3 Percentage of adhered MDA-MB-231 cells overexpressing calpastatin isoforms to endothelial cells. 166

Appendix B

Table B2.1 Cell lines and culture media 266

Table B2.2 Experimental conditions for migration assay.....274

Appendix C

Table C3.1 Summary of transfection conditions and monoclonal population selection in MDA-MB-231 cells.....277

Table C3.2 Summary of transfection conditions and monoclonal population selection in T47D cells 278

List of figures

Chapter 1

Figure 1.1 The invasion-metastasis cascade 13

Figure 1.2 Schematic structure of μ-calpain heterodimer and calpain family members 32

Figure 1.3 Schematic structure of calpastatin protein, cDNA and gDNA. 36

Figure 1.4 Schematic representation of conventional calpain substrates and major events of tumour cell pathophysiology in which conventional calpains are involved 44

Figure 1.5 Calpain and migration 50

Chapter 2

Figure 2.1 PBMC separation by density-gradient centrifugation method 87

Chapter 3

Figure 3.1 Quantitative analysis of the calpain-calpastatin system protein expression across seven breast cancer cell lines by Western blotting.....95

Figure 3.2 Optimisation of a standard serial dilution and sample dilution for RT-qPCR analysis 98

Figure 3.3 Quantitative analysis of CAST mRNA expression across seven breast cancer cells by RT-qPCR 100

Figure 3.4 HA-tagged and total calpastatin expression in CAST1- and CAST3-transfected multiclonal MDA-MB-231 populations detected by Western blotting 104

Figure 3.5 HA-tagged and total calpastatin expression in CAST1-transfected monoclonal MDA-MB-231 populations detected by Western blotting 104

Figure 3.6 HA-tagged and total calpastatin expression in CAST2- and CAST3-transfected monoclonal MDA-MB-231 populations detected by Western blotting 105

Figure 3.7 HA-tagged and total calpastatin expression in CAST1-transfected multiclonal and monoclonal T47D populations detected by Western blotting.....107

Figure 3.8 HA-tagged and total calpastatin expression in CAST2-transfected multiclonal and monoclonal T47D populations established from study 1 detected by Western blotting 108

Figure 3.9 HA-tagged calpastatin and total calpastatin expression in CAST2-transfected multiclonal and monoclonal T47D populations established from study 2 detected by Western blotting.....108
Figure 3.10 HA-tagged and total calpastatin expression in CAST3-transfected multiclonal and monoclonal T47D populations detected by Western blotting. 109
Figure 3.11 Representative blots of quantitative analysis of calpain-calpastatin system protein expression in MDA-MB-231 cells overexpressing calpastatin isoforms by Western blotting. 110
Figure 3.12 Quantitative analysis of calpain-calpastatin system protein expression in MDA-MB-231 cells overexpressing calpastatin isoforms by Western blotting.111
Figure 3.13 Melt curves of CAST1, CAST2 and HPRT mRNA amplified in all standards 114
Figure 3.14 Quantitative analysis of CAST1 expression in transfected MDA-MB-231 and T47D cells by RT-qPCR technique.....115
Figure 3.15 Effects of serial cell passaging on HA-tagged and total calpastatin expression in MDA-MB-231 cells overexpressing calpastatin isoforms detected by Western blotting.....117
Figure 3.16 Effects of G418-free culture medium on HA-tagged and total calpastatin expression in MDA-MB-231 cells overexpressing calpastatin isoforms detected by Western blotting 119
Figure 3.17 Effects of G418-free medium on the migration of transfected MDA-MB-231 cells examined by scratch-wound assay.....121
Figure 3.18 Confocal microscopic images of negative controls in the study of intracellular localisation of calpastatin isoforms in (A) MDA-MB-231 and (B) T47D cells.....122
Figure 3.19 Intracellular localisation of (A) GFP-tagged truncated and (B) HA-tagged full-length forms of calpastatin Type 1 in MDA-MB-231 and T47D cells detected by IF confocal microscopy 123
Figure 3.20 Intracellular localisation of (A) GFP-tagged truncated and (B) HA-tagged full-length forms of calpastatin Type 2 in MDA-MB-231 and T47D cells detected by IF confocal microscopy 124
Figure 3.21 Intracellular localisation of (A) GFP-tagged truncated and (B) HA-tagged full-length forms of calpastatin Type 3 in MDA-MB-231 and T47D cells detected by IF confocal microscopy 124

Figure 3.22 Intracellular localisation of GFP-tagged truncated calpastatin isoforms exon 3 deletion (Δ3) in MDA-MB-231 cells detected by IF confocal microscopy 125

Chapter 4

Figure 4.1 Effect of doxorubicin on breast cancer cell proliferation 130
Figure 4.2 Effect of calpeptin on cell proliferation of breast cancer cells.....132
Figure 4.3 Inhibition of calpain activity in MDA-MB-231 cells by calpeptin (100 µM) 134
Figure 4.4 Inhibition of calpain activity in breast cancer cells by calpeptin (50 µM and 75 µM).....135
Figure 4.5 Effect of A23187 on the integrity of breast cancer cell monolayers.....138
Figure 4.6 Effect of A23187 or calpeptin on calpain activity in MDA-MB-231 cells ..138
Figure 4.7 Calpain activity of MDA-MB-231 cells overexpressing calpastatin isoforms 140
Figure 4.8 Effect of calpeptin or A23187 on calpain activity in the mock-transfected MDA-MB-231 cells.....140
Figure 4.9 Effect of A23187 on calpain activity in MDA-MB-231 cells overexpressing calpastatin isoforms 141
Figure 4.10 Effect of calpastatin isoform overexpression on breast cancer cell proliferation 143
Figure 4.11 Effect of A23187 on cell proliferation in MDA-MB-231 cells overexpressing calpastatin isoforms 145
Figure 4.12 Effect of calpeptin on clonogenicity of MDA-MB-231 cells 147
Figure 4.13 Effect of calpastatin isoform overexpression on MDA-MB-231 clonogenicity 147
Figure 4.14 Effect of A23187 on clonogenic survival of MDA-MB-231 cells overexpressing calpastatin isoforms.....148
Figure 4.15 Optimisation of cell plating density for scratch-wound migration assay. 151
Figure 4.16 Effect of PP2 and calpeptin on MDA-MB-231 cell migration detected by scratch-wound assay 152
Figure 4.17 Effect of cytochalasin D and doxorubicin on breast cancer cell proliferation 154

Figure 4.18 Effect of cytochalasin D on breast cancer cell migration detected by scratch-wound assay 155
Figure 4.19 Effect of calpeptin on breast cancer cell migration detected by scratch-wound assay 156
Figure 4.20 Effects of 0.5% DBS culture medium on the proliferation of parental and transfected T47D cells 157
Figure 4.21 Effect of calpastatin isoform overexpression on breast cancer cell migration detected by scratch-wound assay 159
Figure 4.22 Effect of A23187 or calpeptin on cell migration in MDA-MB-231 cells overexpressing calpastatin isoforms detected by scratch-wound assay 160
Figure 4.23 Effect of A23187 or calpeptin on cell migration in T47D cells overexpressing calpastatin isoform detected by scratch-wound assay 162
Figure 4.24 Effect of CellTracker Green CMFDA labelling on T47D cell proliferation. 164
Figure 4.25 Optimisation of endothelial cell plating density for static adhesion assay. 164
Figure 4.26 PBMC adhesion to endothelial cells 165
Figure 4.27 Adhesion to endothelial cells of MDA-MB-231 cell overexpressing calpastatin isoforms 166
Figure 4.28 T47D cell adhesion to endothelial cells 168
Figure 4.29 Effect of A23187 or calpeptin on adhesion of MDA-MB-231 cells overexpressing calpastatin isoforms to endothelial cells 169

Appendix B

Figure 2B.1 Maps of A) pZsGreen1-N1 plasmid (4708 bp) and B) HA-tagged, GFP-removed, pZsGreen1-N1 plasmid (4018 bp). 268
Figure 2B.2 Maps of HA-tagged, GFP-removed, DNA constructs of full-length calpastatin Type 1 (6351 bp) 268
Figure 2B.3 Maps of HA-tagged, GFP-removed, DNA constructs of full-length calpastatin Type 2 (6306 bp). 269
Figure 2B.4 Maps of HA-tagged, GFP-removed, DNA constructs of full-length calpastatin Type 3 (6102 bp). 269

Appendix C

Figure C3.1 Growth curves of basal-like breast cancer cell lines 275

Figure C3.2 Growth curves of luminal and HER2-enriched breast cancer cell lines ..276

Appendix D

Figure D4.1 Growth curves of parental and stably transfected MDA-MB-231 cell lines 279

Figure D4.2 Growth curves of parental and stably transfected T47D cell lines.....280

Chapter 1 Introduction

1.1 Breast cancer

1.1.1 Epidemiology

Breast cancer occurs principally in women and rarely in men. In the UK, there were around 370 male (< 1%) and 54,800 female new cases diagnosed in 2015 (Cancer Research UK, 2018). One in eight women (12.08%) will be diagnosed with breast cancer in their lifetime, and more than 80% of breast cancers are diagnosed in women over 50 years of age (Cancer Research UK, 2017). In 2018, breast cancer was the most common female cancer diagnosed in the UK with 55,439 new cases (26.7%) as well as in Thailand, my home country, where 19,510 new cases (22.8%) were registered (Global Cancer Observatory, 2019d; Global Cancer Observatory, 2019e). In the same year, breast cancer was also recognised as the most common malignancy amongst women globally with 2.09 million new estimated cases (24.2%), and it was the leading cause of female cancer death worldwide (Global Cancer Observatory, 2019f). Approximately 0.6 million women around the world were estimated to have died from breast cancer (16% of all female cancer deaths) (Global Cancer Observatory, 2019c). In the UK, this disease was the second leading cause of cancer death amongst women with 11,849 deaths (14.3%) following lung cancer (21.4%) (Global Cancer Observatory, 2019b). Over the last decade, however, the mortality rates of female breast cancer in the UK have reduced by around 19%, while the incidence rates have increased by approximately 6% (Cancer Research UK, 2018). In Thailand, breast cancer was ranked third in 2018 with 5,902 deaths (11.8%) following lung (14.7%) and liver carcinomas (13.7%) (Global Cancer Observatory, 2019a). Although the breast cancer incidence is lower in Thailand, the mortality-to-incidence ratio (MIR) is higher ($MIR_{Thailand}$ = 0.3, $MIR_{the\ UK}$ = 0.2) (Global Cancer Observatory, 2019a; Global Cancer Observatory, 2019b; Global Cancer Observatory, 2019d; Global Cancer Observatory, 2019e).

The 5-year survival rate of breast cancer is higher in developed countries at 73% as compared to 57% of patients surviving five years in developing countries (Parkin *et al.*, 2005; Allemani *et al.*, 2015; da Costa Vieira *et al.*, 2017). In the UK, breast cancer survival is improving and has doubled in the last four decades. In England and Wales, 87% and 78% of women diagnosed with breast cancer survive their disease for ≥ 5 and ≥ 10 years, respectively (Cancer Research UK, 2018). Within a decade, the 5-year survival rate in Thailand, regarded as a developing country, has increased from 65.9% (1995-1999) to 71.3% (2005-2009) (Allemani *et al.*, 2015). During 2014 to 2035, the incidence rate for breast cancer in the UK is estimated to increase by 2%, whereas the mortality rate is projected to drop by 26% (Cancer Research UK, 2018). In 2050, the worldwide incidence of new cases is predicted to reach 3.2 million (Hortobagyi *et al.*, 2005). The increases in breast cancer incidence and survival rates in developed countries can be accredited to improving public awareness, and the evolution of public health systems related to early diagnoses through organised mammographic screening programmes. In addition to early detection of the disease, adequacy and accessibility of treatment facilities influence the decrease in mortality rates (Youlden *et al.*, 2012; Rivera-Franco & Leon-Rodriguez, 2018).

1.1.2 Risk factors

1.1.2.1 Age, hormonal status and genetics

The risk of developing breast cancer increases with age. Before 40 years, the likelihood of developing breast cancer is extremely low (1 in 206 or 0.49%), but it dramatically increases approximately 8-fold after the age of 40. The risk for women aged between 40-59 and 60-69 are comparable at 3.75% (1 in 27) and 3.40% (1 in 29) respectively. After the age of 70, the risk doubles to 6.50% (Jemal *et al.*, 2010). The increased risk with age is partially due to increased exposure to the sex hormone oestrogen, and genetic mutations acquired over a lifetime.

The risk of disease development increases in women with early menarche (menstruation beginning before 12 years) as well as in women with a late age of natural menopause (age 55 years or later) (Michaud *et al.*, 2011). Each 1-year delay in menarche reduces the relative risk by 5%; each 1-year delay in menopause increases the relative risk by 3% (Collaborative Group on Hormonal Factors in Breast, 2012). Women with oophorectomy at the age < 35 or bilateral oophorectomy at the age < 40 years are classified into a low-risk group; the relative risk of breast cancer by age at oophorectomy is 3.0 (Shah & Wong, 2006; Michaud *et al.*, 2011). Exogenous sex hormones, e.g., hormonal contraceptives or hormone replacement therapy (HRT), also influence the risk of promoting breast carcinogenesis. The relative risks of developing breast cancer among current and recent users (discontinuation within the previous six months) are 1.19 for combined oral contraceptives (P <0.001) and 1.20 for all hormonal contraceptive products (P = 0.002) compared to the women who never use any of them. The risk increases with the duration of hormonal contraceptive use, from 1.09 with less than a year of use to 1.38 after use for > 10 years (P = 0.002) (Morch *et al.*, 2018). The risk of breast cancer remains higher in the more than 5-year users who have stopped using hormonal contraceptives (Morch *et al.*, 2018), and it will abate over time within 5-15 years of discontinuation of hormonal contraception (Westhoff & Pike, 2018). HRT has been found to increase the relative risk of breast cancer over the time of use; for every five years of use, the relative risk is increased by 10% (Ross *et al.*, 2000). Current users of HRT are more likely than non-users to develop breast cancer (P < 0.0001) and to subsequently die from it (P = 0.05) with 1.66 and 1.22, respectively, relative risk (RR) (Beral, 2003). The risk is substantially higher for combined HRT use (RR = 1.24) than for estrogen replacement therapy use (RR = 1.06) (Ross *et al.*, 2000). In past users, the relative risk remains slightly increased among women who stopped using HRT for about a year (RR = 1.14, P = 0.03), but there is no significant difference between that of never users, for cessation of HRT for less than 5 years, 5–9 years, and ≥ 10 years (Beral, 2003).

Genetic factors and family history also enhance the risk of developing breast cancer in women. Women with a significant family history of breast cancer, especially in first- and second- degree relatives, are at high risk of developing the disease (RR = 2.6) (Shah & Wong, 2006). Less than 30% of hereditary breast cancers are caused directly by mutated forms of susceptibility genes that are inherited from a parent to their child. Approximately 25% of hereditary cases are caused by a mutation in one of the rare but highly penetrant genes, i.e., BRCA1, BRCA2, PTEN, TP53, CDH1, and STK11, which are associated up to an 80% lifetime risk of breast cancer. The other 2–3% of cases are a result of a mutation(s) in the rare, moderate-penetrance genes, e.g., CHEK2, BRIP1, ATM, and PALB2, each of which confers to a two-fold increase in risk (Shiovitz & Korde, 2015). BRCA1 and BRCA2 are the most commonly recognised susceptibility genes of breast cancer as well as of ovarian cancer. They are tumour suppressor genes and play a role in the maintenance of genome integrity (Narod *et al.*, 1995; Filippini & Vega, 2013). Three to eight per cent of female breast cancer cases carry a mutation in one of them (Brody & Biesecker, 1998). The mutations in BRCA1 and BRCA2 increase a lifetime susceptibility of developing breast cancer by 82% (Shiovitz & Korde, 2015). The study by Rakha *et al.* (2008) indicates that mutations in BRCA1 tend to cause tumours with triple-negative basal-like phenotypic property and a high histologic grade. The tumour suppressor gene PTEN is another well-recognised susceptibility gene of breast cancer. The risk of developing breast cancer is increased by 67–85% over a lifetime by mutations of PTEN (Shiovitz & Korde, 2015; Ngeow *et al.*, 2017). Mutation of this gene is also associated with a higher risk of developing endometrial, colorectal, renal, thyroid as well as second breast cancers (Ngeow *et al.*, 2017).

1.1.2.2 Lifestyle factors

Alcohol consumption and smoking are thought to increase the risk of developing breast cancer by altering the level of oxidative stress (Kopp *et al.*, 2017). Alcohol consumption is the only dietary factor that has provided consistent evidence of associating with breast cancer in clinical trials. Studies

indicate a positive dose-response relationship between alcohol consumption and the risk of breast cancer. Every an increment of 10 g of alcohol consumed per day causes an elevated breast cancer risk by approximately 7-10% (Hamajima *et al.*, 2002; Key *et al.*, 2006; Zhang *et al.*, 2007). The relative risk of breast cancer is 1.32-1.43% for 30 g alcohol per day (Zhang *et al.*, 2007) and 1.33-1.61 for ≥45 g per day (Hamajima *et al.*, 2002).

Smoking is a lifestyle factor that provides contradictory evidence of associating with breast cancer. Hamajima *et al.* (2002) state that there is no association between smoking and the development of breast cancer in women who reported drinking no alcohol. The relative risks of breast cancer were 1.03 for former-smokers and 0.99 for current smokers compared to never-smokers. Other studies report a positive association between smoking and the development of breast cancer. A relatively recent publication reports the incidence of breast cancer being higher in current and former smokers than in never-smokers, indicated by hazard ratios (HR) of 1.24 and 1.13, respectively (Gaudet *et al.*, 2013). Breast cancer has been found to be associated with smoking duration of 40 years (HR = 1.57), smoking intensity of 40 cigarettes a day (HR = 1.21), cumulative exposure of 40 pack-years (HR = 1.19), and latency of smoking for 40 years since initiation (HR = 1.19) (Catsburg *et al.*, 2015). Smoking significantly increases the risk of breast cancer in women whose smoking began before the age of 17 (HR = 1.24; $P = 0.002$) (Jones *et al.*, 2017).

Consumption of a high-fat diet, inactivity and obesity have also been associated with an increased risk of cancers (Yee, 2005). In the UK, 5.5% of all cancers in 2010 was contributed by overweight (body mass index or BMI = 25-30), and obesity (BMI ≥ 30) (Parkin & Boyd, 2011). Amongst premenopausal women, BMI ≥ 25 is significantly associated with an increased risk of invasive breast carcinoma ($P = 0.01$); HRs are 1.59 for BMI 25–29.9 and 1.70 for BMI ≥ 30 compared to BMI < 25 (Cecchini *et al.*, 2012). The study of Schoemaker *et al.* (2018), however, has found that the HRs for breast cancer decrease with increasing BMI when compared to the group of underweight (BMI < 17). The

breast cancer risks of BMI > 30 are abated by 23% (HR = 0.77) for younger women aged 18 to 24 years and by 12% (HR = 0.88) for the age of 45-54 years compared to the group of BMI < 17.

1.1.3 Breast cancer classification

1.1.3.1 Histological classification

Breast cancer is broadly divided into non-invasive (*in situ*) and invasive carcinomas. Non-invasive breast carcinoma is comprised of two types - ductal carcinoma *in situ* (DCIS) and lobular carcinoma *in situ* (LCIS). Non-invasive carcinoma cells are confined to the ducts or lobules and do not invade surrounding adipose or connective tissues of the breast. DCIS is the most common form of non-invasive breast cancer (90%) (Sharma *et al.*, 2010) and regarded as a non-obligate precursor to invasive carcinomas. DCIS, however, can progress to invasive cancer within 6-10 years (Dunn *et al.*, 2010; Ryan & Faupel-Badger, 2016), and 14–53% of DCIS will not progress to that stage (Punglia *et al.*, 2018). LCIS is less common and considered to be a risk factor by increasing 7-10 fold of risk for developing invasive breast cancer (Mao *et al.*, 2017). Invasive carcinomas can be further classified based on the morphological feature of the tumour-histological type. The diverse histologic types of breast cancer differ in biological behaviour and consequently have differences in response to therapy and prognoses (Michaud *et al.*, 2011; Nagao *et al.*, 2012). Adenocarcinomas are the most common histology classified as invasive ductal adenocarcinoma (IDC) and invasive lobular adenocarcinoma (ILC) (75-80% and 5-15% of all invasive breast cancer, respectively) (Schnitt & Guidi, 2004; Sharma *et al.*, 2010; Michaud *et al.*, 2011;). Clinical response of IDC to primary anthracycline-based polychemotherapy is significantly better than that of ILC (60% vs 47%; $P = 0.04$) (Bollet *et al.*, 2008). ILC patients (n = 122; 12%), however, have better clinical outcomes compared to patients with IDC (n = 912; 88%) - 87% vs 66% 5-year recurrence-free survival rate ($P = 0.004$), and 93% vs 70% 5-year overall survival rate ($P = 0.001$) (Cristofanilli *et al.*, 2005). In a smaller study by Song *et al.* (2013), the 5-year disease-free and overall survival

rates of patients with IDC (n = 767) were 71.2 and 85.1%, respectively. Inflammatory breast cancer (IBC) is one of the rare types of breast cancer (1-5%) and is classified as an aggressive form of locally advanced disease with poor prognosis (median survival = 2.9 years) (Hance *et al.*, 2005; Tryfonidis *et al.*, 2015). One of the key pathological characteristics of IBC is dermal lymphatic vessel invasion by cancers forming emboli and resulting in blockage of lymphatic drainage and *peau d'orange* (orange peel) appearance of the breast (Edge *et al.*, 2010; Hortobagyi *et al.*, 2017).

1.1.3.2 Molecular classification

Breast cancer is a complex and heterogeneous disease with multiple distinctive characteristics, different morphological features and clinical behaviours (Badve *et al.*, 2011). The heterogeneity of this disease can be confirmed by molecular profiling using DNA microarrays, through gene expression profiling and by the use of the immunohistochemical expression of protein markers. Molecular stratification allows breast cancers to be subdivided into several distinct subtypes; however, five common intrinsic subtypes are typically considered for planning breast cancer management, assessing prognosis and predicting patient outcomes. The five intrinsic subtypes (luminal A and B, HER2-enriched, basal-like, and normal-like) are stratified corresponding to the expression of oestrogen receptor (ER), progesterone receptor (PR) and human epidermal growth factor receptor 2 (HER2) (Perou *et al.*, 2000; Sorlie *et al.*, 2001; Sotiriou *et al.*, 2003; Desmedt *et al.*, 2009; Russnes *et al.*, 2017), as summarised in Table 1.1. The molecular subtypes are potentially predictive of response patterns to specific therapeutic agents.

Table 1.1 Subtypes of breast carcinomas

Subtypes	Characteristics	Frequency	Prognosis
Luminal A	ER^+, $PR^{+/-}$, $HER2^+$, low Ki-67 index	40%	Best
Luminal B	ER^+, $PR^{+/-}$, $HER2^+$, high Ki-67 index	20%	Good
HER2-enriched	ER^-, PR^-, $HER2^+$	10-15%	Poor
Basal-like	ER^-, PR^-, $HER2^-$ (Triple-negative)	15-20%	Poor

Data summarised from Sorlie *et al.* (2001), Sotiriou *et al.* (2003), Desmedt *et al.* (2009), Gemignani and Armstrong (2014), and Ahn *et al.* (2015).

The largest cluster is dominated by ER-positive (ER^+) tumours and can be classified into two subgroups (luminal A and B) by Ki-67 (proliferating cell nuclear antigen) index (Brenton *et al.*, 2005; Cheang *et al.*, 2009). The luminal A type is regarded as the largest subtype (40% of all cases), and is positive for ER (ER^+), negative for HER2 (HER^-) and has low Ki-67 index (< 14%). The luminal B type (20% of all cases) expresses ER^+, $HER2^-$/$HER2^+$ and has a high Ki-67 index (Kim *et al.*, 2012; Gemignani & Armstrong, 2014; Ahn *et al.*, 2015). Luminal B breast cancer commonly has a higher expression of genes related to mitosis and cell proliferation, such as *CCNB1, MKI67*, and *MYBL2*, compare to luminal A type (Cheang *et al.*, 2009). ER and PR statuses are key predictors of the response to hormone therapy (Mosly *et al.*, 2018). The luminal A subtype is considered as a low-risk group, showing a good response to endocrine therapy compared to the luminal B subtype, which generally has a higher grade and exhibits a higher rate of proliferation (Kang *et al.*, 2003a; Ahn *et al.*, 2015; Dowsett *et al.*, 2011; Ahn *et al.*, 2015). Breast cancer with high positivity of the proliferation marker Ki-67 is associated with worse survival (HR = 1.95) (de Azambuja *et al.*, 2007).

The other main cluster is the ER-negative (ER^-) tumours, which are stratified into two subgroups - HER2-enriched and basal-like (10-15% and 15-20% of all breast cancer cases, respectively). The HER2-enriched or $HER2^+$ group is characterised by high expression of erbB2/HER2-related genes/proteins, low to intermediate expression of luminal-related genes/proteins (such as oestrogen receptor gene-1 and progesterone), and low expression of basal-related genes/proteins (e.g., keratin 5 and FOXC1) (Prat *et al.*, 2015). HER2 is a target for HER2-directed therapy, and HER2-positive malignant tumours benefit the most from the use of chemotherapy plus anti-HER2 therapy (Prat *et al.*, 2014; Prat *et al.*, 2017). The basal-like subgroup constitutes 15-20% of breast cancers and is described by negative expression of ER, PR, and HER2, in addition to the expression of genes characteristic of myoepithelial/basal epithelial cells, such as basal cytokeratin 5, 6 and 17 (Perou *et al.*, 2000; Alluri & Newman, 2014). Triple-negative breast cancer (TNBC) and basal-like subtype share the similarity

of lacking expression of such three markers, but they are not biologically-synonymous. Approximately 71-79% of TNBC are basal-like breast cancer, while 68-77% of basal-like cases are identified as TNBC (Bertucci *et al.*, 2008; Prat *et al.*, 2013). Both basal-like and TNBC are associated with aggressive pathologic features and poor prognosis compared to other subtypes (Dent *et al.*, 2007; Banerjee *et al.*, 2006). While ER^+ tumours typically respond to hormone therapy and $HER2^+$ tumours respond to anti-HER2 treatment, there is no currently targeted therapy in widespread use for $ER^-/HER2^-$ breast cancer. Normal-like breast cancer is defined by gene expression similar to patterns found in normal breast tissue (Russnes *et al.*, 2017).

1.1.3.3 TNM classification

According to the American Joint Committee on Cancer (AJCC) staging system, breast cancer is generally diagnosed and categorised into five stages (0 to IV) by TNM Stage Grouping based on extent and size of primary tumour (T), presence and extent of lymph node involvement (N), and presence of distant metastases (M) (Edge *et al.*, 2010; Giuliano *et al.*, 2018). Stage 0 refers to carcinoma *in situ* or disease without invasion of cancer cells into the basement membrane of the breast tissue. Stage I and II refer to early breast cancer that is small invasive tumours with/without nodal micrometastasis in stage I, and with axillary lymph node involvement in stage II (Edge *et al.*, 2010; Giuliano *et al.*, 2017). Most patients with these stages are managed by surgery, followed by adjuvant therapy (chemotherapy, radiotherapy, hormone and/or HER2 targeted therapy) within 31 days after surgery as suggested in the clinical guidelines for the management of breast cancer by the National Health Service (NHS) England (Breast Cancer Expert Advisory Group, 2016). Stage III represents locally advanced disease and is diagnosed by the presence of a large tumour with extensive lymph node involvement in which either the tumour or node is fixed to the chest wall (Edge *et al.*, 2010). The appropriate initial treatment for patients with this stage of the disease is neoadjuvant chemotherapy, followed by local therapy (surgery and radiotherapy) and further adjuvant systemic therapy (Michaud *et al.*, 2011). Stage IV is advanced or metastatic disease and

is characterised as cancer cells spreading to lymph nodes, and migrating beyond the primary site into distant organs through the bloodstream and/or lymphatic system (Edge *et al.*, 2010; Wells *et al.*, 2013). Metastasis is a robust indicator of disease progression, and associates with failure of primary treatments, and difficulty in eradicating cancer by locoregional therapy. It is also a sign of a potentially incurable state and has the worst survival rate of the various tumour types (Scheel and Weinberg, 2012; Wells *et al.*, 2013). In breast cancer, for instance, patients with a higher tumour stage tend to have a worse prognosis. The five-year overall survivals of breast cancer diagnosed in stages 0 to IV are 92, 87, 75, 46 and 13%, respectively (Kumar *et al.*, 2013). The principal therapeutic goals for patients with metastasis are prolonging their survival and improving/maintaining their quality of life. Palliative radiotherapy and systemic treatment (chemotherapy, hormone, or HER2 targeted therapy) can control disease and relieve symptoms associated with the dissemination of cancer (Jutzy *et al.*, 2018).

1.1.3.4 Prognostic classification by Nottingham Prognostic Index (NPI)

The Nottingham Prognostic Index (NPI) is an effective tool for predicting prognosis in patients by combining significant prognostic factors into one unified system. The index is calculated from the primary tumour size, the involvement of the regional lymph node and tumour grade, as shown in the formula below (Haybittle *et al.*, 1982). The lymph node status is classified into three stages: stage 1 no nodal involvement, stage 2 involvement of either up to three low axillary nodes or of the internal mammary node (assessed in medially located tumours) and stage 3 involvement of four or more low axillary nodes and/or the apical axillary node or of both low axillary and internal mammary nodes. Breast cancers can be placed into six prognostic categories regarding NPI - excellent (2.02-2.4), good (2.41-3.4), moderate 1 (3.41-4.4), moderate 2 (4.41-5.4), poor (5.41-6.4), and very poor (6.41-6.8). Table 1.2 shows the frequency and 10-year survival of each NPI group.

$$\text{NPI} = [0.2 \text{ x Tumour size (cm)}] + \text{Lymph node stage (1-3)} + \text{Histological grade (1-3)}$$

Table 1.2 NPI prognostic groups and prognosis

Group	NPI	1980–1986		1990–1999	
		Frequency	10-year survival	Frequency	10-year survival
Excellent	2.02–2.4	12%	88%	15%	96%
Good	2.41–3.4	19%	72%	21%	93%
Moderate 1	3.41–4.4	29%	61%	28%	81%
Moderate 2	4.41–5.4	24%	42%	22%	74%
Poor	5.41–6.4	11%	15%	10%	55%
Very poor	6.41–6.8	5%	12%	4%	38%

Data reproduced from Lee and Ellis (2008). Copyright© 2008 by Elsevier with permission conveyed through Copyright Clearance Centre.

The NPI is an excellent tool to stratify the prognosis of breast cancer patients; in incorporating of predictive factors (ER and HER2 statuses), menopausal status and patient desires, NPI is beneficial for guiding the choice of adjuvant systemic treatments (Lee & Ellis, 2008). The Nottingham Prognostic Index Plus (NPI+) has been developed as a more modern version in an attempt to assist clinicians in offering a more personalised adjuvant treatment plan in all early-stage cases. The NPI+ evolved based on the evaluation of seven biological classes of breast cancer (luminal A and B, luminal N, basal p53 normal, basal p53 altered, $HER2^+/ER^+$ and $HER2^+/ER^-$; Table 1.3) that incorporate additional with six clinicopathological prognostic factors, i.e., positive nodal number, stage, size, mitosis, PR and lymphovascular invasion (LVI) (Rakha *et al.*, 2014).

Table 1.3 Seven core breast cancer NPI+ biological classes

Subtypes	Characteristics
Luminal A	high expression of CK7/8, ER, HER3 and HER4
Luminal B	high expression of CK7/8, ER, HER3 and HER4 but lower expression of PR
Luminal N	high expression of CK7/8 and ER but low expression of HER3 and HER4
HER2+/ER+	HER2 overexpression and ER^+
$HER2^+/ER^-$	HER2 overexpression and ER^-
basal p53 normal	high basal expression and low expression p53
basal p53 altered	high basal expression and high expression p53

Data summarised from Rakha *et al.* (2014).

The NPI+ has not been routinely used yet but is expected to be continuing education (CE) for health care professionals with a launch for NHS (England)

clinical use soon (NIHR Innovation Observatory, 2015). Other breast cancer prognostic tools are available for routine use, e.g., Oncotype DX, MammaPrint, PAM50, IHC4 tests.

1.2 Cancer metastasis and lymphovascular invasion

1.2.1 Metastatic dissemination of cancer

1.2.1.1 Definition and the metastatic cascade

Metastasis is a result of malignant cells disseminating from a primary tumour to establish secondary tumours in an adjacent or distant location (Menezes *et al.*, 2016). It is one of eight core biological hallmarks of cancer that describe biological capabilities acquired during the multistep development of human malignant tumours, including 1) sustaining proliferative signalling, 2) evading growth suppressors, 3) resisting cell death, 4) enabling replicative immortality, 5) inducing angiogenesis, 6) activating invasion and metastasis, 7) reprogramming of energy metabolism to fuel cell growth and division, and 8) evading immune destruction (Hanahan & Weinberg, 2011).

Metastasis symbolises the final-outcome of a complex series of sequentially cell-biological events called 'the invasion-metastasis cascade' (described further below). The process involves 1) acquisition of genetic and/or epigenetic changes within the tumour cells, and 2) coordination of non-neoplastic stromal cells, which supply the initial metastatic cells with essential stimuli to grow and produce macroscopic metastases (Valastyan & Weinberg, 2011). The metastatic property of the tumour cells is acquired from inherited processes. Genetic changes occur in most cells of the primary tumour, providing them with an inherited general predisposition for metastatic dissemination (Weigelt *et al.*, 2005). Two theories have been proposed to describe the acquisition of genetic and/or epigenetic changes. The first theory called 'the late stage or clonal selection theory' explains that only subpopulations of cancer cells in the primary tumour acquire phenotypic alterations, late in tumorigenesis, through an accumulation of various genetic modifications, with the changes, resulting

in the capability of tumour cells to complete the metastatic cascade (Weigelt *et al.*, 2005; Talmadge, 2007). Contrastively, the second theory, based on expression microarray data from human tumours, suggests that most cancer cells in a primary tumour have a metastatic phenotype, suggesting metastasis is an early phenomenon in tumorigenesis (Pantel & Brakenhoff, 2004).

The invasion-metastasis cascade is a complex series of sequential cell-biological events (Figure 1.1). The sequence consists of six steps: 1) a detachment of tumour cells from the original tumour, local invasion and migration through the basement membrane, extracellular matrix (ECM) and stromal layers, 2) intravasation into the blood and/or lymphatic vessels (so-called lymphovascular invasion or LVI), and 3) evasion of the host immune responses. The latter steps are 4) arrest in a distant capillary bed and invasion through the vascular basement membrane and ECM in the process of extravasation from the vessels to new locations, 5) adaptation to survive and grow in the foreign microenvironments of the secondary sites to form micrometastases, and 6) ultimately metastatic colonisation (Pantel & Brakenhoff, 2004; Mohammed *et al.*, 2009b; Valastyan & Weinberg, 2011; Martin *et al.*, 2013).

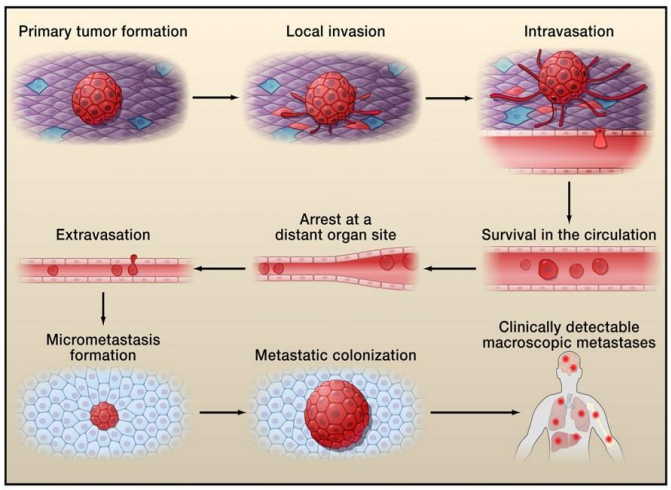


Figure 1.1 The invasion-metastasis cascade. Reproduced from Valastyan & Weinberg, 2011. Copyright© 2019 by Elsevier with permission conveyed through Copyright Clearance Center, Inc.

The metastatic cascade is a series of sequential and interrelated events. Each event can be a rate-limiting step, and a failure at any step would cause a failure of metastasis (Poste & Fidler, 1980; Talmadge & Fidler, 2010). The end-product

of the cascade relies on the intrinsic properties of the malignant cells as well as the host response, in other words, metastatic dissemination is a balance of host-tumour cellular interactions, which vary amongst patients (Talmadge & Fidler, 2010).

1.2.1.2 Incidence and prognosis of metastasis

Metastasis is a sign of disease progression and associated with a poorer prognosis, and shortened survival compared to earlier stages of disease (Shord & Cordes, 2017). The five-year overall survival of breast cancer, for example, diagnosed in an advanced stage is 13% (Kumar *et al.*, 2013). Approximately 30% of new patients diagnosed with solid tumours (melanomas included) is present with clinically evident metastases, while 20% have hidden metastases at the time of diagnosis (Kumar *et al.*, 2018). Microscopic cancer metastases (micrometastases) can be found in newly diagnosed cancer patients. In many cases, cancer relapses at distant organs, even though the primary tumour has been eliminated, suggesting that small clusters of cancer cells exist although clinically undetectable (Medina & Shord, 2011). Even small cancers with <5 mm diameter can generate multiple metastases 5-10 years prior to detection. This phenomenon has been observed in most of the common human solid malignancies, including cancers of the breast, prostate, colon, kidney, lungs, and malignant melanomas (Friberg & Nystrom, 2015). Some patients with micrometastasis can possibly be cured with systemic chemotherapy (Medina & Shord, 2011).

The onset and time course for the development of metastasis generally depend upon the type of cancer, and a variety of patterns of metastasis are observed for different diseases. Breast cancer metastasis, for example, can occur very early (median time = 53 months; an average of time = 69 months after primary surgery without systemic adjuvant treatment), and commonly spreads to the bones (38%), lungs (30%), liver (23%), and brain (5%) (Dillekas *et al.*, 2014; Shord & Cordes, 2017). Prostate cancer frequently metastasises to bone (90%) (Bubendorf *et al.*, 2000), while about 70% of colorectal cancer patients will

develop metastasis in the liver (Rothbarth & van de Velde, 2005), which presents at first diagnosis in 14-18% of all cases, or 10-25% at the time of primary cancer resection (Jegatheeswaran *et al.*, 2013; Valderrama-Treviño *et al.*, 2017). Such different sites of spread according to tumour type suggests different tumour types have individually preferential sites of metastatic dissemination. A number of theories have been put forward to explain the different patterns.

1.2.1.3 Theories to explain metastatic patterns of spread

Metastasis is the spread of a tumour to positions that are physically separated from the primary tumour. The invasiveness of cancer cells allows them to invade adjacent tissue and disseminate to the remote sites by one of three pathways: 1) seeding within body cavities, 2) haematogenous spread, or 3) lymphatic spread (Kumar *et al.*, 2018). Not all of the cells, however, that dissociate from a primary tumour cause a metastatic lesion. The shed cells firstly need to find a favourable environment for growth (Minn & Massave, 2011).

The 'seed and soil' hypothesis was originally proposed by Stephen Paget, since 1889, suggesting that the metastatic process does not happen by chance but occurs in organ-preference patterns and is the result of interactions between metastatic cancer cells (seeds), and their favourable microenvironment for growing (soil) provided by the specific organs (Paget, 1989). The specific characteristics of malignant cells and the biological uniqueness of the microenvironments present within distinct tissues/organs influence tumour cells to disseminate to particular locations and potentially grow in such sites. In addition, endothelial cells in the vasculature of different organs express different cell-surface receptors and growth factors, contributing to supporting or inhibiting extravasation and growth of metastatic cells (Pasqualini & Ruoslahti, 1996; Uehara *et al.*, 2003; Talmadge & Fidler, 2010).

In breast cancer metastasis, for example, CXCR4 receptor has been found to be involved in targeting lymph nodes, bone marrow, liver or pulmonary as the

selective sites for metastasis of breast cancer cells as its ligand, CXCL12 chemokine, is highly expressed there (Huang *et al.*, 2009). Retrospective molecular/histologic analyses of breast cancers have shown that phenotype influences organ-specific metastasis patterns. Bone relapses are most abundant amongst the luminal subtypes, while lung relapses are highly associated with the basal-like subtype (Smid *et al.*, 2008; Kennecke *et al.*, 2010; Yousefi *et al.*, 2018). *In vivo* gene-expression analyses indicate that metastasis of breast cancer to selective organs is mediated by a specific set of genes, e.g. overexpressed IL11, CTGF, CXCR4, and MMP1 in promoting bone metastasis (Kang *et al.*, 2003b), and MMP1, CXCL1 and PTGS2 in lung metastasis (Minn *et al.*, 2005). For another example, in prostate cancer metastasis, platelet-derived growth factor (PDGF) and autophosphorylation of its receptor (PDGF-R) have been found to associate with the growth of metastatic prostate tumour cells in the bone parenchyma. High PDGF and activated PDGF-R expression levels were detected in bone lesions of the mice injected by PC-3MM2 human prostate cancer cells into the tibias, while those increased proteins were not observed in lesions at the adjacent musculature. Endothelial cells within the bone lesions expressed phosphorylated PDGF-R when they were exposed to tumour cells which expressed PDGF (Uehara *et al.*, 2003).

In 1928, James Ewing proposed an opposing hypothesis to the seed and soil theory. The hypothesis states that the anatomical structure of the vascular system is important for the metastatic distribution patterns. In the circulatory network of the primary tumour, tumour emboli appeared in the circulation through intravasation are more likely to be mechanically trapped in the vascular network of the first connected organ (Ewing, 1928). Ewing's hypothesis, however, cannot explain the observation that certain organs which receive a considerable amount of blood supply, such as heart, kidney, spleen, skin, and muscle, are rarely found with metastatic colonisation. Meanwhile, other organs, such as bone, brain, and adrenals, are frequently seen as involvement in sites for metastasis in particular cancer types, even though they are served by a tiny fraction of the circulatory system (Ribatti *et al.*, 2006).

1.2.2 Lymphovascular invasion

1.2.2.1 Lymphovascular invasion in metastasis

Lymphovascular invasion (LVI), an early step in the invasion-metastasis cascade, plays a crucial role in metastases development by allowing disseminated tumour cells to spread to distant tissues or the new organ sites through two endothelial systems - the lymphatic and blood vascular system (Martin *et al.*, 2013), so-called lymphatic/lymphogenous, and haematogenous spreads respectively. Intravasations of disseminated tumour cells into lymphatics or blood vessels are termed as lymphatic invasion (LI) or blood vascular invasion (BVI), respectively. In addition, there is evidence showing that circulating tumour cells can also colonise their tumours of origin in a process called 'tumour self-seeding'. Self-seeding, for instance, of breast, colon, and melanoma tumours in murine models is preferentially mediated by aggressive circulating malignant cells, including those with brain, bone, or lung tropism. In a breast cancer model, self-seeding has been reported to accelerate tumour growth, stromal recruitment, and angiogenesis via seed-derived factors such as the chemokine CXCL1 (Kim *et al.*, 2009).

Lymphatic spread is frequently observed in carcinomas, while haematogenous spread is typical in sarcomas. All forms of cancer, however, may distribute via one or both systems, as several interconnections between the lymphatics and vascular systems exist. Principally, the pattern of lymph node metastasis is governed by the site of the primary tumour, and the local lymphatic drainage pathways. Breast carcinoma, for instance, usually develops in the upper outer quadrant and first disseminates to the axillary nodes, whereas medial breast lesions can spread via the chest wall to the nodes along the internal mammary (thoracic) artery (Kumar *et al.*, 2018).

The presence of LVI is associated with an increased risk of lymph node involvement, local recurrence, and distant metastasis (Lee *et al.*, 2006; Ejlertsen *et al.*, 2009). Lymph node involvement itself is an indicator for that cancer has already developed its ability to metastasise and is also associated

with poor prognosis, as discussed in section 1.2.3 (Nathanson *et al.*, 2009; Song *et al.*, 2011; Ryu *et al.*, 2018). Several tumour types are prone to metastasise to regional lymph node via tumour-associated lymphatics, such as breast cancer, squamous cell carcinoma, and melanoma (Ji, 2016). Expanded lymphatic vessels and lymphangiogenesis have been mainly observed in peritumoural areas of numerous human tumour types (Stacker *et al.*, 2002; Pepper *et al.*, 2003). In breast carcinoma, for instance, the presence of LVI is suggested to help for identifying the disease with high risk for lymph node, and distant metastasis (Davis *et al.*, 1985; Woo *et al.*, 2002; Nathanson *et al.*, 2009; Song *et al.*, 2011). The existence of LVI is significantly associated with increasing numbers of positive axillary lymph nodes ($P < 0.0001$, n = 1713) (Davis *et al.*, 1985); systemic metastasis is significantly associated with LVI but only when regional lymph node is positive ($P = 0.0013$, n = 1668) (Nathanson *et al.*, 2009).

1.2.2.2 Lymphatic vs blood vessel architectural features in lymphovascular invasion

The lymphatic system is a unique vasculature, different yet analogous to the blood vasculature. The blood vascular and the lymphatic systems play functionally harmonising roles in tissue perfusion, and fluid reabsorption (Hong *et al.*, 2004). The lymphatic capillaries transmit tissue fluid (lymph), containing extravasated plasma proteins and cells of the immune system, from extracellular spaces into the larger collecting vessels, the collecting trunks, and eventually to the central venous system, complementing the role of the blood vascular system in maintaining tissue homeostasis. This process is termed 'the blood-lymph circulatory loop' (Witte *et al.*, 2001; Witte *et al.*, 2006). In addition to providing a route for interstitial fluid return to the circulation, the lymphatic system plays an important role in lipogenesis, and a central role in the immunoregulatory network by directional guiding antigen-presenting cells, and lymphocytes to lymph nodes (Pepper *et al.*, 2003; Witte *et al.*, 2006). Lymphatics are also implicated in diverse developmental, growth, repair, and pathologic processes that are either similar to or distinct from such effects by the blood vasculature (Witte *et al.*, 2006). Regarding pathology, the lymphatic

system is found as one of the most important pathways for malignant cell metastasis (Pepper *et al.*, 2003).

Although lymphatic and blood vasculatures share numerous common properties, they also have individually distinct structural features characterised at the ultrastructural level. Lymphatic and blood capillaries are similar structurally, in that they are composed of endothelial cells with flat nuclei, a well-formed basal lamina, deep caveolae, isolated vesicles, intercellular junctions, and adhesion plates (Asioli *et al.*, 2008). Generally, the lymphatic capillaries structurally differ from the blood capillaries in that they have a more irregular, and broader blind-ended structure with incomplete basal lamina, and their endothelium is extremely attenuated. The basal lamina of blood capillaries is covered by pericytes, which are absent in lymphatics (Pepper & Skobe, 2003; Ji *et al.*, 2007). Lymphatic vessels are composed of a single thin layer of lymphatic endothelial cells (LECs) with overlapping intercellular junctions caused by the extensive superimposition of adjacent LECs (Pepper & Skobe, 2003). These vessels are directly bound to the surrounding ECM through an anchoring filament mainly containing fibrillin. Elevated interstitial fluid pressure increases the tension of the anchoring filaments attached to the LECs to pull open the overlapping cell junctions, allowing fluid, macromolecules, and disseminated cells flow into the vessel (Hong *et al.*, 2004; Oliver & Alitalo, 2005; Ohtani & Ohtani, 2012).

Tumour cells, in general, more easily penetrate lymphatics than blood vessels due to looser junctions between the ECs, and their discontinuous basement membrane (Oliver & Alitalo, 2005). The thin-walled initial lymphatic vessels provide less resistance, and more contact area for disseminated tumour cells to penetrate the lymphatic system compared to blood vessels, although a pre-existing blood vascular bed is possibly required to direct lymphangiogenesis (Ji *et al.*, 2007). The lymphatic system has many other pros over the blood circulation as a transport pathway for disseminated tumour cells. The size of the smallest lymphatic vessels are a lot larger than blood capillaries; and flow

velocities are orders of magnitude lower (Pepper *et al.*, 2003). In addition, tumour cells located free in the periductal lymphatic spaces are flushed rapidly, with the high interstitial pressure of tissue fluid (lymph), into the lymphatic labyrinth adjacent to the primary tumour through the sinuses and on into the lymphatic drainage channels (Hartveit, 1990). Lymph is closely identical to interstitial fluid, and that promotes the viability of disseminated tumour cells. Oppositely, in the bloodstream, disseminated tumour cells will confront various obstacles, i.e., serum toxicity, high shear stresses, and mechanical deformation, resulting in an extremely low accomplishment rate for metastasis (Liotta *et al.*, 1991; Weiss & Schmid-Schonbein, 1989; Pepper *et al.*, 2003; Chiang *et al.*, 2016). The lymphatic dissemination pathway, therefore, potentially promotes the survival of disseminated malignant cells, subsequently to improve their metastatic efficiency (Pepper *et al.*, 2003).

1.2.2.3 Molecular mechanisms regulated lymphovascular invasion

LVI is regulated by molecular mechanisms as well as multiple interactions between a variety of molecules and cell types. Once the carcinoma cells have migrated to a location of intravasation, they interact with the surface of the endothelial cells through complex biochemical interactions mediated by proteins, lipids, and carbohydrates. For example, interactions between a complex of glycosphingolipids and α2β1 integrin receptors result in developing adhesion of cancer cells to ECs (Van Slambrouck *et al.*, 2014; Marciel & Hoffmann, 2017). The adhering cells will then penetrate through the basement membrane, and endothelium into the lumina of lymphatic or blood vessels before extravasating the vessels to form metastatic foci at the new sites (Martin *et al.*, 2013). Thus, cell-cell adhesion plays a crucial role to facilitate the attachment of tumour cells to ECs. Calpains and calpastatin, a focus of the current study, have also been implicated in cell adhesion and LVI, as discussed in section 1.3.5.2 and 1.3.5.3. Tumour cells are able to invade into the lymphatic or blood vessels by degrading the vascular ECM and basement membrane through activation of the proteolytic urokinase-type plasminogen activator system (uPA/uPAR), and secretion of proteases such as matrix

metalloproteinases (MMP)-1, −2, and −9 (reviewed in Pachmayr *et al.*, 2017; Chiang *et al.*, 2016). Also, intravasation is stimulated by increasing neoangiogenesis, which is activated by various pathways, including PI3K/Akt, STAT3, and RAS (Samame Perez-Vargas *et al.*, 2013).

Expression of the uPA receptor (uPAR) could be increased by Src through increased activity of activator protein 1 (AP1) in SW480 colon cancer cells. Src expression has been found to promote invasion and intravasation, and the increased invasion depends upon the expression of uPAR. Suppression of uPAR expression was an action of the tumour suppressor PDCD4 (programmed cell death 4), overexpression of which in HEp3 human epidermoid-carcinoma cells has been found to prevent intravasation (Leupold *et al.*, 2007). In RKO colon cancer cells, miR-21 suppressed PDCD4; thus, inhibition of miR-21 resulted in a decrease of intravasation (Asangani *et al.*, 2008). In relevance to the plasminogen activation (PA) system, cleaved CDCP1 (a product of proteolysis activity of plasmin) could form a complex with β_1-integrins, leading to activation of focal adhesion kinase (FAK) and phosphoinositide 3-kinase (PI3K). Inhibition of FAK or PI3K has been observed to decrease intravasation (Casar *et al.*, 2014). In TNBC MDA-MB-231 cell line, direct tumour-promoting interactions of uPAR with uPA or the insulin-like growth factor receptor 1 (IGF1R) were demonstrated, and they could be significantly decreased once uPAR was downregulated. The paired knockdown of uPAR and uPA or IGF1R additively and significantly inhibited cell viability, migration, and invasion of the cell model. In a cohort of patients with TNBC, the complexes formed by uPAR with uPA or with IGF1R significantly correlated with the histological grade as well as with cathepsin B and D, which have been found to be implicated in cell invasion and metastasis (Huber *et al.*, 2016).

The MMP family is also implicated in intravasation (Deryugina & Quigley, 2015). Expression of MMP-1 in HEp3 human epidermoid-carcinoma cells has been found to activate the endothelial protease-activated receptor 1 (PAR1) to facilitate vascular permeability and intravasation (Juncker-Jensen *et al.*, 2013).

By being a source of MMP-9, neutrophils assisted tumour angiogenesis and intravasation. Neutrophil MMP-9 mediated the development of the intravasation-sustaining vasculature through its ability to proteolytic remodel the tumour matrix, resulting in the linked release of angiogenesis factors - vascular endothelial growth factor (VEGF) and basic fibroblast growth factor (bFGF). The released and functionally induced VEGF and bFGF directly regulated the microarchitecture and functions of the intratumoural vasculature, including its capability to sustain tumour cell intravasation, and metastatic dissemination. Epidermal growth factor receptor (EGFR)-mediated regulation of tumour cell intravasation through MMP-9/VEGF pathway has been shown in several cancer cell types, including breast, lung, head and neck squamous carcinomas and glioblastomas - expression and activity of MMP-9 were enhanced by activation of the pathways downstream of EGFR. Conjointly, EGFR inhibitors could suppress MMP-9 expression and indirectly diminish tumour growth via suppressing VEGF production (Deryugina & Quigley, 2015). Downregulation of VEGF production in tumour xenografts treated with an anti-EGFR agent was associated with normalisation of morphology and permeability of tumour-associated vessels (Cerniglia *et al.*, 2009). MMP-2 was also able to activate VEGF expression in A549 lung cancer cells via alphaVbeta3 integrin-mediated PI3K/AKT signalling; recombinant human-MMP-2 restored angiogenesis in MMP-2 downregulated cells (Chetty *et al.*, 2010). PI3K/AKT signalling, as mentioned above, involved with neoangiogenesis, increase of which promoted intravasation (Pachmayr *et al.*, 2017). Paradoxically, suppression of MMP-1, -2, or -9 *in vivo* was shown to increase the intravasation of human fibrosarcoma cells (Deryugina & Quigley, 2015; Chiang *et al.*, 2016).

Murine models of metastatic breast cancer usually feature mutated oncoproteins that activate PI3K, Stat3, and Ras signalling. These three oncogenes were activated together and demonstrated cooperation during primary tumour formation; however, the efficient spread of cancer was only dependent on Ras (Wright *et al.*, 2015). Activation of Ras, which is able to activate cellular invasion, motility, epithelial-mesenchymal transition (EMT),

cell survival, and angiogenesis (Campbell & Der, 2004; Smakman *et al.*, 2005; Pylayeva-Gupta *et al.*, 2011), has been proposed as a key determinant for clinical metastasis and adverse prognosis of ERα^{+}/luminal breast cancer (Wright *et al.*, 2015). In addition to enhancing cell invasion, STAT3 activation has a major role in protecting the tumour cells from immune surveillance through modulating secretion of various inflammatory factors, such as IL6 and TNFα, which function as an immunosuppressor and elevate the survival possibility of tumour cells during their transit through circulation (Nguyen *et al.*, 2009).

1.2.3 Metastasis and lymphovascular invasion in breast cancer

1.2.3.1 Metastasis in breast cancer

Approximately 4-6% of women have advanced or metastatic breast cancer at diagnosis (Cardoso *et al.*, 2012; Sogaard *et al.*, 2008; Louwman *et al.*, 2008), and approximately 30% of women with early disease will develop distant cancer dissemination (O'Shaughnessy, 2005). Ten to fifteen per cent of patients with aggressive breast cancer develop distant metastasis within three years after diagnosis (Weigelt *et al.*, 2005). Approximately one-fifth of patients with metastatic cancer at diagnosis will survive five years (Cardoso *et al.*, 2012); the mean survival of the patients is 18-24 months (Gennari *et al.*, 2005; Martino *et al.*, 2013). Most metastatic breast cancer cases, therefore, are incurable, and palliation is the principal goal of treatment, intending to maintain or improve quality of life, and probably improving survival (Cardoso *et al.*, 2012).

Different tumour types have different preferential sites of metastasis, although most cancers are able to disseminate to various parts of the body. Breast cancers mainly spread to bone (38%), lungs (30%), liver (23%), and brain (5%) (Dillekas *et al.*, 2014; Shord & Cordes, 2017). More than 50% of women who have metastases at primary diagnosis will develop bone metastases (Coleman & Rubens, 1987; Jensen *et al.*, 2011), and 13.6% of patients with stage I-III cancer will develop bone metastasis at 15 years of follow-up (Liede *et al.*, 2016). Kennecke *et al.*, 2010 investigated the incidence of metastases within a 15-year follow-up period in 3,726 patients diagnosed early stage of breast cancer and

found that bone will be the predominant site of metastasis for the luminal A (66.6%), luminal B (71.4%), and luminal/HER2 (65%) groups but is the least common site in the basal subtype (39%). Patients with HER2-positive breast cancer have a higher possibility of brain metastases compared with HER2-negative cases (Kennecke *et al.*, 2010; Musolino *et al.*, 2011; Pestalozzi *et al.*, 2006). The highest incidence of brain metastases, 22.2%, is found in patients diagnosed with HER2-enriched subtype followed by triple-negative basal-like (10.9%), triple-negative nonbasal (7.2%), luminal B (4.7%) and luminal A subtypes (2.2%) (Kennecke *et al.*, 2010). In the brain metastatic breast cancer cell line (231-BR), overexpression of HER2 resulted in stimulating the outgrowth of the cells in the brain (Palmieri *et al.*, 2007). The clinical manifestation of metastatic breast cancer, however, depends on the site of metastases but can include symptoms of bone pain, difficulty breathing, swollen abdomen, jaundice, and altered mental status (Michaud *et al.*, 2011).

1.2.3.2 Lymphovascular invasion in breast cancer

1.2.3.2.1 Incidence and prognosis of lymphovascular invasion

LVI has traditionally been related to poor prognostic breast cancer. However, it is ambiguous, using haematoxylin and eosin (H&E) staining method, whether patients who have the occurrence of LVI should be reconsidered to reclassify from a low risk of recurrence category into a high-risk group (Ejlertsen *et al.*, 2009). Due to false positive and negative results yielded by H&E staining, to improve the detection of LVI, the guidelines of the Danish Breast Cancer Cooperative Group (DBCG) has recommended supplementary use of specific endothelial cell markers, i.e., podoplanin (immunostained by D2-40) for lymphatic endothelium, and CD31 or CD34 for endothelium of all vessels (Ejlertsen *et al.*, 2009). As reported by a systematic review of data published between 1964 and 2012, the rates of LVI and LI using H&E were variable (9-50% and 10-49%, respectively) and less variable using immunostaining (D2-40 for LECs and CD31, CD 34, or Factor VIII for ECs) (32-41% and 21-42%, respectively). However, the BVI rates detected by H&E and/or classical staining approach (4-

46%) and immunostaining (1-29%) were both variable (Gujam *et al.*, 2014a). Due to the evidence showing extremely high sensitivity (97.3%), specificity (98.8%), and accuracy (88.9%) of using D2-40 as a method in detecting LI (Evangelou *et al.*, 2005) as opposed to H&E stain, which could not distinguish LI from BVI, several studies have proposed that relying on D2-40 to detect LI was a much responsible approach in predicting outcomes in patients with breast cancer (He *et al.*, 2017). In comparison, BVI was rarely specifically examined (Gujam *et al.*, 2014a).

By using the specific markers (D2-40, CD31 and CD 34), the current group assessed the incidence of LVI in two cohorts of patients with early invasive lymph node (LN)-negative breast cancer (n = 177 and 1005) and consistently found that although there was a very high microvascular density, in comparison to lymphatic vessel density, LI accounted for 96% of all LVI cases and only 4% for BVI (Mohammed *et al.*, 2007; Mohammed *et al.*, 2011). LI was predominantly detected in the peritumoural areas in breast cancer (76-80%) (Van den Eynden *et al.*, 2006; Mohammed *et al.*, 2011), while intratumoural LI was present in a lesser proportion of cases (24-40%) (Van den Eynden *et al.*, 2006; Mohammed *et al.*, 2007; Mohammed *et al.*, 2011).

The presence of LVI or LI, in particular, has been suggested to help to identify who is at increased risk for axillary LN metastasis (Davis *et al.*, 1985; Lauria *et al.*, 1995; Woo *et al.*, 2002), local recurrence (Pinder *et al.*, 1994; Veronesi *et al.*, 1995; Sundquist *et al.*, 2000; Voogd *et al.*, 2001) or distant metastasis (Veronesi *et al.*, 1995; de Mascarel *et al.*, 1998; Voogd *et al.*, 2001; Lee *et al.*, 2006; Ejlertsen *et al.*, 2009). Both LVI or LI are considered as a poor prognostic factor in patients with operable breast cancer either with (Davis *et al.*, 1985; Song *et al.*, 2011) or without axillary LN involvement who are undergoing adjuvant treatment (Nime *et al.*, 1977; Pinder *et al.*, 1994; Lauria *et al.*, 1995; de Mascarel *et al.*, 1998; Woo *et al.*, 2002; Lee *et al.*, 2006; Mohammed *et al.*, 2011; He *et al.*, 2017). Peritumoural LI, in particular, could be a feature to identify patients with intermediate-risk for recurrence and death from the

disease (Harbeck & Jakesz, 2007). Although BVI has been reported as a minority of LVI, it also showed a correlation with axillary LN involvement, increases of tumour size and grade as well as associations with tumour recurrence (Gujam *et al.*, 2014b) and poor survival (Weigand *et al.*, 1982; Lauria *et al.*, 1995; Gujam *et al.*, 2014b). However, the systemic review mentioned that the role of BVI in predicting breast cancer survival is not clear (Gujam *et al.*, 2014a).

As mentioned, LVI is a negative prognostic factor in breast carcinomas either with or without LN involvement. For instance, fifty-five percents of 349 LN-positive patients with primary invasive breast cancer were detected LVI existence, confirmed by the specific markers when interpretation results by H&E staining were vague (Song *et al.*, 2011). LVI was significantly associated with tumour size ≥2 cm ($P < 0.001$), high histological grade ($P = 0.007$), number of involved LN ($P < 0.001$), ER status ($P = 0.001$), and age ≤40 years ($P = 0.009$). LVI was also a significant independent prognostic factor for disease-free survival (DFS) and overall survival (OS) in LVI-present patients ($P < 0.001$ and $P = 0.006$). For the whole patient cohort, LVI remained an independent prognostic factor for DFS (RR = 2.59; $P = 0.005$) (Song *et al.*, 2011). In a larger study of LN-negative patients, LVI identified in 19% of 2760 tumours was associated with increasing tumour size ($P < 0.0001$), higher histological grade ($P < 0.0001$), younger age ($P < 0.0001$) as well as less favourable NPI group ($P < 0.0001$) (Lee *et al.*, 2006). LVI was an independent prognostic factor in LN-negative operable invasive breast carcinoma for OS in either a group of patients with no adjuvant therapy (RR = 1.64, $P <0.0001$) or a group of selective adjuvant therapy (RR = 1.66, $P = 0.004$) (Lee *et al.*, 2006). The LN-negative patients, however, traditionally fall into the good NPI group, but approximately 20% of these women will, unfortunately, die of breast cancer when followed up for 20+ years. LVI, therefore, can potentially be an early predictor of metastatic dissemination. It has been included in the establishment of the NPI+ index, which aims to provide improved and highly significant patient outcome stratification compared with the traditional NPI (Rakha *et al.*, 2014).

As a majority of LVI, LI is also considered as a negative prognostic factor in breast carcinomas either with or without LN involvement (Mohammed *et al.*, 2014; Mohammed *et al.*, 2011). By using D2-40, the presence of LI (211 of 218 LVI-positive cases) investigated in LN-negative breast cancer (n = 1005) by the current group was significantly associated with 20-year OS and 20-year disease-free interval (DFI) ($P < 0.0001$ and < 0.0001). The presence of even only a single LI was also associated with poorer OS and DFI compared to LI-negative patients ($OS_{LI\text{-}positive}$ = 66%, $OS_{LI\text{-}negative}$ = 85%, $P < 0.001$; $DFI_{LI\text{-}positive}$ = 62%, $DFI_{LI\text{-}negative}$ = 78%, $P < 0.001$) (Mohammed *et al.*, 2011). The subsequent study by the current group in LN-positive breast carcinoma (n = 557) also found that the presence of LI (n = 262, 47%) was a poor prognostic factor for the 20-year OS, DFI, and development of distant metastasis in the whole LN-positive cases. Lower OS rate and DFI rate were present in the group of LI-positive ($OS_{LI\text{-}positive}$ = 54%, $OS_{LI\text{-}negative}$ = 72%, $P < 0.0001$; $DFI_{LI\text{-}positive}$ = 43%, $DFI_{LI\text{-}negative}$ = 61%, $P < 0.0001$). Fifty-one per cent of tumours that developed distant metastasis showed positive LI compared with 36% of cases that do not metastasise ($P < 0.0001$). The most common site of metastasis observed in either LI-present or LI-absent breast cancer cases was bone (16% vs 14%) (Mohammed *et al.*, 2014)

Breast tumours with higher lymph vessel density (LVD) were reported to be associated with the presence of LI ($P < 0.001$), LN metastasis ($P < 0.001$), advanced tumour stage ($P < 0.001$), poor NPI ($P = 0.009$) as well as shorter OS ($P = 0.015$), and DFI ($P = 0.01$) (Mohammed *et al.*, 2009a). In other cancers, high LVD was also associated with adverse clinicopathological variations and outcomes, including in gastric (Gao *et al.*, 2009), colorectal (Chen *et al.*, 2009), and lung carcinomas (Sun *et al.*, 2009). Anti-lymphangiogenic treatment, therefore, is currently developing as a promising strategy for prophylaxis or treatment of metastasis and lymphatic disorders. Amongst a series of anti-angiogenic agents approved by the Food and Drug Administration in the last decade, the most common is bevacizumab, initially accepted as a therapeutic substance in colorectal cancer associated with hepatic metastases. To date,

several anti-angiogenic substances have been characterised, but very few anti-lymphangiogenic agents have been taken into account (Raica *et al.*, 2016).

1.2.3.2.2 Preference of lymphatic invasion in breast cancer and associated factors

Evidence to explain the preference of LI in breast cancer remains sparse. The anatomical and physiological properties of lymphatic vessels, which promote LI over BVI, have been hypothesised and described in section 1.2.2.2. Also, a more active process inducing tumour cells to interact with LECs and enter the lumen of lymphatic capillaries has been suggested. This process involves complex interactions of the three main components - tumour cells, stromal cells and the LECs (Mohammed *et al.*, 2009b). The cellular cross-talk involves a large number of molecules, including macrophage and associated cytokines, chemokine gradients, and the calpain-calpastatin system as discussed below.

Macrophage and associated cytokines

In regulating the process of LVI and metastasis, with data from the current group, macrophage and associated cytokines, such as tumour necrosis factor-α (TNF-α) and Interleukins (IL), may be involved. Safuan *et al.* (2012) demonstrated that breast cancer cells (MDA-MB-231 and MCF7) had higher endogenous *in vitro* adhesive ability to blood endothelial cells (BECs, i.e., HUVEC and hMEC-1) compared to lymphatic endothelial cells (LECs, i.e., hTERT-LEC and HMVEC dLy Neo) ($P < 0.001$). However, while TNF-α treatment of ECs or breast cancer cells alone did not contribute a significant change of tumour–endothelial cell adhesion, double stimulation of both endothelial and tumour cells with TNF-α preferentially caused a significantly-increased LEC interaction ($P < 0.001$) than the adhesion to BECs ($P < 0.01$) (Safuan *et al.*, 2012).

IL-1β also seemed to be an important factor that might play a role in regulating lymphatic invasion and breast cancer metastasis (Safuan, 2012). Upon stimulation with IL-1β, significant increases in cell migration and the number of MDA-MB-231 cells that transmigrated across hMEC-1 and hTERT-LEC were observed with comparable affinity to both ECs, suggesting that IL-1β might be

implicated in the regulation of tumour cell transmigration across and adhesion to ECs as well as LVI. Paradoxically, high cytoplasmic IL-1β expression (combined expression of mature and immature forms) detected by immunohistochemistry (IHC) in breast tumours was significantly associated with the absence of LI (Safuan, 2012). A study by Song *et al.* (2003), however, indicated that the secreted form of mature IL-1β in the extracellular compartment but not the mature cytosolic IL-1β was able to increase tumour growth, invasion, and metastasis. While IL-6 and IL-10 did not affect adhesion patterns of MDA-MB-231 and MCF-7 cells to both hMEC-1 and hTERT-LEC cells, only IL-10 significantly inhibited MDA-MB-231 migration in a dose-dependent manner ($P = 0.03$) (Ahmad *et al.*, 2018). In a cohort of 1380 patients with early-stage invasive disease, high expression of both IL-6 and IL-10 was associated with improved DFI ($P < 0.05$), and only IL-6 was associated with breast cancer-specific survival ($P = 0.017$) (Ahmad *et al.*, 2018). The study of patients diagnosed with cutaneous melanoma (n = 202) revealed that a high macrophage count could be associated with promoting neovascularisation ($P = 0.003$), primary tumour growth (mitotic rate; $P = 0.005$), and the existence of LI ($P = 0.002$) (Storr *et al.*, 2012b).

Chemokines

Chemokines have been recognised as a key player in a role that providing directional signals for cancer cell invasion and metastasis (Zlotnik, 2008; Talmadge & Fidler, 2010). Chemokine receptor CXCR4 was found to play a potential role in targeting lymph nodes, bone marrow, and pulmonary tissue, as the selective sites for the dissemination of breast cancer, as they expressed the ligand CXCL12 (Huang *et al.*, 2009). CCL21/CCR7 axis was also involved in lymph node metastasis; CCR7 expression positively correlated with lymph node metastasis of triple-negative breast cancer ($P = 0.0096$, n = 181) (Li *et al.*, 2017b). The expression of CCL21/CCR7 by breast cancer showed the ability to promote tumour-induced lymph-vascular recruitment *in vivo* and regulate the expression and secretion of lymphangiogenic factor VEGF-C, leading to the promotion of proliferation, migration, and tube formation of the primary

human LECs *in vitro* (Tutunea-Fatan *et al.*, 2015). In oesophageal squamous cell carcinoma (ESCC), enhanced adhesive ability of CCR7-expressing ESCC cell line was observed in response to CCL21/secondary lymphoid-tissue chemokine (SLC), in particular, in the presence of HMVEC-LLy LECs ($P = 0.005$).

Calpastatin

Calpastatin, the focus of the current study, has been first discovered by the current group in the extent that involving with breast cancer LI. A cohort of 177 patients with breast cancer showed that downregulation of calpastatin protein ($P < 0.025$, n = 53) and exon3-containing variant (CASTexon3) ($P < 0.014$, n = 56) was significantly associated with a presence of LI (Storr *et al.*, 2011b). The implication of calpastatin in LVI has been confirmed in a subsequence larger cohort of early-stage invasive breast cancer. This study demonstrated a significant association between high calpastatin expression and the absence of intra-tumoural LI ($P = 0.014$, n = 1266) (Storr *et al.*, 2012a). These two studies suggest that resultant altered calpain activity via differed expression of calpastatin may be involved in regulating LI in breast cancer. The associations between calpastatin level and other clinicopathological variations will be described in section 1.3.5.3.4.

1.3 Calpains and calpastatin

Calpastatin is the specific endogenous inhibitory protein of calpain (Carragher & Frame, 2002). μ-Calpain and m-calpain, also known as conventional calpains, are ubiquitously expressed and are the most intensely studied calpains among fifteen members of the family (reviewed in Leloup & Wells, 2011; Storr *et al.*, 2011a). Both calpains are recognised as important regulators of various physiological pathways, such as cell proliferation, survival, apoptosis, adhesion, and migration (Fei *et al.*, 2013). An imbalance between the level of calpain and calpastatin is postulated to be an important factor causing dysregulation of calpain activity and subsequently leading to a wide range of diseases and pathologies (Potz *et al.*, 2016), including, for example, muscular dystrophies (Tidball & Spencer, 2000), degenerative nerve diseases (Tsuji *et al.*, 1998; Elkind

et al., 2011), Alzheimer's disease (Higuchi *et al.*, 2012), degenerative vascular disorders (Miyazaki & Miyazaki, 2018), diabetes (Gurlo *et al.*, 2016), cataract formation (Carragher, 2006), myocardial infarction (Sandmann *et al.*, 2001), and cancer. Dysregulation of calpain activity is related to tumour invasion (Mamoune *et al.*, 2003), metastasis (Storr *et al.*, 2011a), and response to anticancer therapies (Kulkarni *et al.*, 2010; Kulkarni *et al.*, 2012; Liu *et al.*, 2006; Mlynarczuk-Bialy *et al.*, 2006). Calpastatin expression, as mentioned in 1.2.3.2.2, is also associated with cancer progression, in particular of the presence of LI (Storr *et al.*, 2011b; Storr *et al.*, 2012a).

1.3.1 Calpain family

Calpains are a conserved family of intracellular Ca^{2+}-dependent cysteine proteases (EC 3.4.22.17 Clan CA, family C02). They mediate the activities of a large number of specific substrates by partial cleavage that is somewhat similar to post-translational modification rather than performing digestion or degradation. Thus, calpain is considered as a modulator/regulatory protease rather than a digestive/degradative enzyme (Sorimachi *et al.*, 2011b). Typical cellular digestive proteases are usually independent of calcium and are active to degrade their substrates completely in acidic compartments. In comparison, the regulatory proteases of the calpain family are entirely inactive in the absence of Ca^{2+} as well as at resting cytoplasmic Ca^{2+} levels but activated at neutral pH in the presence of Ca^{2+}. The calpain-mediated proteolysis modifies the structure and/or function of their target substrate proteins by partial truncation at one or a few sites (Baudry *et al.*, 2013; Sorimachi *et al.*, 2011b). This subsequently impacts various physiological phenomena, including cell signal transduction, morphogenesis, proliferation, migration, apoptosis and death (Sorimachi *et al.*, 2010; Sorimachi *et al.*, 2011a; Leloup & Wells, 2011; Baudry *et al.*, 2013). The ubiquitous μ- and m-calpains are the most well-characterised members in modulating these physiological pathways. In regulating the cellular biological activities, only one or two calpain molecules are required to act on its substrate, whereas the proteasomal and lysosomal proteases function in a co-ordinated step-wise pathway together with proteins

mediating ubiquitination and intracellular compartmentalisation (e.g. autophagosomes and endosomes) (Sorimachi *et al.*, 2011b).

Based upon the primary sequence characteristics of the calpain-like cysteine protease sequence motif defined in the conserved domain (the CysPc domain), calpain homologs have been identified in a wide range of living organisms (Croall & DeMartino, 1991; Sorimachi *et al.*, 2011b; Ono & Sorimachi, 2012). They are observed in almost all eukaryotes and a few bacteria, but not in archaebacterial (Sorimachi *et al.*, 2011a). In human, calpains are expressed in a wide range of cells and tissues (Goll *et al.*, 2003). Thus far, fifteen human calpain genes (CAPNn, n = 1-3, and 5-16) encoding fifteen calpains and two genes for small regulatory subunits (CAPNS1 and CAPNS2; 30 kDa) have been identified (Sorimachi *et al.*, 2011a). Calpastatin, the specific endogenous calpain inhibitor, is sometimes also considered as a member of the calpain family. Calpains are classified based on the presence/absence of the EF-hands of protein domain structure into classical/typical EF domain calpains (i.e. conventional and unconventional EF-calpain subunits) and non-classical/atypical non-EF domain calpains (Storr *et al.*, 2011a). Classical calpains are comprised of four domains I-IV (DI-DIV), while non-classical calpains have certain domains of the classical calpains deleted or replaced (Suzuki *et al.*, 2004) (Figure 1.2). The members of the calpain family are listed in Table 1.4.

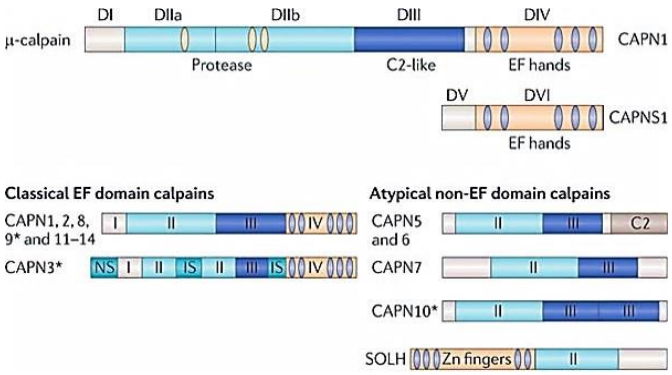


Figure 1.2 Schematic structure of μ-calpain heterodimer and calpain family members. Reproduced from Storr *et al.*, 2011a. Copyright© 2011 by Nature Publishing Group with permission conveyed through Copyright Clearance Center, Inc.

The classical calpains (80K) are comprised of four domains (DI-DIV) with the presence of penta EF-hands (PEF). This class consists of calpain-1, -2, -3, -8, -9,

-11, -12, -13, and -14 (Ono & Sorimachi, 2012). Calpain-1 and calpain-2 are the 80-kDa calpain large catalytic subunits that separately interact with a smaller 30-kDa regulatory subunit (CAPNS1 or calpain-4; domain V-VI) to form functional heterodimeric calpains called micro (μ)-calpain and milli (m)-calpain, respectively (Kawasaki *et al.*, 1986; Leloup & Wells, 2011). μ-Calpain and m-calpain are known as the 'conventional calpains'. Both are ubiquitously expressed, and, as mentioned, they are the most intensely studied and well-characterised among all members of the calpain family. Their names are designated based upon the levels of Ca^{2+} requirement for their activity *in vitro*. μ-Calpain and m-calpain can be activated at neutral pH by the micromolar range (3-50 μM) and the millimolar range (0.4-0.8 mM) of Ca^{2+}, respectively, for *in vitro* half-maximal activation (Cong *et al.*, 1989; Kapprell & Goll, 1989; Baudry *et al.*, 2013). The unconventional EF domain calpains (calpains-3, -8, -9, -11, -12, -13, and -14) are composed of four domains, which are originally found in the large catalytic subunit of the conventional calpains (Suzuki *et al.*, 2004).

Table 1.4 The calpain family

Protein	Gene	Other names	Class	Expression
Calpain-1	CAPN1	μ-calpain large subunit, CAPN1[μCL]	Classical	Ubiquitous
Calpain-2	CAPN2	m-calpain large subunit, CAPN2[mCL]	Classical	Ubiquitous, except erythrocytes
Calpain-3	CAPN3	p94, nCL-1, CAPN3[p94]	Classical	Skeletal muscle, lens, retina
Calpain-5	CAPN5	hTRA-3, nCL-3, CAPN5[hTRA-3]	Non-classical	Ubiquitous
Calpain-6	CAPN6	CAPNX, CAPN6[CANPX]	Non-classical	Embryonic muscles, placenta
Calpain-7	CAPN7	PalBH, CAPN7[PalBH]	Non-classical	Ubiquitous
Calpain-8	CAPN8	nCL-2, CAPN8[nCL-2]	Classical	GI tract
Calpain-9	CAPN9	nCL-4, CAPN9[nCL-4]	Classical	GI tract
Calpain-10	CAPN10	CAPN10	Non-classical	Ubiquitous
Calpain-11	CAPN11	CAPN11c	Classical	Testis
Calpain-12	CAPN12	CAPN12	Classical	Hair follicle
Calpain-13	CAPN13	CAPN13	Classical	Ubiquitous
Calpain-14	CAPN14	CAPN14	Classical	Ubiquitous
Calpain-15	CAPN15	SOLH, CAPN15[SOLH]	Non-classical	Ubiquitous
Calpain-16	CAPN16	CAPN16[demi-calpain, C6orf103]	Non-classical	Ubiquitous
CAPNS1	CAPNS1	calpain small subunit (CSS)1, calpain-4, calpain S1, 30K, CAPNS1		Ubiquitous
CAPNS2	CAPNS2	CSS2, calpain S2, CAPN14, CAPNS2		Lens

Data summarised from Suzuki *et al.*, 2004; Saez *et al.*, 2006; Leloup & Wells, 2011; Sorimachi *et al.*, 2011a; Sorimachi *et al.*, 2011b; Ono & Sorimachi, 2012.

In addition to calpain-1 and -2, calpain-9 also forms heterodimers with small subunits (30K) but calpains-3 and -13 form homodimers (Ravulapalli *et al.*, 2009). CAPN8/9[G-calpain] is the first hybrid heterodimer of two distinct calpain catalytic subunits (calpain-8 and -9) observed *in vivo*; heterodimer formation is crucial to stabilise the CAPN8/9[G-calpain] existence (Hata *et al.*, 2010; Sorimachi & Ono, 2012). Others do not apparently interact with 30K, although they have a similar calmodulin-like domain associating to domain IV, which is critical for heterodimerisation with 30K subunit (Suzuki *et al.*, 2004).

DI is the N-terminal anchor helix region of the large subunit. It is autolysed when calpains are activated by Ca^{2+}, but this does not seem to be a requirement as a prior condition for the activation (Nakagawa *et al.*, 2001; Storr *et al.*, 2011a). The autolysis, however, contributes to a lower requirement for Ca^{2+} (Suzuki *et al.*, 1981; Imajoh *et al.*, 1986b), a substrate specificity change (Nakagawa *et al.*, 2001), and the dissociation of heterodimeric calpains into subunits driven by factors such as crystal formation or autolysis of active enzymes (Zhang & Mellgren, 1996; Pal *et al.*, 2001; Nakagawa *et al.*, 2001; Sorimachi *et al.*, 2010).

The conserved protease (CysPc) domain II, also known as a catalytic domain, is a common structural and functional element for the calpain family. In the absence of Ca^{2+}, the inactive DII is divided into two protease core subdomains (PC1 and PC2 or DIIa and DIIb), which, upon Ca^{2+} binding onto each core domain, fold into a single functional CysPc domain that contains an active cysteine catalytic cleft (Strobl *et al.*, 2000; Moldoveanu *et al.*, 2004) to interact with substrates or calpastatin (Hanna *et al.*, 2008).

DIII contains a C2 domain-like (C2L) domain, which binds Ca^{2+} and phospholipids (Tompa *et al.*, 2001). This domain is a highly conserved region in the calpain family, and it is involved in calcium-mediated conformational changes that are required for calpain activity and inhibition of calpain by calpastatin (described in section 1.3.4) (Hanna *et al.*, 2008; Moldoveanu *et al.*,

2008). It may play a crucial role in the Ca^{2+}-dependent membrane translocation of calpains (Kawasaki & Kawashima, 1996; Tompa *et al.*, 2001).

The carboxy-terminal DIV is a calmodulin-like Ca^{2+}-binding domain. It is highly homologous to the carboxy-terminal DVI of the regulatory subunit (30K CAPNS1). DIV and DVI both contain five EF-hand motifs (PEF-hand), which is involved in Ca^{2+} binding except the fifth EF-hand (Minami *et al.*, 1987; Hosfield *et al.*, 1999). The fifth EF-hands of the small subunit and the large subunit interact to each other, resulting in the heterodimer formation (Imajoh *et al.*, 1987; Blanchard *et al.*, 1997; Suzuki *et al.*, 2004). In the presence of Ca^{2+}, the structural changes in DIV are not noticeable (Saez *et al.*, 2006).

DV is the N-terminus of the regulatory subunit (30K CAPNS1) which contains a glycine-rich region, so-called a glycine-rich hydrophobic (GR) domain (Baudry *et al.*, 2013). This domain possibly facilitates interaction with the plasma membrane and/or membrane proteins through hydrophobic interactions. The majority of this domain is autolysed during calpain activation, indicating that this region does not engage in protease activity (Imajoh *et al.*, 1986a; Sorimachi *et al.*, 2010). In humans, the physiological roles of a regulatory subunit homologue encoded by the *CAPNS2* remain unclear (Schad *et al.*, 2002).

The non-classical calpains (atypical non-EF domain calpains) is composed of the molecules that lack PEF-hand motifs with/without C2L domain. PEF and C2L are normally present in DIV and DIII of the classical calpains, respectively (Sorimachi *et al.*, 1993; Ono & Sorimachi, 2012). Regarding the missing of domain IV, non-classical calpains cannot form a dimer with 30K (Suzuki *et al.*, 2004). Calpain-5, -6, -7, -10, -15, and -16 are categorised into this class.

In addition to the structure-oriented classification, calpain can be classified based upon their localisation - ubiquitous or tissue-specific. Six out of fifteen calpains are regarded as tissue-specific calpains expressed mainly in a particular tissue, i.e., calpain-3 (skeletal muscle), -6 (embryonic muscle and placenta), -8 and -9 (gastrointestinal (GI) tracts), -11 (testis), and -12 (hair follicles). The other

calpains are ubiquitously expressed (Suzuki *et al.*, 2004; Sorimachi *et al.*, 2011a; Storr *et al.*, 2011a; Ono & Sorimachi, 2012), as summarised in Table 1.4.

1.3.2 Calpastatin

Calpastatin was first proposed, in 1979, as the name for the protein inhibitor of calpains by Takashi Murachi (Murachi, 1989). Calpastatin, as shown in Figure 1.3, comprises of five domains - a region of 150-230 amino acid residues on its N-terminal Leader domain (XL and L domains) followed by four mutually homologous C-terminal regions of approximately 140 amino acid residues (inhibitory domains I-IV).

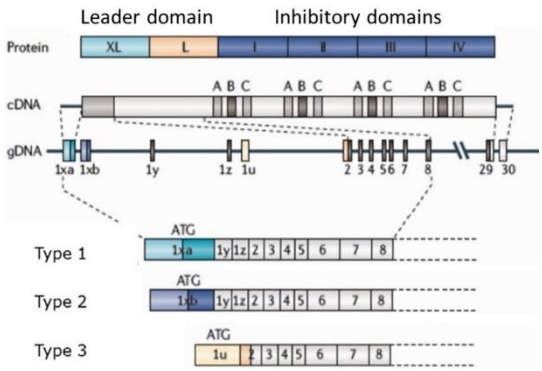


Figure 1.3 Schematic structure of calpastatin protein, cDNA and gDNA. Reproduced from Storr *et al.*, 2011a, Nature Reviews Cancer, 11, 364-374; Copyright© 2011 by Nature Publishing Group with permission conveyed through Copyright Clearance Center, Inc.

Calpastatin is regarded as a unique inhibitor as the amino acid sequence of the inhibitory domains have no homology with any other polypeptides (Emori *et al.*, 1988; Kawasaki *et al.*, 1989). Each inhibitory domain is capable of reversibly binding to, and inhibiting one calpain molecule in the presence of Ca^{2+}, i.e., a single calpastatin molecule is capable of simultaneously binding up to four heterodimer calpain molecules. The four domains differ in their ability to inhibit calpains in the order of domain I ≥ domain IV ≥ domain II ≥ domain III (Kawasaki *et al.*, 1989; Wendt *et al.*, 2004; Hanna *et al.*, 2007). Calpastatin has more efficiency in inhibiting m-calpain than it does μ-calpain, with the IC50 for m-calpain being 2- to 10-fold lower than the IC50 for μ-calpain (Maki *et al.*, 1987a; Maki *et al.*, 1987b; Maki *et al.*, 1988; Emori *et al.*, 1988; Wendt *et al.*, 2004).

Amongst the four repetitive inhibitory domains, conserved residues are not evenly distributed but are clustered in restricted regions termed subdomains A, B, and C (Asada *et al.*, 1989; Maki *et al.*, 1989; Takano *et al.*, 1988) encoded by separate exons in the human gene (Lee *et al.*, 1992b), suggesting individual functional roles toward inhibition of calpain. Although subdomains A and C have no inhibitory activity either individually (Uemori *et al.*, 1990) or when together (Ma *et al.*, 1994), both are a requirement for enhancing the inhibitory activity of subdomain B; missing of A has more effect to the inhibitory capacity of calpastatin than missing of C subdomain (Maki *et al.*, 1988; Uemori *et al.*, 1990; Ma *et al.*, 1994). Subdomain B contains a conserved amino acid sequence (LGXK(R)D(E)XYIPPXYRXLL) that seems to be a requirement for inhibitory activity but that, paradoxically, has only slight inhibitory activity by itself (Emori *et al.*, 1988; Kawasaki *et al.*, 1989; Uemori *et al.*, 1990; Wendt *et al.*, 2004).

The single CAST gene located on chromosome 5q15 (National Center for Biotechnology Information, 2019) encodes for multiple calpastatin isoforms. Differential promoter usage and alternative splicing produce a variety of calpastatin mRNA transcripts primarily involving the leader or L domain, which is composed of 8 exons, or in the first inhibitory domain, resulting in various calpastatin polypeptide production with specific exon composition and N-terminal variation (Lee *et al.*, 1992b; Takano *et al.*, 1999; Takano *et al.*, 2000; Parr *et al.*, 2001a; Parr *et al.*, 2004; Minobe *et al.*, 2006).

Calpastatin Types 1, 2, 3 and 4 are the most intensely studied amongst all isoforms. They are encoded by the mRNA transcripts generated by differential promoter usage. The properties of calpastatin transcripts and proteins are summarised in Table 1.5. Calpastatin Type 1 and Type 2 both contain the XL domain but different N-terminal sequences generated from tandem promoters associated with exons 1xa and 1xb, respectively. Calpastatin Type 3 is generated from a promoter associated with the untranslated exon 1u, resulting in a protein in which lacks XL region from the L domain (Takano *et al.*, 2000; review in Storr *et al.*, 2011a). Calpastatin Type 4 is a testis-specific isoform (Li &

Goldberg, 2000; Li *et al.*, 2000) lacking the L domain and the inhibitory domain I due to the production of a promoter between exons 14 and 15 (14t-L or 14t-S exon in a domain II) (Takano *et al.*, 2000; review in Storr *et al.*, 2011a).

Table 1.5 Summary of calpastatin isoforms identified in tissues.

Properties of transcript	Properties of protein
Type 1; contains 1xa, 1y, 1z, 2, 3, 4, 5, 6, 7, 8 exons for XL-L domain and exons for all four inhibitory domains; predicts an 85-kDa polypeptide.	Rate of migration in SDS-PAGE and tissue expression is unknown.
Type 2; contains 1xb, 1y, 1z, 2, 3, 4, 5, 6, 7, 8 exons for XL-L domain and all four inhibitory domains; predicts an 84-kDa polypeptide.	Migrates as a 145-kDa polypeptide in four SDS-PAGE; contains XL domain that has three protein kinase A sites in some species; present in cardiac tissue.
Type 3; prototypal; contains 1u, 2, 3, 4, 5, 6, 7, 8 exons for L domain and exons for all four inhibitory domains; predicts a 77–78-kDa polypeptide.	Migrates as 135-kDa in SDS-PAGE; present in mammalian skeletal muscle and many other tissues.
Deletion of exon 3 in domain L; contains all four repeating domains; predicts a 74–75-kDa polypeptide.	Migrates as 125-kDa in SDS-PAGE; present in mammalian skeletal muscle and other tissues.
Deletion of exons 3 and 6 in domain L; contains all four repeating domains; predicts a 72–73-kDa polypeptide.	Rate of migration in SDS-PAGE unclear (110–115-kDa??); tissue distribution has not been characterised.
Lacks domains L and I; 46-kDa polypeptide.	Migrates as 70-kDa in SDS-PAGE; in human, pig, rabbit erythrocytes; possibly also in other cells where it may have been identified as a degradation product.
Type 4; lacks domains L and I and part of domain II; molecular weight unknown.	Rate of migration in SDS-PAGE is unknown; transcript found in testis.
Lacks domains L, I, and II; predicts a 35-kDa polypeptide.	Rate of migration in SDS-PAGE ~55 kDa; found in human placenta.
Lacks domains L, I, II, and III: predicts an 18.7-kDa polypeptide.	Rate of migration in SDS-PAGE unknown; found in human testis.

Data adapted from Wendt *et al.*, 2004. Copyright© 2004 by Walter de Gruyter and Company with permission conveyed through Copyright Clearance Center, Inc.

Alternative splicing is also responsible for producing several types of calpastatin. It occurs variously in different species. Deletion of the region corresponding to exon 3 has been observed partially in calpastatin human cDNA clones (Lee *et al.*, 1992a; Lee *et al.*, 1992b) but has been found in all calpastatin cDNA clones of rat (Ishida *et al.*, 1991; Lee *et al.*, 1992a; De Tullio *et al.*, 1998). In mouse, either non-deleted isoform or the exon-3-deleted type of calpastatin are detected in tissues and cultured myoblast cell line (Takano *et al.*, 1999). Isoforms with exons 4 and/or exon 6 deleted are present in rat calpastatin, while an exon 5-deleted isoform is found in human. Such isoforms,

however, are undetectable in mouse (Takano *et al.*, 1999). Isoforms deleted in the inhibitory domain I are also present in human (exon 11), and mouse (exon 12) calpastatins (Lee *et al.*, 1992b; Takano *et al.*, 1999). In human tissues, the exon 11-deleted isoform is expressed in brain tissues and neuroblastoma cell lines but cannot be detected in heart nor liver (Lee *et al.*, 1992b).

The cellular consequence of expression of the various calpastatin splice variants has not been fully described. The absence of exon 6 promotes the formation of intracellular storage aggregates (De Tullio *et al.*, 2009), while the lack of exon 3 eliminates a stretch of basic amino acids, Lys-Lys-Arg-His-Lys-Lys, from the L domain. This part of the L domain has been described to be involved in binding calpastatin to biomembranes (Goll *et al.*, 2003). In addition, a calpastatin exon 3-containing mRNA (CASTexon3) has been suggested to play a crucial role in regulating LVI, the initial process of metastatic dissemination, of breast cancer. Down-regulation of an exon 3 containing variant (CASTexon3 mRNA) ($P < 0.014$, n = 56) and the low level of calpastatin ($P < 0.025$, n = 53) was shown to be significantly associated with the presence of LI in breast cancer (Storr *et al.*, 2011b). Calpastatin exon 3 containing Types 1, 2 and 3 are, therefore, the focus of the current study.

1.3.3 Calpain and calpastatin distribution in subcellular and tissue levels

Calpain and calpastatin principally co-localise in the cytoplasm, with a slight multitude around the nuclear region (Gil-Parrado *et al.*, 2003). Under calcium-stimulating conditions, dissociation of calpain from calpastatin is crucial for calpain activation, resulting in re-localisation of calpain to the plasma membrane where it cleaves and regulates downstream targets including cell adhesion- or migration-modulating regulators, while calpastatin remains in the cytoplasm (Gil-Parrado *et al.*, 2003; Stifanese *et al.*, 2010). Nuclear calpain is believed to be implicated in promoting cell survival via several signalling pathways, including NF-κB, Ku80, and PI-3K/Akt (Baghdiguian *et al.*, 1999; Tremper-Wells & Vallano, 2005; Baek *et al.*, 2016; Burchett *et al.*, 2019). Perinuclear localisation of calpastatin might be a consequence of accumulated

aggregation of calpastatin after being disassociated from binding to calpain (Averna *et al.*, 2003), possibly causing an elevation of cell migration but a reduction of nuclear calpain-mediated pro-survival effects. Likewise, the accumulation of calpastatin in the nuclei may promote cell death through suppressing the pro-survival effects mediated by nuclear calpain (Burchett *et al.*, 2019).

In breast cancer tissues, distribution of calpain-1, -2 and calpastatin investigated by IHC has been observed predominantly in the cytoplasm with some granularity and heterogeneity between adjacent tumour cells, but extremely infrequently detected in the nucleus (Storr *et al.*, 2011c; Storr *et al.*, 2012a; Storr *et al.*, 2016). The localisation of calpain-4, however, has not been shown in breast cancer tissue but in the tissue of ovarian tumour, showing that calpain-4 principally distributed in the cytoplasm (Yang *et al.*, 2017).

1.3.4 Calpain activation and calpain-calpastatin interaction

Ca^{2+} tightly controls calpain function by activating calpain activity and plays a role as an inducer of the inhibitory action of calpastatin - the only known protein inhibitor specific for calpain (Branca, 2004; Storr *et al.*, 2011a). Thus, efficient control of intracellular Ca^{2+} concentration is critical for the physiological functions of the calpain-calpastatin system (Croall & DeMartino, 1991; Ono & Sorimachi, 2012). Aberrant calpain activity due to a shift of Ca^{2+} homeostasis is associated with various pathological conditions, e.g., neuronal injury, neurodegenerative diseases (Higuchi *et al.*, 2012; Stifanese *et al.*, 2010; Vosler *et al.*, 2008), retinal neurodegeneration (Hoffmann *et al.*, 2013), dystrophic skeletal muscle (Zhao *et al.*, 2012), and myocardial infarction (Garcia-Dorado *et al.*, 2012). In addition to Ca^{2+} and calpastatin, there are additional mechanisms regulating calpain activity, including calpain expression level, post-translational modifications, phosphorylation of substrates or calpains themselves, the intervention of phospholipids, and formation of multiprotein complexes containing calpains (Lebart & Benyamin, 2006; Fei *et al.*, 2013).

1.3.4.1 Calpain activation

Calpain distributes and localises in the cytosol as an inactive protease before translocating to membranes in response to increase in cellular Ca^{2+} concentration and being activated in the presence of Ca^{2+} (Suzuki *et al.*, 2004). During activation, DI is autocatalytically hydrolysed, resulting in dissociation of 30K from the 80K subunit. The activated calpain, or the free 80K subunit, hydrolyses substrate proteins at membranes or in the cytosol after being released from membranes (Suzuki *et al.*, 1995; Suzuki *et al.*, 2004). Studies on the mechanism of calpain activation have thus far been performed using mainly μ- or m-calpains (Moldoveanu *et al.*, 2002b). m-Calpain contains at least three different Ca^{2+}-binding sites - a protease DII, an acidic loop region in C2L DIII, and calmodulin-like DIV and DVI.

The mechanism for calpain activation regulated by Ca^{2+} comprises of two stages. The first stage is the binding of Ca^{2+} to release constraints imposed by domain interactions. In the absence of Ca^{2+}, the nonfunctional conformation of the catalytic DII contains subdomains DIIa and DIIb separated by structural constraints imposed by an interaction between DI and DVI on one side and the strong electrostatic bonds between DIIb and DIII on the other side (Strobl *et al.*, 2000; Reverter *et al.*, 2001; Moldoveanu *et al.*, 2002b; Suzuki *et al.*, 2004). Binding of Ca^{2+} to DIV, DVI, and DIII results in separation of DI from DVI and DII from DIII, subsequently leading to conformation changes and dissociation, as mentioned, of 30K from the 80K subunit. The second stage is the formation of the active site cleft occurring only after the previous step by two Ca^{2+} atoms bound to DII (one each to DIIa and DIIb) (Moldoveanu *et al.*, 2002b; Suzuki *et al.*, 2004). Upon Ca^{2+} binding, DIIa and DIIb are folded into a single functional CysPc domain containing an active cysteine catalytic cleft (Strobl *et al.*, 2000; Moldoveanu *et al.*, 2004) to interact with substrates or calpastatin (Hanna *et al.*, 2008).

1.3.4.2 Calpain-calpastatin interaction

The activity of the calpains is tightly controlled by calpastatin, which is an intrinsically unstructured protein capable of reversibly binding and inhibiting up to four molecules of calpain in the presence of Ca^{2+}. Calpastatin, located in intracellular storage aggregates, is released into the cytosol, by intracellular calcium influx, to interact with calpain. Calcium also acts as an inducer of the inhibitory action of calpastatin by restructuring calpain to allow the A, B and C subdomains within each inhibitory domain of calpastatin to bind; A binds to domain IV, and C binds to domain VI of the calpains in a Ca^{2+}-dependent manner (Ma *et al.*, 1994; Yang *et al.*, 1994; Wendt *et al.*, 2004). Although binding of subdomain B to the calpains has been assumed to be Ca^{2+}-independent, the synthetic 24-residue peptide designed to mimic subdomain B of calpastatin binds to bovine calpain with higher specificity and a higher rate of binding in the presence of Ca^{2+} compared with binding in the absence of Ca^{2+} (Croall & McGrody, 1994). The Ca^{2+} concentration requirement for binding of calpastatin to calpain is associated with calpain but not with calpastatin (Kapprell & Goll, 1989). There is no evidence that calpastatin binds Ca^{2+} (Wendt *et al.*, 2004).

Subdomains A and C fold as amphipathic α-helices binding to the exposed Ca^{2+}-induced hydrophobic pockets on DIV and DVI, respectively (Hanna *et al.*, 2008; Moldoveanu *et al.*, 2008). Ca^{2+}-binding to the EF-1 hand initiates exposure of the hydrophobic pocket due to the movement of the first helix in the EF-1 hand (Todd *et al.*, 2003). The B-region binds to calpain only after calpain has been activated by Ca^{2+} (Wendt *et al.*, 2004; Hanna *et al.*, 2008; Moldoveanu *et al.*, 2008), and have inhibitory property only if it contains 13 amino acids or more. A longer amino acid sequence has higher inhibitory activity, suggesting that inhibition necessitates interaction over a huge area of the calpain molecule (Ma *et al.*, 1994; Wendt *et al.*, 2004). Region B inhibits calpain by occupying both sides of the catalytic cleft (DI-DIII) to obstruct the active site in the extended substrate-like orientation (Moldoveanu *et al.*, 2008). While passing through the active site cleft, calpastatin escapes proteolytic cleavage, by looping out and around the active site cysteine (Hanna *et al.*, 2008;). The presence of DIII to DVI

is necessary for the regulatory effects of calpastatin; calpains which lack these domains can evade the inhibition by calpastatin, in the other word, calpastatin can inhibit only dimeric calpains, e.g., μ- and m-calpain (Moldoveanu *et al.*, 2002a).

1.3.5 Roles of calpains and calpastatin in cancer

As mentioned, the calpain-calpastatin system has been implicated in the development, progression and response to therapies of various cancers, such as carcinomas of the pancreas, bile duct and ampulla (Storr *et al.*, 2012d), ovarian (Storr *et al.*, 2012c; Zhang *et al.*, 2019), gastric (Peng *et al.*, 2016b), lung (Xu *et al.*, 2019), and breast (Storr *et al.*, 2015). In breast cancer, the calpain-calpastatin system, in particular the conventional calpains (μ- and m-calpain), their catalytic subunits (calpain-1 and calpain-2) and specific inhibitor calpastatin have been investigated in a wide range of *in vitro* and *in vivo* studies focussing on their association with cellular functions related to cancer progression and metastasis as well as clinical outcomes and treatment responses.

1.3.5.1 Cell proliferation, survival, and apoptosis

Calpains are involved in cell proliferation, survival or apoptosis via regulating various crucial regulators, such as Myc, β-catenin, cyclin E, tumour-suppressor protein p53, nuclear factor-κB (NF-κB), and caspases. Figure 1.4 shows a schematic representation of conventional calpain substrates and major events of tumour cell pathophysiology in which conventional calpains are involved.

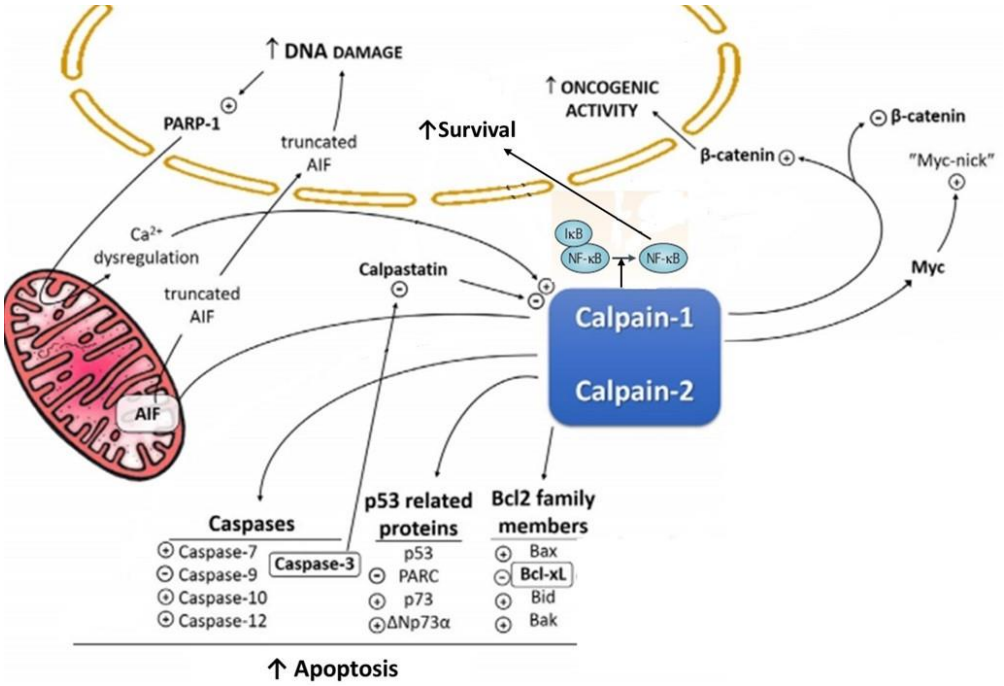


Figure 1.4 Schematic representation of conventional calpain substrates and major events of tumour cell pathophysiology in which conventional calpains are involved. Reproduced from Moretti *et al.*, 2014. Copyright© 2011 by Elsevier Inc. with permission conveyed through Copyright Clearance Center, Inc.

Calpain activity involves Myc and β-catenin, the two important regulators of cell proliferation and survival. The Myc family of nuclear oncogenes encodes transcription factors generally promoting cell growth, proliferation, and apoptosis in mammalian cells. They are one of the most commonly activated genes in human cancers, and uncontrollable Myc expression is one of the most important hallmarks of the hyperproliferation associated with most cancers (Dang, 2012; McMahon, 2014). In Eμ-myc lymphoma cells, c-Myc activation was found together with highly increased calpain activity, leading to tumorigenesis, while calpastatin expression was detected at much lower levels compared to the normal splenic B cells (Li *et al.*, 2012). In rat fibroblasts, c-Myc enhanced calpain activity through suppressing calpastatin expression. Silencing of calpastatin in c-Myc-negative cells resulted in the restoration of calpain activity, leading to stimulated cell growth, cell cycle redistribution, tumorigenicity as well as anchorage independence, which is a crucial feature for cancer cell detachment from a primary tumour before floating around in the blood vessels/lymph nodes without undergoing anoikis (Niapour *et al.*, 2008). Thus,

knockdown of calpastatin promoted transformation in c-Myc-negative cells. In primary chicken embryo fibroblasts, calpain activity was increased during oncogenic transformation induced by various common oncoproteins, including v-Myc, v-Src, v-Jun, k-Ras, and v-Fos. Anchorage-independent growth of all transformed cells could be inhibited by calpain inhibition (Carragher et al., 2004). While increased calpain activity caused oncogene-induced apoptosis associated with transformation by v-Myc (Carragher *et al.*, 2004), apoptosis induced by the calpain inhibitor (PD150606 or knockdown of calpain-4) was strongly dependent on c-Myc (Niapour et al., 2008). Myc could be up-regulated under improper conditions for cancer growth, such as nutrient deficiency and hypoxia, resulting in enhancing apoptosis. However, cancer cells were able to escape Myc-induced apoptosis through calpain-mediated proteolysis of Myc to a transcriptionally inactive form called 'Myc-nick', which refers to augmented anchorage-independent growth and cell survival. Myc-nick has been found to delay colon cancer cell death following treatment with chemotherapy agents (e.g., imatinib, cisplatin, and etoposide) and promote the disease progression and metastasis through inducing cell survival, the actin-bundling protein fascin, filopodia formation, and cell motility (Conacci-Sorrell *et al.*, 2014).

β-Catenin, a substrate for calpain, functions as a transcriptional coactivator of genes that are able to stimulate cell proliferation and suppress apoptosis. β-Catenin mutations, which are commonly present in human cancers, cause the constitutive transcriptional coactivation of tumour-promoting genes. In breast and prostate cancers, where mutations of β-catenin rarely occur, the calpain-mediated proteolysis of β-catenin contributed to aberrant stabilisation of the protein and enhanced oncogenic activity (Rios-Doria *et al.*, 2004). However, in colon carcinoma cells, calpain caused degradation of β-catenin promoted by Gq signalling (Li & Iyengar, 2002), resulting in a decrease of cell proliferation, and anchorage-independent growth (Benetti *et al.*, 2005). Silencing of endogenous calpain, in colon cancer cells, contributed to an increase of the free transcriptional competent pool of endogenous β-catenin. Calpain inhibitors (calpastatin and growth arrest-specific protein 2 (Gas2)) could control the level,

localisation and functions of β-catenin through regulating calpain. In comparison, Gas2DN (Gas2 dominant negative) induced calpain activity *in vitro*, increased degradation of stabilised/mutated β-catenin *in vivo*, and reduced anchorage-independent growth and proliferation of colon cancer cells *in vitro* (Benetti *et al.*, 2005).

Cyclin E is a required protein for the G1/S transition of the cell cycle. Calpain-mediated cleavage of cyclin E has been found to produce a hyperactive low-molecular-weight cyclin E (Wang *et al.*, 2003). Overexpression of cyclin E in MCF-7 breast cancer cells could transactivate calpain-2 expression, resulting in cleavage of cyclin E itself and other calpain substrates, i.e., FAK, pp60src, p53, and calpastatin. In a murine breast tumour model, high expression of proteolysed cyclin E and FAK was observed with higher metastatic potential. In human breast cancer, high expression of cyclin E was detected together with the expression of the low molecular weight isoforms, high level of calpain-2, and proteolysis of FAK (Libertini *et al.*, 2005). In breast cancer patients, cyclin E overexpression was observed in 10-25% of all cases and may be associated with expression or activity of calpain-2. In addition, the upregulation of cyclin E was clinically associated with greater genomic instability, more aggressive behaviour, a poor response to tamoxifen (P = 0.001 for poor relapse-free survival, HR = 4.01, n = 108), and poor clinical outcome ($P < 0.001$, HR for death = 13.3, n = 256) (Span *et al.*, 2003; Keyomarsi *et al.*, 2002).

Calpain activity has been shown to involve in pro-survival activities of tumour-suppressor protein p53 and nuclear factor-κB (NF-κB). Protein p53 is activated in response to DNA damage to prevent the replication of cells sustaining genetic injury by inducing cell cycle arrest or apoptosis. To sustain high accumulated levels of p53 within the cell following DNA damage, stabilisation of p53 is co-occurred with the activation of the protein (Kubbutat & Vousden, 1997). Wild-type p53 is a substrate for proteolytic cleavage by μ- and m-calpains (Pariat *et al.*, 1997), indicating a role for both proteases in regulating p53 stability and avoidance of p53 dependent apoptosis (Gonen *et al.*, 1997; Kubbutat &

Vousden, 1997). GAS2, which was cleaved during apoptosis to allow rearrangement of the actin cytoskeleton, could enhance p53 stability through its physical association with calpain to impede cleavage of p53 (Benetti *et al.*, 2001). Calpain inhibition by calpain inhibitor 1 increased the levels of activated p53, the level of p21 protein, and the activation of caspases, contributing to cell arrest in G0/G1 and apoptosis in various tumour cell lines (Atencio *et al.*, 2000). Mutation of p53 is the most common genetic change identified in human neoplasia, and mutant p53 proteins, with altered tertiary structures, have been reported their various susceptibilities to calpains - some of them being resistant to degradation and others having more sensitivity (Pariat et al., 1997). Although p53 mutation in breast cancer has been found at a lower incident compared to other solid tumours, it was associated with more aggressive diseases (ER^- tumours: $P = 0.044$, n = 11/37; PR^- tumours: $P = 0.012$, n = 13/42) (Mazars *et al.*, 1992), and worse overall survival ($P = 0.01$, relative hazard (RH) = 2.0, n = 2319) (Pharoah *et al.*, 1999; Gasco *et al.*, 2002).

Activation of NF-κB rapidly leads to the transcription of various genes involving with cell survival and apoptosis as well as other multiple aspects of oncogenesis, such as cell proliferation, cycle progression, neoplastic transformation, and migration, (Piva *et al.*, 2006; Pianetti *et al.*, 2001). In breast cancer, while calpain inhibition by calpeptin was reported to increase TNF-α-induced NF-κB activation *in vitro* (Fei *et al.*, 2013), calpain also promoted NF-κB activation *in vitro and in vivo* by mediating degradation of tumour suppressor PTEN, which was able to prevent HER-2-induced NF-κB activation via inhibiting Akt kinase signalling pathway (Pianetti *et al.*, 2001). Calpain-2 has been reported to be responsible for PTEN degradation (Briz *et al.*, 2013). In addition, calpain also modulated the activity of NF-κB through regulating its inhibitor, IκBα. IκBα could be cleaved by calpain in HepG2 liver cells (Han *et al.*, 1999), while calpastatin overexpression inhibited calpain activity, degradation of IκBα, and NF-κB activation in murine models (Li *et al.*, 2014). Proteolytic cleavage of IκBα was found to be responsible by μ-calpain (Shumway *et al.*, 1999), m-calpain (Han *et al.*, 1999) as well as calpain-3 (Baghdiguian *et al.*, 1999).

Calpain also plays a role to cooperate with some cellular apoptotic pathways. Storr *et al.* (2015) reviewed the implications of calpain activity in inducing apoptosis through the caspase cysteine protease machinery, as caspase-7, -9, -10 and -12 are substrates for calpain-mediated proteolysis. Calpain cleavage leads to activation of caspase-7, -10 and -12, but inactivation of caspase-9 (Chua *et al.*, 2000; Tan *et al.*, 2006; Gafni *et al.*, 2009). For caspase-7, it was found to be cleaved by calpain-1 and caspase-3, and two different products produced from calpain-1-dependent cleavage were more active than the products produced from the cleavage mediated by caspase-3 (Gafni et al., 2009). During endoplasmic reticulum (ER) stress, caspase-12 was activated by calpain, contributing to apoptotic cell death (Tan *et al.*, 2006; Martinez *et al.*, 2010). Interestingly, caspase-8, which is a pro-apoptotic protease, has been discovered to impede neuroblastoma metastasis through inducing apoptosis; however, it also stimulated cell migration amongst non-apoptotic cells, suggesting that caspase-8 is able to stimulate metastasis when apoptosis is compromised (Barbero *et al.*, 2009). Caspase-8 prevented calpastatin-mediated inhibition of calpain-2 by restricting their interaction, leading to enhancement of calpain-2-mediated cleavage of FAK, and further promoting cell migration (Barbero et al., 2009). During apoptosis, calpastatin was cleaved by calpain-1, -2, and caspases (Porn-Ares *et al.*, 1998; Wang *et al.*, 1998). The high-molecular-weight form of calpastatin was cleaved by caspase-1, -3, and -7, while calpastatin with missing of domain L and inhibitory domain I was sensitive to proteolysis by caspase-1 but resistant to caspase-3 and -7 (Wang *et al.*, 1998). In calpastatin-silenced mice, calpain inhibition appeared to facilitate the apoptotic responses without the activation of caspase 3 (Takano *et al.*, 2005).

Calpain also assists pro-apoptotic pathways through cleaving numerous substrates involved with caspase-dependent apoptosis, such as BAX, BCL-2, CDK5, APAF1, JNK, JUN, FOS, Cain, and calpastatin (reviewed in Storr *et al.*, 2011a; Storr *et al.*, 2015). Calpain located in mitochondria is implicated in caspase-independent apoptosis through modulating proteolytic cleavage of

apoptosis-inducing factor (AIF) (Polster *et al.*, 2005; Liu *et al.*, 2009). Activation of poly(ADP-ribose) polymerase 1 (PARP1) DNA repair enzyme, following DNA damage, contributed to mitochondrial calcium dysregulation, leading to calpain activation and further promote AIF-induced apoptosis (Vosler *et al.*, 2009; Storr *et al.*, 2011a).

1.3.5.2 Cell migration, adhesion, and invasion

Cell motility is a crucial property of tumour cells to promote metastasis. Before invading into lymphatic or blood vessels, tumour cells detach themselves from the growing tumour cell mass, followed by invasion and migration through the ECM, and eventually adhere to the vascular walls. These phenomena are considered prerequisites for the LVI event (Pantel & Brakenhoff, 2004; Aleskandarany *et al.*, 2015). Likewise, after leaving the vessels, tumour cells also require invasive, migratory, and adhesive abilities to move and grow at a new site. Cellular movement involves multiple steps: 1) creating membrane protrusions at a leading edge and attachment to a new site by a cell front; 2) connecting actin cytoskeleton to the ECM substratum; and 3) producing pulling force to promote cell detachment at the trailing edge and that allows cells to move forward (Wells *et al.*, 2005).

Calpains have been implicated in regulating several key steps to allow cellular movement, including destabilising cell adhesion to ECM, promoting turnover of focal adhesion, membrane protrusion, invadopodia formation, cell spreading, rear detachment, and chemotaxis (Franco & Huttenlocher, 2005; Storr *et al.*, 2011a). These phenomena are involved with numerous key regulators of cell-matrix and cell-cell interactions, many of which are identified as proteolytic substrates for conventional μ- and m-calpains, such as focal adhesion complex components (e.g., FAK and talin), cell adhesion molecules (e.g., cadherins), and other related molecules (e.g., PKC) (Hoskin *et al.*, 2015; reviewed in Franco & Huttenlocher, 2005, and Storr *et al.*, 2011a). Figure 1.5 shows calpain-mediated signalling mechanisms in the regulation of cell migration and invasion.

Calpains have been demonstrated to modulate the dynamic turnover of integrin-associated focal adhesion structures and influence cell migration through mediating proteolytic cleavages of central molecules of focal adhesion complexes, i.e., talin (Franco *et al.*, 2004b), and FAK (Chan *et al.*, 2010), as well as other focal adhesion-related proteins, such as ezrin, vinculin, fodrin, and α-actinin (Storr *et al.*, 2011a).

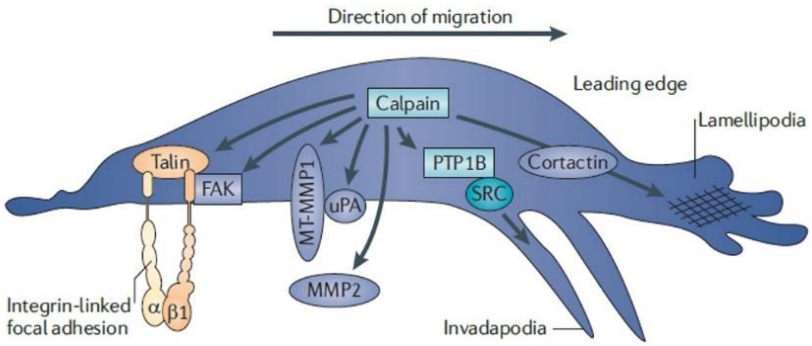


Figure 1.5 Calpain and migration. Pharmacological and molecular intervention studies that target calpain activity suggest a role for multiple calpain substrates, and thus several distinct calpain-mediated signalling mechanisms, in the regulation of cell migration and invasion. Reproduced from Storr *et al.*, 2011a. Copyright© 2011 by Nature Publishing Group with permission conveyed through Copyright Clearance Center, Inc.

In a breast cancer cell model, the membrane-cytoskeleton linker protein ezrin, a specific substrate for calpain-1 (Yao *et al.*, 1993), plays a role in regulating focal adhesion and invadopodia dynamics through altering calpain activity. Downregulation of ezrin by shRNA was accompanied by a reduction of calpain-mediated proteolytic cleavage of the focal adhesion- and invadopodia-associated proteins talin, FAK, and cortactin (Hoskin *et al.*, 2015). Rodriguez-Fernandez *et al.* (2016) proposed calpain as a potential target in regulating cancer progression and metastasis, particularly in breast cancer. This study showed that calpain inhibitors (calpeptin, calpain inhibitor VI, and ALLN) suppressed calpain (recombinant calpain-1, and -2)-mediated cleavage of lactating mammary gland focal adhesion protein talin-1 as well as cell adhesion molecules (E-cadherin, β-catenin, and δ-catenin). This suggests that both calpain-1 and -2 were able to precisely recognise and cleave those adhesion proteins from mammary gland epithelia. Also, knockdown of calpain-1 significantly prevented calpain-mediated cleavage of all those adhesion-related

proteins and reduced the migration ability of MCF-7 and MDA-MB-231 breast cancer cells (not determined (ND) for knockdown of calpain-2) (Rodriguez-Fernandez *et al.*, 2016). Paradoxically, calpain-dependent cleavage of paxillin, a focal adhesion-associated protein, has been found to generate paxillin delta, which functioned as a paxillin antagonist and negatively regulated focal adhesion disassembly and turnover, leading to a reduction of migration in HeLa cervical cancer and HEK 293 embryonic kidney cell lines (Cortesio *et al.*, 2011).

Alternative pro-migratory mechanisms for calpain have been explored. Calpain is likely to regulate membrane protrusions, depending on the cleavage of proteins that modify the actin cytoskeleton such as cortactin (Storr *et al.*, 2011a), which is a substrate for calpain-2 (Perrin *et al.*, 2006). Calpain-resistant cortactin increased transient membrane protrusion and decreased cell migration in fibroblasts (Perrin *et al.*, 2006), suggesting that calpain proteolysis of cortactin regulates migration through stabilising lamellipodia and pseudopod. Franco *et al.* (2004a) revealed that calpain-2 plays a role in preventing membrane protrusions and regulating lamellipodial dynamics at the leading edge of migrating fibroblast cells. Downregulation of calpain-2 and -4 similarly resulted in the cells with a protrusive morphology, increased transient membrane activity, and altered protrusion kinetics (Franco *et al.*, 2004a).

Calpains are also involved in cell invasion. In highly metastatic rat mammary adenocarcinoma MTLn3 cells, calpain-2 depletion contributed to impaired invadopodia development, which could be recovered by expression of a truncated fragment of PTP1B, a product of calpain cleavage. This suggests that calpain proteolysis regulates PTP1B–Src mediated invadopodia (Cortesio *et al.*, 2008). Calpain activity was also required for augmenting expression and activity of MMP2 and MMP9, which are the main ECM enzymes produced and released from protrusive invadopodia to degrade collagen, as well as uPAs (Popp *et al.*, 2003; Jang *et al.*, 2010; Postovit *et al.*, 2002) and MT-MMP1 (or called MMP14) in various cells (Kwak *et al.*, 2012), resulting in ECM remodelling and cell invasion. Adipose-derived stromal/stem cells (ASCs) cultured in breast cancer

condition media had increased mRNA expression of MMP-15 and calpain-4 as well as decreased calpastatin mRNA expression. Such dysregulated mRNA expression was associated with the enhanced cell invasion of ASCs, and silencing of each protease or protease inhibitor confirmed that they play a role in ASCs invasion (Strong *et al.*, 2012). These findings support the previous studies indicating that ASCs are associated with enhancing cell invasion and metastasis of either *in vitro* (Jotzu *et al.*, 2011) or clinical breast cancer cells (Zimmerlin *et al.*, 2011).

Calpain is also involved in the epithelial-mesenchymal transition (EMT) in various cancer cells. In A549 lung adenocarcinoma cell line, calpain-2 was upregulated during TGF-β-induced EMT (Keshamouni *et al.*, 2009), while fibronectin seemed to activate cell migration/invasion through ERK1/2-calpain-2 signalling (Meng *et al.*, 2009), indicating a potential role of calpain in fibronectin-induced EMT. In breast tissue, fibronectin is a primary component of the mammary mesenchymal compartment and undergoes dramatic changes during breast cancer development. Increased fibronectin expression was observed in the stroma of breast tumours (Ioachim *et al.*, 2002) and associated with an invasive and metastatic breast cancer phenotype (Zhou *et al.*, 2015). In MCF-7 breast cancer cells, fibronectin induced an EMT-like morphological alteration as well as cell migration and invasive abilities with increased calpain-2 expression and increased calpain-mediated proteolysis of FAK1. Calpain inhibitors (calpeptin, calpain inhibitor I and IV) was able to reverse the fibronectin-induced EMT and inhibit FAK proteolysis (Li *et al.*, 2017a).

In short, a growing body of evidence indicates the crucial roles of calpain in regulating breast tumour cell proliferation, survival, adhesion, migration and invasion through a variety of pathways, with such involvement contributing to disease progression and metastasis. In a similar vein, calpain inhibition either by silencing calpain expression or the use of inhibitors (endogenous/synthetic inhibitors) has provided evidence to support that the calpain/calpastatin system is a potential target for anti-metastasis therapy.

1.3.5.3 Prognosis and clinical outcomes in breast cancer patients

Clinically aberrant expression of calpains and calpastatin was reported in several cancer types, and that irregularity has been found to be associated with clinicopathological variables and clinical outcomes.

1.3.5.3.1 Calpain-1

Calpain-1 expression is heterogeneous in different cancers in comparison with normal or non-malignant counterparts. Calpain-1 expression level was relatively higher in chronic lymphocytic leukaemia (B-CLL) ($P < 0.01$, 15 cases of B-CLL vs 15 age- and sex-matched healthy volunteers) (Witkowski *et al.*, 2002), but lower in ovarian cancer (Salehin *et al.*, 2011). The unchanged calpain-1 level was also observed in numerous types of cancer, including gastric cancer (n = 51 pairs of cancerous and matched normal peritumoral gastric mucosa) (Liu *et al.*, 2017), colorectal adenocarcinoma (n = 50 pairs of tumour tissues and normal adjacent colonic mucosa) (Lakshmikuttyamma *et al.*, 2004), and endometrial cancer (29 endometrial cancerous vs 18 benign tissues) (Salehin *et al.*, 2010).

In a large cohort of early-stage invasive breast cancer (n = 1315), high calpain-1 expression was associated with various clinicopathological variations, including positive status of ER ($P = 0.001$) and PR ($P = 0.005$) as well as low-grade tumours ($P = 0.014$) (Storr *et al.*, 2012a). In term of clinical outcomes, calpain-1 expression was associated differently with different breast cancer types and conditions. Although there was no correlation between calpain-1 and HER2 gene amplification or HER2 expression, high calpain-1 was significantly associated with poor relapse-free survival ($P = 0.001$, n = 93) in HER2-positive patients treated with trastuzumab following adjuvant chemotherapy. This suggests calpain-1 as a biomarker to predict relapse-free survival in patients with such condition (Storr *et al.*, 2011c). This suggestion was subsequently confirmed by the two following cohorts, conducted by the current group, also showing that high calpain-1 was significantly associated with poor relapse-free survival ($P = 0.01$, n = 194; $P = 0.019$, n = 87) (Pu *et al.*, 2016). Moreover, the negative association between calpain-1 level and relapse-free survival

remained present when those two cohorts were combined (P = 0.01, n = 281) (Pu *et al.*, 2016). Conversely, in large but operable inflammatory breast cancer treated with neoadjuvant chemotherapy, low calpain-1 expression had a significant association with adverse breast cancer-specific survival (P = 0.003, n = 43) (Storr et al., 2016). In other cases, the association between calpain-1 level and clinical outcomes was not present, such as in the cohorts of patients with early-stage invasive breast carcinomas that were unclassified (n = 1371) or classified as triple-negative/basal-like tumours (n = 387) (Storr *et al.*, 2012a).

1.3.5.3.2 Calpain-2

Calpain-2 is highly expressed in cancers compared to normal/non-cancerous counterpart, including in gastric cancer (P < 0.0001, 51 pairs of cancerous and normal peritumoural gastric mucosa) (Liu *et al.*, 2017), and colorectal adenocarcinoma (P < 0.05, 50 pairs of tumour tissues and normal adjacent colonic mucosa) (Lakshmikuttyamma *et al.*, 2004). Calpain-2 expression has also been detected at a reduced level in ovarian cancer (Salehin *et al.*, 2011), but unchanged in endometrial cancer (29 endometrial cancerous vs 18 benign tissues) (Salehin *et al.*, 2010), and chronic lymphocytic leukaemia (B-CLL) (15 pairs of B-CLL cases and age- and sex-matched healthy volunteers) (Witkowski *et al.*, 2002).

In an extensive cohort of patients with early-stage invasive breast cancer conducted by the current group, high calpain-2 expression was positively associated with a presence of peri-tumoural LI (P = 0.022, n = 1286) and negatively associated with relapse-free survival (P = 0.043, n = 1286) (Storr *et al.*, 2012a). In an independent cohort of ER^- cases (n = 387), a presence of high calpain-2 was also significantly associated with worse prognoses - breast cancer-specific- and relapse-free survivals (P = 0.003 and < 0.001, respectively), suggesting that calpain-2 could prognostically stratify patients with breast cancer (Storr *et al.*, 2012a). Both cohorts have been further independently performed analyses on patients with triple-negative or basal-like tumours, showing that high calpain-2 expression remained statistically associated with

both disease-specific- and relapse-free survivals for either basal-like (*P* = 0.025, n = 270/1371; *P* = 0.020, n = 149/387 respectively) or triple-negative subgroups (*P* = 0.043, n = 236/1371; *P* = 0.033, n =253/387 respectively) (Storr *et al.*, 2012a). This study discovered the interesting findings showing that in the presence of low calpain-2 expression, patients diagnosed triple-negative/basal-like tumours had comparable breast cancer-specific survival to the patients with non-basal or receptors (ER, PR or HER2)-positive disease. Paradoxically, high calpain-2 expression has been found to be significantly associated with high overall survival (*P* = 0.031, n = 94) in large but operable non-inflammatory breast cancer treated with neoadjuvant therapy (Storr *et al.*, 2016). In HER2-positive patients treated with trastuzumab following adjuvant chemotherapy, there was no correlation between calpain-2 expression and HER2 expression, HER2 gene amplification, or relapse-free survival (n = 92) (Storr *et al.*, 2011c).

1.3.5.3.3 Calpain-4

Calpain-4 has been frequently detected at a higher level in various cancers compared to normal/non-cancerous tissues, such as ovarian carcinomas (*P* < 0.01 determined in 91 cases with ovarian carcinomas, 5 borderline ovarian tumour tissues, and 5 normal ovarian epithelial tissues) (Yang *et al.*, 2017), glioma (*P* < 0.01; 279 gliomas vs 21 normal tissues) (Cai *et al.*, 2014), non-small cell lung cancers (NSCLC) (8 pairs of NSCLC and matched adjacent noncancerous tissues) (Gu *et al.*, 2015), melanoma (*P* < 0.01; 120 melanoma vs 34 normal tissues) (Wang *et al.*, 2017), and gastric cancer (*P* = 0.026, 33 paired gastric cancer and adjacent normal tissues) (Peng *et al.*, 2016a).

Higher calpain-4 mRNA expression was also detected together with high expression of the protein in various cancers, including nasopharyngeal carcinoma (*P* < 0.05 and < 0.05 respectively; 7 tumour samples vs 2 normal tissues) (Zheng *et al.*, 2014), intrahepatic cholangiocarcinoma (*P* = 0.003 and < 0.001 respectively; 33 tumour tissues vs 13 normal liver tissues from healthy donors) (Zhang *et al.*, 2013a), and renal carcinoma (*P* = 0.013 and 0.005

respectively, 40 paired tumour and adjacent non-tumour tissues) (Zhuang *et al.*, 2014).

Although calpain-4 expression or the correlation of which with the clinical outcome of patients diagnosed with breast cancer remain unrevealed, high calpain-4 expression in ovarian cancer was reported to be significantly associated with shorter overall survival ($P = 0.0331$, n = 91) (Yang *et al.*, 2017). The roles of calpain-4 in cell survival, migration or invasion have also been demonstrated, as described in section 1.3.5.1 and 1.3.5.2.

1.3.5.3.4 Calpastatin

Aberrant expression of calpastatin has been observed in various cancers; with clinical studies showing low calpastatin levels correlating with cancer progression and worse outcome, such as in the operable inflammatory breast cases (Storr *et al.*, 2016), and patients with bile duct and ampullary carcinomas (Storr *et al.*, 2012d). Low expression of calpastatin in comparison to normal/adjacent tissue has been reported in gastric cancer ($P < 0.0001$, n = 51 pairs of cancerous tissues and matched normal peritumoral gastric mucosa) (Liu *et al.*, 2017), colorectal adenocarcinoma ($P < 0.05$, 50 paired tumour tissues and adjacent colonic mucosa) (Lakshmikuttyamma *et al.*, 2004), and ovarian cancer (Salehin *et al.*, 2011). On the other hand, higher calpastatin expression was reported in endometrial cancer (n = 29) compared to benign tissue (n = 18) ($P = 0.037$) (Salehin *et al.*, 2010), while unchanged expression was present in chronic lymphocytic leukaemia (B-CLL; n=15) compared with non-malignant cells (15 age- and sex-matched healthy volunteers) (Witkowski *et al.*, 2002).

In breast cancer, downregulation of calpastatin protein ($P = 0.025$, n = 53) and exon3-containing variant ($P = 0.014$, n = 56) was significantly associated with the presence of LI (Storr *et al.*, 2011b). Calpastatin has been confirmed to be involved with LI in a subsequent larger cohort showing that high calpastatin expression was associated with the absence of intra-tumoural LI ($P = 0.014$, n = 1266) (Storr *et al.*, 2012a). This suggests that calpastatin may play a crucial role in regulating the initial process of metastatic dissemination of breast cancer via

regulating LVI. Calpastatin expression was also negatively associated with clinicopathological variations of the high-risk group for breast cancer recurrence. Low calpastatin exon 3-containing mRNA was significantly associated with larger tumour size (>2 cm, *P* = 0.003), higher NPI (*P* = 0.012), and negative HER (*P* = 0.042). Low calpastatin protein was associated with negative status of ER (*P* = 0.010) and PR (*P* = 0.022) as well as basal phenotypic tumour (*P* = 0.008) (Storr *et al.*, 2011b). On the other hand, high calpastatin expression significantly associated with clinicopathological features of the low-risk group, including older patients (≥40 years, *P* = 0.002), small tumours (<2 cm, *P* = 0.022), low grade (*P* = 0.002), low NPI (*P* = 0.001), ER-positive (*P* = 0.001), and PR-positive (*P* < 0.001), and non-basal phenotypic breast cancer (*P* = 0.003) (Storr *et al.*, 2012a). Also, in HER2-positive patients treated with trastuzumab following adjuvant chemotherapy (n = 93), calpastatin expression was found to be correlated with NPI (*P* = 0.003), lymph node status (*P* = 0.007), HER2 expression level (r = 0.350, *P* = 0.001), and HER2 gene amplification (r = 0.258, *P* = 0.027) (Storr *et al.*, 2011c).

Calpastatin expression was also associated with clinical outcomes in patients with breast cancer. In a cohort of large but operable primary breast cancer patients treated with neoadjuvant chemotherapy, low expression of calpastatin was significantly associated with adverse breast cancer-specific survival in inflammatory breast cancers (*P* = 0.020, n = 43). In contrast, high expression was significantly associated with adverse disease-specific survival in non-inflammatory disease (*P* = 0.035, n = 94) (Storr *et al.*, 2016). In other words, low calpastatin was associated with improved breast cancer-specific survival in non-inflammatory large but operable primary breast cancer treated with neoadjuvant chemotherapy, while high calpastatin was associated with improved disease-specific survival in inflammatory cases. However, in other cases, the association between calpastatin expression and clinical outcomes (disease-specific or relapse-free survivals) was not present, such as in the cohorts of patients with early-stage invasive breast cancer (*P* = 0.094, n = 53, Storr *et al.*, 2011b; n = 1371, Storr *et al.*, 2012a), primary breast cancer treated

with trastuzumab following adjuvant chemotherapy (*P* = 0.298, n = 93) (Storr *et al.*, 2011c), or triple-negative or basal-like tumours (n = 387) (Storr *et al.*, 2012a). Furthermore, calpastatin mRNA expression was not correlated with breast cancer-specific survival (*P* = 0.204, n = 56) or disease recurrence (*P* = 0.097, n = 56) in lymph node-negative patients (Storr *et al.*, 2011b).

Amongst all types of breast cancer, calpastatin expression may be more important in inflammatory breast cancer. Calpain-1 expression level also associated with the survival in the inflammatory cases, as described in sections 1.3.5.3.1.

1.4 Hypothesis, aim, and objectives

Hypothesis:

A growing body of evidence mostly indicates negative involvement of calpastatin expression to calpain activity and physiological pathways/ clinicopathological characteristics related to breast cancer progression and metastasis *in vitro*, *in vivo* animal models, or clinical studies (sections 1.3.5.1, 1.3.5.2, and 1.3.5.3.4). Low expression of calpastatin protein or exon 3-containing CAST mRNA is negatively associated with the presence of LI, which is a predominant form of LVI and a poor prognostic factor in patients with operable breast cancer either with or without LN-involvement (section 1.2.3.2.1). Although various calpastatin isoforms originate from a single gene, the mechanism whereby each regulates calpain activity is mostly unknown, with no prior studies investigating their differential ability to regulate cancer progression and LVI. In this study, therefore, we hypothesise that calpastatin isoform overexpression suppresses calpain activity as well as breast cancer cell phenotypic endpoints related to cancer progression and LVI.

Aim:

The overall aim of the thesis is to study the role of overexpression of calpastatin isoforms (Type 1, 2, and 3) encoded by exon 3-containing CAST mRNA in

regulating calpain activity and phenotypic behaviours related to breast cancer progression and LVI.

Objectives:

1. Establish stably transfected monoclonal breast cancer cell models overexpressing calpastatin Type 1, 2, and 3, using cell lines representing two different subtypes of breast cancer, by DNA transfection.
2. Explore intracellular localisation of calpastatin isoforms in the established transfected cell lines using immunofluorescence confocal microscopy.
3. Investigate the role that individual calpastatin isoforms play in regulating breast cancer cell proliferation and clonogenicity to understand processes involved in regulating breast cancer progression, using growth curve and clonogenic survival assays, respectively.
4. Investigate the role that individual calpastatin isoforms play in regulating breast cancer cell migration and tumour cells-endothelial interactions to understand processes involved in regulating breast cancer LVI, using scratch-wound migration and static adhesion assays, respectively.

Chapter 2 Materials and methods

2.1 Cell culture

2.1.1 Cell lines and growth medium

Seven breast cancer cell lines representing various subtypes of breast cancer were used in this study, including basal-like/triple-negative (MDA-MB-231, MDA-MB-468 & SUM149), luminal (MCF-7 & T47D), and HER2-positive (SKBR3 & JIMT-1) cell lines. All cells were obtained from the American Type Culture Collection (ATCC) except for SUM149, an inflammatory breast cancer cell line, that was a kind gift from Dr Fedor Bertidchevski, University of Birmingham. All breast cancer cell lines were used within a passage window of fifteen. The immortalised human microvascular endothelial cell line (hMEC-1) was purchased from ATCC, and the human telomerase reverse transcriptase lymphatic endothelial cell line (hTERT-LEC) was kindly provided by Prof Sebastian F. Schoppmann, University of Vienna, Austria. The endothelial cells were used in static adhesion assays within a passage window of 8. All cells were cultured in the defined growth media listed in Table B2.1 (Appendix B) at 37˚C in an incubator maintained at 95% relative humidity and a CO_2 level of 5%. Stably transfected MDA-MB-231 and T47D cell lines established from section 2.6 were routinely cultured with selection medium (750 µg/mL G418 in complete medium) (section 2.6.1) that was replaced by regular medium, without G418, two days before cells being used in experiments. Iron supplemented donor bovine serum (DBS) (Gibco, Life Technologies, USA) was heat-inactivated by incubating for 30 minutes in a 56°C water bath before being used to prepare complete media. All cell culture related reagents were pre-warmed to 37˚C in a water bath, and cell culture was performed under aseptic conditions in a Class II biological safety cabinet.

To ensure there is no misidentification or cross-contamination of cell lines, short tandem repeating (STR) DNA profiling can be applied to identify human cell lines derived from the tissue of a single individual (Nims *et al.*, 2010; Reid *et al.*, 2013). Thus, all cell lines were regularly verified for authenticity using the

Promega Powerplex® 16 short tandem repeat (STR) system, conducted by postdoctoral researchers within the group, Dr Sarah Storr or Dr Aula Ammar, approximately every six months. All cell lines were also routinely screened for mycoplasma infection, one of the main problems in cell culture, that can extensively affect cell physiology and metabolism (Nikfarjam & Farzaneh, 2012). Mycoplasma infection was assessed by senior technicians every 4-6 months using the MycoProbe® Mycoplasma Detection Kit (R&D Systems, USA).

2.1.2 Subculture of adherent cell lines

Adherent cells were cultured in tissue culture flasks with routine culture media and subcultured when the confluency reached 70-80%. To subculture, the culture medium was removed, and the cell layer was washed once with Dulbecco's phosphate-buffered saline (PBS) (Sigma-Aldrich, UK). The cell layer was then entirely covered by excess volume of 0.5 mg/mL trypsin-EDTA (Sigma-Aldrich, UK) for 30 seconds (1 mL in a T25cm^2 flask, 3 mL in a T75cm^2 flask, or 5 mL in a T175cm^2 flask). The excess trypsin-EDTA was removed, and the adherent cells were incubated at 37°C, 5% CO_2 for 2 minutes for MDA-MB-231 cells and 4 minutes for the other cell lines, to detach from the flask surface. Cells were checked under a microscope to ensure complete detachment. Complete culture media was added to deactivate the trypsin-EDTA before harvesting the cells. The homogeneous suspension of harvested cells was split into a new tissue culture flask with different cell subcultivation ratios depending on the level of confluence and the cell type. Cultures with 70-80% confluence were split in a subcultivation ratio of 1:5 to 1:10 for MDA-MB-231 cells and 1:4 to 1:6 for the other cell lines. Fresh complete medium was then added to an appropriate total volume (5 mL in a T25cm^2 flask, 15 mL in a T75cm^2 flask, or 25 mL in a T175cm^2 flask) before transferring the flask containing the subcultured cells into the incubator.

2.1.3 Cryopreservation and recovery from cryopreservation

To control for genetic drift, limit the risk of bacterial, fungal, viral or cellular cross-contamination, and to ensure low passage number for subsequent

experiments, cells were initially obtained from a master cell stock before being expanded, frozen down and kept in liquid nitrogen as stocks. To freeze cell down, once the culture reached 70-80% confluence, cells were harvested with trypsin-EDTA and homogeneously suspended in complete medium. The total number of cells and the percentage of viability were determined using trypan blue exclusion dye method; cells were counted with a haemocytometer or a Countess® Automated Cell Counter (Life Technologies, USA). The cell suspension was then centrifuged at 170 x g for 5 minutes. The supernatant was discarded, and the cell pellet resuspended in an appropriate volume of freezing medium (mix of 10% dimethyl sulfoxide (DMSO) and 90% complete medium) to achieve a final concentration of $1x10^6$ to $1x10^7$ cells/mL. The cell suspension was stored in labelled cryovials (1 mL in each vial) before being placed in a CoolCell® alcohol-free cell freezing container which ensures a -1°C/minute freezing rate. Cells were placed at -70°C overnight before being transferred for long-term storage in liquid nitrogen (-180°C) for future use.

To recover frozen cells from liquid nitrogen, vials were thawed in a 37°C water bath, and cells immediately transferred into a 15-mL conical centrifuge tube containing 9 mL of pre-warmed complete culture medium. To remove DMSO, the cell suspension was centrifuged at 170 x g for 5 minutes. The supernatant was discarded, and the cell pellet resuspended in fresh culture medium before being transferred into a T25cm^2 tissue culture flask. Culture medium was refreshed the following day, and cells were cultured following routine procedures.

2.2 Chemicals and drug preparation

Stock solution of drugs and chemicals were prepared in DMSO (D2650, Sigma-Aldrich, Germany) to a concentration of 100 mM calpeptin (03-34-0051, Calbiochem, EMD Millipore, USA), 10 mM A23187 calcium ionophore (aka calcimycin, C7522, Sigma-Aldrich, Germany), 50 mM doxorubicin (D1515, Sigma-Aldrich, Germany), 100 mM PP2 (P0042, Sigma-Aldrich, Germany), 10 mM cytochalasin D (C8273, Sigma-Aldrich, Germany), 2 mM t-Boc-Leu-Met-

CMAC (A6520, Invitrogen, USA), and 10 mM CellTracker Green CMFDA (C7025, Invitrogen, USA). TNF-α (300-01A, Peprotech, USA) stock solution was prepared by dissolving 0.1 mg in 1 mL of 0.1% bovine serum albumin (or BSA, Sigma-Aldrich, Germany) in PBS. The stock solutions of all drugs were stored at -20°C. Mitomycin C (M0503, Sigma-Aldrich, Germany) stock solution, at a concentration of 1 mg/mL, was freshly prepared in sterile dH_2O on an experimental day before being sub-diluted using complete culture medium to achieve the final working concentrations for cell treatment. The solvent for preparing drug stock solution, i.e., DMSO or dH_2O, was added to the negative control at the same volume equivalent to that in the drug treatment group. The final percentage of DMSO did not exceed 0.1% v/v in any groups.

2.3 Cell growth curve analysis and evaluation of cell proliferation

Cell growth analysis was started by seeding two millilitres of cell suspension per well in 6-well tissue culture plates at the following seeding densities: $5x10^4$/mL for MDA-MB-231 cells, $1x10^5$/mL for MDA-MB-468, SUM149, MCF-7, and JIMT-1 cells, and $2x10^5$/mL for T47D and SKBR3 cells. The stably transfected cells established from section 2.6 were plated at the densities that were used for their parental cell lines. Cells in triplicate wells were trypsinised (section 2.1.2) and counted using a haemocytometer every 24 hours after cell seeding over a 96-hour time course. The growth curves were then plotted as the average total cell number vs time points on a linear scale and a semi-log scale. The doubling time of each cell line was calculated from log phases of their growth curves, using the following equation where N1 is an initial cell number; N2 is a final cell number; T is a time interval. Data represent the average cell doubling time ± standard deviation (SD) of at least two independent experiments, each performed in triplicate.

$$\text{Doubling time} = \text{T x } [\log(2)/(\log(\text{N2}) - \log(\text{N1}))]$$

To evaluate the effects of drug treatment on cell proliferation, cells were seeded in a 6-well plate at the seeding densities described above and treated by drugs the next day. Cells were treated with various concentrations of drugs:

calpeptin (25, 50, 100 and 200 µM for MDA-MB-231; 25, 50, 75, 100 and 200 µM for T47D), A23187 (0.5 and 1 µM for MDA-MB-231), cytochalasin D (0.01, 0.1, 1, 2, and 10 µM for both cells), CellTracker Green CMFDA (1 µM for T47D), and doxorubicin (a positive control at 0.25, 0.5, and 1 µM for both cells). DMSO at 0.1% was used as a negative control. At 24, 48 and 72 hours after exposure to drugs, cells from triplicate wells were trypsinised (section 2.1.2) and counted using a haemocytometer. The total cells in drug treatment wells were calculated as percentages of the total cells relative to control wells at each time point. Data represent the average percentage cell number ± SD of three independent experiments, each performed in triplicate. The dose- or time-response curves were generated by plotting the average percentages of cell number versus drug concentrations or the exposure time, respectively.

2.4 Western blotting

2.4.1 Cell treatment and preparation of cell lysate

Subconfluent cell cultures were harvested by trypsinisation (section 2.1.2). Cell pellets ($5x10^6$ cells) collected by centrifugation at 170 x g for 5 minutes were washed twice in 10 mL of PBS each time to removed residual serum proteins. After centrifugation, PBS was aspirated, and the pellets were lysed by incubation at 4°C for 10 minutes with 1 mL of RIPA lysis buffer (R0278, Sigma-Aldrich, Germany) supplemented with 1X Halt Protease Inhibitor Cocktail containing protease inhibitors, phosphatase inhibitors and EDTA (ThermoFisher, USA). Cell lysates were centrifuged at 4°C for 10 minutes at 15000 rpm to remove debris, and supernatants were collected and stored at -70˚C. Frozen lysates were thawed on ice prior to use and repeat freeze-thaw cycles avoided.

To assess the effect of serial cell passaging on levels of HA-tagged calpastatin isoform and total calpastatin expression in the stably transfected cells (231CAST1 and 231CAST2 cells established from section 2.6), they were subcultured ten times from master stocks (passage number 0 or P. 0). Cell lysates from subconfluent cell cultures at P. 2, 4, 6, 8, and 10 were collected

using the method described above. The effect on marker expression, of HA-tagged calpastatin and total calpastatin in 231CAST1 and 231CAST2 cells, was measured following short-term cell culturing once the selection agent G418 was removed. Cells were initially routinely cultured with the selection medium (750 µg/mL G418) to reach subconfluence before being harvested using trypsinisation (section 2.1.2) and split into three cultures. One culture was lysed to prepare a cell lysate that was used as a reference sample of Day 0, while the other two cultures were grown in parallel in G418-deficient or containing medium to reach subconfluence at Day 3. For each culture condition (with/without G418), cells from Day 3 were harvested and separated to prepare cell lysates and to continue culturing in a new flask with the same culture medium until Day 7. Cell lysates from Day 7 were then collected. This process of cell lysate preparation was repeated three times.

2.4.2 SDS-polyacrylamide gel electrophoresis (SDS-PAGE)

SDS-PAGE separates proteins according to their molecular weight by them migrating through a gel matrix by electrophoresis; smaller proteins migrate faster. The rate of migration, however, can be influenced by the structure and charge of the proteins that are eliminated by the use of sodium dodecyl sulphate (SDS) and polyacrylamide gel in SDS-PAGE, resulting in the formation of denatured proteins with a net negative charge. The protein separation by SDS-PAGE, therefore, is merely based on polypeptide chain length, which is proportional to the molecular weight of the proteins.

Protein samples were prepared by mixing cell lysate (13 volumes) with sample buffer (4X) (5 volumes), and reducing agent (2 volumes). Details of materials are shown in Table 2.1. Before loading the samples equally (15 or 20 µL) into each well of the gel, they were denatured using a heat block at 100°C for 5 minutes and cooled immediately on ice. Magic Marker (LC5602, Invitrogen, USA) and Rainbow Marker (GE Healthcare, USA) or SeeBlue® plus2 Prestained Standard (LC5925, Invitrogen, USA) were loaded into the same gel to allow comparison against known molecular weight proteins.

Table 2.1 Materials for determination of protein expression by Western blotting

Processes	The calpain-calpastatin system proteins in seven cell lines	HA-tagged calpastatin and the calpain-calpastatin system proteins in transfected cells
Sample preparation	A mix of cell lysate (13 volumes), NuPAGE® LDS sample buffer (4X) (ThermoFisher, USA) (5 volumes) and NuPAGE® Reducing Agent (ThermoFisher, USA) (2 volumes)	A mix of cell lysate (13 volumes), Bolt® LDS Sample Buffer (4X) (ThermoFisher, USA) (5 volumes), Bolt® Sample Reducing Agent (10X) (ThermoFisher, USA) (2 volumes)
Protein separation	Gels: NuPAGE®4-12 % Bis-Tris Protein Gels (ThermoFisher, USA)	Gel: Bolt® 4-12 % Bis-Tris Plus Gels (ThermoFisher, USA)
	Running buffer: 50 mL NuPAGE MOPS SDS Running Buffer (20X) (ThermoFisher, USA) and 950 mL dH_2O	Running buffer: 50 mL Bolt® MES SDS Running Buffer (20X) (ThermoFisher, USA) and 950 mL dH_2O
	Electrophoresis: 125 V for 120 minutes	Electrophoresis: 200 V for 35 minutes
Protein transfer	Transfer buffer: 25 mL NuPAGE® Transfer Buffer (20X) (ThermoFisher, USA), 100 mL methanol and 375 mL dH_2O.	Transfer buffer: 25 mL Bolt® Transfer Buffer (20X) (ThermoFisher, USA), 100 mL methanol and 375 mL dH_2O
	Electrophoresis: 10 V for 90 minutes	Electrophoresis: 25 V for 60 minutes

As defined in Table 2.1, for investigating the expression of calpain-calpastatin system proteins in seven breast cancer cell lines, proteins contained in cell lysates were isolated by electrophoresis at 125 V for 120 minutes using materials and reagents of NuPAGE® (ThermoFisher, USA). For the experiments assessing the expression of conventional calpains and calpastatin in stably transfected cell lines established from section 2.6, proteins were isolated using materials and reagents of Bolt® (ThermoFisher, USA) at 200 V for 35 minutes.

2.4.3 Immunoblotting

The separated bands of proteins bound on the gel were transferred onto a 0.2-micron nitrocellulose membrane (Millipore, USA) by electrophoresis in 1X transfer buffer (5 % v/v of 20X transfer buffer and 20 % v/v methanol in dH2O), as defined in Table 2.1. The membrane with transferred proteins was then placed into a 50-mL centrifuge tube containing 10 mL of blocking buffer (5% w/v nonfat milk (Marvel Dried Skimmed Milk, UK) in 0.1 % v/v Tween20/PBS),

and incubated at room temperature for 1 hour on a tube roller mixer. The blocking buffer was used to block the remaining surface of the membrane to prevent nonspecific binding of the detection antibodies during subsequent steps. To detect the expression of target proteins, the blocking buffer was replaced with the primary antibody diluted in blocking buffer. The dilution ratios and details of each antibody are listed in Table 2.2. The membrane was incubated with primary antibody at 4°C overnight on a tube roller mixer before being washed three times with 10 mL of 0.1 % Tween20/PBS for 5 minutes at room temperature.

Table 2.2 Sources and dilutions of primary antibodies used in Western blotting

Antibody	Company	Catalogue number	Host	Dilution
Mouse calpastatin monoclonal antibody (PI-11)	EMD Millipore, Merk, Germany	MAB3084	Mouse	1 in 1000
Mouse calpain 1 large subunit monoclonal antibody (P-6)	Santa Cruz Biotechnology, USA	sc-81171	Mouse	1 in 1000
Rabbit calpain-II (m-Calpain) polyclonal antibody	Chemicon®, Millipore, USA	AB1625	Rabbit	1 in 2500
Mouse calpain small subunit (μ-or m-Calpain) monoclonal antibody (P1)	EMD Millipore, Merk, Germany	MAB3083	Mouse	1 in 1000
Mouse HA tag monoclonal antibody [HA.C5]	Abcam, USA	ab18181	Mouse	1 in 1000
Mouse α-fodrin monoclonal antibody (AA6)	Enzo Life Sciences, USA	BML-FG6090-0100	Mouse	1 in 1000
Rabbit β-actin polyclonal antibody	Abcam, USA	ab8227	Rabbit	1:1000
Mouse β-actin monoclonal antibody [mAbcam8226](HRP)	Abcam, USA	ab20272	Mouse	1 in 5000
Polyclonal rabbit anti-mouse Immunaglobulin/HRP	Dako, USA	P0206	Rabbit	1:1000
680 Donkey anti-Mouse IgG (H+L)	IRDye®, LI-COR, USA	926-32222	Donkey	1 in 5000
800CW Donkey anti-Rabbit IgG (H+L)	IRDye®, LI-COR, USA	926-32213	Donkey	1 in 5000

To ensure equal loading amount amongst all samples, the level of β-actin expression was used as an internal loading control, with it being detected by incubating the membrane with an anti-human β-actin antibody (with or without horseradish peroxidase (HRP) tag) for 1 hour at room temperature. The HRP tagged β-actin antibody was applied in chemiluminescent Western blotting used in the selection of transfected monoclonal cells (section 2.6.3). The membrane was rewashed three times, with 10 mL of 0.1 % Tween20/PBS for 5 minutes at room temperature.

The nitrocellulose membrane was then incubated with secondary antibodies for 1 hour at room temperature to probe primary antibody-bound target proteins. The secondary antibodies used in the experiments were produced in a species different from those of the primary antibody, and cell lines. A combination of two fluorescent secondary antibodies (680 Donkey anti-Mouse IgG and 800CW Donkey anti-Rabbit IgG, IRDye®, LI-COR, USA) was applied for fluorescent Western blotting. In chemiluminescent Western blotting, proteins of interest were probed by a polyclonal rabbit anti-mouse immunoglobulin/HRP, while β-actin was probed by an HRP-tagged β-actin antibody, as mentioned previously. The membrane was washed three times, with 0.1 % Tween20 in PBS.

The fluorescently probed proteins were visualised using an Odyssey FC Imager (LI-COR Biosciences, USA). The fluorescence intensity was quantified by Image Studio Software Version 4.0. The quantitative expression of target proteins was calculated by normalising the signals of the target proteins to the signal of β-actin. Data represent the average protein expression or the percentage relative protein expression to the respective control ± SD of three independent experiments. Chemiluminescent Western blotting is considered to be more sensitive compared to fluorescent Western blot technique (Kondo *et al.*, 2018). The HRP-labelled proteins were visualised using the enhanced chemiluminescence (ECL) (GE Healthcare, Life Sciences, USA) with X-ray films (GE Healthcare Amersham™ Hyperfilm™ ECL, USA).

2.5 Measurement of mRNAs expression

2.5.1 Purification of total RNA from cultured cells

The working area, micropipettes and microcentrifuge were cleaned thoroughly with RNaseZapTM cleaning agent (Sigma-Aldrich, Germany) for removing RNase, and the materials used in the experiment were RNase-free, such as pipette tips, and collection tubes. Total RNA from each cell line was independently collected in triplicate from subconfluent cultured cells by using QIAamp RNA Blood Mini Kit (52304, Qiagen, Netherlands) or RNeasy Plus Mini Kit (74134, Qiagen, Netherlands) for the evaluation of CAST mRNA expression from the seven breast cancer cells or the established transfected cell lines, respectively.

2.5.1.1 Purification of total RNA from seven breast cancer cell lines

Total RNA was extracted, using the QIAamp RNA Blood Mini Kit (52304, Qiagen, Netherlands), following the manufacturer's instructions. Monolayer cells in a T25cm^2 flask were lysed directly by adding 350 µL of RLT buffer to ≤ 5x10^6 cells or 600 µL RLT buffer to 5x10^6-1x10^7 cells after completely aspirating cell-culture medium. The number of cells was assessed from a representative flask cultured in parallel. The cell lysate was collected using a sterile cell scraper (Falcon, USA) then vortexed or pipetted to mix. No cell clumps were visible before pipetting the lysate directly into a QIAshredder spin column placed in a 2 mL collection tube. The homogenised lysate was collected by centrifugation for 2 minutes at 13000 rpm. To precipitate nucleic acids, 350 µL of 70% ethanol was added to the homogenised lysate and mixed well by pipetting. The sample, including any precipitate which may have formed, was then carefully pipetted into a new QIAamp spin column in a 2 mL collection tube without moistening the rim and centrifuged for 15 seconds at 13000 rpm. The QIAamp spin column was transferred into a new 2 mL collection tube.

To eliminate gDNA contamination, on-column DNase digestion was performed using the RNase-Free DNase Set (79254, Qiagen, Netherlands). The spin-

column membrane was washed by adding 350 µL RW1 Buffer and centrifuged for 15 seconds at 10000 rpm. The flow-through was discarded. DNase I stock solution (10 µL) was gently mixed with 70 µL Buffer RDD by inverting the tube before being directly added to the QIAamp spin column membrane and placed on the benchtop (20-30°C) for 15 minutes. A volume of 350 µL RW1 Buffer was added to the QIAamp spin column then centrifuged for 15 seconds at 13000 rpm to remove DNA contamination.

The QIAamp spin column was washed twice by adding 500 µL of RPE Buffer and centrifuged at 13000 rpm for 15 seconds and 3 minutes, respectively. To eliminate the chance of possible Buffer RPE carryover, the QIAamp spin column was placed in a new 2 mL collection tube and centrifuged at 13000 rpm for 1 minute. The QIAamp spin column was then transferred into a 1.5 mL collection tube. To elute RNA from the column, RNase-free water (30-50 µL) was directly pipetted onto the QIAamp membrane and centrifuged for 1 minute at 13000 rpm. RNA in the collection tube was stored in -70°C for further cDNA synthesis.

2.5.1.2 Purification of total RNA from transfected breast cancer cell lines

RNAprotect Cell Reagent (76526, Qiagen, Netherlands) and RNeasy Plus Mini Kit (74134, Qiagen, Netherlands) were used in the preparation of total RNA from stably transfected breast cancer cell lines established from section 2.6. The culture media was first removed before subconfluent cultures in a T25cm^2 flask being washed three times with 3 mL PBS. To detach adherent cells, 500 µL RNAprotect Cell Reagent was directly added to cell monolayer. The mix of cells and RNAprotect Cell Reagent was pipetted up and down then stored in a 1.5 mL sterile Eppendorf tube at -80°C or directly performed isolation and purification of total RNA by using RNeasy Protect Mini Kit according to the following instructions. The mix of cells and RNAprotect Cell Reagent (1 volume) was transferred into a 15 mL centrifuge tube containing DNase/RNase free distilled water (9 volumes) before being centrifuged for 5 minutes at 4100 rpm. After centrifugation, the white cell pellet has appeared at the tube bottom. The supernatant was completely removed by pipetting, and the pellets were

loosened by flicking the tube. Cells were then lysed by adding Buffer RLT Plus (up to $5x10^6$ cells/ 350 µL RLT or $5x10^6$ to $1x10^7$ cells/ 600 µL RLT) and vortexing for 1 minute to completely dissolve pellets. The lysate was homogenised by transferring directly into a QIAshredder spin column placed in a 2 mL collection tube before centrifugation for 2 minutes at 13000 rpm.

To remove gDNA contamination, the homogenised lysate was transferred to a gDNA Eliminator spin column placed in a 2 mL collection tube and centrifuged for 30 seconds at 13000 rpm. To precipitate nucleic acids, a volume of 70% ethanol was added to the flow-through then mixed well by pipetting but not centrifuged. The sample, including any precipitate that may have formed, was transferred to an RNeasy spin column placed in a 2 mL collection tube before being centrifuged for 15 seconds at 13000 rpm. The RNA contained in the RNeasy spin column was washed using RW1 Buffer and RPE Buffer and extracted by RNase-free water by the processes described in section 2.5.1.1.

The RNA preparations were measured for both the amount of total RNA and their purity by using a Nanodrop spectrophotometer ND100 (ThermoFisher, USA). The ratio of absorbance at 260 nm and 280 nm were used to assess the purity of RNA; a ratio of ~2.0 is commonly accepted as pure for RNA (Desjardins & Conklin, 2010). The volume of the total RNA solution contained 1 or 2 µg RNA was prepared for further cDNA synthesis.

2.5.2 cDNA synthesis by reverse transcription

2.5.2.1 cDNA conversion for the seven breast cancer cell lines

Reverse transcription (RT) is the process by which RNA is converted into complementary DNA (cDNA) by the retroviral enzyme reverse transcriptase. One microgram of total RNA prepared from section 2.5.1.1 was reverse transcribed to cDNA by using oligo(dT)15 priming and the GoScriptTM Reverse Transcription System (A5000, Promega, USA). The RNA and primer mix was prepared in 0.2 mL PCR tubes using the components listed in Table 2.3

Table 2.3 Components of RNA sample preparation and reverse-transcription reaction mix.

Components	Volume (µl)
RNA sample preparation	
RNA (1 µg/reaction)	X µL
Oligo(dT)15 (0.5 µg/reaction)	1 µL
Nuclease-Free Water (to a final volume of 5 µL)	Y µL
Final volume	5 µL
Reverse transcription reaction mix	
Nuclease-Free Water (to a final volume of 15 µl)	X µL
GoScript™ 5X Reaction Buffer	4 µL
$MgCl_2$ (25 mM)	4 µL
PCR Nucleotide Mix (final concentration 0.5 mM each dNTP)	1 µL
Recombinant RNasin® Ribonuclease Inhibitor (40 u/µl)	0.5 µL
GoScript™ Reverse Transcriptase	1 µL
Final volume	15 µL

Five microlitres of RNA sample was placed into a preheated 70°C heat block for 5 minutes then immediately chilled on ice for at least 5 minutes. Each tube was centrifuged for 10 seconds using a microcentrifuge to collect the condensate and maintain the original volume. The reverse transcription reaction mix was prepared in a microcentrifuge tube to allow 15 µL for each cDNA synthesis reaction by combining the components of the GoScript™ Reverse Transcription System in the order listed in Table 2.3. Each component was combined, and the mix was then gently vortexed before dispensing into the reaction tubes. All procedures were performed on ice.

The 5 µL mix of RNA and primer was added to 15 µL reaction mix for a final reaction volume of 20 µL per tube. The transcription reaction was performed on a controlled-temperature heat block using the following conditions: 5 minutes at 25°C (annealing), 55 minutes at 42°C (extension), and 15 minutes at 70°C (to inactivate reverse transcriptase). The reaction tubes were frozen at -20°C for long-term storage before proceeding to a real-time quantitative polymerase chain reaction (RT-qPCR) (section 2.5.3.1).

2.5.2.2 cDNA conversion for transfected breast cancer cell lines

cDNAs of the stably transfected breast cancer cell lines were synthesised from 1 or 2 µg of the total RNA extracted as described in section 2.5.1.2 by using the RT^2 First Strand Kit (330404, Qiagen, Netherlands). To eliminate gDNA contamination, the gDNA elimination mix for each RNA sample was prepared by combining the components shown in Table 2.4. All components, including RNA, were mixed gently by pipetting up and down and centrifuged briefly. The mix was then incubated at 42°C for 5 minutes and placed immediately on ice for at least 1 minute.

Table 2.4 Components of gDNA elimination mix and reverse-transcription reaction mix

Components	Volume (µl)
gDNA elimination mix	
RNA (1 or 2 µg)	X µL
Buffer GE	2 µL
RNase-free water (to a final volume of 10 µl)	Y µL
Total volume	10 µL
Reverse-transcription reaction mix	
5X Buffer BC3	4 µL
Control P2	1 µL
RE3 Reverse Transcriptase Mix	2 µL
RNase-free water	3 µL
Total volume	10 µL

The reverse-transcription reaction mix was prepared from the components listed in Table 2.4. A 10 µL aliquot of the reverse-transcription mix was added into each reaction tube containing 10 µL genomic DNA elimination mix (1 or 2 µg RNA existed) and mixed gently by pipetting up and down. To synthesise cDNA, the transcription reaction was performed on a controlled-temperature heat block using the following conditions: incubated at 42°C for precisely 15 minutes (annealing and extension), then immediately incubated at 95°C for 5 minutes to stop the reaction. The reactions were maintained frozen at -20°C for long-term storage prior to RT-qPCR analysis described in section 2.5.3.2.

2.5.3 Real-time quantitative polymerase chain reaction analysis

2.5.3.1 CAST isoform expression in the seven breast cancer cell lines

Expression of calpastatin mRNAs, i.e., total CAST, CAST containing exon3 (CASTexon3), CAST1, CAST2 and CAST3, in seven breast cancer cell lines was evaluated relative to the expression of HPRT, a reference gene, using RT-qPCR. The gene expression levels were analysed using the relative standard curve method. Amplification of the target genes and a reference gene in samples took place alongside standard curve analysis, allowing the quantification of gene expression within the cell lines. Before studying CAST expression in all samples, optimisations of a serial dilution of the standard cDNA and sample dilution ratio were performed. A serial dilution of the standard (5, 1, 0.2, 0.04, 0.008, and 0.0016 µg) was prepared from JIMT-1 cell cDNA stock synthesised from 1 µg total RNA, while sample dilutions (1 in 20 and 1 in 50) were prepared from cDNA stocks of JIMT-1 and T47D cells. Following optimisation, as described in the section of results, a dilution of 1:70 was used for all samples, while a standard serial dilution defined above was remained to be used for creating standard curves.

A Stratagene MX3000p real-time cycler (Stratagene, USA) was used to perform RNA amplification and quantification. In a total volume of 10 µL reaction, 1 µL of each cDNA sample was amplified by the SYBR green detection method using 9 µL of SYBR master mix (0.5 µL of each forward and reverse primers, 5 µL of SYBR master mix (2X) (4309155, Life Technologies, USA), and 3 µL of RNase-free water (AM9935, Invitrogen, USA). Concentrations of all calpastatin primers in the reactions were 10 µM, while the concentration of HPRT primers was 2 µM. Sequences of specific oligonucleotide forward and reverse primers complementary to a specific sequence on the target genes, designed by Prof Tim Parr, School of Biosciences, are presented in Table 2.5.

Table 2.5 Sequences of specific oligonucleotide forward and reverse primers

Genes	Primers
HPRT	forward primer 5'-AAATTCTTTGCTGACCTGCTG-3'
	reverse primer 5'-TCCCCTGTTGACTGGTCATT-3'
Total CAST	forward primer 5’-ACCTGCAGATGACCAAGACCCCA-3’
	reverse primer 5’-TGCTTTGGAGCTGGAAGCAGCC-3’
CASTexon3	forward primer 5’-AACCAGCAAGTCTTCCAGTATGAA-3’
	reverse primer 5’-GTCCTTCCATCTGTTGGCTGA-3’
CAST1	forward primer 5’-CCGCCGCACCCA-3’
	reverse primer 5’-CCTTTCTTTTCTCCTGGTTTGGA-3’
CAST2	forward primer 5'-CCAGCCGGTTGTTGCC-3'
	reverse primer 5'-GGCGATTCACTGGTTTTTTCA-3'
CAST3	forward primer 5’-AGAGAGCTGGGCTGGAGCTC-3’
	reverse primer 5’-TTTTCAGGAGGTCTGCATTCCT-3’

The reactions for each sample were performed in triplicate in an optical 96-well reaction plate (ThermoFisher, USA). Three negative control samples, where RNase-free water was substituted for cDNA, were included in each run (no template control, NTC). Reaction conditions were started by heating to 95°C for 10 minutes to activate the AmpliTaq Gold® DNA Polymerase, followed by 40 amplification cycles consisting of 95°C for 15 seconds to denature the DNA, and 60°C for 1 minute to allow annealing of the primers and extension. After 40 cycles, samples were denatured, and melting curve analyses were taken over 40 cycles, in 1°C steps from 60°C to 95°C. Real-time PCR results were analysed using 7500 software v2.0.1. CAST expression in each cell line was presented relative to its HPRT reference gene content. Data represent the average expression of CAST or the average relative gene expression to the respective control ± SD of three independent experiments, each performed in triplicate.

2.5.3.2 CAST isoform expression in transfected cell lines

Expression of CAST1 or CAST2 in CAST-transfected cell lines was evaluated relative to the expression of HPRT, a reference gene, using RT-qPCR. To optimise standard serial dilution, standard curves of CAST1, CAST2 and HPRT

were created from a 2-fold standard serial dilution (18, 9, 4.5, 2.25, 1.125, 0.563, and 0.281 µg) of cDNA mix of 231CAST1 and 231CAST2 cells (1:1 ratio). cDNA of each cell line was reversed transcribed from 1 µg of total RNA. By running 40 PCR cycles using the protocol mentioned in section 2.5.3.1, the Ct values of CAST2 standards were detected at the late cycles (~30 and more) or undetectable (for 0.281 µg standard). In an attempt to increase CAST2 cDNA template, standard serial dilution was then prepared from only 231CAST2 cells' cDNA to generate standard curves of all investigated mRNA.

cDNA samples which reverse-transcribed from 2 µg of total RNA (section 2.5.2.2) were prepared as a 1 in 20, 1 in 5, or 1 in 40 cDNA dilution to measure the expression of CAST1, CAST2 or HPRT, respectively. A standard serial dilution prepared from the synthesised cDNA stock of 231CAST2 cells was used to create standard curves (CAST1 and CAST2: 100, 66.67, 44.44, 29.63, 19.75, and 13.17 µg; HPRT: 10, 5, 2.5, 1.25, 0.625, and 0.3125 µg). In a total volume of 10 µL reaction, 1 µL of each cDNA sample was amplified by SYBR green detection method using 9 µL of SYBR master mix (1 µL of each forward and reverse primers, 5 µL of SYBR Green ROX qPCR Mastermix (2x) (330523, Qiagen, Netherland), and 2 µL RNase-free water (AM9935, Invitrogen, USA)). Concentrations of HPRT, CAST1 and CAST2 primers in the reactions were 100, 100, and 50 nM, respectively. Three negative control samples, where the RNase-free water was substituted for cDNA, were included in each run. The amplification and quantification of genes, as well as melt curve analysis, were performed as described in section 2.5.3.1. Expression levels of CASTs were estimated from standard curves, as explained in section 2.5.3.1.

2.6 Establishment of stably transfected breast cancer cell lines overexpressing calpastatin isoforms

2.6.1 Optimisation of G418 concentration in the selection medium

Before transfection, the concentration of G418 selective antibiotic (Geneticin) (10131, Gibco, Life Technologies, UK) was optimised to select cells transfected with HA-tagged, GFP removed, pZsGreen1-N1 plasmids modified from

pZsGreen1-N1 plasmids (632448, Clontech, USA). A neomycin resistance cassette (Neo^r) contained in the plasmid allows stably transfected eukaryotic cells to be selected by G418. By that, optimal selection G418 concentration in complete medium (termed selection medium) should kill all untransfected cells within 7-10 days. For MDA-MB-231 cells, 750 µg/mL G418 supplemented culture medium was the optimal selection medium previously optimised by Dr Sarah Storr, a postdoctoral researcher in the group. The current study sought to confirm such data by repeating the optimisation twice, each in duplicate. Subconfluent cells (70%) in a 6-well tissue culture plate were treated by G418 at different concentrations (0, 200, 300, 400, 500, 600, 700, 750, 800, 900, 1000 µg/mL) for 7-10 days. Medium supplemented with/without G418 was refreshed every 3-4 days. Cells were examined visually, each day, by phase-contrast microscopy to ascertain the lowest concentration that could kill all parental cells within 7-10 days. Experiments with T47D cells were also conducted independently three times, in duplicate each time.

2.6.2 DNA transfection

From section 3.2.1, two breast cancer cell lines (MDA-MB-231 and T47D) were chosen to produce stably-transfected cells overexpressing calpastatin isoform 1, 2 or 3 following DNA transfection. DNA constructs of CAST1, CAST2 or CAST3 were designed by Dr Kirsty Jewell within Prof Tim Parr's Group, School of Biosciences. Cloning of CAST1, CAST2 or CAST3 cDNA genes into the HA-tagged, GFP removed, pZsGreen1-N1 plasmids was performed in the high-efficiency JM109 *Escherichia coli* (Promega, USA) by Dr Kirsty Jewell. Maps of pZsGreen1-N1 & HA-tagged, GFP-removed pZsGreen1-N1 plasmids and cDNA constructs of full-length calpastatin are shown in Appendix B (Figure 2B.1, Figure 2B.2, Figure 2B.3 and Figure 2B.4). Nucleotide sequences of HA-tagged CAST1, CAST2, or CAST3, as well as of a plasmid, are also present in Appendix B. Three different transfection reagents, i.e., FuGENE®HD (Promega, USA), Lipofectamine®3000 (Life Technologies, USA) or Viromer®Red transfection reagents (Lipocalyx, UK), were used to optimise the transfer of DNA constructs into MDA-MB-231 and T47D cells.

The transfection reagents are commonly applied to deliver RNA or plasmid DNA into cells *in vitro* by facilitating negatively charged nucleic acid genetic materials to overcome the electrostatic repulsion of the negatively charged cell membrane. Lipofectamine®, a chemical transfection formulation of cationic lipids, forms liposomes in an aqueous condition before interacting with nucleic acids to form the liposome-nucleic acid transfection complexes (lipoplexes) (Felgner *et al.*, 1994; Rao *et al.*, 2015). Liposomal or cationic lipid-based transfection reagents have dominated the field of nonviral gene delivery since 1987 (Rao *et al.*, 2015) and offer a wide range of applications; however, they may not be efficient in all cell types. Ambrosini *et al.* (1999), additionally, indicated the limitations of cationic lipid-based technology, including colloidal stability, cytotoxicity, and their effects on the lipid metabolism of the cell.

Nonliposomal transfection reagents, including FuGENE® HD and Viromer®Red, are an alternative to liposome-mediated transfection methods. These reagents include polymers that can form complexes with DNA or RNA (polyplexes) and other types of lipids that are capable of forming micelles in aqueous solutions. Viromer®Red is a transfection formulation of the polymers called polyethylenimine (PEI), which is the most highly studied cationic polymers and has been found to perform comparably to Lipofectamine® 3000 in transfecting diverse cells lines including glial cells. However, Viromer®Red requires further modification to minimalise the effects on cell viability (Rao *et al.*, 2015). FuGENE®HD is a chemical transfection formulation of cationic lipids that form micelles in aqueous solutions before forming complexes with DNA or RNA. FuGENE®HD is recognised as the most preferred transfection reagent, as indicated by its maximal transfection efficiency for several cell lines (MC3T3-E1, C3H10T1/2, HeLa, C2C12, Hep G2, and HCT116) compared to other six commercially available reagents, including jetPEI® (a formulation of PEI) and Lipofectamine®2000 (Yamano *et al.*, 2010). However, transfection efficiency comparison between FuGENE®HD and Lipofectamine®3000, to our knowledge, has not been tested.

A day before performing transfection, cells were seeded in a tissue culture plate to form 70% confluent cells in the following day. MDA-MB-231 cell were seeded by $3.6x10^5$, $1.8x10^5$, or $0.75x10^5$ cells/well in a 6-, 12-, or 24-well plate, respectively; T47D cells were seeded by $7x10^5$, $2.5x10^5$, $1x10^5$, or $1.5x10^4$ cell/well in a 12-, 24-, 48- or 96-well plate, respectively. On the day of performing transfection, the culture medium was replaced with Opti-MEM I reduced serum medium (without antibiotics) (ThermoFisher, USA). For optimisations, transfection reagent/DNA mixtures were prepared in different ratios (1.7-3.5 µL FuGENE®HD per 1 µg DNA; 1.5-3 µL Lipofectamine®3000 per 1 µg DNA; 0.4 µL Viromer®Red per 1 µg DNA). To prepare the mixtures from FuGENE®HD or Lipofectamine®3000 reagents, the reagent and DNA constructs were mixed in Opti-MEM medium as described in the manufacturer's instructions before incubation at room temperature for 10 or 5 minutes, respectively. To use Viromer®Red, Buffer RED supplied with the reagent was used as a diluent of the mixtures as described in the manufacturer's instructions; the mixture of transfection reagent and DNA constructs were incubated at room temperature for 15 minutes before use. The transfection reagent/DNA mixtures were then added dropwise to the wells while gently swirling the plate. The final amount of DNA construct in each well was 2000, 500, 250, and 88 ng for a 12-, 24-, 48- and 96-well plate, respectively. In each transfection experiment, the dilution of the transfection reagent without a DNA construct was added into a negative control well, which would have no living cell after selection.

At 24, 48 or 72 hours following transfection, the 750 µg/mL G418 selection medium, optimised from section 2.6.1, was applied to select transfected MDA-MB-231 or T47D cells (multiclonal populations). The selection medium was refreshed every 3-4 days. To validate and assess the success of transfection, cell lysates collected from the CAST-transfected cells were examined by Western blotting (section 2.4) for the expression of HA-tagged and total calpastatin with results compared to that of parental and mock-transfected control cells.

2.6.3 Selection of monoclonal cell populations expressing the highest level of HA-tagged calpastatin isoforms

Individual cells from the multiclonal mixed population were transferred into 96-well plates (1 cell/well) by adding 100 µL of 10 cells/mL cell suspension in each well and maintained cultured in the selection medium in an attempt to make monoclonal populations. The established monoclonal populations were assessed for HA-tagged and total calpastatin expression levels using chemiluminescent Western blotting, as described in section 2.4, to select the one with the highest levels of the proteins for using as cell models of the current project.

2.7 Immunofluorescence microscopy

Immunofluorescence (IF) microscopy is a widely-used technique for investigating intracellular localisation of proteins (Shakes *et al.*, 2012). In the current project, intracellular localisation of the HA-tagged full-length forms of calpastatin Type 1, Type 2 and Type 3 in the established transfected cell lines (section 2.6) was examined and compared with that of GFP-tagged truncated forms (only XL and L domains), encoded by exon3-containing/lacking variants, previously investigated by Dr Sarah Storr (unpublished data).

A day before performing immunolabelling of HA-tagged calpastatin, cells were seeded onto a collagen-coated round coverslip (Corning® BioCoat™, Germany), which was placed at the bottom of a 6-well plate. Cell plating density for MDA-MB-231 cell lines was $5x10^5$ cells/well and $8x10^5$ cells/well for T47D cell lines. After overnight incubation, the culture medium was gently removed using a 1000 µL micropipette, and adherent cells were gently washed with 500 µL of PBS for 5 minutes, three times. Cells were then fixed on the coverslip with 1 mL of 4% paraformaldehyde solution in PBS for 15 minutes at room temperature before being washed three times with 500 µL of PBS, for 5 minutes each time. Cells were incubated with a blocking buffer (10% normal goat serum (Sigma-Aldrich, Germany) and 0.3% Triton™ X-100 (Sigma-Aldrich, Germany) in PBS) for 60 minutes at room temperature. Following the blocking step, cells were

incubated in the dark at 4°C overnight with a mouse monoclonal antibody of HA tag (6E2) conjugated with green fluorescent Alexa® 488 dye (2350S, Cell Signalling Technology, USA); dilution ratio of the antibody was 1 in 800 in antibody dilution buffer (1% bovine serum albumin (A9418, Sigma-Aldrich, Germany) and 0.3% Triton™ X-100 in PBS). Cells were then washed with 1 mL of 0.1% Tween20/PBS for 5 minutes, three times. To visualise cell morphology, F-actin staining using phalloidin conjugated with far-red fluorescent Alexa Fluor™ 635 dye (A34054, Invitrogen, USA) (1:40 dilution in PBS) was performed in the dark at room temperature for 30 minutes followed by washing with 1 mL PBS for 5 minutes repeated three times. To visualise nuclei, cells were counterstained with a 1:5000 dilution in PBS of blue fluorescent Hoechst33258 dye (10 mg/mL) (H3569, Invitrogen, USA) in the dark for 10 minutes at room temperature then washed with 1 mL PBS for 5 minutes repeated three times. The coverslips covered with adherent cells were mounted with 50% glycerol in PBS and sealed with clear nail polish on a microscope slide before scanning using a Leica SP8 Confocal Laser Scanning Microscope (Germany). The laser excitation and emission wavelengths to detect HA tag, F-actin and nuclei are shown in Table 2.6. GFP (green fluorescent protein) contained in the truncated forms of calpastatin is a visual marker of calpastatin that can be directly detected by the confocal microscope without immunolabelling.

Table 2.6 Confocal laser scanning microscope settings

Target	Marker	Laser excitation	Emission
Nuclei	Blue fluorescent Hoechst33258 dye	405 nm	415 – 480 nm
HA-tag	Green fluorescent Alexa® 488 dye	488 nm	500 – 600 nm
GFP	GFP	488 nm	500 – 600 nm
F-actin	Red fluorescent phalloidin	635 nm	650 – 750 nm

2.8 t-Boc calpain activity assay

Calpain activity can be examined by various assays. Many of them detect the activity level in cell lysates. During the preparation of cell lysates, however, the subcellular structure is disrupted then causes the rapid association between

calpastatin and active calpain (Han *et al.*, 1999). To avoid false determination of cellular calpain activity, the current assay, therefore, assessed calpain activity in living intact cells by detecting fluorescent intensity of a cleaved fragment of a membrane-permeant calpain substrate t-BOC-Leu-Met (tert-Butyloxycarbonyl-L-Leucyl-L-Methionine-7-Amino-4-Chloromethylcoumarin or CMAC). This calpain substrate has an excitation/emission maxima ~330/403. After entering the cell, the coumarin moiety of t-Boc-Leu-Met conjugates to glutathione, resulting in the formation of t-butoxycarbonyl-Leu-Met-7-amino-4-methylcoumarin glutathione conjugate (t-Boc-Leu-Met-MAC-SG) which is nonfluorescent and membrane-impermeant (Rosser *et al.*, 1993). After cleavage by calpain, the cleaved fragments produce blue fluorescence with excitation/emission maxima ~351/430 from the coumarin moiety, allowing the measurement of intracellular calpain activity.

In the current work, $5x10^5$ MDA-MB-231 or $1x10^6$ T47D cells were plated in T25cm^2 tissue culture flasks. After 24-hour incubation, cells were treated with calpeptin (a calpain inhibitor) or A23187 (an inducer of calcium ions influx). Concentrations and incubation periods of calpeptin treatment were optimised for cells using 50 or 75 µM calpeptin treatment for 0.5, 1, 2 and 24 hours. To examine the effect of A23187 on calpain activity, MDA-MB-231 or the transfected cells made from section 2.6 were treated with a single dose of 0.5 µM A23187 for 24 hours, 2 µM A23187 for 30 minutes, or 50 µM calpeptin for 30 minutes as well as a double treatment of A23187 treatment condition as indicated followed by calpeptin for 30 minutes. Negative control cells were treated by 0.1% DMSO in the culture medium. Cells were then harvested by trypsinisation (section 2.1.2) and diluted to $5x10^5$/mL in 600 µL serum-free RPMI-1640 medium, which was aliquoted into two groups (250 µL each). Two microlitres of pre-warmed t-BOC-Leu-Met (2 mM stock) or 2 µL DMSO (final concentration = 0.8%) was added to each group to assess the total fluorescence intensity or to assess the background fluorescence intensity, respectively. The samples were transferred into a 96-well optical-bottom plate in duplicate wells (100 µL/well) before being red fluorescence intensity using a BMG FLUOstar

OPTIMA Microplate Reader (Germany) (pre-heated to 37°C). Fluorescence was continuously measured on a ten cycle kinetic window (excitation/emission 350/430, gain 2000, ~4 minutes interval) at 37°C.

To obtain the absolute fluorescence intensity of the cleaved t-BOC representing calpain activity, the background fluorescence intensity obtained from the reading of medium containing 0.8% DMSO was subtracted from the total fluorescence intensity of each sample. The reading of the first cycle baseline was then subtracted from the reading at each cycle. The percentage of calpain activity was calculated using the equation shown below. Data represent the average ± intra-experimental SD for one experiment or ± inter-experimental SD for at least two independent experiments, each in duplicate.

$$\text{Calpain activity } (\%) = \frac{\text{Fluorescence intensity of treated cells}}{\text{Fluorescence intensity of untreated cells}} \times 100$$

2.9 Clonogenic survival

The clonogenic survival assay can be used to evaluate the ability of single cells to form colonies, as represented by the plating efficiency (PE), or to examine cell survival by calculating the surviving fraction (SF) which represents the reproductive integrity of cells after receiving an experimental treatment. The colony-forming ability of each cell is represented by colony-forming units, each containing ≥50 cells. PE values of MDA-MB-231 or T47D cell lines were assessed by incubating cells at low density (e.g. 100, 200, 300, 400, 600, and 800 cells) per T25cm^2 tissue culture flask in six parallel set for each cell line. MDA-MB-231 or T47D cells were incubated undisturbed for 14 or 21 days, respectively, allowing single cells to form colony-forming units. The incubation time for both cell types has been optimised previously by PhD students in the group, including Dr Abdullah (2019). After incubation, the culture medium was aspirated, and flasks were gently washed with PBS. Colonies were then fixed with 50% methanol in 0.9% saline solution for 5 minutes, followed by absolute methanol for 10 minutes. Colonies staining was performed at room temperature for 2 hours using a 0.5% crystal violet solution. After aspirating the

staining reagent, flasks were washed gently in running tap water and left to dry at room temperature. Colony-forming units were counted. PE was generated from untreated controls and calculated as the following equation. The PE values of transfected MDA-MB-231 or T47D cells established from section 2.6 were assessed and compared to those of parental cells.

$$\mathrm{PE} = \frac{\text{Number of colonies formed}}{\text{Number of cells plated}} \times 100\%$$

SF values of MDA-MB-231 cells and the stably transfected 231Ctrl, 231CAST1 and 231CAST2 cells in response to the effects of doxorubicin (10 nM; a positive control), calpeptin (50 µM) or A23187 (0.5 and 1 µM) were assessed. Cells were initially seeded in triplicate wells at $1x10^5$ cells per well of a 6-well culture plate and incubated for 24 hours before being treated by drugs for 24 or 72 hours. DMSO (0.1%) was used as a negative control. After 24 or 72 hours of drug treatment, cells in triplicate wells were harvested by trypsinisation (section 2.1.2), pooled and seeded at low-density in T25cm^2 tissue culture flasks in six parallel set for each treatment. Flasks were incubated undisturbed for 14 days. SF values of cells following treatment were calculated according to the following equation (Woolston & Martin, 2011).

$$\mathrm{SF} = \frac{\text{Number of colonies formed after treatment}}{\text{Number of cells plated} \times \mathrm{PE}}$$

Data represent the average PE or SF ± SD of at least three independent experiments, with each experiment containing six parallel data sets.

2.10 Haptotaxis scratch-wound migration assay

The haptotaxis scratch-wound migration assay is a simple, reproducible technique (Cory, 2011) and is commonly used to study the collective and directional movement of populations of cells (Moutasim *et al.*, 2011). The assay is generally applied to evaluate basic cell migration parameters, e.g., speed, persistence, and polarity. In this assay, cells are grown to form a confluent monolayer, and a thin wound (cell-free area) is introduced by scratching with a pipette tip. At the wound edge, cells polarise and migrate into the wound gap.

Advantages of this technique are that there is no requirement of the use of gradient chambers or specific chemoattractants, and the assay produces a robust directional migratory response, even in cell types that do not express their strong responses in single cell migration assays (Cory, 2011). A disadvantage of this assay, however, is that it completely oversimplifies the complex process of invasion, lacking the tumour structural architecture and stromal components (Moutasim *et al.*, 2011). To truly assess migration, the influence of proliferation closing the wound has to be taken into account - this was accomplished by using mitomycin C, an anti-proliferative agent, for the experiment of MDA-MB-231 cells or 0.5% DBS containing culture medium for T47D cells' migration assessment.

In the current work, optimisation of tumour cell seeding density was performed before conducting scratch-wound assays to ensure a greater than 90% confluent monolayer was formed before drug treatment and wound production. Cells, suspended in complete culture medium at various densities, were seeded in 12-well tissue culture plates (1 mL/well) in duplicate wells. The seeding densities of parental MDA-MB-231 cells and their stably transfected cells (231Ctrl, 231CAST1 and 231CAST2) were tested at $2x10^5$, $2.5x10^5$, and $3x10^5$ cells/well; and $9x10^5$, $10x10^5$, $11x10^5$ and $12x10^5$/well were tested for parental T47D and their stably transfected cells (T47DCtrl and T47DCAST1).

Scratch wound migration assays were initiated by plating $2.5x10^5$/well of parental MDA-MB-231 and their transfected cells, or $10x10^5$/well of parental T47D and their transfected cell lines, to form confluent monolayers following a 24-hour incubation (as optimised previously). Before wound scratching, cells were pre-treated with PP2, cytochalasin D, calpeptin, or A23187 (concentrations are shown in Appendix B, Table B2.2) for 24 hours. PP2 and cytochalasin D were first optimised in an attempt to use as a cell migration inhibitor, while calpeptin and A23187 were examined for their effect on cell migration through regulating calpain activity.

After drug treatment, a 10 or 200 µL pipette tip was used to produce a wound at an angle of 90° on the confluent cell monolayer of T47D or MDA-MB-231 cells, respectively, through the centre of the well with one flowing movement to give a clean straight edge. A 200 µL pipette tip was too large to produce a proper width of T47D wound. Wound scratch at 90° angle to the tissue culture plate was shown to produce a more consistent and reproducible width as compared to wounds made by 45° angle scratch, investigated by Dr Yimin Zhang (a previous PhD student of the group) (Safuan, 2012). The monolayer was then rinsed twice with 500 µL of PBS to remove cellular debris and the released stimuli from ruptured cells, e.g., extracellular signal-regulated kinase, growth factors (Dieckgraefe *et al.*, 1997; Xu *et al.*, 2004; Yin *et al.*, 2007), and to smooth the edge of the scratch. Complete medium containing 10 µg/ml mitomycin C or 0.5% DBS containing medium was added to inhibit cell proliferation of MDA-MB-231 or T47D clones, respectively. To monitor the wound healing, two areas of a wound were then imaged at 100X magnification at 0 hours and the other time points after scratch, as indicated in the section of results. The wound areas were measured using Image J 1.43u software (National Institute Health, USA), and the percentage of wound closure at each time point calculated relative to the initial wound area obtained at 0-hour post-scratch. Data represent the average percentage of wound closure ± SD of at least two independent experiments, each in triplicate. Optimised experimental conditions for examining migration ability for each cell line are present in Appendix B, Table B2.2.

The effect of G418-removed culture medium, on migratory ability, was examined on the transfected 231Ctrl, 231CAST1 and 231CAST2 clones produced from section 2.6; these cells were routinely cultured with the selection medium (750 µg/mL G418). G418 was removed from the culture medium of the transfected cells for 0, 1, 3, 5, 7, 10 or 14 days before performing cell migration assessment.

2.11 Endothelial adhesion assays

2.11.1 Peripheral blood mononuclear cell isolation

Peripheral blood mononuclear cells (PBMCs) were used as a positive control in static adhesion assays (described in section 2.11.2). PBMCs were isolated from whole blood using a density-gradient centrifugation method, as described in the study of Safuan *et al.* (2012). Blood was collected, under informed consent, from three healthy donors (25 mL/donor), in a vacutainer tube (BD, UK) containing 170 IU heparin as an anticoagulant. PBMC isolation was performed in a sterile 50 mL centrifuge tube (Falcon, UK) by firstly adding 12.5 mL Histopaque® 1119 (Sigma-Aldrich, Germany) into a tube to separate the granulocytes, then tilting the tube and slowly adding Histopaque® 1077 (Sigma-Aldrich, Germany) on top of the layer of Histopaque 1119 to separate the mononuclear cells. Twenty-five millilitres heparinised blood was then layered on top of the Histopaque 1119 and Histopaque 1077, followed by centrifuging at 670 x g for 30 minutes, at room temperature. After centrifugation, several layers of cells and liquid were formed. The second layer, containing PBMCs (Figure 2.1), from three separate tubes of three donors was collected and pooled before being washed twice with RPMI-1640 growth medium supplemented with 10% DBS and cryo-preserved, as described in section 2.1.3, in RPMI-1604 medium containing 10% DBS and 10% DMSO (1×10^6 cell/mL/vial). Frozen PBMCs were stored in liquid nitrogen until use and were used throughout all endothelial adhesion assays to demonstrate reproducibility and appropriate endothelial response.

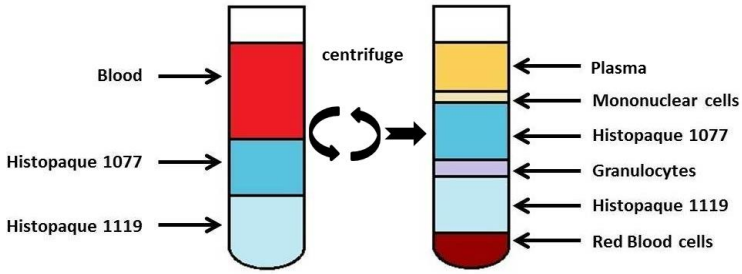


Figure 2.1 PBMC separation by density-gradient centrifugation method. Left tube represents blood layered on top of Histopaque 1077 and Histopaque 1119. Right tube represents the formed cell layers after centrifugation. PBMCs are in the second layer.

2.11.2 Static adhesion assays

Optimisation of endothelial cell plating density was carried out before conducting static adhesion assays, to ensure confluent monolayers were formed after 24 hours. Endothelial cell (EC) suspensions, in complete medium (500 µL), at different densities were plated in a 24-well plate and incubated for 24 hours. Seeding densities in the optimisations were $2.5x10^5$, $3x10^5$, and $3.5x10^5$ cells/mL for hMEC-1 blood vascular ECs and $1.5x10^5$, $2x10^5$, and $2.5x10^5$ for hTERT-LEC lymphatic ECs. After 24 hours incubation, $3x10^5$ cells/mL hMEC-1 and $2x10^5$ cells/mL hTERT-LEC cells produced confluent monolayers.

As a positive control, determination of PBMC adhesion to TNF-α-stimulated ECs (a 24-hour treatment with 5 ng/mL TNF-α) was assessed immediately before conducting each tumour cell adhesion assay to demonstrate that ECs were responding appropriately. ECs were seeded to form a confluent monolayer after 24 hours. Culture medium was then removed and replaced by the medium with or without 5 ng/mL TNF-α (300-01A, Peprotech, USA). After 24 hours of drug treatment, monolayers were washed once with medium and incubated for 5 minutes at 37°C with $1x10^5$ cells PBMCs in a total volume of 500 µL/well. Non-adherent cells were removed from the endothelial layer by washing twice with pre-warmed RPMI-1640 serum-free medium, and then the RPMI-1640 containing 10% DBS was added. Two fields at the central area marked by grid lines on the bottom of the plates were imaged using phase-contrast microscopy (Leica, Switzerland) at 100X magnification. Adherent PBMC number from the two areas were counted. Data represent the average sum of adherent cell number from the two fields ± SD of at least three independent experiments, with each experiment performed in triplicate.

For tumour cell adhesion assays, following 24 hours of EC seeding, the culture medium was removed, and monolayers were refreshed and incubated with complete medium for another 24 hours. On the day of investigating tumour cell adhesion, the experiment was started after ensuring that the ECs responded appropriately to the cytokine from the PMBC adhesion assay. Tumour cells, i.e.,

MDA-MB-231, T47D parental cells and their respective transfected cell lines (231Ctrl, 231CAST1, and 231CAST2; T47DCtrl, and T47DCAST1), which had been pre-treated with/without 50 µM calpeptin or 0.5 µM A23187 for 24 hours in T25cm^2 tissue culture flasks, were harvested by trypsinisation (section 2.1.2). Safuan *et al.* (2012) indicated that trypsin had no effect in altering tumour cell adhesion to ECs. One million tumour cells were labelled with 1 µM CellTracker Green CMFDA (ThermoFisher, USA) at 37°C for 30 minutes. CellTracker Green CMFDA had no effect on the proliferation of MDA-MB-231 (Safuan, 2012) or T47D cells after 72 hours of exposure (optimised in the current study). After labelling, the cell suspension was centrifuged at 170 x g for 5 minutes to remove CellTracker Green CMFDA, and tumour cell pellets were re-suspended in 10 mL of RPMI-1640 containing 10% DBS to produce 1x10^5 cells/mL cell suspension.

The endothelial cell monolayers were washed once with the medium before being incubated with 500 µL of tumour cell suspension at 37°C for 35 minutes. The incubation period for determining MDA-MB-231 cell adhesion to the ECs was optimised by Dr Safuan (2012), and the same incubation condition also applied in the studies with T47D cells. Non-adherent cells were then removed from the endothelial layers by washing twice with pre-warmed RPMI-1640 serum-free medium, followed by addition of RPMI-1640 containing 10% DBS. Two fields at the central area marked by grid lines on the bottom of the plates were pictured using a fluorescence microscope (Leica SP8, Switzerland) at 400X magnification, and the number of adherent tumour cells was counted from those two fields. Data represent the average sum of adherent cell number from the two fields or as the percentage of absolute adherent cell number relative to the respective control ± SD of at least three independent experiments, with each experiment performed in triplicate.

2.12 Statistical analysis

All results are presented as average ± intra-experiment standard deviation (SD) of one experiment or inter-experiment SD of at least two independent experiments, each performed in duplicate or triplicate. Inter-experiment SDs

were calculated as combined SD using the following formula where SD1 and SD2 are intra-experiment SD of individual experiment 1 and 2, respectively; n_1 and n_2 are the numbers of replicate in each experiment; y is the number of experiments. The formula was confirmed as appropriate following discussions between Dr Abhik Mukherjee, Professor Stewart Martin, and a biostatistician at the University of Nottingham, UK (Mukherjee, 2004).

$$\mathrm{SD}_{\mathrm{combined}} = \sqrt{\frac{\left[(n_1 - 1) \times {SD_1}^2 + (n_2 - 1) \times {SD_2}^2\right]}{n_1 + n_2 - y}}$$

IC50 values were calculated from dose-response curves using a GraphPad Prism7 non-linear regression model between logarithms of concentrations and normalised response. All of the figures were plotted using Microsoft Excel software version 2016 or GraphPad Prism7 software. Statistical analysis was performed using GraphPad Prism7 software. Data were analysed using the Student t-test for comparison between two groups or one-way ANOVA test for comparison between more than two groups. Statistical analysis was performed when at least three independent experiments were conducted. Values of $P < 0.05$ were considered statistically significant.

Chapter 3 Calpastatin isoform overexpression and intracellular localisation

3.1 Hypotheses and aims

Several studies, as described in section 1.3.5, have indicated that calpain and calpastatin expression is associated with breast cancer progression, chemotherapeutic response or clinical outcomes in different stages and subtypes of breast cancer (Storr *et al.*, 2011b; Storr *et al.*, 2011c; Storr *et al.*, 2012a; Storr *et al.*, 2016; Pu *et al.*, 2016). Expression of calpastatin protein or exon 3-containing CAST mRNA was negatively associated with the presence of LI, and ER^-, PR^-, or basal phenotypic tumours in early-stage breast cancer cases (Storr *et al.*, 2011b; Storr *et al.*, 2012a). Calpastatin expression also positively correlated with the levels of HER2 expression and HER2 gene amplification in HER2-positive patients treated with trastuzumab following adjuvant chemotherapy (Storr *et al.*, 2011c). Together, the heterogeneity and differential expression of the calpain-calpastatin system may present in different breast cancer cell types.

In addition, the correlation between calpastatin and calpain expression has been reported in various cancers, such as gastric cancer (Liu *et al.*, 2017), ovarian carcinoma (Storr *et al.*, 2012c; Zhang *et al.*, 2019), endometrial cancer (Salehin *et al.*, 2010), and breast cancer (Storr *et al.*, 2011c; Davis *et al.*, 2014; Storr *et al.*, 2016). In a cohort of large but operable breast tumours, treated with neoadjuvant chemotherapy, calpastatin expression was significantly correlated with the expression of calpain-1 but not with calpain-2 (Storr *et al.*, 2016). Paradoxically, in early-stage breast cancer cohorts, the expression of calpastatin correlated with the expression of calpain-9 (Davis *et al.*, 2014), and calpain-2, but not calpain-1 (Storr *et al.*, 2011c).

Calpain and calpastatin have been reported to colocalise in the cytoplasm with a slight multitude around the nuclear region (Gil-Parrado *et al.*, 2003). By IHC studies in breast cancer tissues, calpain-1, calpain-2 and calpastatin distributed

predominantly in the cytoplasm with some granularity and heterogeneity between adjacent tumour cells, but infrequently detected in the nucleus (Storr *et al.*, 2011c; Storr *et al.*, 2012a; Storr *et al.*, 2016). Although various calpastatin isoforms originate from a single CAST gene (section 1.3.2), the differential intracellular localisation of each isoform is mostly unknown.

Thus, the hypotheses of this chapter were as follow:

1. Calpain-calpastatin system proteins (calpain-1, -2, -4 and calpastatin) and calpastatin mRNA (total CAST, CASTexon 3, CAST1, CAST2 and CAST3) are differentially expressed in different breast cancer phenotypes.
2. Overexpression of calpastatin isoforms alters the expression levels of calpains.
3. Calpastatin isoforms localise in cytoplasm, nuclei, or at the perinuclear location.

Aims:

1. Examine expression of the calpain-calpastatin system proteins (calpain-1, -2, -4 and calpastatin) and CAST mRNA (total CAST, CASTexon 3, CAST1, CAST2 and CAST3) in different breast cancer phenotypes *in vitro*.
2. Establish stably transfected monoclonal populations of breast cancer cell lines overexpressing different calpastatin isoforms (Type 1, 2, and 3), using cell lines representing two different subtypes of breast cancer.
3. Examine the effect of calpastatin isoform overexpression on the expression levels of conventional calpain subunits (calpain-1, -2 and -4) in the transfected cell lines.
4. Investigate the effect of cell culture factors (serial cell passaging and influence of G418-presence and removal) on calpastatin expression or the migratory ability of the transfected cell lines.
5. Explore intracellular localisation of calpastatin isoforms in the transfected cell lines.

3.2 Establishment of stably transfected breast cancer cell lines overexpressing calpastatin isoforms

This study aimed to establish stably transfected monoclonal breast cancer cell clones overexpressing calpastatin isoform 1, 2 or 3 from two breast cancer cell lines representing different subtypes of breast cancer. Seven breast cancer cell lines from different subtypes were included in the study, i.e., basal-like (MDA-MB-231, MDA-MB-468 and the inflammatory SUM149 cells), luminal (MCF-7 and T47D), and HER2+ (SKBR3 and JIMT-1) breast cancer cells. Amongst all cells, two cells were selected to be transfected with cDNA constructs encoded for full-length calpastatin Type 1, 2, or 3 upon their low calpastatin protein or CAST mRNA expression but high calpain as well as rapid proliferation.

3.2.1 Selection of breast cancer cell lines to overexpress calpastatin isoforms

3.2.1.1 Cell growth characteristics of seven breast cancer cell lines

Growth curve analyses were conducted to evaluate the growth characteristics of breast cancer cell lines and included evaluating the population of doubling times (DTs). Generally, rapid proliferation is an important characteristic of cells, potentially contributing to the successful establishment of transfected monoclonal clones. In addition, the growth curve also allows the determination of the best time range for evaluating the effects of interventions such as drug treatment on the proliferation of cells (Assanga & Lujan, 2013). In the current study, population doubling times of seven breast cancer cell lines, summarised in Table 3.1, were calculated from the log phase of their growth curves (shown in Appendix C Figure C3.1 and Figure C3.2). Cells ranked from shortest to longest DTs were MDA-MB-231 cells (19.07 ± 0.76 hours), T47D (29.53 ± 1.48 hours), MDA-MB-468 (32.15 ± 0.24 hours), JIMT-1 (37.19 ± 3.28 hours), MCF-7 (38.29 ± 4.98 hours), SUM149 (42.88 ± 1.18 hours), and SKBR3 (74.45 ± 2.07 hours), respectively.

Table 3.1 Doubling times of breast cancer cell lines calculated from current data and reviewed from publications

Cell lines (subtype)	DTs from current data (hours)	DTs from publications (hours)
MDA-MB-231 (TNBC/ basal-like)	19.07 ± 0.76 (n=3)	20.00 ± 1.60 (Abdullah, 2019), 27.78 ± 5.14 (Limame *et al.*, 2012), 28.1 ± 1.2 (Watanabe *et al.*, 2001)
MDA-MB-468 (TNBC/ basal-like)	32.15 ± 0.24 (n=2)	29.9 ± 0.5 hours (Watanabe *et al.*, 2001), ~30-40 hours (DSMZ),
SUM149 (TNBC/ basal-like/ inflammatory type)	42.88 ± 1.18 (n=2)	33.95 hours (SIB, 2019)
T47D (luminal)	29.53 ± 1.48 (n=3)	31.1 ± 0.6 hours (Watanabe *et al.*, 2001), 34.00 ± 0.51 hours (Abdullah, 2019)
MCF-7 (luminal)	38.29 ± 4.98 (n=2)	34 hours (Silva *et al.*, 2013), 35 hours (Maldonado *et al.*, 2014), 38.5 hours (Yue *et al.*, 2012), 44.2 hours (Risinger *et al.*, 2015)
SKBR3 (HER2+)	74.45 ± 2.07 (n=2)	~2-3 days (Stengl *et al.*, 2017), 65.1 hours (Yue *et al.*, 2012)
JIMT-1 (HER2+)	37.19 ± 3.28 (n=2)	~30-40 hours (DSMZ)

Subtypes of breast cancer cell lines are reviewed from Tanner *et al.* (2004), Subik *et al.* (2010), Barnabas and Cohen (2013), Menon *et al.* (2014), and Mota *et al.* (2017). DTs is doubling times; TNBC is triple-negative breast cancer; n is the number of independent experiments.

Table 3.1 shows the comparable cell doubling times of seven cell types between calculated from the current data and indicated in publications, indicating that all seven cell lines behaved properly, and the experimental technique was reliable. Cells were further examined for their expression of calpain-calpastatin system proteins and CAST mRNA to select the cell models for transfection.

3.2.1.2 Expression of the calpain-calpastatin system proteins across seven breast cancer cell lines

Quantitative analysis of the calpain-calpastatin system protein expression provided important information to choose two breast cancer cells expressing low calpastatin but high calpains (calpain-1, -2 and -4) to be used as cell models for calpastatin isoform overexpression by DNA transfection. The intrinsic expression of the proteins of interest in the different cell lines was quantified by fluorescent Western blotting (section 2.4). Results are presented as the relative expression ratio of the target protein to β-actin in Figure 3.1.

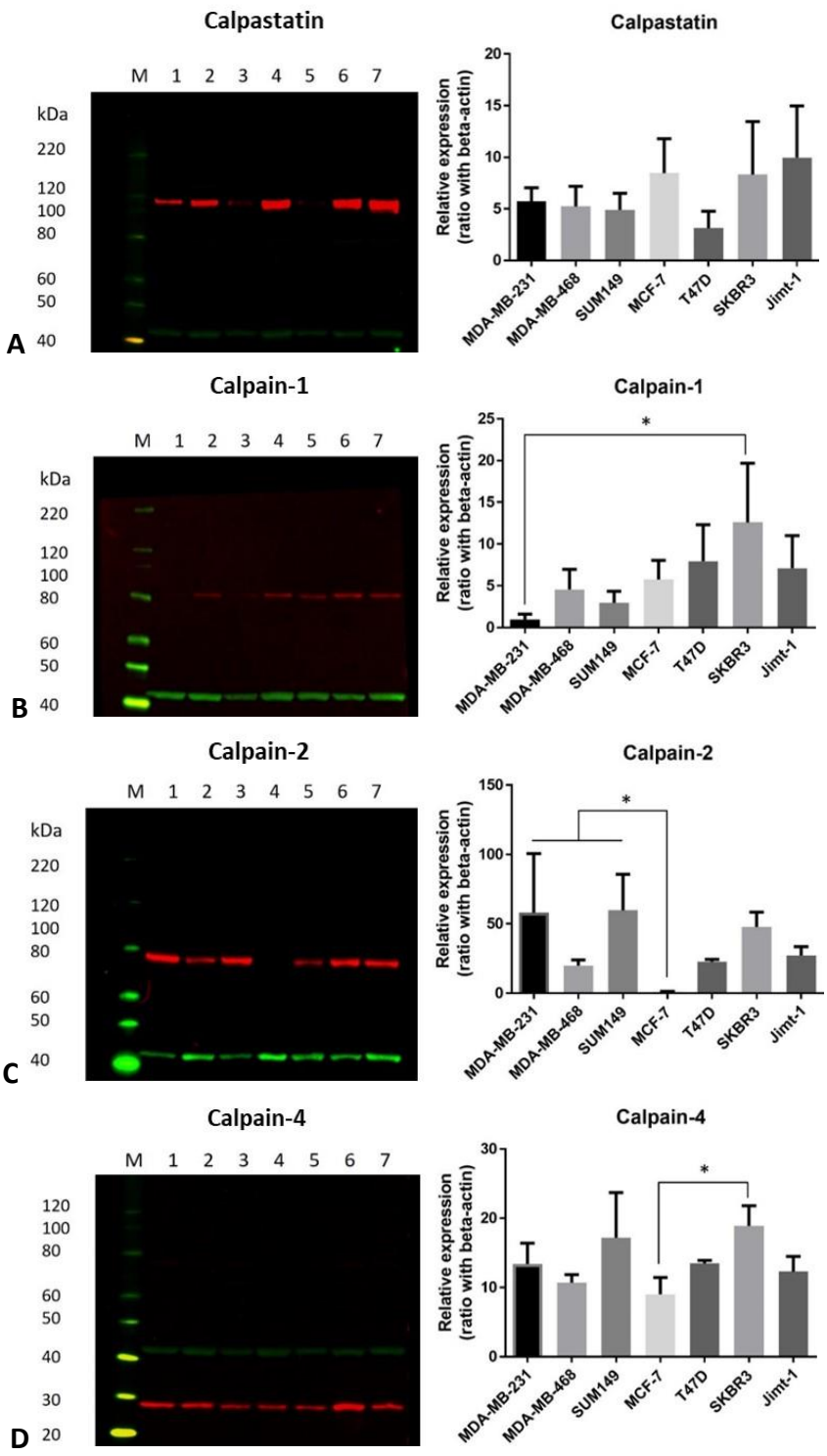


Figure 3.1 Quantitative analysis of the calpain-calpastatin system protein expression across seven breast cancer cell lines by Western blotting. Lysates were independently prepared in triplicate from different passages. Representative blots of three independent experiments are presented. β-actin was used as the sample loading control (42 kDa, green bands). Red bands indicate (A) calpastatin (100-120 kDa), (B) calpain-1 (82 kDa), (C) calpain-2 (80 kDa) and (D) calpain-4 (28 kDa). Lane M: protein markers, Lane 1: MDA-MB-231, Lane 2: MDA-MB-468, Lane 3: SUM149, Lane 4: MCF-7, Lane 5: T47D, Lane 6: SKBR3, and Lane 7: JIMT-1. Relative expression of (A) calpastatin, (B) calpain-1, (C) calpain-2 and (D) calpain-4 are presented as ratios to β-actin expression. Data represent the average ± SD of three independent experiments, each performed without replicate. P-values express the level of statistical differences between the two groups; * $P < 0.05$.

Calpastatin, as shown in Figure 3.1-A, had duplicate bands localised between 100 and 120 kDa, representing the expression of various calpastatin isoforms that show heterogeneity in molecular weights (Parr *et al.*, 2001b). The duplicate bands of calpastatin were also observed previously by the PhD projects of the current group in the various breast (Pu, 2016), and ovarian cancer cell lines (Zhang, 2018). The relative levels of calpastatin were not significantly different amongst the seven breast cancer cells. T47D cells showed the relatively lowest level of the protein followed by all basal-like types, including MDA-MB-231, MDA-MB-468 and SUM149, then MCF-7, SKBR3 and JIMT-1, respectively (Figure 3.1-A).

In the study of calpains, the relatively highest level of calpain-1 (Figure 3.1-B) was detected in SKBR3 cells, followed by T47D, JIMT-1, MCF-7, then the basal-like MDA-MB-468, SUM149, and MDA-MB-231 cells, respectively. A significant difference of calpain-1 expression was observed between SKBR3 and MDA-MB-231 cells (P = 0.0251). Calpain-2 levels in MDA-MB-231 and SUM149 cells were relatively highest amongst all cells and approximately 50-fold higher than MCF-7's expression (P = 0.0375 and 0.0304 respectively), which was barely detectable. Relative moderate levels of calpain-2 were detected in SKBR3, JIMT-1, T47D, MDA-MB-468 cells, respectively (Figure 3.1-C). The levels of calpain-4 from high to low were found in SKBR3, SUM149, T47D, MDA-MB-231, JIMT-1, MDA-MB-468, and MCF-7, respectively (Figure 3.1-D). A significant difference in calpain-4 expression was found only between the highest level in SKBR3 and the lowest level in MCF-7 (P= 0.0256).

Briefly, luminal T47D and basal-like subtype cells (MDA-MB-231, MDA-MB-468 and SUM149) were the cells of choices for establishing cells overexpressing calpastatin isoforms, as they were ranked the first and second places, respectively, amongst all cells in expressing the lowest calpastatin expression. T47D cells expressed the medium-to-high level of all calpains (calpain-1, -2 and -4) relative to the other cells. Meanwhile, all basal-like subtype cells expressed comparable levels of calpain-1 and -4, while the highest calpain-2 expression

was observed in MDA-MB-231 and SUM149 cells amongst all seven cells. To select two cells for overexpressing calpastatin isoforms, supportive data acquired from the RT-qPCR analysis of CAST mRNAs expression shown in the following section 3.2.1.3 were also applied.

3.2.1.3 Expression of CAST mRNAs across seven breast cancer cell lines

To select two breast cancer cells expressing low CAST mRNA expression for overexpressing calpastatin isoforms, RT-qPCR analyses for quantifying the expression levels of total CAST, CAST-containing exon3 (CASTexon3), CAST1, CAST2 and CAST3 were performed in seven breast cancer cells lines defined in section 3.2.1.2, using the relative standard curve method (section 2.5). Standard curves of CASTs and HPRT reference gene were produced from a standard serial dilution prepared from cDNA of JIMT-1 cells, the cells that expressed the highest level of calpastatin protein amongst all seven cell types (section 3.2.1.2).

3.2.1.3.1 Optimisation of a standard serial dilution and sample dilution

A standard serial dilution and sample dilution were initially optimised. As shown in Figure 3.2-A and -B, a standard serial cDNA dilution (5, 1, 0.2, 0.04, 0.008, and 0.0016 µg) prepared from JIMT-1 cells' cDNA stock solution was used to create standard curves of total CAST and HPRT mRNA. The amplification efficiencies (%E) of both total CAST (E = 115.764%) and HPRT mRNA amplification (E = 100.686%) were around 90-110%, which is the range of reliability of quantitative PCR analysis (Broeders *et al.*, 2014). A strong linear correlation between cycle threshold (Ct) values and log quantities of total CAST or HPRT was observed and indicated by $R^2 > 0.99$. This indicates that the experimental design used in the current work was optimal.

The current work also aimed to optimise the dilution ratio of cDNA samples that made the Ct values fell near the middle of the range of the standard curves. cDNA stock solution of the cells expressing the highest and lowest levels of calpastatin protein amongst all seven cell lines (JIMT-1 and T47D cells

respectively; section 3.2.1.2) was diluted 1:20 or 1:50 before being assessed the expression of total CAST and HPRT (Figure 3.2).

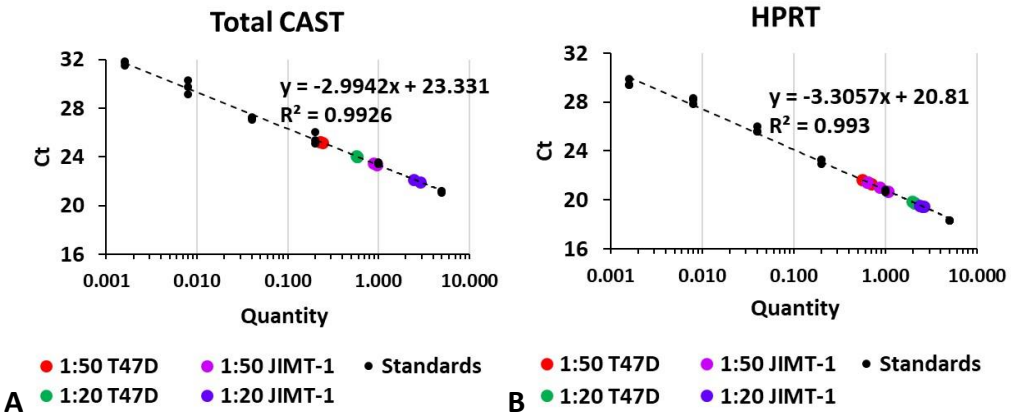


Figure 3.2 Optimisation of a standard serial dilution and sample dilution for RT-qPCR analysis. Standard curves of (A) total CAST and (B) HPRT were created as the relationship between the cycle threshold (Ct) values and log quantities of cDNA. A standard serial dilution (5, 1, 0.2, 0.04, 0.008, and 0.0016 µg) was prepared from JIMT-1 cells' cDNA stock (black spots). Samples were prepared as 1:50 and 1:20 dilution solution from T47D cells' cDNA stock solution (red and green spots, respectively) or JIMT-1 cells' cDNA stock solution (purple and blue spots, respectively). In the linear equation, y is Ct value, and x is log quantity. Data represent Ct values of each standard and sample from one experiment performing in triplicate.

As demonstrated in Figure 3.2-A and -B, the Ct values of all samples were present at the lower part of the standard curves, even the samples of T47D cells diluted 1:50 (red spots) which was assumed to have the lowest content of total CAST mRNA. Meanwhile, the Ct values of the JIMT-1 samples diluted 1:20 were present around the edge of the standard curves (blue spots). Therefore, in the following experiments, cDNA samples should be more diluted by using a 1:70 dilution ratio, while standard curves were remained to produce from a standard serial dilution used in optimisation.

3.2.1.3.2 CAST mRNA expression across seven breast cancer cells

Expression levels of total CAST, CASTexon3, CAST1, CAST2, CAST3, and HPRT reference gene in seven breast cancer cell lines were measured and calculated using the linear equations of standard curves, as shown in Table 3.2. R^2 values at > 0.9 were observed for all standard curves, indicating a linear correlation between the cycle threshold (Ct) value and log quantity of all mRNA. The amplification efficiencies of most PCR reactions (total CAST, CAST1 and CAST3)

fell in the ideal range for quantitative analysis (90-110%; Broeders *et al.*, 2014). Although the efficiencies of PCR reactions of CASTexon3 (E = 116.567%), CAST2 (E = 78.588%) and HPRT (E = 75.539%) were slightly out of the range, the information required to compare those mRNA expression levels across seven cell lines were obtained.

Table 3.2 Linear equations of standard curves and amplification efficiencies of PCR reactions for evaluating CAST and HPRT mRNA expression in seven breast cancer cell lines

Genes	Linear equations of the standard curves	R^2	Efficiencies of PCR reaction (%)
Total CAST	$y = -3.301x + 21.559$	0.977	100.868
CASTexon3	$y = -2.980x + 29.584$	0.971	116.567
CAST1	$y = -3.347x + 23.034$	0.994	98.977
CAST2	$y = -3.971x + 22.359$	0.924	78.588
CAST3	$y = -3.560x + 24.48$	0.952	90.955
HPRT	$y = -4.092x + 28.622$	0.968	75.539

In the linear equation, y is Ct value, and x is log quantity.

Figure 3.3 displays CAST mRNA expression levels as ratios to HPRT levels. Figure 3.3-A shows that the lowest level of total CAST mRNA was detected in T47D (relative expression (R) = 0.36), followed by SUM149 (R = 0.5), MDA-MB-231, JIMT-1, and MDA-MB-468 (R < 1), then SKBR3 and MCF-7 cells (R > 1). T47D cells' total CAST expression was significantly different from that in SKBR3 and MCF-7 cells (*P* = 0.0296 and 0.0041 respectively), while the level of total CAST mRNA in SUM149 cells was significantly lower than that in MCF-7 cells (*P* = 0.0152). The lowest expression of CASTexon3 was also observed in T47D cells (R = 0.1) followed by SUM149 (R = 0.4), MDA-MB-468 cells (R = 0.8) then MCF-7, SKBR3, JIMT-1 cells (R ~ 1), and lastly MDA-MB-231 cells (R = 6.4), which expressed CASTexon3 to a level that was significantly higher than the expression in all other cell lines (*P* < 0.0001) (Figure 3.3-B). Besides MDA-MB-231, T47D cells' CASTexon3 expression was statistically different from that in MCF-7, SKBR3 and JIMT-1 cells (*P* = 0.0097, 0.0090 and 0.0050, respectively), whereas such expression in SUM149 cells was different from that in JIMT-1 cells (*P* = 0.0473).

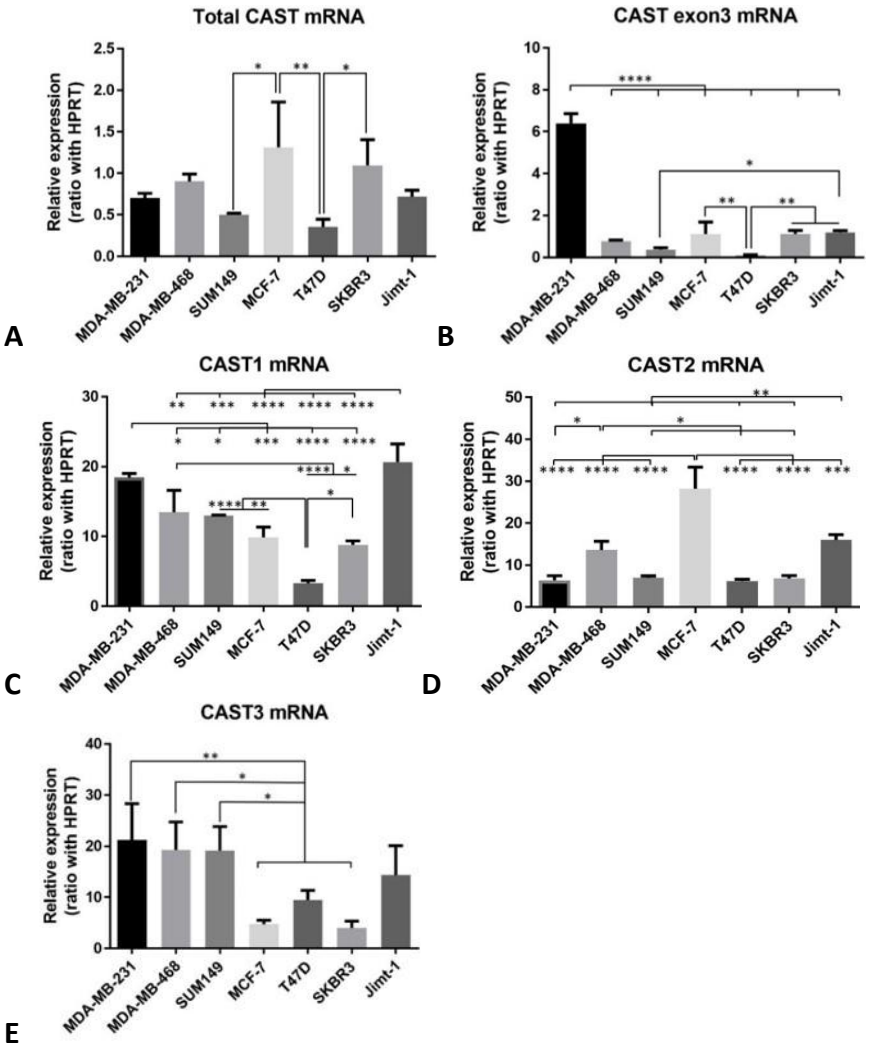


Figure 3.3 Quantitative analysis of CAST mRNA expression across seven breast cancer cells by RT-qPCR. Samples were independently prepared in triplicate from different passages, and each was assessed mRNA expression in triplicate. Relative expression of (A) total CAST, (B) CASTexon3, (C) CAST1, (D) CAST2, and (E) CAST3 was presented as ratios to HPRT expression. Data represent the average ± SD of three independent experiments, each in triplicate. P-values were assessed for showing the level of statistical differences between the two groups; * $P < 0.05$, ** $P < 0.01$, *** $P < 0.001$, and **** $P < 0.0001$.

T47D's CAST1 expression (R ~ 2) was the lowest amongst all cell lines followed by SKBR3, MCF-7 (R = 8-9), SUM149, MDA-MB-468 (R ~ 13) then MDA-MB-231 (R = 18.4) and JIMT-1 cells (R = 20.7), respectively (Figure 3.3-C). The CAST1 expression level of T47D cells was significantly lower than the levels detected in all other cells (*P*-values presented in Figure 3.3-C). The expression in SKBR3 cells was significantly different only to the first three cells expressing the highest level of CAST1, i.e., JIMT-1, MDA-MB-231, and MDA-MB-468 cells ($P <$ 0.0001, < 0.0001 and 0.0458 respectively). The levels in JIMT-1 and MDA-MB-231 cells were significantly different from the expression in all other cells. For

CAST2 expression (Figure 3.3-D), the lowest level of CAST2 was found in T47D, MDA-MB-231, SKBR3, and SUM149 (R ~ 6-7) followed by MDA-MB-468 and JIMT-1 (R ~ 14-16), and finally MCF-7 cells (R ~ 28). The CAST2 levels of MCF-7 or JIMT-1 cells were significantly higher than the level detected in all other cell lines, while MDA-MB-468 cells significantly expressed CAST2 in different levels from all cells except JIMT-1 (description of *P*-values presented in Figure 3.3-D). The lowest CAST3 expression levels were detected in SKBR3 and MCF-7 cells (R ~4), followed by T47D (R = 9.5), then JIMT-1 (R ~14), and, lastly, basal-like SUM149, MDA-MB-468, and MDA-MB-231 cells, respectively (R ~ 19-21) (Figure 3.3-E). The highest content of CAST3 detected in the top three cells statistically differed from the levels expressed in the last bottom two cells, MCF-7 and SKBR3 lines (description of *P*-values presented in Figure 3.3-E).

In summary, based upon the results from the current section 3.2.1 two cell lines, representing different breast cancer subtypes, were chosen to overexpress calpastatin isoforms. One of the selected cells was luminal T47D cells due to their lowest calpastatin expression and medium-to-high levels of all conventional calpain subunits (calpain-1, -2 and -4) relative to all other six cells (section 3.2.1.2). In addition, the RT-qPCR analysis of CAST mRNA expression (section 3.2.1.3) provided supportive information for choosing T47D cells as a cell model – all CAST mRNA levels in T47D cells were detected either in the relatively lowest or very low levels compared to other cells. The basal-like cells (MDA-MB-231, MDA-MB-468 and SUM149) expressed the lowest levels of calpastatin following T47D cells. These three cells expressed similar levels of calpain-1 and -4, while amongst all seven cells, the highest calpain-2 expression was observed in MDA-MB-231 and SUM149 cells. MDA-MB-231 and SUM149 cells, generally, expressed similar levels of all investigated CAST mRNA, except for CASTexon3 and CAST1 that were detected at the lower level in SUM149 cells. However, MDA-MB-231 cells have been found to grow approximately two times faster than SUM149 cells (DTs = 19.07 and 42.88 hours respectively; section 3.2.1.1), suggesting a higher potential in MDA-MB-231 cells to establish transfected monoclonal populations after DNA transfection. T47D cells also

proliferated rapidly. Amongst seven cells, T47D doubling time (29.53 hours) was ranked a second place behind MDA-MB-231 cells (section 3.2.1.1). Therefore, the luminal T47D and the basal-like MDA-MB-231 cells were selected to overexpress calpastatin isoforms in the following section 3.2.2.

3.2.2 Calpastatin DNA transfection and selection of transfected monoclonal cells

MDA-MB-231 and T47D cells were used to generate monoclonal cell models overexpressing full-length calpastatin Type 1, Type 2, and Type 3 by DNA transfection technique (section 2.6). Before transfection, the concentration of the antibiotic G418 was optimised to select the transfected cells. Non-transfected T47D and MDA-MB-231 cells were observed to be killed using 750 µg/mL G418 within 7 and 10 days, respectively.

MDA-MB-231 and T47D cells were transfected by the DNA constructs encoding for HA-tagged calpastatin Type 1, 2 or 3, using transfection reagents (Lipofectamine®3000, Fugene®HD, and Viromer®Red). HA-tagged, GFP removed, pZsGreen1-N1 plasmid (an empty vector) was also transferred into the cells to produce mock-transfected controls. Transfection was performed with various dilution ratios between DNA constructs and the transfection reagents, various incubation periods (24-72 hours) in different multiple-well cell culture plates, as defined in Appendix C (Table C3.1 and Table C3.2). Areas of multiple-well cell culture plates seemed to matter to transfection in T47D cells, as discussed further in Chapter 5. The transfected multiclonal populations were then selected and expanded by complete culture medium supplemented with 750 µg/mL G418 before being examined for HA-tagged calpastatin isoform expression to confirm transfection using Western blotting (section 2.4). Single cell clones were then generated and tested for HA-tagged calpastatin isoform expression, and the clones showing the highest expression were used as cell models for the current project.

3.2.2.1 Transfected monoclonal MDA-MB-231 clones

MDA-MB-231 cells were successfully transfected by the DNA constructs of the empty vector (3874 bp) and CAST2 (6306 bp) by the same condition - a 48-hour incubation of a 1.7: 1 ratio of Fugene®HD : DNA in a 12-well plate. Amongst all, a CAST1 DNA construct (6351 bp) was the largest one and could not be delivered into MDA-MB-231 cells by such conditions but by a 48-hour transfection with 1.5:1 and 3:1 of Lipofectamine®3000: DNA in a 24-well plate to produce multi-clonal populations A and B, respectively.

From the multiclonal population of mock-transfected MDA-MB-231 control (231Ctrl), five 231Ctrl clones were established, and clone 1 was chosen due to its morphology that, amongst all clones, looked the most similar to the parental cells. To confirm the transfection of CAST1 in MDA-MB-231 cells using Western blotting, firstly, a positive control lysate of HEK293 cells transfected with an HA-tagged minigene (HEK293-HA tag) was used to show that the anti-HA tag antibody used in this study was specific. An HA-tagged protein expressed in HEK293 cells was detected at around 60 kDa by Western blotting (Figure 3.4-A). As expected, MDA-MB-231 parental cells did not express the HA-tagged protein (Figure 3.4-A) but expressed total calpastatin (100-120 kDa, Figure 3.4-B). β-actin used as the sample loading control was detected at similar expression levels in all samples at 42 kDa. Both multiclonal CAST1-transfected MDA-MB-231 (231CAST1) populations A and B overexpressed total calpastatin compared to parental MDA-MB-231 positive control cells (Figure 3.4-B). However, the population A expressed HA-tagged calpastatin (100-120 kDa), representing calpastatin isoform 1 expression, at a higher level compared to the population B (Figure 3.4-A). Therefore, monoclonal cell selection was performed starting from the population A. Amongst all eleven 231CAST1 clones established from the multiclonal population A, eight of them expressed HA-tagged calpastatin. 231CAST1 clone 5, showing the highest level of the HA-tagged protein (Figure 3.5-A) and overexpressing total calpastatin (Figure 3.5-B) relative to the negative controls (MDA-MB-231 and 231Ctrl clone1), was selected and used as a cell model in the current project.

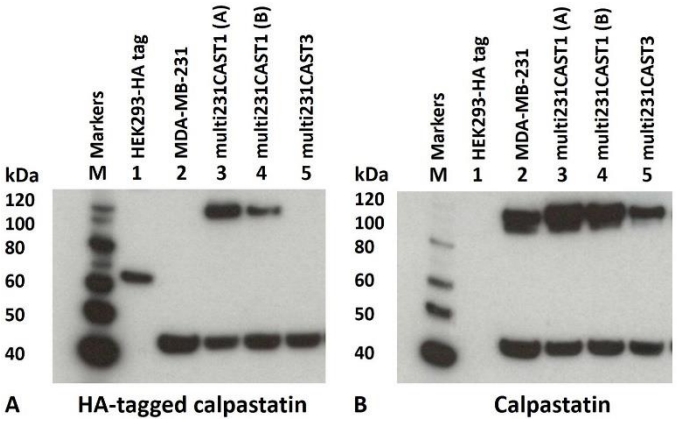


Figure 3.4 HA-tagged and total calpastatin expression in CAST1- and CAST3-transfected multiclonal MDA-MB-231 populations detected by Western blotting. Blots of the experiments are presented. Both (A) HA-tagged and (B) total calpastatin localise at 100-120 kDa. β-actin was used as the sample loading control (42 kDa). Lane M: protein markers, Lane 1: a positive control for HA tag expression - HEK293 cells transfected with HA-tagged minigene (HEK293-HA tag), Lane 2: a positive control for total calpastatin expression - parental MDA-MB-231 cells, Lane 3-4: multiclonal 231CAST1 populations A and B (multi231CAST1(A) and multi231CAST1(B) respectively), and Lane 5: multiclonal 231CAST3 population (multi231CAST3).

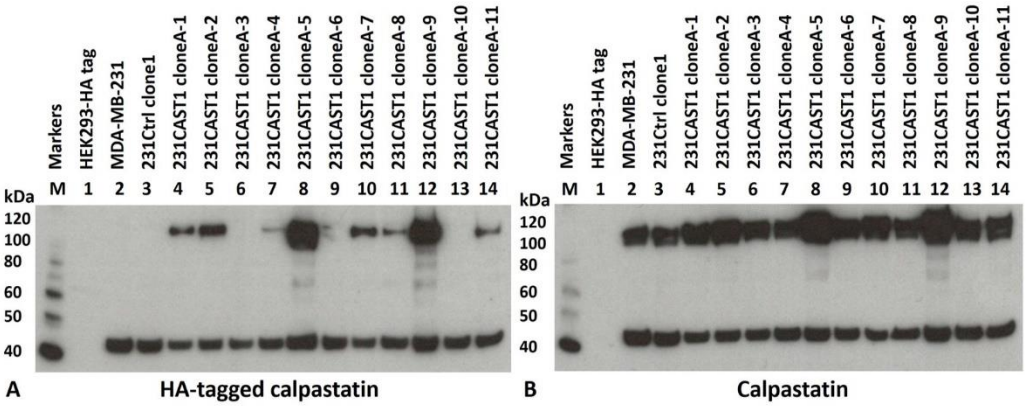


Figure 3.5 HA-tagged and total calpastatin expression in CAST1-transfected monoclonal MDA-MB-231 populations detected by Western blotting. Blots of the experiments are presented. Both (A) HA-tagged and (B) total calpastatin localise at 100-120 kDa. β-actin was used as the sample loading control (42 kDa). Lane M: protein markers, Lane 1: a positive control for HA tag expression - HEK293 cells transfected with HA-tagged minigene (HEK293-HA tag), Lane 2: a positive control for total calpastatin expression - parental MDA-MB-231 cells, Lane 3: a negative control for HA tag expression - 231Ctrl clone 1, Lane 4-14: 231CAST1 clones A-1 to A-11 established from the multiclonal 231CAST1 population A.

As shown in Figure 3.6-A, amongst all five monoclonal cell lines established from the multiclonal population of CAST2-transfected MDA-MB-231 cells (231CAST2), 231CAST2 clone 1 showed the highest levels of calpastatin Type 2, represented by the level of HA-tagged protein. Also, this clone 1 expressed a higher level of total calpastatin relative to the other four clones as well as the negative MDA-MB-231 control cells (Figure 3.6-B). Thus, 231CAST2 clone 1 was then used as a cell model for this project.

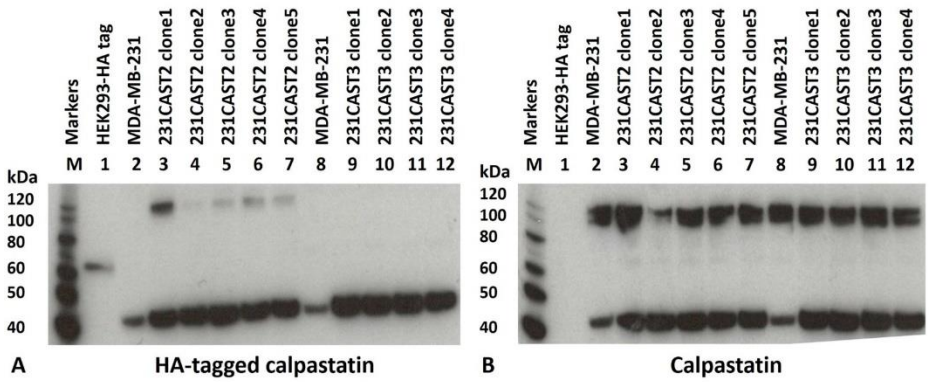


Figure 3.6 HA-tagged and total calpastatin expression in CAST2- and CAST3-transfected monoclonal MDA-MB-231 populations detected by Western blotting. Blots of the experiments are presented. (A) HA-tagged and (B) total calpastatin localise at 100-120 kDa. β-actin was used as the sample loading control (42 kDa). Lane M: protein markers, Lane 1: a positive control for HA tag expression - HEK293 cells transfected with HA-tagged minigene (HEK293-HA tag), Lane 2, 8: a positive control for total calpastatin expression - parental MDA-MB-231 cells, Lane 3-7: 231CAST2 clones 1 to 5, Lane 9-12: 231CAST3 clones 1 to 4.

MDA-MB-231 cells transfected with CAST3 DNA construct (6102 bp), termed 231CAST3, could survive and expand in the selection medium following transfection using the same condition as used for producing the empty vector- and CAST2-transfected multiclonal populations. However, neither the multiclonal population produced after CAST3 transfection (Figure 3.4-A) nor their four established monoclonal cell lines (Figure 3.6) had a detectable expression of HA-tagged calpastatin. After several attempts of MDA-MB-231 transfection with CAST3, the cells could not be transfected. Due to time restrictions, transfection of CAST3 in MDA-MB-231 cells was discontinued.

As a summary, the current work was successful in establishing monoclonal 231Ctrl, 231CAST1 and 231CAST2 cell lines for using as cell models in the current project.

3.2.2.2 Transfected monoclonal T47D clones

Transfection in T47D cells was more difficult and took more experiments to succeed compared to MDA-MB-231 cells, as summarised in Appendix C (Table C3.2). Similar to MDA-MB-231 cells, transfection of the largest DNA construct of CAST1 in T47D cells was also more challenging compared to the other smaller DNA constructs, as it took more attempts to be successful. Lipofectamine seemed to be an optimal transfection reagent to delivery CAST1 constructs into

the cells. CAST1-transfected multiclonal T47D cells were a pooled population of all survived transfected populations produced from a 72-hour incubation with 1.5:1 of Lipofectamine:DNA as well as a 48- or 72-hour incubation with 2:1, 2.5:1 and 3:1 ratios of Fugene:DNA. In comparison, all other DNA constructs could be transferred into the cells by incubation with a 2.5:1 ratio of Fugene:DNA – a 48-hour incubation for the empty vector and a 72-hour incubation for CAST2 and CAST3 DNA constructs. Importantly, the density of multiclonal population survived after transfection and selection using the selection medium seemed to matter (discussed further in Chapter 5). Transfections of CAST1 and CAST2 in T47D cells were successful after being performed in a 96-well plate instead of using a plate containing a larger surface area (defined in Table C3.2, Appendix C).

Three empty vector-transfected T47D cell clones (T47DCtrl) were established and expanded in the selection medium. Amongst them, T47DCtrl clone 2 was chosen due to its morphology showing the most similarity to the parental cells. For confirmation of CAST1 transfection using Western blotting, as presented in Figure 3.7-A, a positive control (HEK293-HA tag) showed a signal of HA-tagged protein at around 60 kDa, whereas the parental T47D and the selected mock-transfected T47DCtrl clone 2 did not show a signal of HA-tagged calpastatin. The CAST1-transfected multiclonal T47D cells (multiT47DCAST1) expressed HA-tagged calpastatin localised around 100-120 kDa. For the selection of monoclonal T47DCAST1 cell lines (Figure 3.7-B), amongst all ten monoclonal populations, clone 7 was the only one expressing HA-tagged calpastatin localised at the same position as the protein observed in 231CAST1 clone 5 (the selected cell model from section 3.2.2.1), which was used as another positive control in addition to HEK293-HA tag. Thus, T47DCAST1 clone 7 was used as another cell model of calpastatin Type 1 overexpression in addition to the 231CAST1 clone in the following experiments.

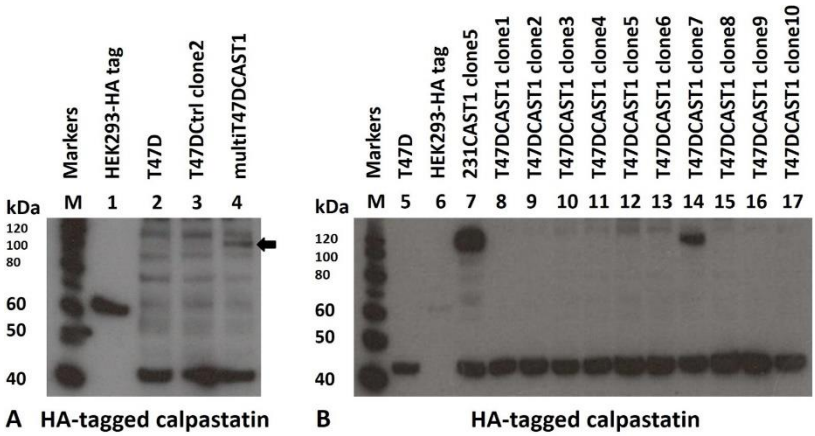


Figure 3.7 HA-tagged and total calpastatin expression in CAST1-transfected multiclonal and monoclonal T47D populations detected by Western blotting. Blots of the experiments are presented. (A) HA-tagged and (B) total calpastatin localise at 100-120 kDa. β-actin was used as the sample loading control (42 kDa). Lane M: protein markers, Lane 1 and 6: a positive control lysate of HEK293 cells transfected with HA-tagged minigene (HEK293-HA tag), Lane 2 and 5: a negative control lysate of parental T47D, Lane 3: a negative control lysate of T47DCtrl clone 2, Lane 4: multiclonal CAST1-transfected T47D population (multiT47DCAST1), Lane 7: a positive control lysate of 231CAST1 clone 5, Lane 8-17: T47DCAST1 clones 1 to 10.

T47D cells transfected with CAST2 DNA construct could survive and expand in the selection medium following transfection by incubating cells with the 2.5:1 ratio of Fugene:DNA for 48 hours in a 12-well plate (study 1; Figure 3.8). However, neither the multiclonal population produced after CAST2 transfection (Figure 3.8-A) nor its two established monoclonal populations (Figure 3.8-C) had a detectable expression of HA-tagged protein. After several attempts of T47D transfection with CAST2, the cells could be transfected the second time (study 2; Figure 3.9). Multiclonal T47DCAST2 populations 2A, 2B and 2C were independently produced from the same transfection conditions - a 72-hour transfection with the 2.5:1 ratio of Fugene:DNA in a 96-well plate. HA-tagged calpastatin expression was detected in the population 2B but not in the population 2A (Figure 3.9-A); population 2C was not examined the protein expression. The population 2B was, therefore, subsequently performed monoclonal cell selection, and only two clones could survive and expand in the selection medium. However, the expression of HA-tagged calpastatin was detected in positive controls (HEK293-HA tag and the selected 231CAST2 clone 1 from section 3.2.2.1) but not observed in both T47DCAST2 clones (Figure 3.9-C). Due to time constraints, the monoclonal population selection for T47DCAST2 cells could not be completed by the current project.

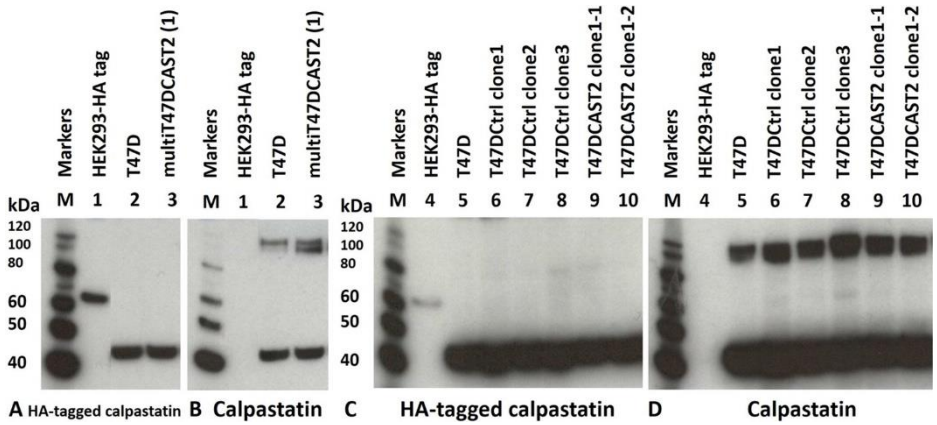


Figure 3.8 HA-tagged and total calpastatin expression in CAST2-transfected multiclonal and monoclonal T47D populations established from study 1 detected by Western blotting. Blots of the experiments are presented. (A, C) HA-tagged and (B, D) total calpastatin localise at 100-120 kDa. β-actin was used as the sample loading control (42 kDa). Lane M: protein markers, Lane 1, 4, 11 and 17: a positive control lysate of HEK293 cells transfected with HA-tagged minigene (HEK293-HA tag), Lane 2, 5, 12 and 16: a negative control lysate of parental T47D cells. Lane 3: the multiclonal T47DCAST2 population survived in the selection medium (multiT47DCAST2 (1)), Lane 6-8: T47DCtrl clones 1 to 3, Lane 9-10: T47DCAST2 clone 1-1 and 1-2 established from multiT47DCAST2 (1) population.

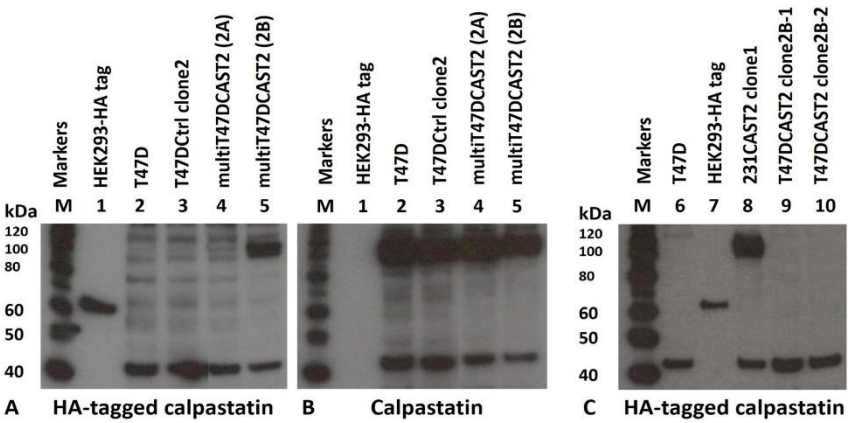


Figure 3.9 HA-tagged calpastatin and total calpastatin expression in CAST2-transfected multiclonal and monoclonal T47D populations established from study 2 detected by Western blotting. Blots of the experiments are presented. Both (A, C) HA-tagged and (B) total calpastatin localised at 100-120 kDa. β-actin was used as the sample loading control (42 kDa). Lane M: protein markers, Lane 1, 7: a positive control lysate of HEK293 cells transfected with HA-tagged minigene (HEK293-HA tag), Lane 2, 6: a negative control lysate of parental T47D, Lane 3: a negative control lysate of T47DCtrl clone 2 (T47DCtrl clone2), Lane 4-5: multiclonal T47DCAST2 populations 2A and 2B (multiT47DCAST2 (2A) and (2B)), Lane 8: a positive control lysate of 231CAST2 clone 1, Lane 9-10: T47DCAST2 clones 2B-1 and 2B-2 establish from multiT47DCAST2 (2B) population.

CAST3 DNA constructs were successfully delivered into T47D cells - multiclonal T47DCAST3 cells expressed HA-tagged calpastatin (Figure 3.10-A), representing overexpression of calpastatin Type 3, and overexpressed total calpastatin relative to the parental T47D cells (Figure 3.10-B). Amongst five established monoclonal T47DCAST3 populations, there were only two clones expressing

the HA-tagged protein (clone 2 and 5), and T47DCAST3 clone 2 had higher HA-tagged calpastatin expression compared to clone 5. By comparison with the parental cells, total calpastatin expression was evidently higher in clone 2 but weakly detected in clone 5. Thus, T47DCAST3 clone 2 was chosen as one of the cell models used in the current study. As a summary, the current work was successful in establishing monoclonal T47DCtrl, T47DCAST1 and T47DCAST3 cell lines.

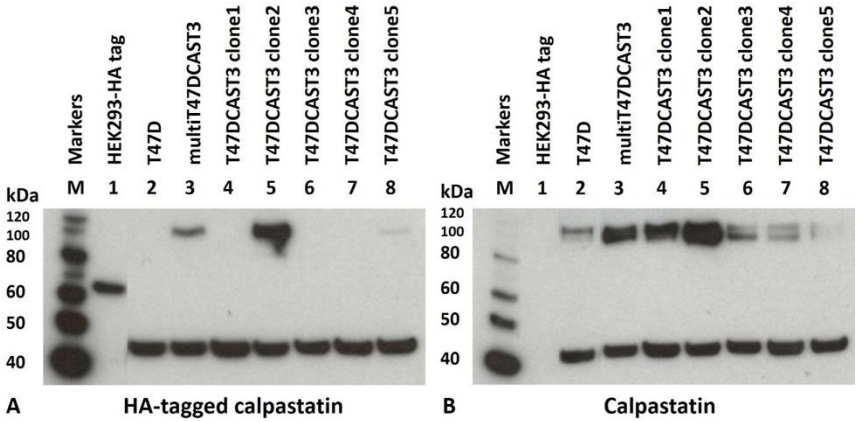


Figure 3.10 HA-tagged and total calpastatin expression in CAST3-transfected multiclonal and monoclonal T47D populations detected by Western blotting. Blots of the experiments are presented. Both (A) HA-tagged and (B) total calpastatin localise at 100-120 kDa. β-actin was used as the sample loading control (42 kDa). Lane M: protein markers, Lane 1: a positive control lysate of HEK293 cells transfected with HA-tagged minigene (HEK293-HA tag), Lane 2: a negative control lysate of parental T47D cells, Lane 3: multiclonal T47DCAST3 population (multiT47DCAST3), Lane 4-8: T47DCAST3 clone 1 to 5.

Briefly, monoclonal breast cancer cells overexpressing calpastatin isoforms 1, 2 or 3 could not be all established from the same cell line, neither MDA-MB-231 nor T47D cells. The current project successfully created six stable monoclonal cell lines, i.e., the cells overexpressing calpastatin Type 1 (231CAST1 and T47DCAST1), Type 2 (231CAST2), Type 3 (T47DCAST3), and the respective mock-transfected controls (231Ctrl and T47DCtrl). Based upon a difference between CAST1 and CAST 2 mRNA sequences by only one exon, overexpression of calpastatin Type 1 and Type 2, especially in MDA-MB-231 cells, was selected to fully examine and compare their roles to each other in regulating breast cancer progression and LVI (Chapter 4).

3.3 Expression of the calpain-calpastatin system proteins and CAST mRNA in the cells overexpressing calpastatin isoforms

The current work sought to quantitatively evaluate the overexpression levels of HA-tagged calpastatin isoform and the particular CAST mRNA in the transfected cell clones established from section 3.2. The cells overexpressing calpastatin Type 1 (231CAST1 and T47DCAST1) and Type 2 (231CAST2) were used as cell models after being ensured that they significantly overexpressed calpastatin isoform protein or mRNA. The expression of conventional calpain subunits was also quantified whether it was affected by altered calpastatin expression.

3.3.1 Expression levels of the calpain-calpastatin system proteins

The current study aimed to quantify the expression levels of HA-tagged calpastatin isoform and total calpastatin in 231CAST1 and 231CAST2 clones compared to mock-transfected 231Ctrl and parental MDA-MB-231 cells. Calpastatin overexpression was also examined for its impact on conventional calpain subunit (calpain-1, -2 and -4) expression. The protein expression was assessed using fluorescent Western blotting (section 2.4), and representative blots of three independent experiments are shown in Figure 3.11.

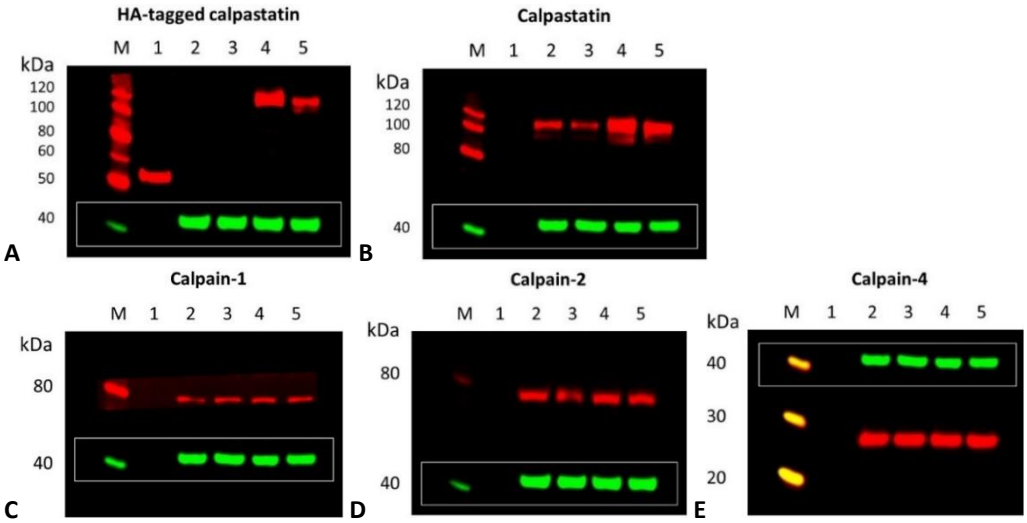


Figure 3.11 Representative blots of quantitative analysis of calpain-calpastatin system protein expression in MDA-MB-231 cells overexpressing calpastatin isoforms by Western blotting. Representative blots of three independent experiments are presented. Red bands indicate (A) HA-tagged calpastatin (100-120 kDa), (B) calpastatin (100-120 kDa), (C) calpain-1 (82 kDa), (D) calpain-2 (80kDa), and (E) calpain-4 (28-kDa). β-actin was used as the sample loading control (42 kDa, green bands). Lane M: protein markers, Lane 1: a positive control lysate of HEK293 cells transfected with HA-tagged minigene (HEK293-HA tag), Lane 2: MDA-MB-231, Lane 3: 231Ctrl, Lane 4: 231CAST1, Lane 5: 231CAST2.

Results were presented as the relative expression ratio (R) of the target protein to β-actin (Table 3.3) that subsequently being calculated as fold expression relative to that in mock-transfected 231Ctrl control (except for HA-tagged protein) (Figure 3.12).

Table 3.3 Calpain-calpastatin system protein expression in MDA-MB-231 cells overexpressing calpastatin isoforms assessed by Western blotting.

Cell clones	Relative protein expression ratio (R) to β-actin				
	HA-tagged calpastatin	Calpastatin	Calpain-1	Calpain-2	Calpain-4
231Ctrl	0	0.49	0.19	4.11	3.49
		± 0.48	± 0.03	± 0.47	± 0.46
MDA-MB-231	0	0.75	0.17	4.30	3.36
		± 0.53	± 0.01	± 0.71	± 0.28
231CAST1	1.10	1.71	0.26	4.60	3.86
	± 0.46	± 1.58	± 0.07	± 0.49	± 0.20
231CAST2	0.73	1.12	0.25	4.22	3.68
	± 0.25	± 0.93	± 0.07	± 0.58	± 0.38

Data represent the average relative expression ratios of calpains or calpastatin to β-actin ± SD of independent experiments (n = 6 for HA-tagged and total calpastatin, n = 3 for calpain-1, -2, and -4), each performed without replicate; n is the number of independent experiments.

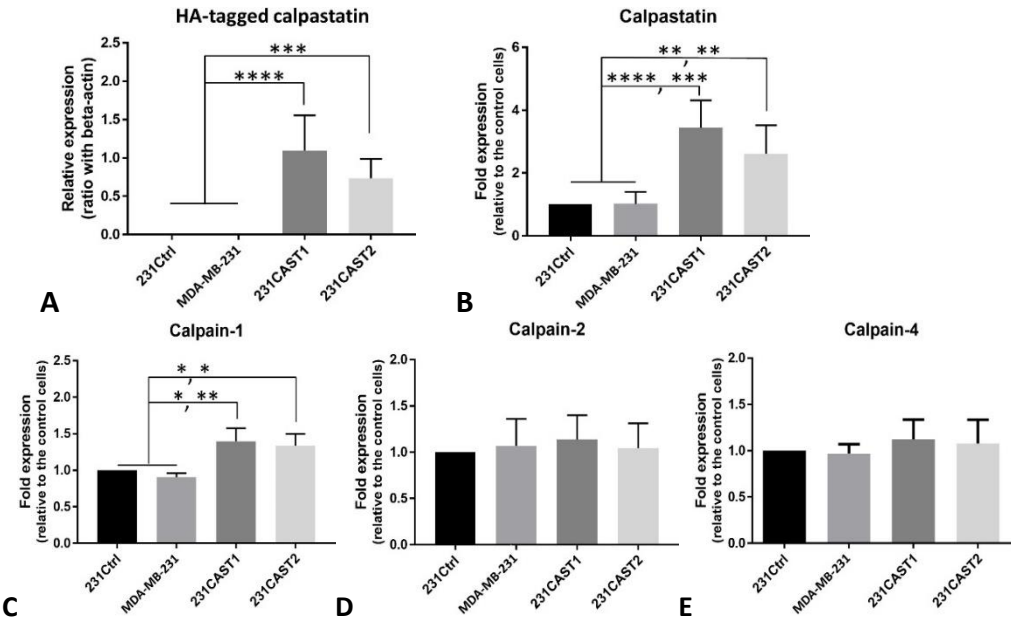


Figure 3.12 Quantitative analysis of calpain-calpastatin system protein expression in MDA-MB-231 cells overexpressing calpastatin isoforms by Western blotting. Cell lysates were prepared independently in triplicate from different cell passages of 231Ctrl, parental MDA-MB-231, 231CAST1 and 231CAST2 cells. (A) HA-tagged calpastatin expression in each line is presented as a ratio to β-actin expression; the expression of (B) calpastatin, (C) calpain-1, (D) calpain-2, and (E) calpain-4 in each cell line is presented as fold expression relative to 231Ctrl cells. Data represent the average ± SD of three independent experiments for calpains and six independent experiments for HA-tagged and total calpastatin, each performed without replicate. *P*-values were assessed for showing the level of statistical differences between CAST-overexpressing cells and the mock-transfected control or parental MDA-MB-231 cell lines; **P* < 0.05, ***P*<0.01, ****P*<0.001, and *****P*<0.0001.

The mock-transfected 231Ctrl cells expressed all investigated proteins in a similar pattern to parental cells, i.e., HA-tagged calpastatin (no expression), total calpastatin (1 vs 1.023 fold, $P > 0.9999$), calpain-1 (1 vs 0.90 fold, $P = 0.7788$), calpain-2 (1 vs 1.067 fold, $P = 0.9848$) and calpain-4 (1 vs 0.97 fold, $P = 0.9964$) (Figure 3.12). Such data indicate that the empty-vector transfection and the selective agent (G418) had no effect on the expression of the calpain-calpastatin system proteins in MDA-MB-231 cells. The 231CAST1 and 231CAST2 clones expressed similar levels of the HA-tagged calpastatin (R = 1.1 and 0.73, respectively; $P = 0.1096$; Table 3.3 and Figure 3.12). As expected, the expression of HA-tagged protein in 231CAST1 and 231CAST2 clones was significantly higher than that found in the mock-transfected control ($P < 0.0001$ and = 0.0005, respectively) or the parental cells ($P < 0.0001$ and = 0.0005, respectively). Total calpastatin levels in 231CAST1 and 231CAST2 cells, as presented in Figure 3.12, were also similar ($P = 0.1941$) and significantly increased in comparison to the mock-transfected 231Ctrl cells by 3.44 fold in 231CAST1 cells ($P < 0.0001$) and 2.61 fold in 231CAST2 cells ($P = 0.0035$). Also, 231CAST1 and 231CAST2 cells significantly expressed higher total calpastatin levels than the parental cells ($P = 0.0002$ and 0.0099, respectively).

Figure 3.12 shows that amongst all conventional calpain subunits, only a calpain-1 expression significantly increased in both MDA-MB-231 clones overexpressing calpastatin Type 1 (231CAST1 cells) by 1.40 fold ($P = 0.0188$) and Type 2 (231CAST2 cells) by 1.33 fold ($P = 0.0446$) in comparison to the expression in the mock-transfected 231Ctrl cells. The increased calpain-1 levels were not different between in 231CAST1 and 231CAST2 clones ($P = 0.9215$). In comparison to parental cells, calpain-1 expression was also statistically higher in both 231CAST1 ($P = 0.0055$) and 231CAST2 cells ($P = 0.0122$). However, significant changes in the expression of calpain-2 or -4 were undetectable by Western blotting analysis in both 231CAST1 and 231CAST2 clones compared to that of 231Ctrl and parental cells.

3.3.2 Expression levels of CAST mRNA

This study aimed to evaluate CAST1 and CAST2 mRNA expression levels in the CAST1-transfected cells (231CAST1 and T47DCAST1) and the CAST2-transfected clone (231CAST2), respectively, in comparison with that in the respective control cells, including the mock-transfected controls (231Ctrl or T47DCtrl) or parental cells (MDA-MB-231 or T47D), using RT-qPCR technique (section 2.5). The levels of mRNA were quantified using the relative standard curve method.

Firstly, standard curves of CAST1, CAST2 and HPRT reference gene were created from a 2-fold standard serial dilution (0.28-18 µg) of cDNA mix of 231CAST1 and 231CAST2 cells (1:1 ratio) (section 2.5.3.2). The PCR reactions of CAST1 and HPRT had high amplification efficiencies (E = 85.62% and 93.20%, respectively) and contributed to the linearity of the standard curves (R^2 = 0.9959 and 0.9820, respectively). However, CAST2 PCR amplification efficiency (E = 64.06%) and the linearity of the CAST2 standard curve (R^2 = 0.7630) were low. By running forty PCR cycles using the protocol mentioned in section 2.5.3.1 with a range of standard concentrations (0.28-18 µg), the Ct values of CAST2 standards were detected at the late cycles (~30 and more) to undetectable (for 0.28 µg standard), suggesting deficient amounts of CAST2 cDNA templates in standards. In an attempt to increase CAST2 cDNA template, standard serial dilution was then prepared from only 231CAST2 cells' cDNA to generate standard curves of all investigated mRNA.

Standard curves of CAST1, CAST2 and HPRT were then created from a standard serial dilution of 231CAST2 clone's cDNA - a 1.5-fold serial dilution (13.17-100 µg) for CAST1 and CAST2 expression analyses and a 2-fold serial dilution (0.3125-10 µg) for HPRT expression assessment. Melt curves of CAST1, CAST2 and HPRT showed that there was only one PCR product of a target gene amplified in each reaction (Figure 3.13), indicating specificity of primers as well as absences of contamination with gDNA and primer-dimers. There was also no peak of primer-dimer or contamination presented in the no template control (NTC; flat red lines, Figure 3.13).

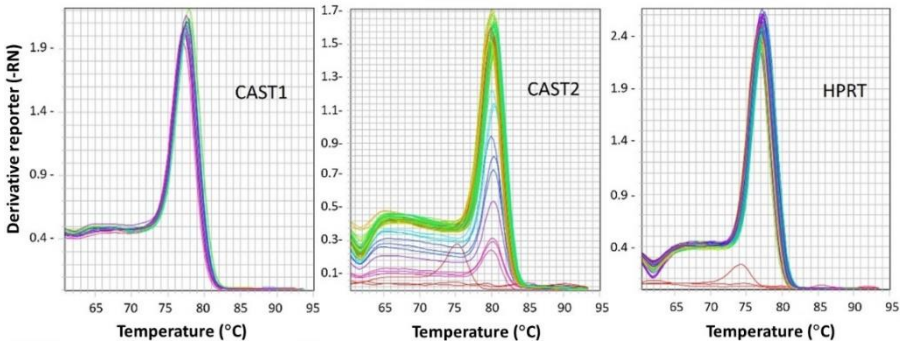


Figure 3.13 Melt curves of CAST1, CAST2 and HPRT mRNA amplified in all standards. Standard serial dilution was prepared as a 1.5-fold dilution (13.17-100 µg) for CAST1 and CAST2 expression analyses or a 2-fold dilution (0.3125-10 µg) for HPRT expression assessment. Red lines represent the melt curves of no template control.

In CAST2 PCR reaction, the peak heights of the melt curves generated from the lowest two concentrations of the standards (13.17 and 19.75 µg indicated by pink and purple peaks, respectively) were very low (Figure 3.13). Moreover, most of the CAST2 standards had late Ct values (>30), indicating low concentrations of the amplicon presented in the reactions, as supported by very poor PCR efficiency (27.44%, Table 3.4). Such results suggest that CAST2 expression levels could not be assessed by using the current protocol. Due to time constraints, it was not possible to optimise and repeat the PCR reactions using a new protocol for CAST2 expression analysis in the transfected cells. Therefore, the quantitative analysis of CAST2 expression was discontinued in the current project.

Table 3.4 Linear equations of standard curves and amplification efficiencies of PCR reactions for evaluating CAST and HPRT mRNA expression

mRNA	Linear equations of the standard curves	R^2	Efficiencies of PCR reaction (%)
CAST1	$y = -3.9647x + 34.071$	0.9851	78.74
CAST2	$y = -9.4976x + 46.683$	0.9915	27.44
HPRT	$y = -3.5808x + 24.955$	0.9688	90.22

In the linear equation, y is C_t value, and x is log quantity of cDNA.

As shown in Table 3.4, the standard curves of CAST1 and HPRT showed linearity by R^2 = 0.9855 and 0.9688, respectively. The amplification efficiencies were 90.22% for HPRT PCR and 78.74% for CAST1 PCR. Quantities of CAST1 and HPRT mRNA expressed in the target sample cells were calculated from the linear

equations derived from the standard curves (shown in Table 3.4). The expression levels of CAST1 in 231CAST1 and T47DCAST1 cells were calculated as a relative expression calculated by normalisation to HPRT levels, then shown as a relative ratio out of CAST1 expression in the respective mock-transfected controls (231Ctrl or T47DCtrl) (Figure 3.14).

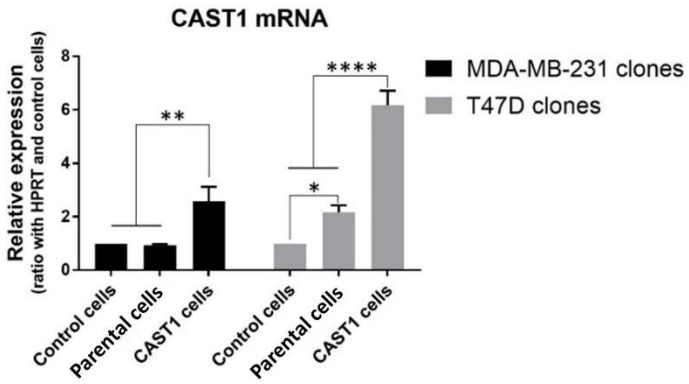


Figure 3.14 Quantitative analysis of CAST1 expression in transfected MDA-MB-231 and T47D cells by RT-qPCR technique. Samples were independently prepared in triplicate from different passages of the control cells (231Ctrl or T47DCtrl), parental cells (MDA-MB-231 or T47D), and CAST1-transfected cells (231CAST1 or T47DCAST1). Expression of CAST1 and HPRT reference gene were extrapolated from the standard curves. Relative expression of CAST1 was calculated by normalising to HPRT expression and calibrating with the expression of the respective mock-transfected controls (231Ctrl or T47DCtrl). Data represent the average ± SD of three independent experiments, each performed in triplicate. *P*-values were assessed for showing the level of statistical differences between CAST1-overexpressing cells and the mock-transfected controls or parental cell lines;* $P < 0.05$, ** $P < 0.01$, *** $P < 0.001$, and **** $P < 0.0001$.

As shown in Figure 3.14, mock-transfected 231Ctrl and parental MDA-MB-231 cell lines expressed a comparable level of CAST1 mRNA with no statistical difference ($P = 0.9695$). On the other hand, T47DCtrl cells expressed lower levels of CAST1 than that detected in the parental T47D cells (~2 fold difference, $P = 0.0155$), indicating that plasmid transfection or G418 affected CAST1 expression in T47D cell line. Both 231CAST1 and T47DCAST1 cells significantly overexpressed CAST1 mRNA compared to their respective mock-transfected controls (2.60 and 6.22 fold increases, respectively; $P = 0.0020$ and < 0.0001, respectively) and parental cells ($P = 0.0016$ and < 0.0001, respectively).

As a brief summary, 231CAST1 and T47DCAST1 clones were confirmed for their overexpression of HA-tagged and total calpastatin (section 3.3.1) and/or CAST1 mRNA (section 3.3.2) in comparison to the respective mock-transfected and parental cells. Although CAST2 mRNA expression in 231CAST2 clone could not

be examined due to poor efficiency of the RT-qPCR, 231CAST2 cells were confirmed for their HA-tagged and total calpastatin overexpression compared to the mock-transfected and parental cells (section 3.3.1). Therefore, T47DCAST1, 231CAST1, and 231CAST2 clones could be used to assess the effects of calpastatin isoform overexpression on phenotypic endpoints related to breast cancer progression and LVI (Chapter 4).

3.4 Effects of cell culture factors on calpastatin expression and migration of transfected cells

3.4.1 Effects of serial cell passaging on calpastatin expression in transfected cells

To ensure that the level of calpastatin isoform overexpression in the CAST-transfected cells remained stable during the study, the effect of serial cell passaging on the expression of HA-tagged and total calpastatin was assessed. MDA-MB-231 cells overexpressing calpastatin Type 1 and Type 2 (231CAST1 and 231CAST2 cells respectively) were serially subcultured for ten times from the master stocks (passage number 0 or P. 0), and the cell lysates at P. 2, 4, 6, 8 and 10 were analysed for the protein expression using the fluorescent Western blotting technique (section 2.4).

Figure 3.15 shows representative blots of (A) HA-tagged and (B) total calpastatin expression analyses as well as (C, D) the relative expression ratio (R) of the β-actin normalised calpastatin level in the cells at each passage number against the expression in the passage number 2. 231CAST1 cells at all investigated passage numbers (P. 2, 4, 6, 8 and 10) expressed similar levels of both HA-tagged calpastatin (R = 1, 0.84, 1.01, 0.96 and 0.63, respectively) and total calpastatin (R = 1, 0.69, 0.90, 0.66 and 0.72, respectively). There was no statistical difference between the protein expression in 231CAST1 cells at passage number 2 and the following passage number 4, 6, 8 or 10 (HA-tagged calpastatin: P = 0.9907, > 0.9999, > 0.9999, and 0.8279, respectively; total calpastatin: P = 0.6001, 0.9859, 0.5111, and 0.6724, respectively).

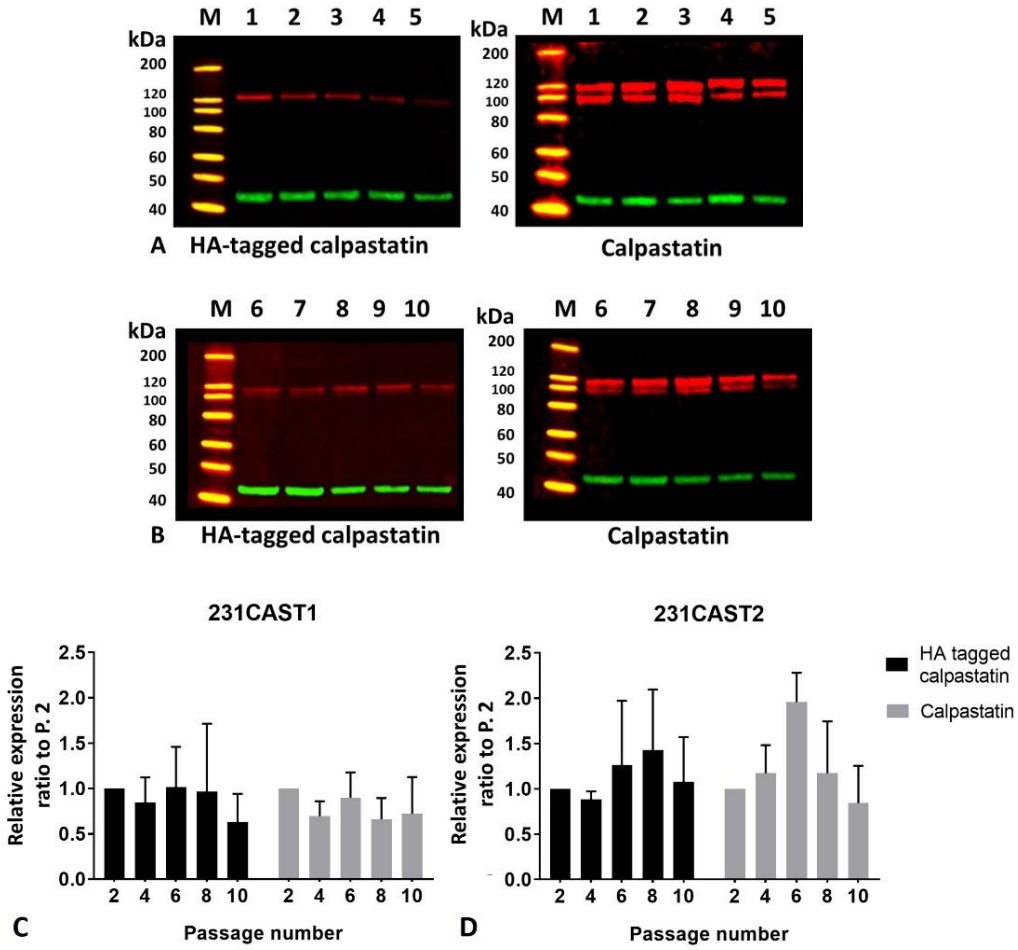


Figure 3.15 Effects of serial cell passaging on HA-tagged and total calpastatin expression in MDA-MB-231 cells overexpressing calpastatin isoforms detected by Western blotting. Cells were serially subcultured from the master stock (P. 0) before being collected cell lysates in triplicate from different passages. Representative blots of three independent experiments in (A) 231CAST1 and (B) 231CAST2 clones are shown here. Red bands indicate HA-tagged and total calpastatin (100-120 kDa). β-actin was used as the sample loading control (42 kDa, green bands). Lane M: protein markers, Lane 1-5: 231CAST1 at P. 2, 4, 6, 8, and 10, respectively, and Lane 6-10: 231CAST2 at P. 2, 4, 6, 8, and 10, respectively. Expression levels of HA-tagged and total calpastatin in (C) 231CAST1 and (D) 231CAST2 clones were normalised by β-actin expression before being calculated as the relative expression ratio to P. 2. Data represent the average ± SD of three independent experiments, each performed without replicate. No statistical difference is present between each passages and P.2.

Similarly, 231CAST2 cells at P. 2, 4, 6, 8 and 10 also expressed the similar levels of HA-tagged calpastatin (R = 1, 0.89, 1.26, 1.43, and 1.08, respectively) and total calpastatin (R = 1, 1.18, 1.96, 1.17, and 0.85, respectively) (Figure 3.15-D). The levels of both proteins in 231CAST2 cells at P. 4, 6, 8 and 10 were not significantly different from that at P. 2 (HA-tagged calpastatin: P = 0.9981, 0.9607, 0.8136 and 0.9996, respectively; total calpastatin: P = 0.9767, 0.0628, 0.9767 and 0.9839, respectively).

To summarise, subculturing transfected cells up to ten times from the master cells did not significantly affect the levels of HA-tagged and total calpastatin expression. Therefore, in the current project, all transfected cells established from section 3.2 were used until they reached passage number 10.

3.4.2 Effects of G418-free culture medium on calpastatin expression and cell migration in transfected cells

Mock-transfected 231Ctrl cells significantly proliferated with a longer doubling time in the selection medium compared to the parental cells (section 4.3.1.1). Yallop and Svendsen (2001) have reported that G418 slowed down cell growth and affected the metabolism of the stably transfected baby hamster kidney BHK 570 cell line. This raised the question of whether G418 may affect phenotypic endpoints of transfected cells. To avoid such effects, the current work intended to culture the transfected cells in the short-term and conduct experiments using G418-free culture medium after ensuring that G418 removal had no effect on calpastatin expression or cell migration, a representative phenotypic endpoint, in the transfected MDA-MB-231 cells.

3.4.2.1 Effects of G418-free culture medium on calpastatin expression

The current work aimed to compare the calpastatin expression levels between transfected cells cultured with G418-containing and removed medium. Figure 3.16 shows the expression levels of HA-tagged and total calpastatin after culturing cells for three (Day 3) and seven days (Day 7) in the culture medium with/without G418 relative to that in the primary cells, which were routinely cultured in the selection medium (Day 0).

In 231CAST1 cells, culturing cells with the G418-free medium for either three or seven days did not alter the levels of HA-tagged and total calpastatin expression compared to routinely culturing cells with the selection medium (HA-tagged calpastatin: 1.23 vs 1.12 (P = 0.9963) and 1.64 vs 1.99 (P = 0.8031) for Day 3 and Day 7 respectively; total calpastatin: 1.05 vs 1.07 (P = 0.9999) and 0.80 vs 1.33 (P = 0.1893) for Day 3 and Day 7 respectively). Likewise, no

difference of either HA-tagged or total calpastatin expression was observed between the 231CAST2 cells cultured with the G418-free and G418-containing culture medium for either three days (HA-tagged calpastatin: 1.27 vs 0.81, P = 0.6009; total calpastatin: 1.61 vs 0.91, P = 0.3557) or seven days (HA-tagged calpastatin: 1.05 vs 1.06, P > 0.9999; total calpastatin: 0.74 vs 0.70, P > 0.9999).

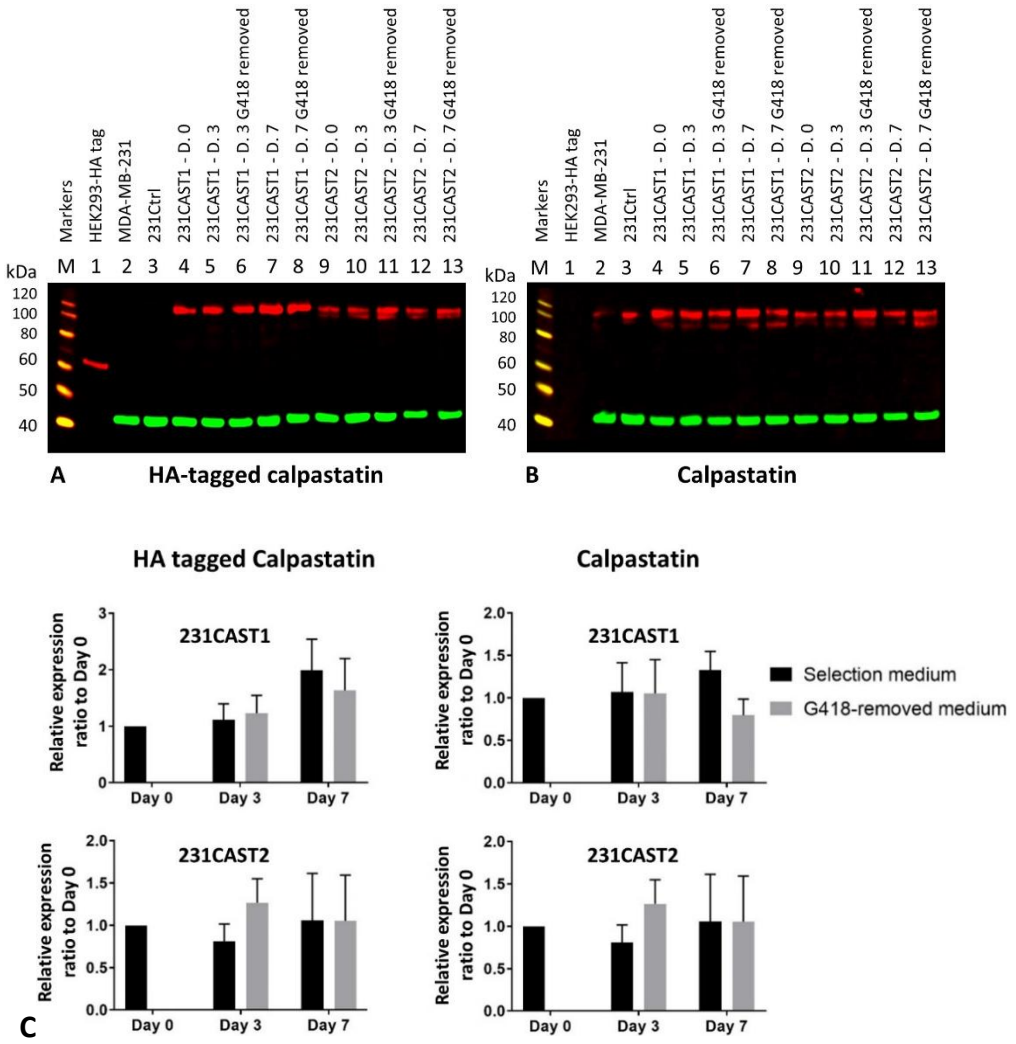


Figure 3.16 Effects of G418-free culture medium on HA-tagged and total calpastatin expression in MDA-MB-231 cells overexpressing calpastatin isoforms detected by Western blotting. Representative blots of three independent experiments are presented. Red bands indicate (A) HA-tagged and (B) total calpastatin (100-120 kDa). β-actin was used as the sample loading control (42 kDa, green bands). Lane M: protein markers, Lane 1: a positive control lysate of HEK293 cells transfected with HA-tagged minigene (HEK293-HA tag), Lane 2: MDA-MB-231, Lane 3: 231Ctrl, Lane 4, 5, and 7: 231CAST1 cultured with selection medium at day (D.) 0, 3, and 7, respectively, Lane 6 and 8: 231CAST1 cultured with G418-free medium at day 3 and 7 respectively, Lane 9, 10 and 12: 231CAST2 cultured with selection medium at day (D.) 0, 3, and 7, respectively, Lane 11 and 13: 231CAST2 cultured with G418-free medium at day 3 and 7, respectively. (C) Expression levels of HA-tagged and total calpastatin were normalised by β-actin expression before being calculated as the relative expression ratio to Day 0. Data represent the average ± SD of three independent experiments, each performed without replication. No statistical difference is present between Day 0 and other groups as well as between selection medium and G418-removed medium groups.

In comparison with the initial control cells on Day 0, the levels of HA-tagged and total calpastatin expression were not significantly changed in the cells cultured either with or without G418 for three of seven days. In 231CAST1 cells, the relative expression of HA-tagged calpastatin, as well as total calpastatin, was not altered after three days (P = 0.9497 and 0.9991) or seven days (P = 0.3476 and 0.8809) of cell culture using the G418-removed medium compared to the control. 231CAST2 cells also remained to express similar levels of both HA-tagged and total calpastatin compared to the control cells (day 0) after being cultured with the G418-removed medium for three (P = 0.9054 and 0.4786 respectively) or seven days (P = 0.9998 and 0.9479 respectively).

Briefly, G418 removal from culture medium for up to seven days did not affect the expression of HA-tagged or total calpastatin in both 231CAST1 and 231CAST2 cells.

3.4.2.2 Effects of G418-free culture medium on cell migration

The current study aimed to investigate the effect of G418-removed culture medium on the migration of the transfected MDA-MB-231 cell lines. The transfected cells were assessed for their migration activity using scratch-wound assay (section 2.10) after being pre-cultured with the G418-free medium for 1, 3, 5, 7, 10 or 14 days compared with the control cells cultured routinely in the selection medium (0 days of exposure to the G418-free medium).

Figure 3.17 shows the percentage of wound closure, representing cell migration activity, at 24 hours post-scratch. As shown in Figure 3.17-A, mock-transfected 231Ctrl cells pre-incubated with G418-free culture medium for 1-14 days showed a similar migratory ability (40.04–51.21 %wound closure) to the control cells (0 days) (49.77 ± 2.73 %wound closure) but remained to migrate significantly slower than the parental cells at all exposure periods to G418-free medium (65.27–79.60 %wound closure). G418 removal from the incubation medium up to 14 days also did not affect the migration activities of 231CAST1 (Figure 3.17-B) and 231CAST2 cells (Figure 3.17-C). There was no significant difference between the migratory activities of the CAST-transfected cells pre-

cultured in the G418-free medium for 1-14 days (59.55-67.10 %wound closure for 231CAST1; 34.91-54.79 %wound closure for 231CAST2 cells) compared to the control cells cultured with the selection medium (0 days) (56.12 ± 4.96 %wound closure for 231CAST1; 60.31 ± 7.62 %wound closure for 231CAST2 cells) (Figure 3.17-B, -C).

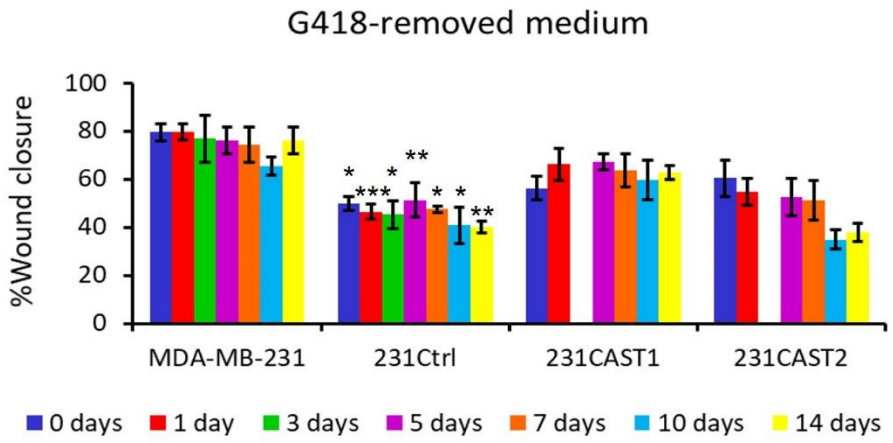


Figure 3.17 Effects of G418-free medium on the migration of transfected MDA-MB-231 cells examined by scratch-wound assay. Before conducting migration assessments, 231Ctrl, 231CAST1 and 231CAST2 cells were cultured in the G418-free culture medium for 0, 1, 3, 5, 7, 10 or 14 days, while MDA-MB-231 parental cells were routinely cultured in the complete medium. Mitomycin C was used for the inhibition of cell proliferation after wound-scratch. Wound closure was examined at 24 hours post-scratch. Data represent the average ± SD of three independent experiments, each performed in triplicate. Significant differences between the percentage wound closures of MDA-MB-231 and 231Ctrl cells were observed at all periods of exposure (* $P < 0.5$, ** $P < 0.01$, and *** $P < 0.001$ vs MDA-MB-231). No significant difference is present within each cell line in comparison with the control group (0 days).

In summary, the levels of calpastatin expression and migration activity of the transfected MDA-MB-231 cells were not affected by G418 removal from cell culture for up to 7 and 14 days, respectively. Thus, in the following phenotypic assessments, to avoid the possible effect of G418 on phenotypic features, the regular culture medium was used in culturing the transfected cells for two days before performing experiments and also used in experimentation.

3.5 Intracellular localisation of calpastatin isoforms

This study aimed to investigate intracellular localisation of full-length calpastatin Type 1, Type 2 or Type 3 in breast cancer cells and compare to that of the respective truncated forms (only XL and L domains) assessed previously by Dr Sarah Storr, a doctoral researcher of the current group (unpublished

data). The truncated version of calpastatin was encoded by exon3-containing/lacking cDNA. The IF confocal microscopy was used to explore the intracellular localisation of calpastatin isoforms in addition to being used for monitoring CAST transfection in the established transfected cells (section 2.7).

Cellular distribution of the HA-tagged full-length version of Type 1 was tracked in 231CAST1 and T47DCAST1 cells, Type 2 in 231CAST2 cells, and Type 3 in T47DCAST3 cells, by using the green Alexa Fluor®488 conjugated anti-HA-tag antibody. Phalloidin was used to label F-actin to visualise cell outline (red), and Hoechst was used to label nuclei (blue). Figure 3.18-A and -B display the confocal microscopic images of the negative controls showing no expression of HA-tagged protein. The figures present parental (MDA-MB-231 and T47D) and mock-transfected cells (231Ctrl and T47DCtrl) showing no expression of HA-tagged calpastatin as well as the cells (231CAST2 and T47DCAST1) expressing HA-tagged proteins that were not probed with the anti-HA-tag antibody.

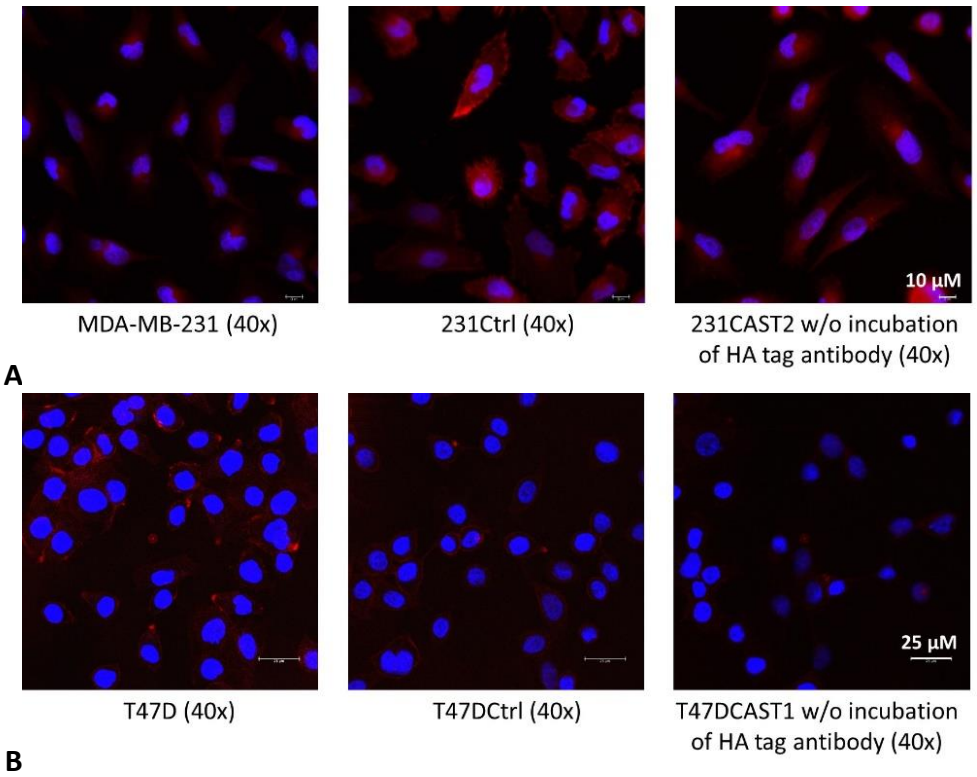


Figure 3.18 Confocal microscopic images of negative controls in the study of intracellular localisation of calpastatin isoforms in (A) MDA-MB-231 and (B) T47D cells. The left panel shows images of parental cells (MDA-MB-231 and T47D). The middle panel shows images of mock-transfected cells (231Ctrl and T47DCtrl). The right panel shows images of 231CAST2 and T47DCAST1 clones unprobed with the anti-HA-tag antibody.

Figure 3.19, Figure 3.20 and Figure 3.21 show the subcellular distribution of calpastatin Type 1, 2, and 3, respectively. Results revealed that both full-length and truncated forms of all types localised in the same fashion in breast cancer cells. The distribution of each calpastatin isoform within the basal-like MDA-MB-231 cells and the luminal T47D cells seemed no different. Type 1 and Type 3 were expressed mostly throughout the cytoplasm and slightly distributed in the nuclei, as shown in Figure 3.19 and Figure 3.21, respectively. Type 2 localisation was unique and different from the other isoforms as its expression was cytoplasmic with a predominant perinuclear expression. Figure 3.20 shows representative images of Type 2 calpastatin as visible spots in the MDA-MB-231 line and fibre-like aggregation in T47D cells.

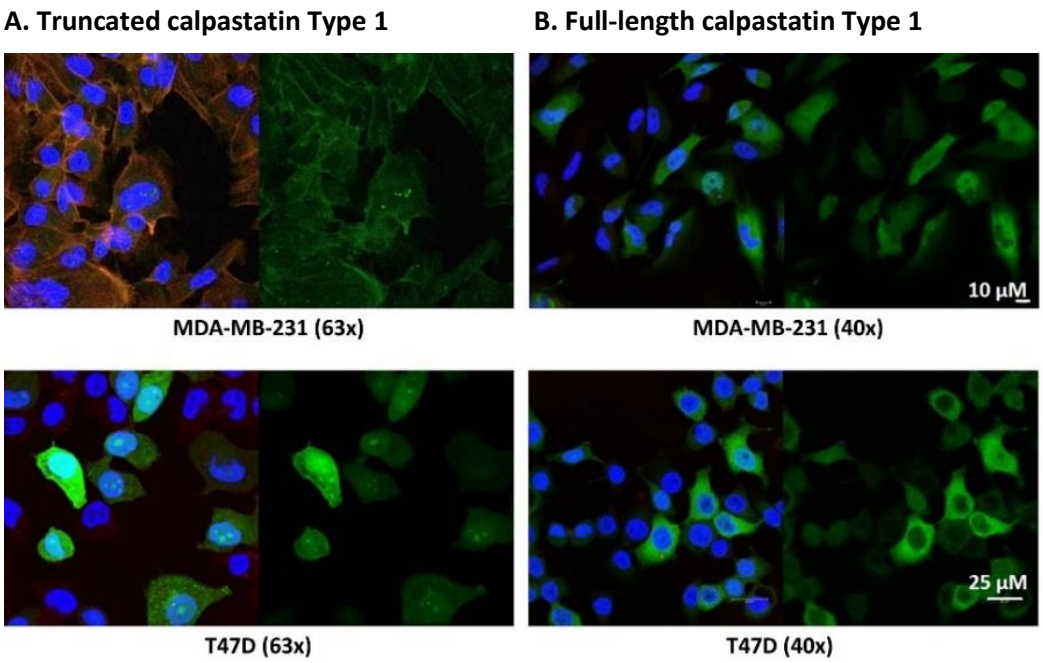


Figure 3.19 Intracellular localisation of (A) GFP-tagged truncated and (B) HA-tagged full-length forms of calpastatin Type 1 in MDA-MB-231 and T47D cells detected by IF confocal microscopy. The left column of each panel shows labelling confocal images of GFP or HA tag (green), nuclei (blue), and F-actin (red); the right column of each panel shows a singular expression of GFP or HA tag (green).

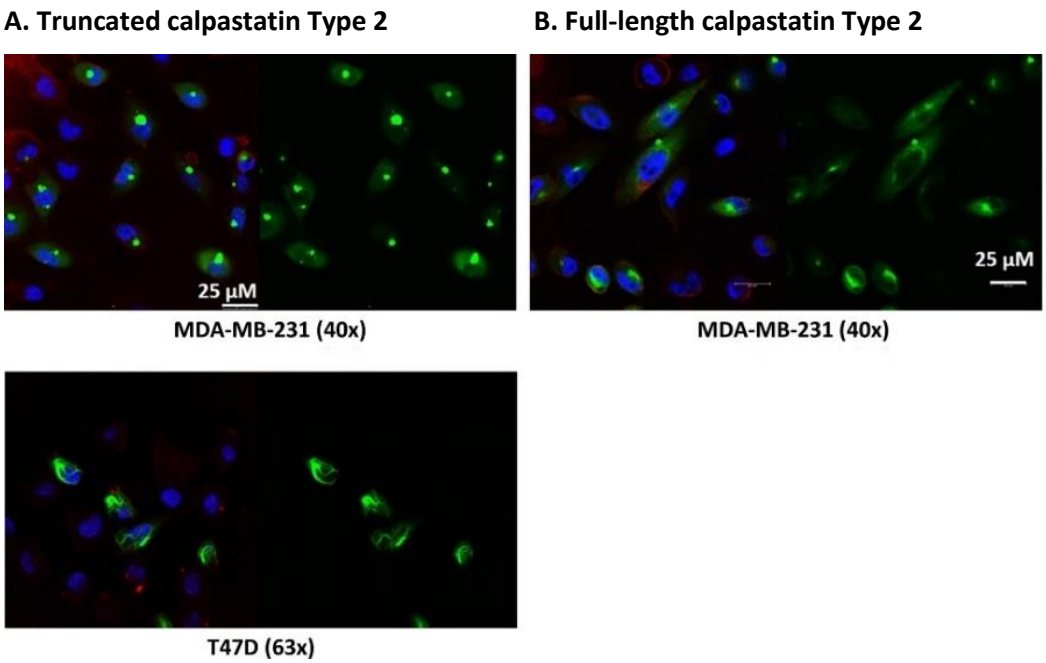


Figure 3.20 Intracellular localisation of (A) GFP-tagged truncated and (B) HA-tagged full-length forms of calpastatin Type 2 in MDA-MB-231 and T47D cells detected by IF confocal microscopy. The left column of each panel shows labelling confocal images of GFP or HA tag (green), nuclei (blue) and F-actin (red); the right column of each panel shows a singular expression of GFP or HA tag (green).

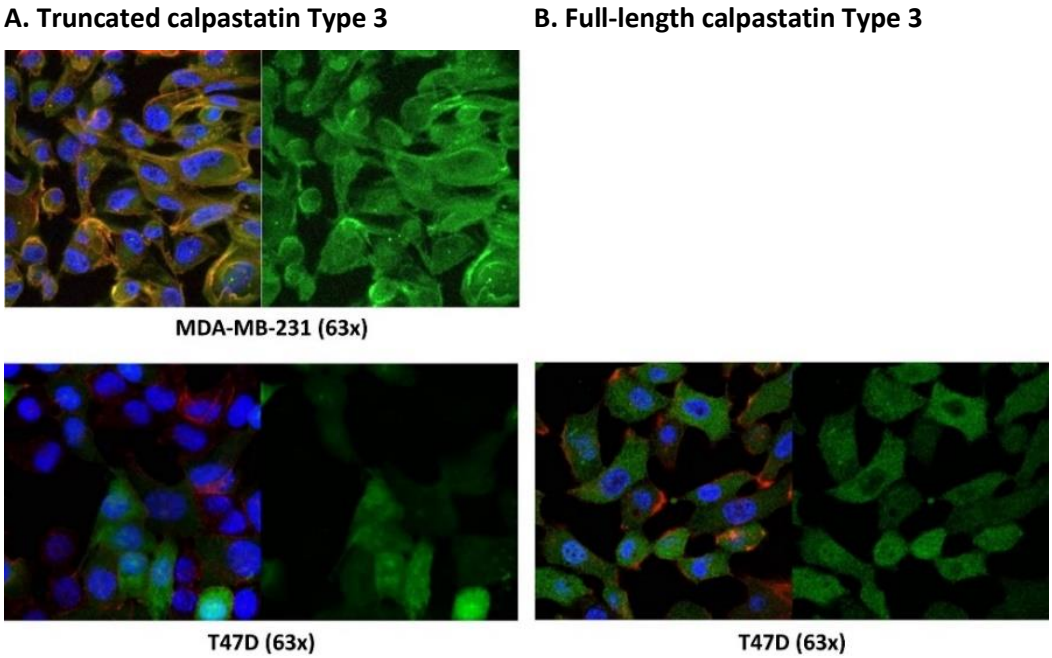


Figure 3.21 Intracellular localisation of (A) GFP-tagged truncated and (B) HA-tagged full-length forms of calpastatin Type 3 in MDA-MB-231 and T47D cells detected by IF confocal microscopy. The left column of each panel shows labelling confocal images of GFP or HA tag (green), nuclei (blue) and F-actin (red); the right column of each panel shows a singular expression of GFP or HA tag (green).

Also, the intracellular localisation of an exon 3-deleted version of the truncated calpastatin Type 1 (Type1Δ3), Type 2 (Type1Δ3) and Type 3 (Type1Δ3) has been investigated by Dr Storr (unpublished data). As shown in Figure 3.22, they distributed similarly to both truncated and full-length forms, encoded by exon3-containing cDNA of CAST, in MDA-MB-231 cells.

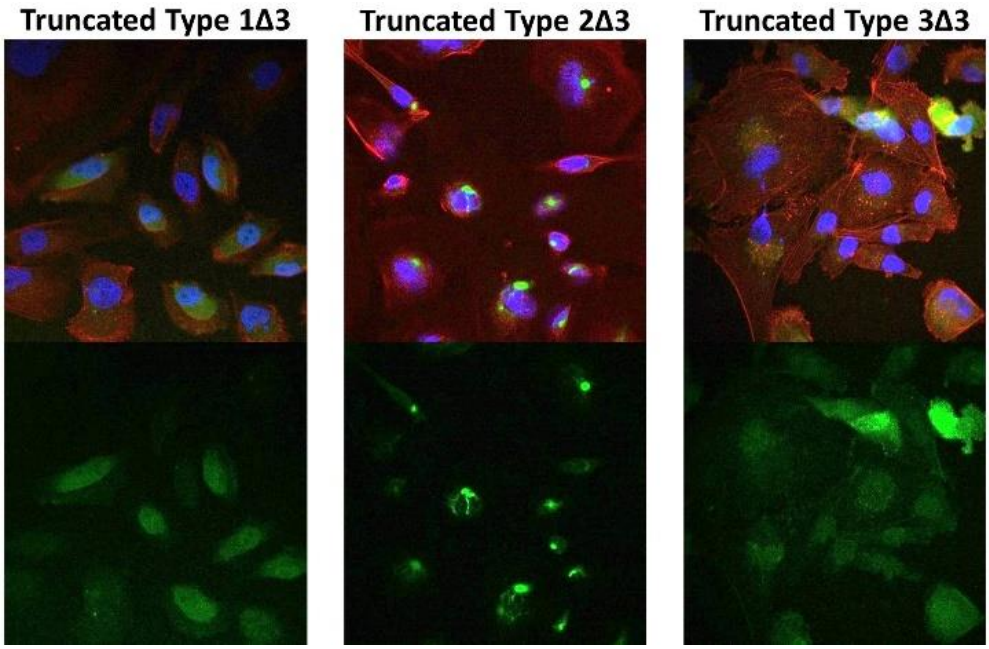


Figure 3.22 Intracellular localisation of GFP-tagged truncated calpastatin isoforms exon 3 deletion (Δ3) in MDA-MB-231 cells detected by IF confocal microscopy. The upper row shows labelling confocal images (63x) of GFP (green), nuclei (blue), and F-actin (red); the lower row shows a singular expression of GFP (green).

Briefly, the stably transfected monoclonal breast cancer cells overexpressing calpastatin Type 1, Type 2 and Type 3 were not wholly created from the same breast cancer cell line, neither MDA-MB-231 nor T47D (section 3.2). The current project successfully overexpressed Type 1 in MDA-MB-231 and T47D cells, Type 2 in MDA-MB-231 cells, and Type 3 in T47D cells. The difference between Type 1 and Type 2 in subcellular localisation (section 3.5) and their mRNA sequences differing by only one exon suggested to examine and compare the roles of calpastatin isoforms, mainly between Type 1 and 2, in regulating phenotypic endpoints related to breast cancer progression and LVI in MDA-MB-231 cell models. T47DCAST1 clone was also included in the phenotypic assessment to compare the role of full-length calpastatin Type 1 in different cell types.

3.6 Summary

1. MDA-MB-231 and T47D cells were chosen as *in vitro* cell models amongst seven cell lines to overexpress calpastatin isoforms based upon their low expression of calpastatin protein/mRNA and high calpains.

2. Stably transfected monoclonal cells overexpressing HA-tagged full-length calpastatin Type 1 (231CAST1 and T47DCAST1 cells), Type 2 (231CAST2 cells), and Type 3 (T47DCAST3 cells) and their respective mock-transfected monoclonal control cells (231Ctrl and T47DCtrl cells) were generated.

3. HA-tagged calpastatin expression, representing the expression of calpastatin isoforms, significantly increased in both 231CAST1 and 231CAST2 cells relative to mock-transfected cells ($P < 0.0001$ and $= 0.0005$, respectively). Total calpastatin was also significantly overexpressed relative to mock-transfected cells by 3.44 fold in 231CAST1 cells ($P < 0.0001$) and 2.61 fold in 231CAST2 cells ($P = 0.0035$).

4. Amongst all conventional calpain subunits, only calpain-1 expression significantly increased in both 231CAST1 (1.40 fold increase, $P = 0.0188$) and 231CAST2 cells (1.33 fold increase, $P = 0.0446$) in comparison to the expression in the mock-transfected cells.

5. CAST1 mRNA significantly overexpressed in the CAST1-transfected cell clones, i.e., 231CAST1 cells (2.60 fold increase; $P = 0.0020$) and T47DCAST1 clones (6.22 fold increase; $P < 0.0001$), relative to mock-transfected controls.

6. CAST2 mRNA expression in 231CAST2 cells could not be examined due to the poor amplification efficiency (27.44%) of the RT-qPCR method. However, overexpression of HA-tagged and total calpastatin observed in the cells allowed 231CAST2 clone to be another *in vitro* cell model for the current project.

7. 231CAST1 and 231CAST2 cell lines were confirmed for their persistent expression of HA-tagged and total calpastatin after being serially subcultured from the master cells (passage number 0) for ten times. Thus, all transfected cells were routinely cultured with the selection medium (750 µg/mL G418) and used in routine experiments up to passage number 10.

8. Short-term removal of G418 from the culture medium did not affect the HA-tagged and total calpastatins expression (up to 7 days) and the migration (up to 14 days) of 231CAST1 and 231CAST2 cells, compared to the cells routinely cultured in the selection medium. To avoid the possible effect of G418 on cell behaviours, the G418-free culture medium was used to culture all transfected cells for two days before performing and while conducting the experiments.

9. Type 1 and Type 3 calpastatin localised in MDA-MB-231 and T47D cells generally throughout the cytoplasm and slightly in the nuclei. Type 2 was found to have a cytoplasmic expression with a predominant perinuclear localisation – spots in MDA-MB-231 cells and fibre-like aggregation in T47D cells.

10. Full-length calpastatin isoforms distributed in breast cancer cells similarly to their truncated forms (only XL and L domains), encoded by cDNA either containing or lacking exon 3.

11. Calpastatin Type 1 and Type 2 were selected to examine and compare their roles to each other in regulating phenotypic endpoints related to breast cancer progression and LVI (Chapter 4) due to the differences between them in subcellular distribution and mRNA sequences by only one exon.

Chapter 4 Roles of calpastatin isoform overexpression in breast cancer progression and LVI

4.1 Hypotheses and aims

Calpastatin, as described in section 1.3.5.3.4, is the specific endogenous inhibitor of conventional calpains, with the current group reporting calpastatin involvement in breast cancer progression and LVI, in particular LI. The expression levels of calpastatin protein or exon3-containing calpastatin variants were negatively associated with the presence of LI and other clinicopathological characteristics of the high-risk group for cancer recurrence (such as ER-, PR-, and basal phenotypic tumours) (Storr *et al.*, 2011b; Storr *et al.*, 2012a), as well as lymph node involvement in breast cancer (Storr *et al.*, 2011c). This suggests that calpastatin may play a crucial role in regulating breast cancer progression and LVI. As described in section 1.3.5, generally, calpain activity, which can be activated by Ca^{2+} but limited by calpastatin, is positively implicated in several cellular physiological functions related to cancer progression and metastasis, such as cell proliferation, survival, apoptosis, migration, and invasion. In addition to activating calpain, Ca^{2+} influx plays a significant role in enhancing calpain inhibition by calpastatin, suggesting that calpastatin might attenuate activated calpains rather than prevent activation (Wells & Leloup, 2010). As mentioned by several studies (sections 1.3.5.1 and 1.3.5.2), reduction of calpain activity by calpastatin overexpression, pharmacological calpain inhibitors (e.g., calpeptin) or genetic disruption of calpain, generally, contributes to inhibition of cancer progression-related or metastasis-related physiological functions. The calcium ionophore A23187, a well-characterised mobile ion-carrier, has been previously used to increase intracellular Ca^{2+} content and calpain activity in several cell lines, including MDA-MB-231 breast cancer cells (Varga *et al.*, 2018; Pu, 2016), before examining the implications of an enhanced calpain activity on cellular functions.

Thus, the hypotheses of the current chapter were as follow:

1. Calpastatin isoform overexpression suppresses calpain activity in breast cancer cells.
2. Calpastatin isoform overexpression suppresses breast cancer cell phenotypic endpoints related to cancer progression and LVI.
3. A23187 increases calpain activity, leading to the promotion of breast cancer cell phenotypic endpoints related to cancer progression and LVI.

Aims: The current project focused on the role of calpastatin isoform overexpression in regulating phenotypic endpoints related to breast cancer progression and LVI *in vitro* using stably transfected breast cancer cells overexpressing calpastatin Type 1 (231CAST1 and T47DCAST1 cells), Type 2 (231CAST2 cells), or Type 3 (T47DCAST3 cells), established from the section 3.2, as cell models. The effects of Type 1 overexpression and Type 2 overexpression on the phenotypic endpoints were principally assessed and compared with each other in MDA-MB-231 cells, due to the differences between calpastatin Type 1 and Type 2 in intracellular localisation (section 3.5) and their mRNA sequences differing by only one exon. The present chapter aimed to:

1. Assess the effect of calpastatin isoform overexpression on calpain activity in breast cancer cells in the presence/ absence of A23187.
2. Evaluate the role that overexpression of individual calpastatin isoforms plays in regulating breast cancer cell proliferation and clonogenicity, to understand processes involved in regulating breast cancer progression *in vitro*, in the presence/ absence of A23187.
3. Evaluate the role that overexpression of individual calpastatin isoforms plays in regulating breast cancer cell migration and vascular endothelial interactions to understand the processes involved in regulating breast cancer LVI *in vitro*, in the presence/ absence of A23187.

4.2 Role of calpastatin isoform overexpression in regulating calpain activity *in vitro*

4.2.1 Effects of calpeptin on cell proliferation

Calpeptin is a cell-permeable peptide aldehyde inhibitor, which binds to the active site of calpain and reversibly inhibits protease activity (Tsujinaka *et al.*, 1988). The current project selected calpeptin to use as a comparator to the effect of calpastatin isoform overexpression on calpain activity and *in vitro* phenotypic endpoints because it shows more selectivity to inhibit calpain activity over the chymotrypsin-like activity of the eukaryotic proteasome compared to other protease inhibitors, including calpain inhibitors 1 (ALLN) and 2 (ALLM) (Figueiredo-Pereira *et al.*, 1994). In addition, calpeptin is the universal calpain inhibitor used in many studies, allowing them to compare their results to each other.

The effect of calpeptin on cell proliferation was evaluated in basal-like MDA-MB-231 and luminal T47D cells over 72 hours. Response to treatment by doxorubicin, a positive control, was initially assessed to ensure that cells were responding as expected. The effect of doxorubicin at multiple concentrations (0, 0.25, 0.5 and 1 µM) on cell proliferation was evaluated and is presented as dose-response curves in Figure 4.1**.** Table 4.1 shows the IC50 values of doxorubicin on the proliferation of both cell lines at each time point.

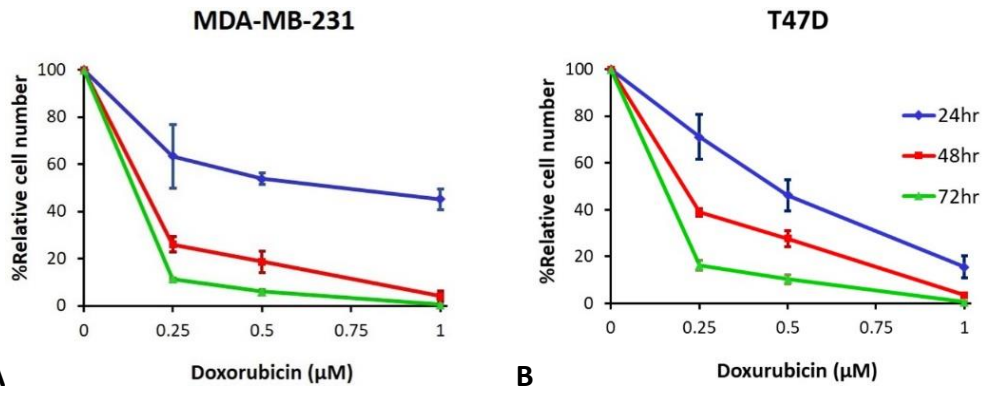


Figure 4.1 Effect of doxorubicin on breast cancer cell proliferation. (A) MDA-MB-231 and (B) T47D cells were treated with multiple concentrations of doxorubicin (0.25, 0.5, and 1 µM) for 24, 48 or 72 hours. Data represent the percentage cell proliferation as the average percentage of cell number relative to the no-treatment control ± SD of three independent experiments, each performed in triplicate.

Table 4.1 IC50 values of doxorubicin on breast cancer cells proliferation (n = 3).

Cell lines	IC50 of doxorubicin (µM)		
	24 hours	48 hours	72 hours
MDA-MB-231	0.72 ± 0.17	0.10 ± 0.03	0.06 ± 0.01
T47D	0.43 ± 0.08	0.19 ± 0.01	0.07 ± 0.01

No significant difference between IC50 values of doxorubicin in MDA-MB-231 and T47D cells was observed at each time points; n is the number of experiment. No significant difference in the IC50 values observed between both cell lines at each time-point.

Doxorubicin reduced MDA-MB-231 and T47D cell proliferation in a time- and dose-dependent manner. IC50 values of doxorubicin in inhibiting the proliferation of MDA-MB-231 vs T47D cells were 0.72 ± 0.17 µM vs 0.43 ± 0.08 µM, 0.10 ± 0.03 µM vs 0.19 ± 0.01 µM, and 0.06 ± 0.01 µM vs 0.07 ± 0.01 µM, at 24, 48, and 72 hours, respectively, of drug treatment. There was no significant difference in the IC50 values observed between both cell lines at each time-point. In clinical practice, the ESMO clinical practice guidelines suggested doxorubicin for breast cancer treatment; the recommended dose of doxorubicin hydrochloride is 60 mg/m^2 administered as an intravenous bolus every 21 days for 4 cycles of therapy, in combination with cyclophosphamide (Cardoso *et al.*, 2019).

A previous PhD project conducted by the current group also obtained comparable IC50 values for doxorubicin in MDA-MB-231 and T47D cell lines at all time points - 0.42 ± 0.09 µM vs 0.61 ± 0.21 µM, 0.16 ± 0.06 µM vs 0.15 ± 0.01 µM, and 0.10 ± 0.03 µM vs 0.07 ± 0.03 µM for 24, 48, and 72 hours of drug exposure (Abdullah, 2019). Also, the IC50 values from the current work correspond well to previously reported studies. Twenty-four-hour treatment with doxorubicin exhibited anti-proliferative effect with an IC50 value of 1-2.7 µM for MDA-MB 231 (Aroui *et al.*, 2009; Pilco-Ferreto & Calaf, 2016), and 0.383 µM for T47D (Putri *et al.*, 2016). The reported IC50 values of the 48-hour drug treatment in MDA-MB-231 cells were 0.14-1 µM (Pichot *et al.*, 2009; Wu *et al.*, 2013; Pilco-Ferreto & Calaf, 2016), while 0.25-0.29 µM IC50 values were indicated in T47D cells (Barzegar *et al.*, 2015; Pichot *et al.*, 2009). Treatment of 0.088-0.1241 µM doxorubicin for 72 hours caused a 50% reduction of MDA-MB-231 proliferation (Gouaze-Andersson *et al.*, 2007; Zhang *et al.*, 2012).

Therefore, both MDA-MB-231 and T47D cells, in the current study, responded to doxorubicin as expected, indicating that cells behaved properly in culture.

At 24 hours after drug exposure, as presented in Figure 4.1**,** MDA-MB-231 cells were more resistant to the anti-proliferative effect of doxorubicin compared to T47D cells, especially at the highest concentration (1 µM). Doxorubicin at 1 µM caused 45.10% and 15.47% cell proliferation in MDA-MB-231 and T47D cells, respectively. At this time point, 0.5 µM doxorubicin inhibited approximately 50% cell proliferation of MDA-MB-231 and T47D cells (53.80 ± 2.46 and 46.09 ± 6.65% cell proliferation, respectively). Treatment with 0.5 µM doxorubicin was therefore used as a positive control in subsequent proliferation assays to evaluate the effects of other agents on the proliferation of both cell types.

The impacts of calpeptin at multiple concentrations on the proliferation of MDA-MB-231 (5, 25, 50, 100 and 200 µM) and T47D cells (25, 50, 75, 100 and 200 µM) were assessed and are presented in dose-response curves in Figure 4.2. Anti-proliferative effects of calpeptin are more evident in T47D than that in MDA-MB-231 cells.

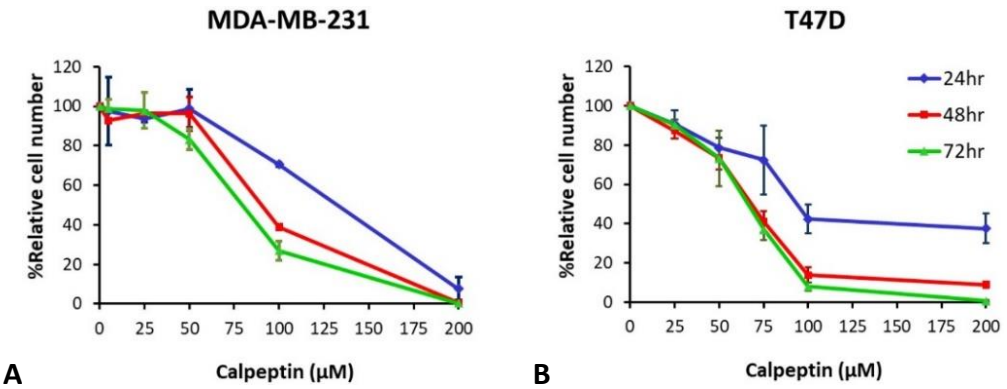


Figure 4.2 Effect of calpeptin on cell proliferation of breast cancer cells. (A) MDA-MB-231 and (B) T47D cells were treated with multiple concentrations of calpeptin (0-200 µM) for 24, 48 and 72 hours. Data are from cell counts before being calculated as the average percentage of cell number relative to the no-treatment control ± SD of three independent experiments, each performed in triplicate.

MDA-MB-231 responded to calpeptin in a time- and dose-dependent manner. The anti-proliferative effect of calpeptin started with a concentration higher than 50 µM in the first 48 hours of treatment. Treatment with 50 µM calpeptin for 24 to 48 hours caused 96-99% proliferation and started showing a small

anti-proliferative activity after 72 hours of drug treatment (83.20% proliferation). Pu (2016), another former member of the current group, previously reported similar data showing that 25 and 50 µM calpeptin were non-toxic to MDA-MB-231 cell growth after 24 and 48 hours of exposure. These two concentrations, however, were slightly toxic if the duration of treatment was extended to 72 hours (Pu, 2016). In the current study, marked decreases of MDA-MB-231 cell proliferation started from 100 µM calpeptin at all treatment periods (70.48, 38.80 and 26.88 %cell proliferation for 24-, 48- and 72-hour time points, respectively). Dr Pu also observed the effects of 100 µM calpeptin on MDA-MB-231 cells, causing approximately 60%, 40% and 30% cell proliferation for each time point (Pu, 2016). Calpeptin at 200 µM, in the current work, substantially inhibited MDA-MB-231 cell proliferation (7.69, 0.48 and 0.24 %cell proliferation for each time point) with more evident effects compared to 100 µM calpeptin.

Calpeptin also affected the T47D cell proliferation in a time- and dose-dependent manner. A small anti-proliferative ability of calpeptin on T47D cells was initially observed at higher than 25 µM at all time-points. Treatments with 50 and 75 µM calpeptin for 24 hours caused a reduction to 78.64% and 72.41% cell proliferation, respectively. Marked anti-proliferative effects of calpeptin were observed from 100 µM for the 24-hours drug exposure (42.27% cell proliferation), and 75 µM for the longer treatments (40.90 and 36.91 %cell proliferation for 48 and 72 hours of drug exposure, respectively). Calpeptin at 100 µM vs 200 µM substantially inhibited T47D cell proliferation by causing 42.27% vs 37.54%, 13.79% vs 8.92%, and 8.00% vs 0.69% proliferation for the 24-, 48-, and 72-hour treatment, respectively.

Although calpain inhibitory effect of treatment with 100 µM calpeptin for 24 hours was significantly detected in MDA-MB-231, as indicated in the study of Pu (2016), this concentration evidently demonstrated a cytotoxic effect on both MDA-MB-231 and T47D cells. Thus, experiments were conducted to identify a calpeptin concentration causing minimal cytotoxicity but maximal inhibition of calpain activity in MDA-MB-231 and T47D cells.

4.2.2 Inhibitory effect of calpeptin on calpain activity

The effective concentration of calpeptin required to inhibit calpain activity in MDA-MB-231 and T47D cells was optimised in the current section using t-Boc assay (section 2.8). A previous PhD study by the current group indicated that 100 µM calpeptin treatment for 0.5, 6, or 24 hours significantly inhibited calpain activity in SKBR3, MCF-7, and MDA-MB-231 breast cancer cells (Pu, 2016). Calpeptin at 100 µM was initially used, in the current study, in an attempt to verify the t-Boc assay assessment of calpain activity. Figure 4.3 shows fluorescence intensities of the cleaved substrate t-BOC-Leu-Met at cycle 1-10 (Figure 4.3-A) and the percentages of calpain activity in MDA-MB-231 at cycle 10 (Figure 4.3-B) in response to calpeptin treatment. The fluorescence intensities are presented as pooled data from three independent experiments, and the percentages of calpain activity were calculated independently from each experiment before being averaged. Treatment with 100 µM calpeptin for 30 minutes significantly reduced calpain activity in MDA-MB-231 cells by 21.89 ± 4.49% (P = 0.0011), confirming and corroborating the previous data (20-30% reduction) by Pu (2016), indicating that t-Boc assay provided consistent results.

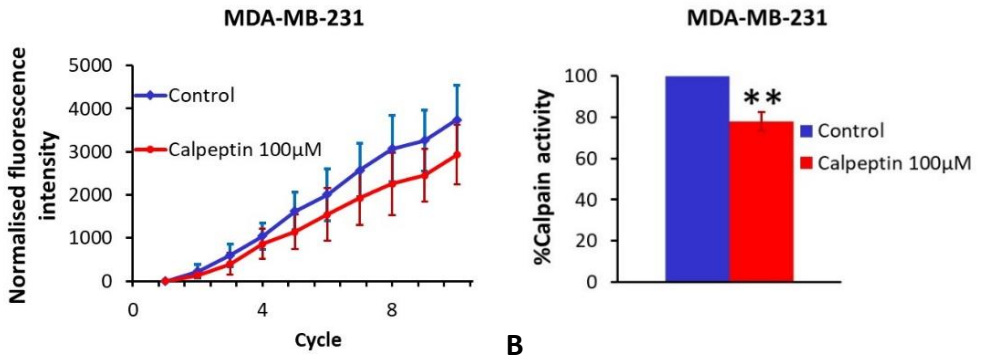
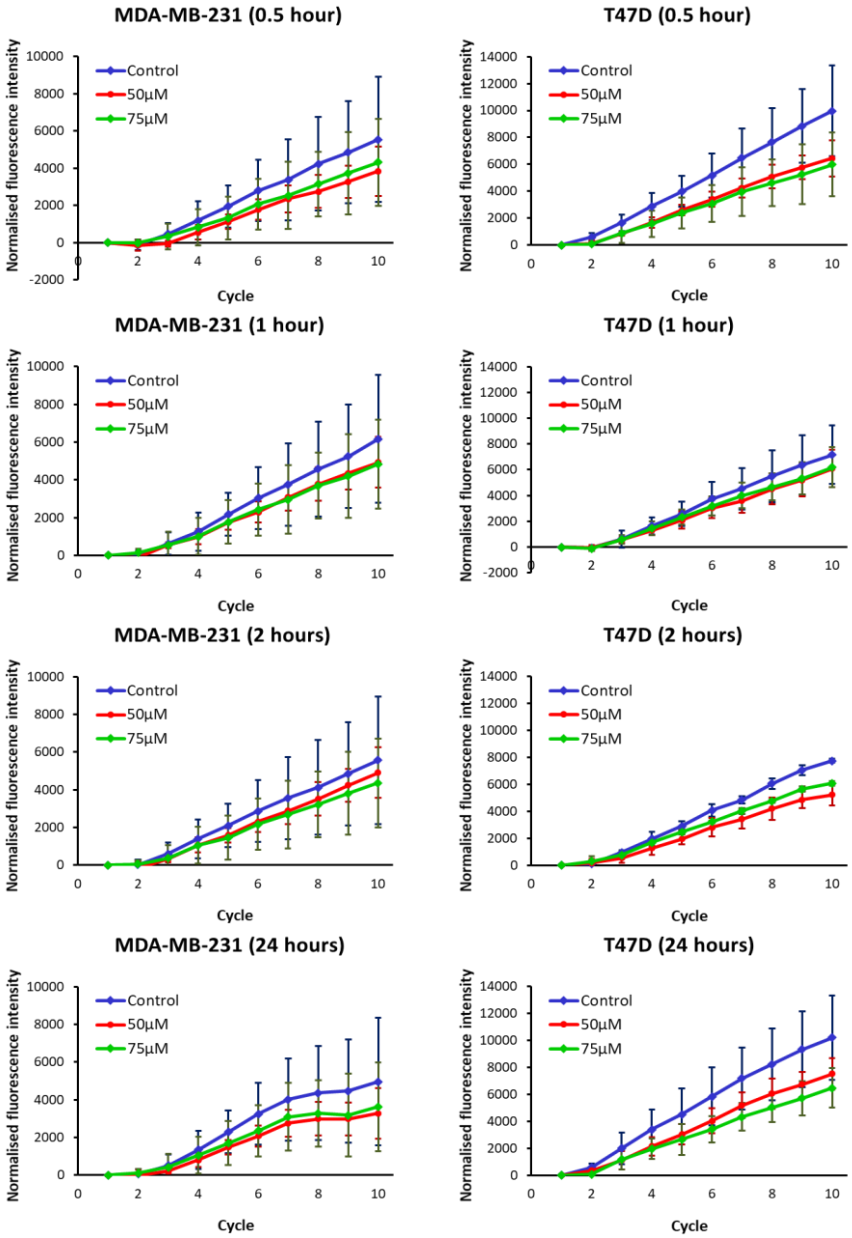


Figure 4.3 Inhibition of calpain activity in MDA-MB-231 cells by calpeptin (100 µM). MDA-MB-231 cells treated with 100 µM calpeptin for 30 minutes were examined for their calpain activity by t-Boc assay. Results are presented as (A) fluorescence intensities of the cleaved substrate t-BOC-Leu-Met at cycle 1-10, and (B) percentages of calpain activity at cycle 10. Data represent the average ± SD of three independent experiments, each in duplicate. *P*-values were assessed for showing the level of statistical difference between a calpeptin treatment group and no-treatment control;** $P < 0.01$.

To optimise calpeptin treatment conditions to generate a significant reduction of calpain activity but with minimal toxicity, calpeptin at 50 and 75 µM was examined on both cell lines at various incubation periods (0.5, 1, 2 or 24 hours), as shown in Figure 4.4.

A. Fluorescence intensities of the cleaved t-BOC-Leu-Met at cycle 1-10



B. Percentages of calpain activity at cycle 10

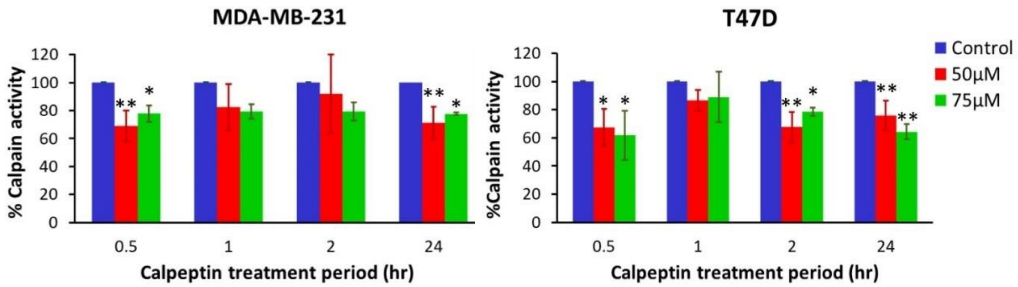


Figure 4.4 Inhibition of calpain activity in breast cancer cells by calpeptin (50 μM and 75 μM). MDA-MB-231 or T47D cells treated with 50 or 75 μM calpeptin for 0.5, 1, 2 and 24 hours were examined for their calpain activity using t-Boc assay. Results are presented as (A) fluorescence intensities of the cleaved substrate at cycle 1-10, and (B) percentages of calpain activity at cycle 10. Calpain activity assessment of each condition was performed independently. Data represent the average ± SD of three independent experiments, each performed in duplicate. P-values were assessed for showing the level of statistical differences between calpeptin treatment groups and no-treatment control; $*P < 0.05$, $**P < 0.01$.

As shown in Figure 4.4, calpeptin at 50 µM and 75 µM exhibited similar capabilities to reduce calpain activity in both cells for all incubation periods. In MDA-MB-231 cells, 50 µM calpeptin in comparison to 75 µM calpeptin reduced calpain activity with the similar abilities - 31.02% vs 22.18% (P = 0.2923), 17.57% vs 20.83% (P = 0.8160), 7.97% vs 20.68% (P = 0.4906), and 28.76% vs 22.29% (P = 0.5039) for the 0.5-, 1-, 2-, and 24-hour treatment, respectively. Similarly, calpeptin at 50 µM compared to 75 µM calpeptin also attenuated calpain activity in T47D cells by similar levels - 32.54% vs 38.15% (P = 0.6796), 13.42% vs 10.94% (P = 0.8355), 32.38% vs 21.40% (P = 0.1698), and 24.13% vs 35.59% (P = 0.1703) for the 0.5-, 1-, 2-, and 24-hour treatment, respectively.

The incubation period seemed to be a significant parameter in the calpain inhibitory activity of calpeptin (Figure 4.4-B). In MDA-MB-231 cells, significant calpain inhibition by both 50 and 75 µM calpeptin was observed only in the 0.5-hour treatment (P = 0.0036 and 0.0173, respectively) and at the most prolonged 24-hour treatment (P = 0.0088 and 0.0213, respectively). The treatment for 1 hour (P = 0.1509 and 0.0981) or 2 hours (P = 0.7922 and 0.2942) did not significantly inhibit calpain activity and produced a relative lower effect compared to the 0.5-hour treatment. Similarly, calpain activity of T47D cells was significantly decreased by treatment with 50 and 75 µM calpeptin for 0.5 hours (P = 0.0345 and 0.0179, respectively), 2 hours (P = 0.0017 and 0.0128, respectively), and 24 hours (P = 0.0091 and 0.0013, respectively). The 1-hour treatment did not show a significant effect in T47D cells (P = 0.3102 and 0.4313), and its effect was relatively lower than the effect of the 0.5-hour treatment. Together, the depletion of calpain inhibition by calpeptin observed when the breast cancer cells exposed to the drug for longer than 30 minutes might be due to cellular compensation of calpain activity occurring shortly (at least for 1 hour) before recovery of calpain inhibitory effect by calpeptin was significantly re-detected.

In summary, the conditions of calpeptin treatment for MDA-MB-231 and T47D cells were optimised by considering the concentration required to significantly inhibit calpain activity with minimal effect on cell proliferation as well as the

incubation period required to get maximal calpain inhibition. Calpeptin at 50 µM, therefore, was selected for future experiments due to its significant calpain inhibitory effect with no toxic on MDA-MB-231 cell proliferation or a small effect on the proliferation of T47D cells (section 4.2.1). As the 24-hour treatment of 50 µM calpeptin showed a significant impact to inhibit calpain activity in both cells, this condition was used in subsequent experiments.

4.2.3 Inductive effect of A23187 calcium ionophore on calpain activity

A23187 calcium ionophore is commonly used to enhance the intracellular Ca^{2+} influx and calpain activity in various cell lines, including MDA-MB-231 and MCF-7 breast cancer cells (Journé *et al.*, 2004; Varga *et al.*, 2018). In the current study, A23187 was investigated its effect on calpain activity detected by the t-Boc assay in MDA-MB-231 wild type before being used in experiments of their transfected cell clones.

Previous studies by the current group suggested that treatment with A23187 at 2 µM for 30 minutes was able to increase calpain activity in MDA-MB-231 cells by 94% detected by the Suc-LLVY-AMC assay (Pu, 2016). The 24-hour treatment with complete culture medium containing 2 µM A23187 was reported to cause only 5.1% MDA-MB-231 induction of cell apoptosis and necrosis (conducted by Dr Yimin Zhang). However, this treatment, by visual estimation, damaged approximately 50% integrity of cell monolayers in parental MDA-MB-231 and the respective transfected cell lines (Figure 4.5). The integrity of cell monolayers is an important factor if wishing to evaluate cell migration by scratch-wound assay. While A23187 at 1 µM slightly damaged cell monolayers by around 20%, 0.5 µM A23187 showed no effect. Thus, A23187 at 0.5 µM was assessed its ability to induce calpain activity in MDA-MB-231 cells in comparison to 2 µM A23187.

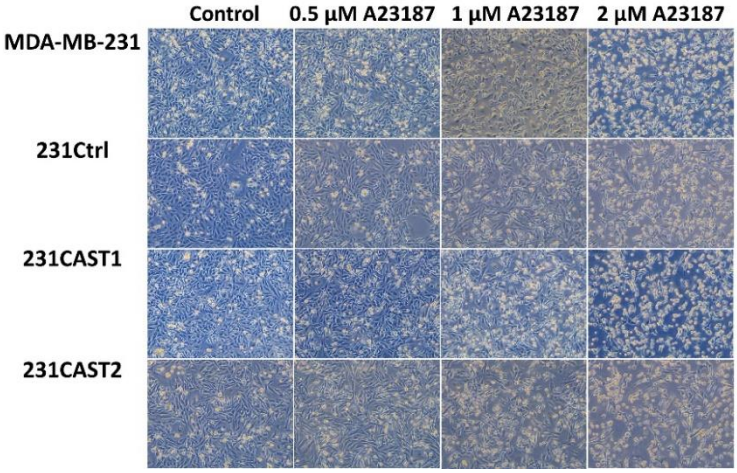


Figure 4.5 Effect of A23187 on the integrity of breast cancer cell monolayers. Representative images of cell monolayers of MDA-MB-231 parental and the stably transfected cell lines (231Ctrl, 231CAST1 and 231CAST2) treated with A23187 at 0, 0.5, 1 and 2 µM for 24 hours (100x magnification).

Calpain activity in MDA-MB-231 cells was assessed in response to a single treatment with 2 µM A23187 for 30 minutes, 0.5 µM A23187 for 24 hours, or 50 µM calpeptin for 30 minutes; and by a double treatment of 2 µM A23187 for 30 minutes/ 0.5 µM A23187 for 24 hours followed by 50 µM calpeptin for 30 minutes, as presented in Figure 4.6.

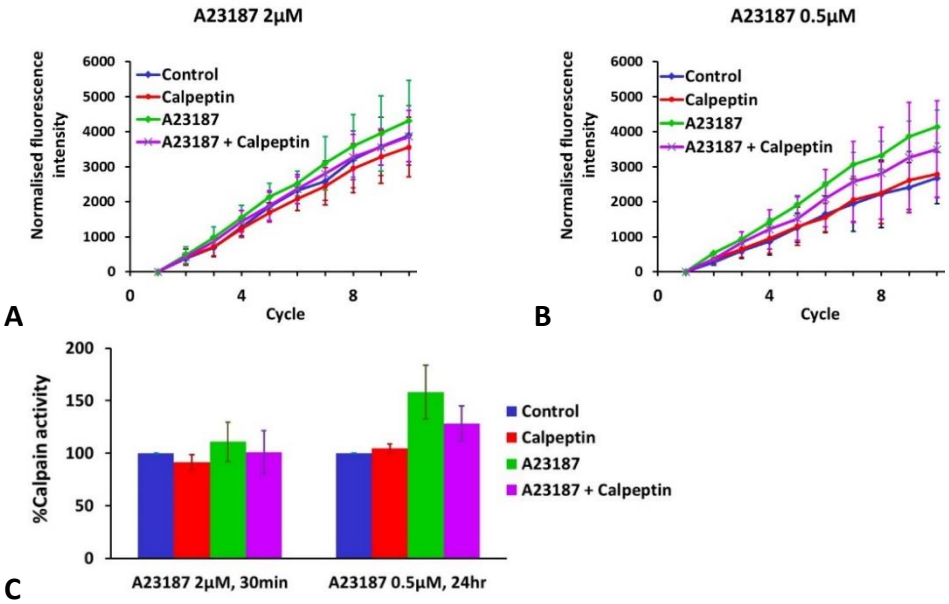


Figure 4.6 Effect of A23187 or calpeptin on calpain activity in MDA-MB-231 cells. Results are presented as (A, B) fluorescence intensities of the cleaved substrate at cycle 1-10, and (C) percentages of calpain activity at cycle 10. (A) Cells were treated with 2 µM A23187 or 50 µM calpeptin alone for 30 minutes, or treated with A23187 for 30 minutes followed by calpeptin for 30 minutes; (B) cells were treated with 0.5 µM A23187 for 24 hours or 50 µM calpeptin for 30 minutes alone; or treated with A23187 for 24 hours followed by calpeptin for 30 minutes. (C) A bar chart shows cellular calpain activity in response to 2 µM or 0.5 µM A23187 from the experiments performed separately. Data represent the average ± SD of (A) three or (B) two independent experiments, each performed in duplicate.

As shown in Figure 4.6-A, and -C, calpain activity in MDA-MB-231 cells treated with 2 µM A23187 alone for 30 minutes was increased by approximately 10% (110.79% calpain activity) relative to control. While calpeptin alone reduced calpain activity by around 9%, the double treatment produced approximately 100% calpain activity, suggesting that calpeptin normalised A23187-enhanced calpain activity. However, changes in calpain activity compared to the untreated cells were not significant in any single or combined drug treatments. For the treatment with 0.5 µM A23187 for 24 hours (Figure 4.6-B and -C), A23187 alone increased calpain activity by 58% relative to basal activity of control (158% calpain activity). The double treatment caused 128% calpain activity, again suggesting that the A23187-enhanced calpain activity could be attenuated by calpeptin.

In summary, treatment with A23187 at 0.5 µM for 24 hours increased calpain activity to a level that was higher than the calpain activity influenced by the treatment with 2 µM A23187 for 30 minutes (58% vs 10% increased calpain activity). A23187-increased calpain activity could be attenuated by calpain inhibition using calpeptin. Treatment with 0.5 µM A23187 for 24 hours was therefore used in subsequent experiments.

4.2.4 Effects of calpastatin isoform overexpression on calpain activity

4.2.4.1 Calpain activity in calpastatin isoform overexpressing MDA-MB-231 cells

The current section sought to determine the consequences of upregulation of individual calpastatin Type 1 or Type 2 on calpain activity in MDA-MB-231 cell, using the t-Boc assay. As reviewed in sections 1.3.5.1 and 1.3.5.2, calpain activity in the calpastatin-overexpressing cells was postulated to be lower than the basal activity in the mock-transfected cells. In this study, however, the unexpectedly opposing results, as shown in Figure 4.7, were observed. Overexpression of calpastatin Type 1 and Type 2 significantly contributed to relative increases of calpain activity in 231CAST1 (139.82%, P = 0.0157) and 231CAST2 cells (170.78%, P = 0.0009), respectively, compared to the calpain

activity level in the mock-transfected 231Ctrl cells. Difference between calpain activity in 231CAST1 and 231CAST2 was not observed (P = 0.0727).

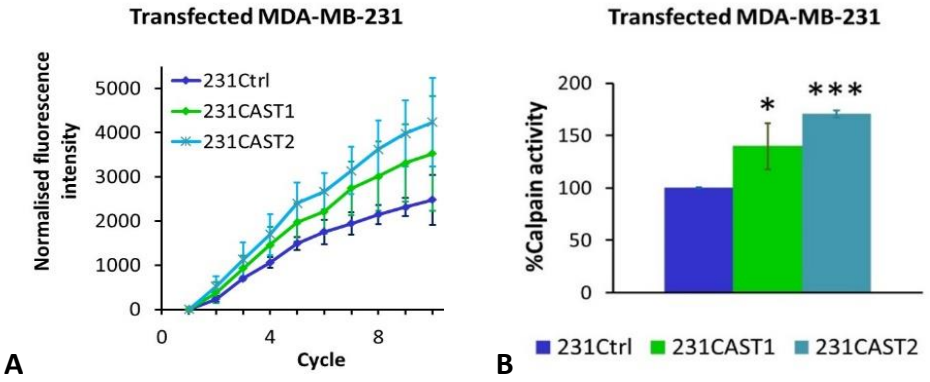


Figure 4.7 Calpain activity of MDA-MB-231 cells overexpressing calpastatin isoforms. MDA-MB-231 cells overexpressing calpastatin Type 1 (231CAST1) or Type 2 (231CAST2) or the mock-transfected cells (231Ctrl) were examined for their calpain activity using the t-Boc assay. Results are shown as (A) fluorescence intensities of the cleaved t-BOC-Leu-Met at cycle 1-10 and (B) percentages of calpain activity at the cycle 10 relative to the mock-transfected control. Data represent the average ± SD of three independent experiments, each performed in duplicate. P-values were assessed for showing the level of statistical differences between CAST-overexpressing cells and the mock-transfected control; *P < 0.05 or *** P < 0.001.

4.2.4.2 Effects of A23187 calcium ionophore on calpain activity

The effect of A23187 on calpain activity in MDA-MB-231 cells overexpressing different calpastatin isoforms was examined. Calpain activity in mock-transfected 231Ctrl cells was first examined whether the cells respond to the presence of A23187 or calpeptin similarly to the parental cells, explored in section 4.2.3. The results are shown in Figure 4.8.

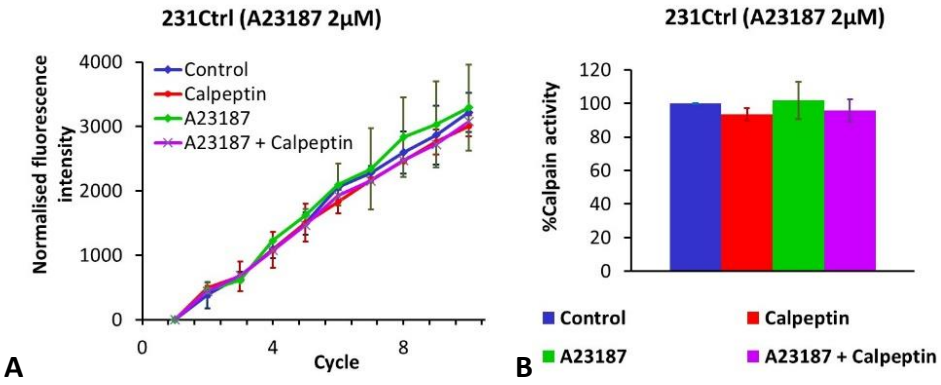


Figure 4.8 Effect of calpeptin or A23187 on calpain activity in the mock-transfected MDA-MB-231 cells. Results are shown as (A) fluorescence intensities of the cleaved substrate t-BOC-Leu-Met at cycle 1-10, and (B) percentages of calpain activity at cycle 10. The mock-transfected 231Ctrl cells were treated with 50 µM calpeptin or 2 µM A23187 alone for 30 minutes, or treated with A23187 for 30 minutes, followed by calpeptin for 30 minutes. Data represent the average ± SD of two independent experiments, each in duplicate.

Figure 4.8 shows that while treatment with 2 µM A23187 for 30 minutes did not affect calpain activity in 231Ctrl cells (101.78%), a double treatment (A23187 and calpeptin, respectively) resulted in the similar calpain activity level to the effect of the 30-minute calpeptin treatment alone (95.75% vs 93.79%), suggesting that a small calpain inhibitory effect observed in the double treatment was caused by calpeptin. However, neither single treatments nor double treatment of the calpain regulators significantly affected calpain activity in 231Ctrl, or wild type cells (section 4.2.3).

The role that calpastatin isoform overexpression plays in regulating calpain activity of MDA-MB-231 cells in the presence of A23187 was investigated using 231CAST1 and 231CAST2 cells treated with different A23187 conditions - 2 µM A23187 for 30 minutes or 0.5 µM A23187 for 24 hours. As shown in Figure 4.9, the treatment of 2 µM A23187 remained to cause no effect in inducing calpain activity in mock-transfected cells but seemed to slightly increase calpain activity in both 231CAST1 and 231CAST2 cells by 13.52 % and 12.21%, respectively.

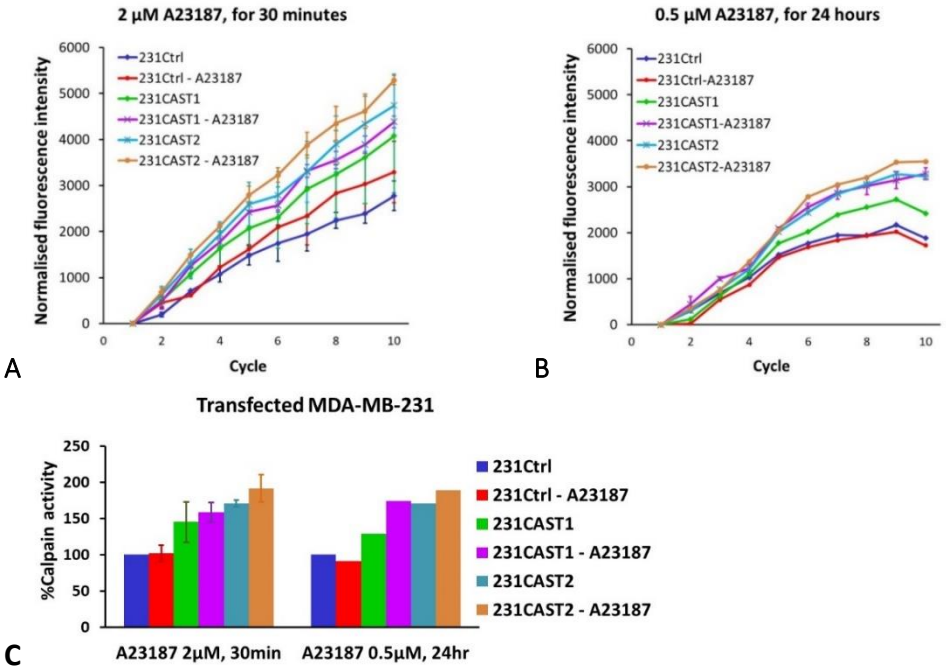


Figure 4.9 Effect of A23187 on calpain activity in MDA-MB-231 cells overexpressing calpastatin isoforms. MDA-MB-231 overexpressing calpastatin Type 1 (231CAST1) or Type 2 (231CAST2) or the mock-transfected cells (231Ctrl) were treated with (A) 2 µM A23187 for 30 minutes or (B) 0.5 µM A23187 for 24 hours. Results are presented as (A, B) fluorescence intensities of the cleaved substrate at cycle 1-10, and (C) percentages of calpain activity at cycle 10 relative to the mock-transfected control. The experiments of 2 µM and 0.5 µM A23187 were performed separately. Data represent the average ± intra-experimental SD for one experiment of 0.5 µM A23187 treatment or ± inter-experimental SD for two independent experiments of 2 µM A23187 treatment, each in duplicate.

For the prolonged treatment (Figure 4.9-B and -C), 0.5 µM A23187, which caused 58% increase of calpain activity in parental MDA-MB-231 (section 4.2.3), seemed to be ineffective in stimulating calpain activity of the mock-transfected 231Ctrl cells but effective in the treated 231CAST1 and 231CAST2 compared to the no-treatment controls - 91.52% vs 100% for 231Ctrl cells, 174.25% vs 128.70% for 231CAST1 cells or 188.49% vs 171.17% for 231CAST2 cells. In other words, the 0.5 µM A23187-treated cells had higher calpain activity relative to their respective no-treatment controls by 35.39% and 10.12% in 231CAST1 and 231CAST2 cells, respectively. The results of this study, however, were generated from only one experiment due to unstable fluorescence signals observed in repeated experiments (data not shown), and the study was not resumed due to time limitations.

4.3 Role of calpastatin isoform overexpression on *in vitro* models of breast cancer progression (proliferation and clonogenic survival)

The calpain-calpastatin system has been implicated in various cancer progression-related cellular functions, such as cell proliferation, survival, and apoptosis (section 1.3.5.1). The role of calpastatin isoforms in regulating phenotypic characteristics related to cancer progression, however, has not been previously examined. This section aimed to evaluate the role that overexpression of individual calpastatin isoforms plays in regulating breast cancer cell proliferation and clonogenicity, to understand processes involved in regulating cancer progression *in vitro*, in the presence/absence of A23187.

4.3.1 Cell proliferation

4.3.1.1 Effects of calpastatin isoform overexpression on cell proliferation

The effect of calpastatin isoform overexpression on cell proliferation was examined using all stably transfected monoclonal MDA-MB-231 or T47D cells, established from section 3.2, as *in vitro* cell models. Growth curves are shown in Appendix D (Figure D4.1 and Figure D4.2). Figure 4.10 and Table 4.2 show

and compare cell growth characteristics and doubling times, respectively, amongst all transfected cells.

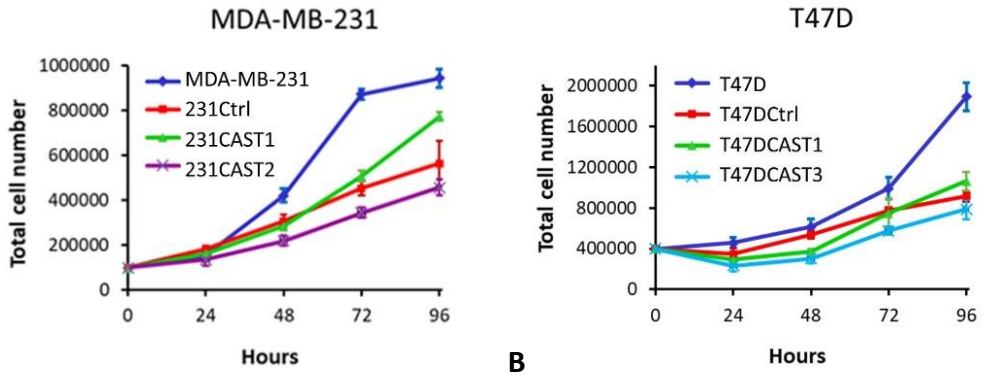


Figure 4.10 Effect of calpastatin isoform overexpression on breast cancer cell proliferation. (A) MDA-MB-231, (B) T47D parental cells and their respective transfected cells overexpressing calpastatin Type 1 (231CAST1 and T47DCAST1), Type 2 (231CAST2), Type 3 (T47DCAST3), and the mock-transfected controls (231Ctrl and T47DCtrl) were examined for their proliferation over 96 hours. Growth analyses of each cell line were performed independently. Growth characteristics of parental cells are from section 3.2.1.1. Data represent the average cell number per well ± SD of three independent experiments, each in triplicate.

Table 4.2 Cell doubling times of parental and stably transfected breast cancer cell lines.

Transfection	Doubling time (hours)	
	MDA-MB-231	T47D
No (Parental cells)	19.07 ± 0.76**	29.53 ± 1.48
Empty vector	38.41 ± 7.51	41.97 ± 5.01
CAST1	29.13 ± 0.65	33.11 ± 8.62
CAST2	35.63 ± 3.83	-
CAST3	-	37.09 ± 6.46

Growth analyses of each cell line were performed independently. Doubling times of parental cells are from section 3.2.1.1. Data represent the average cell doubling time ± SD of three independent experiments, each performed in triplicate. *P*-values were assessed for showing the level of statistical differences between each cell line and the mock-transfected controls;** $P < 0.01$.

As shown in Figure 4.10 and Table 4.2, the mock-transfected 231Ctrl cells proliferated significantly slower than the corresponding parental cells, causing the longer doubling time (38.41 vs 19.07 hours, $P = 0.0018$). Likewise, the mock-transfected T47D cells (T47DCtrl) seemed to have longer doubling time relative to parental cells, although there was no statistical difference (41.97 vs 29.53 hours, $P = 0.0822$). In this study, growth curve analyses of all transfected cells were performed in the selection medium (750 µg/mL G418), suggesting that

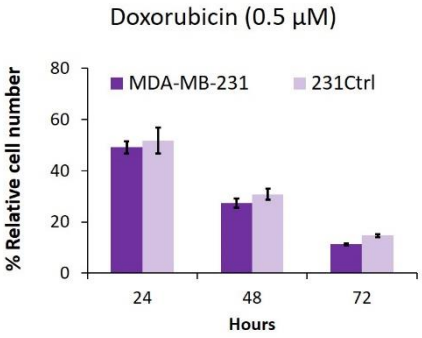
the longer doubling times of both mock-transfected 231Ctrl and T47DCtrl cells might be as a consequence of G418 or the empty-vector contained in both cells.

Amongst all CAST-transfected cells, calpastatin Type 1 overexpression in both 231CAST1 (29.13 vs 38.41 hours, *P* = 0.0676) and T47DCAST1 cells (33.11 vs 41.97 hours, *P* = 0.2382) seemed to influence cell proliferation, leading to a shorter doubling time compared to the respective mock-transfected cells, although a significant difference was not detected. The doubling times of 231CAST2 cells overexpressing Type 2 calpastatin (35.63 hours, *P* = 0.7664), as well as T47DCAST3 cells overexpressing Type 3 protein (37.09 hours, *P* = 0.6445), were not different from that of their mock-transfected controls.

4.3.1.2 Effects of A23187 calcium ionophore on cells proliferation

This study aimed to 1) optimise the non-toxic concentration of A23187 on cell proliferation for using in subsequent experiments and 2) investigate the impact of A23187 on the proliferation of the cells overexpressing calpastatin isoforms. The parental MDA-MB-231 and their transfected cells were treated with A23187 at 0.5 or 1 µM for 24, 48, and 72 hours then cell proliferation assessed. As shown in Figure 4.11, mock-transfected 231Ctrl cells responded to 0.5 µM doxorubicin, a positive control, similarly to parental MDA-MB-231 cells. The percentages of cell proliferation of the parental cells vs 231Ctrl mock-transfected cells were 51.81% vs 49.13%, 30.82% vs 27.40% and 14.62% vs 11.31% after being treated by the drug for 24, 48 and 72 hours, respectively. The parental cells consistently responded to the positive control, as they did previously in section 4.2.1, suggesting that the parental cells behaved as expected, and the experimental technique was robust.

A. Doxorubicin



B. A23187

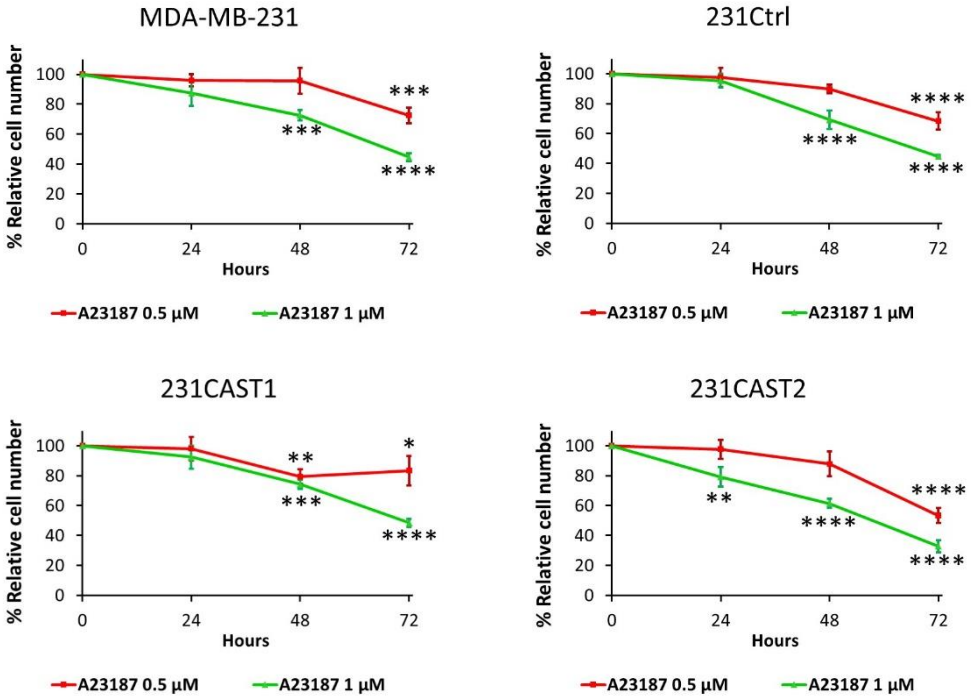


Figure 4.11 Effect of A23187 on cell proliferation in MDA-MB-231 cells overexpressing calpastatin isoforms. Parental MDA-MB-231 cells and their transfected cell lines overexpressing calpastatin Type 1 (231CAST1), and Type 2 (231CAST2), and the mock-transfected cells (231Ctrl) were treated with (A) doxorubicin (0.5 µM) or (B) A23187 (0.5 and 1 µM) for 24, 48, and 72 hours. Data represent the average percentages of cell number relative to the no-treatment control ± SD of three independent experiments, each performed in duplicate. *P*-values were assessed for showing the level of statistical differences between the A23187 treatment groups and no-treatment control within each cell line; * $P < 0.5$, ** $P < 0.01$, *** $P < 0.001$ or **** $P < 0.0001$. No significant difference observed between parental and mock-transfected cell lines at each time-point in the study of doxorubicin.

A23187 treatment similarly affected cell proliferation in all cell lines in a dose- and time-dependent manner. A23187 treatment at 0.5 µM for 24 hours did not significantly affect cell proliferation of any cell line (> 95% cell proliferation). For prolonged treatment, 0.5 µM A23187 caused a small anti-proliferative effect in all cell lines. More than 80% cell proliferation was demonstrated at 48 hours of

drug treatment; 95.65, 89.84, 79.42, and 87.84 %cell proliferation was observed for the parental MDA-MB-231, 231Ctrl mock-transfected, 231CAST1, and 231CAST2 cells, respectively. After 72 hours of drug exposure, A23187 decreased cell proliferation to approximately 70% for all cells, except for 231CAST2 cells (~ 53.41%).

A23187 at a higher concentration (1 µM) exhibited higher proliferative inhibition in all cell lines. A 24-hour drug treatment contributed to approximately 90% or more of cell proliferation in the parental MDA-MB-231 (87.42%), 231Ctrl (95.30%), and 231CAST1 cells (92.41%) but caused a higher effect on 231CAST2 cell proliferation (79.20%). The 48-hour treatment inhibited cell proliferation by ~30% in the parental MDA-MB-231, 231Ctrl, and 231CAST1 cells (72.55, 69.30, 74.37% cell proliferation, respectively), and ~40% for 231CAST2 cells (61.45% cell proliferation). After extending the treatment of 1 µM A23187 up to 72 hours, the cell proliferation was inhibited by approximately 50% in parental MDA-MB-231, 231Ctrl, and 231CAST1 cells but 67.22% in 231CAST2 cell line. Amongst all cells, 231CAST2 cells seemed to be more sensitive to A23187.

4.3.2 Clonogenicity

4.3.2.1 Effects of calpastatin isoform overexpression on clonogenicity

The effect of calpastatin isoform overexpression on clonogenicity of breast cancer cells was examined using stably transfected MDA-MB-231, as cell models. Calpeptin was used in the current study to demonstrate the effect of calpain inhibition on clonogenic survival. Clonogenic survival assays of all cells were performed in the regular culture medium, without G418, and the results presented as plating efficiency (PE) or surviving fraction (SF).

As shown in Figure 4.12, within 14 days, parental MDA-MB-231 cells were able to form colonies with 42.25 ± 4.73% PE, which is comparable to the previous data (52.89 ± 13.69%) obtained by Dr Abdullah (2019), a former PhD student of the current group. The 24-hour treatment of 50 µM calpeptin that had no anti-

proliferative effect on MDA-MB-231 cells (section 4.2.1) also showed no effect on clonogenic survival of the cells (SF = 0.99 ± 0.17, *P* = 0.9607). Thus, the treatment of calpeptin was not included in the following assays to be used as a comparator for calpastatin overexpression's effect on clonogenic survival.

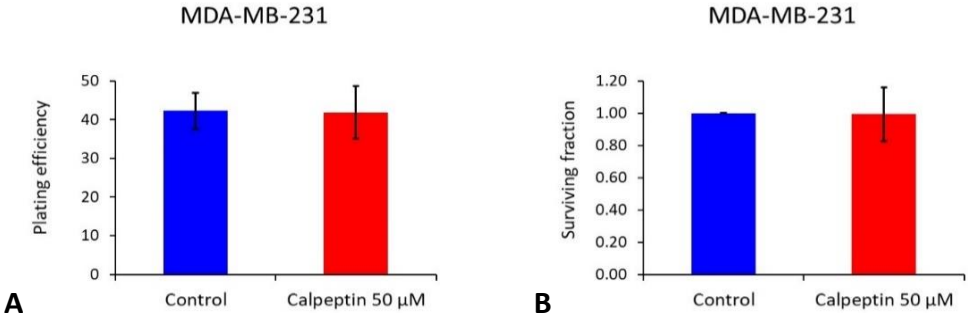


Figure 4.12 Effect of calpeptin on clonogenicity of MDA-MB-231 cells. Cells were treated with 50 µM calpeptin for 24 hours before being plated for clonogenic survival. Data represent the average percentages of (A) plating efficiency or (B) surviving fraction ± SD of three independent experiments, each experiment containing six parallel data sets. No significant difference is present between the calpeptin treatment group and no-treatment control.

For transfected cell lines (Figure 4.13), the PE value of mock-transfected 231Ctrl cells was significantly lower than the parental cells (PE = 46.85 ± 4.37% vs 69.07 ± 6.74%, *P* = 0.0009). SF of 231Ctrl cells relative to parental cells was 0.68 ± 0.05 (*P* < 0.0001), perhaps indicating that the empty vector is having an effect. There was no significant effect of isoform overexpression on clonogenicity in either 231CAST1 (PE = 49.32 ± 6.08%, *P* = 0.9427; SF = 1.04 ± 0.20, *P* = 0.9147) or 231CAST2 cells (PE = 45.35 ± 3.82%, *P* = 0.9860; SF = 0.96 ± 0.23, *P* = 0.9147) in comparison with that of the mock-transfected control.

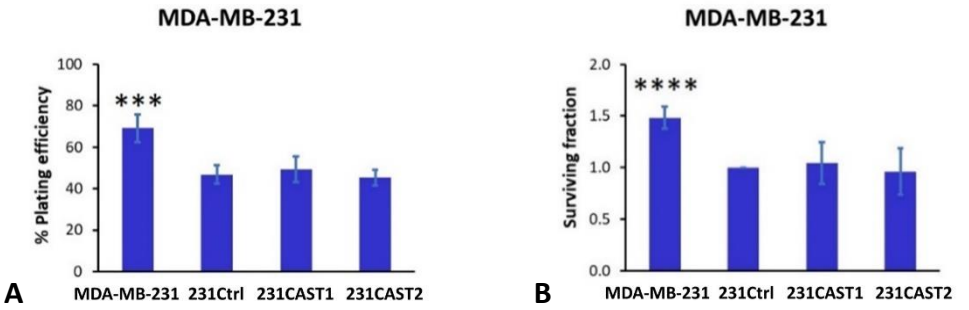


Figure 4.13 Effect of calpastatin isoform overexpression on MDA-MB-231 clonogenicity. Clonogenic survival assays were performed in parental MDA-MB-231 cells and their transfected cell lines overexpressing calpastatin Type 1 (231CAST1), and Type 2 (231CAST2), and the mock-transfected cells (231Ctrl). Colonies were formed within 14 days. Data represent the average plating efficiency or surviving fraction ± SD of nine independent experiments, each containing six parallel data sets. P-values were assessed for showing the level of statistical differences between each cell line and the mock-transfected control; *** *P* < 0.001 or **** *P* < 0.0001.

4.3.2.2 Effects of A23187 calcium ionophore on clonogenic survival

This study aimed to 1) optimise the non-cytotoxic concentration of A23187 on clonogenic survival for using in subsequent experiments and 2) interpret the impact of A23187 on clonogenicity of the cells overexpressing calpastatin isoforms. Figure 4.14 shows the clonogenic survival, represented by SF values, of stably transfected MDA-MB-231 cells overexpressing calpastatin Type 1 (231CAST1) and Type 2 (231CAST2) as well as control cells (the wild type and the mock-transfected cells) after pre-treated with A23187 for 24 or 72 hours.

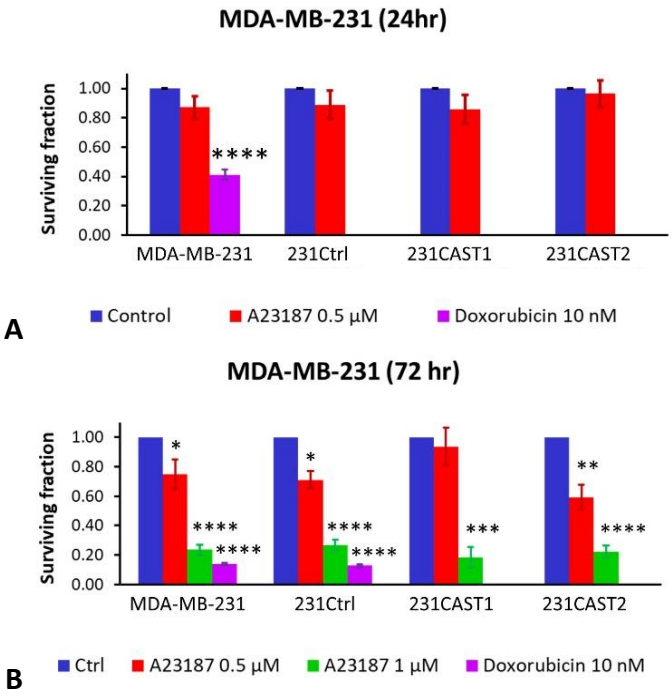


Figure 4.14 Effect of A23187 on clonogenic survival of MDA-MB-231 cells overexpressing calpastatin isoforms. Parental MDA-MB-231 cells, and their transfected cell lines overexpressing calpastatin Type 1 (231CAST1), Type 2 (231CAST2), and mock-transfected cells (231Ctrl) were treated with A23187 (0.5 and 1 µM) or 10 nM doxorubicin for (A) 24 or (B) 72 hours before being plated to form colonies. For (A) the 24-hour treatment, PE values were 73.03 ± 5.30% (MDA-MB-231), 47.42 ± 5.31% (231Ctrl), 53.61 ± 9.26% (231CAST1), 43.19 ± 5.35% (231CAST2). For (B) the 72-hour treatment, PE values were 62.64 ± 9.96% (MDA-MB-231), 42.57 ± 4.90% (231Ctrl), 40.17 ± 4.92% (231CAST1), and 36.31 ± 3.42% (231CAST2). Data represent the average percentages of surviving fraction ± SD of three independent experiments, each experiment containing six parallel data sets. P-values were assessed for showing the level of statistical differences between drug treatment groups and no-treatment control within each cell line; * $P < 0.05$, ** $P < 0.01$, *** $P < 0.001$, and **** $P < 0.0001$.

In the current study, 10 nM doxorubicin was used as a positive control. It caused approximately 60-66% MDA-MB-231 colony inhibition following exposure to doxorubicin for 24 hours ($P < 0.0001$), or 84-89% colony inhibition for the 72-hour drug exposure ($P < 0.0001$). The mock-transfected 231Ctrl cells responded

to doxorubicin similarly to the parental cells. Pre-incubation with the drug for 72 hours resulted in 83-91% colony inhibition in 231Ctrl cells ($P < 0.0001$).

A23187 calcium ionophore suppressed clonogenic survival of all cell lines in a dose- and time-dependent manner. Clonogenic survival of all cells, including 231CAST1, 231CAST2, and their negative control cells (parental MDA-MB-231 and 231Ctrl cells), was not affected by pre-treatment with 0.5 µM A23187 for 24 hours (4-14% inhibition, SF = 0.86-0.96, Figure 4.14). For the prolonged pre-incubation (72 hours), 0.5 µM A23187 significantly inhibited colony formation by 25% for parental MDA-MB-231 (SF = 0.75, $P = 0.0305$), 29% for 231Ctrl (SF = 0.71, $P = 0.0156$), and 41% for 231CAST2 (SF = 0.59, $P = 0.0011$), but did not significantly affect clonogenic survival of 231CAST1 cells (SF = 0.95, $P = 0.7262$). Pre-incubation for 72 hours with 1 µM A23187 showed significant effect in suppressing colony formation by 76% (SF = 0.24, $P < 0.0001$), 72% (SF = 0.28, $P < 0.0001$), 82% (SF = 0.18, $P = 0.0002$), and 78% (SF = 0.22, $P < 0.0001$) for MDA-MB-231, 231Ctrl, 231CAST1, and 231CAST2 cells, respectively.

In summary, the 24-hour treatment with 0.5 µM A23187 showed the ability to increase calpain activity (section 4.2.3 and 4.2.4.2) but had no toxicity on the integrity of cell monolayers (section 4.2.3), cell proliferation (section 4.3.1.2) and clonogenic survival (section 4.3.2.2) in all MDA-MB-231 cell clones. Therefore, this condition was used in subsequent experiments.

4.4 Role of calpastatin isoform overexpression in breast cancer LVI *in vitro*

As previously mentioned, calpastatin has been reported to be associated with breast cancer LVI, in particular LI (Storr *et al.*, 2011b; Storr *et al.*, 2012a). Although the calpain-calpastatin system has been shown to regulate cellular functions related to LVI, such as cell migration and adhesion (section 1.3.5.2), the mechanism whereby each calpastatin isoform regulates such phenotypic endpoints remains unknown. The current work, therefore, aimed to investigate the role that overexpression of calpastatin Type 1 and 2 individually play in regulating haptotaxis cell migration and endothelial interactions (specifically

cancer cell adhesion to lymphatic vs blood vessel ECs), using transfected breast cancer cell overexpressing Type 1 (231CAST1 and T47DCAST1 cells) and Type 2 (231CAST2 cells) as *in vitro* cell models, in the presence/absence of A23187.

To regulate calpain activity, 0.5 µM A23187 treatment for 24 hours was used in the current experiments. This A23187 condition seemed to be active at inducing calpain activity in parental MDA-MB-231 (section 4.2.3), 231CAST1, and 231CAST2 cells (section 4.2.4.2) but had no significant effect on cell proliferation (section 4.3.1.2), clonogenic survival (section 4.3.2.2), or the integrity of cell monolayers (section 4.2.3) in all parental and transfected MDA-MB-231 cells. Due to time limitations, the effect of A23187 on calpain activity in wide-type or transfected T47D cells was not examined. The treatment with 0.5 µM A23187 for 24 hours optimised in MDA-MB-231 cells, therefore, was used in the studies of T47D cell lines. Calpeptin treatment at 50 µM for 24 hours, which significantly inhibited calpain activity in MDA-MB-231 and T47D cells (section 4.2.2), was used to show the effect of calpain inhibition on the investigated cellular functions.

4.4.1 Cell migration

4.4.1.1 Optimisation of cell plating density to form cell monolayers

Optimisation of cell plating density to form confluent cell monolayer (90-100%) was performed before conducting the scratch-wound (haptotaxis) migration assay. Figure 4.15 shows representative images of cell monolayers formed at 24 hours after cell plating at various cell densities, as indicated. A density of $2.5x10^5$ cells/well produced confluent monolayers for all parental and stably transfected MDA-MB-231 cell lines (mock-transfected 231Ctrl, 231CAST1 and 231CAST2). Plating cells at a slightly lower concentration ($2x10^5$ cells/well) did not produce 90-100% confluent cell monolayers, whereas over confluent monolayers were formed with a density of $3x10^5$ cells/well. In comparison to MDA-MB-231 cells, all parental and transfected T47D cells (mock-transfected T47DCtrl and T47DCAST1; no image available) required a higher cell density (one million cells/well) to form confluent cell monolayers. At higher cell

densities (1.1 and 1.2 million cells/well), over confluent T47D cell monolayers were created.

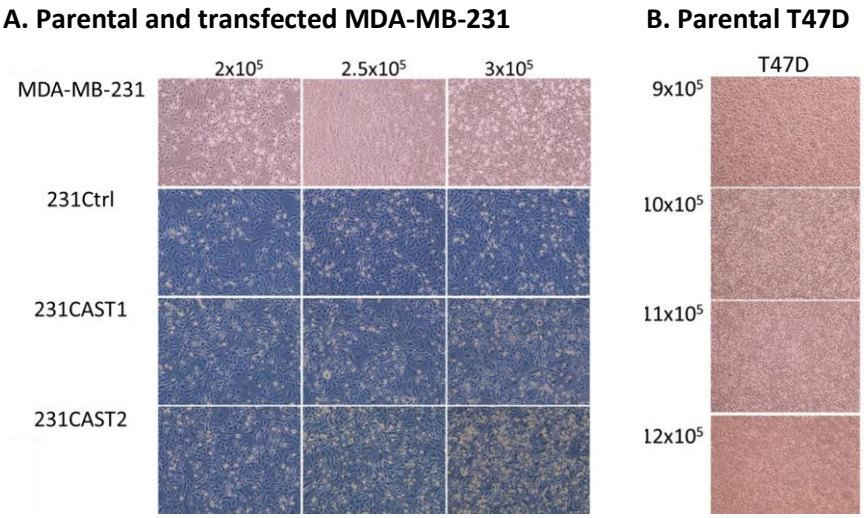


Figure 4.15 Optimisation of cell plating density for scratch-wound migration assay. Representative images (100x magnification) of (A) parental and transfected MDA-MB-231 cells, and (B) T47D parental cells at 24 hours after plating cell at the indicated cell densities (cells/well).

4.4.1.2 Optimisation of positive control for inhibiting cell migration

4.4.1.2.1 PP2

PP2 is a c-Src kinase inhibitor that has been shown to inhibit the migration of various cell lines (Bartscht *et al.*, 2012), including breast cancer cells (e.g., MDA-MB-231, MCF-7, SKBR3 and T47D) (Li et al., 2010; Liu & Feng, 2010; Fan et al., 2012). PP2 reportedly significantly inhibited migration of MDA-MB-231 cells after pre-incubating cells with 5 µM PP2 for an hour (Tang *et al.*, 2011), while treatment with the drug for 24 hours had no effect on cellular viability or proliferation (Nelson *et al.*, 2014). In the current study, the effect of pre-incubation with PP2 on MDA-MB-231 cell migration was studied using a range of concentration up to 5 µM compared to the effect of calpain inhibition using 100 µM calpeptin. The scratch-wound assay was used to examine the migration activity of the cells (section 2.10). Representative images of wound healing in response to 0, 1.25, 2.5 and 5 µM PP2 are shown in Figure 4.16. The inhibitory effect of PP2 on MDA-MB-231 cell migration, represented by a decrease of the percentage of wound closure, was observed with increasing concentration of PP2 (Figure 4.16). However, the effect of PP2 in inhibiting cell migration was

not significant. At 20 or 24 hours post-scratch, 5 µM PP2 prevented MDA-MB-231 cell migration by 10.66% (*P* = 0.4897) and 11.63% (*P* = 0.1121), respectively.

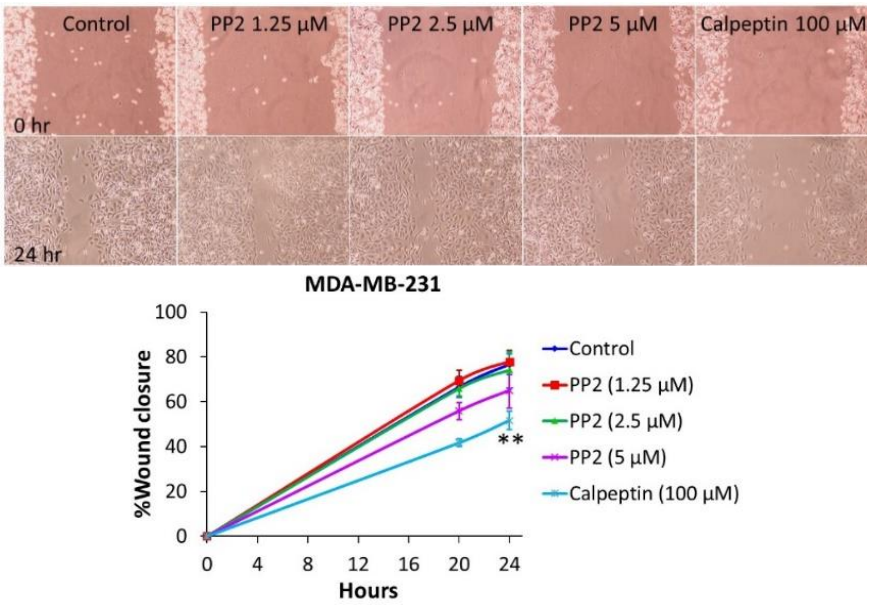


Figure 4.16 Effect of PP2 and calpeptin on MDA-MB-231 cell migration detected by scratch-wound assay. Cells were treated with PP2 (1.25, 2.5, and 5 µM) or 100 µM calpeptin for 24 hours before scratch-wound. Mitomycin C was used for the inhibition of cell proliferation after wounding. Representative images of wounds at indicated time points are shown (100x magnification); %wound closure at 20 and 24 hours post-scratch was calculated relative to the initial wound area. Data represent the average ± SD of three independent experiments, each performed in triplicate. P-values were assessed for showing the level of statistical differences between the treatment groups and no-treatment control; ** $P < 0.01$.

Additional PP2 optimisation, to use as a positive control for migration assay, was attempted by increasing concentration > 5 µM; however, turbidity was detected in the PP2 working preparations at 1, 10, and 25 µM prepared in 0.1% DMSO/complete culture medium. The precipitation of PP2 remained present at the bottom of the tube after centrifuging at 1000 rpm for 5 minutes even though heat was applied to facilitate solubility of PP2. As mentioned in the product sheet, PP2 is a non-polar molecule that can be dissolved by approximately 0.15, 1.4, and 3 mg in 1 mL of ethanol, DMSO, and dimethylformamide (DMF), respectively (Cayman Chemical, 2015). Although 100 mM PP2 in DMSO stock solution was an absolute solution, PP2 contained in the working preparations of 0.1% DMSO/complete medium became insoluble due to the sparingly soluble property of PP2 in aqueous buffers (Cayman Chemical, 2015). The incompletely dissolved drug can lead to variation

and wrong interpretation of the results. Thus, PP2 was discontinued to verify as a positive control for cell migration assessment.

The activity of 100 µM calpeptin on cell migration was also determined at this time. Although the calpain inhibitor at 100 µM caused a significant inhibition in wound healing by 24.98% (P = 0.0015) at 24 hours post-scratch, it seemed to slightly affect the integrity of the MDA-MB-231 cell monolayer (no image) and affected cell proliferation (~30% inhibition, section 4.2.1), suggesting that the decreased wound healing was more likely a consequence of cytotoxicity of calpeptin on cell proliferation.

4.4.1.2.2 Cytochalasin D

Cytochalasin D, a potent inhibitor of actin polymerisation, has been reported to inhibit cell migration (Shuster *et al.*, 1996), with 1 µM cytochalasin D reported to inhibit the migratory ability of MDA-MB-231 cells (Glenn *et al.*, 2016). The current section aimed to optimise the concentration of cytochalasin D that did not affect MDA-MB-231 and T47D cell proliferation but effectively inhibited cell migration.

4.4.1.2.2.1 Effects of cytochalasin D on cell proliferation

MDA-MB-231 and T47D cell proliferation was assessed 24 hours after being treated with various concentrations of cytochalasin D (0.01, 0.1, 1, 2 and 10 µM) or with 0.5 µM doxorubicin (positive control). Figure 4.17-A shows that exposure to doxorubicin for 24 hours caused 52.19 ± 9.05% and 44.94 ± 10.94% cell proliferation in MDA-MB-231 and T47D cells, respectively. The proliferative inhibition by doxorubicin, shown in this study, was similar to the previous results in both cells (section 4.2.1), suggesting that the breast cancer cells behaved as expected and the experimental technique was robust.

Cytochalasin D inhibited proliferation of MDA-MB-231 and T47D cells in a dose-dependent manner (Figure 4.17-B); the cell number was reduced with increasing concentrations. MDA-MB-231 cells were relatively more resistant to cytochalasin D compared to T47D's. Cytochalasin D at 0.01 and 0.1 µM had no

effect on the proliferation of MDA-MB-231 (97.60 ± 2.12% and 99.80 ± 5.60% cell proliferation, respectively), whereas the higher concentrations (1, 2 and 10 µM) caused a substantial decrease of cell number (40-50% reduction). For T47D cells, cytochalasin D at 0.01 µM did not affect cell proliferation (92.80 ± 5.49% proliferation) but started to show the anti-proliferative effect at 0.1 µM (32.58 ± 5.41% inhibition); > 70% cell proliferative inhibition was observed in the treatment with higher concentrations.

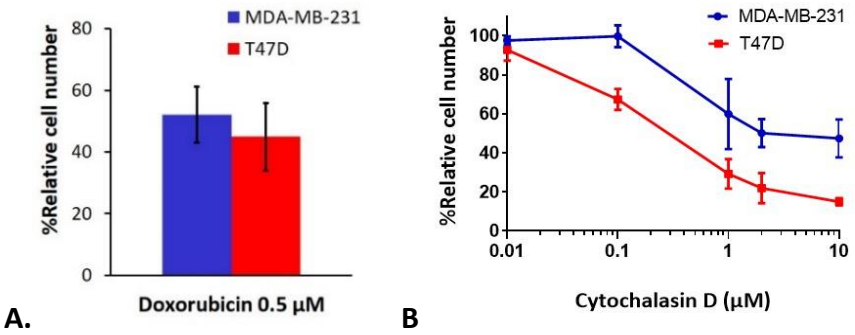


Figure 4.17 Effect of cytochalasin D and doxorubicin on breast cancer cell proliferation. MDA-MB-231 and T47D cells were treated with (A) 0.5 µM doxorubicin or (B) cytochalasin D (0.01, 0.1, 1, 2 and 10 µM) for 24 hours. Data represent the average percentages of cell number relative to the no-treatment control ± SD of three independent experiments, each performed in duplicate for T47D or triplicate for MDA-MB-231.

The 24-hour treatment with cytochalasin D at the concentrations that did not markedly alter cell proliferative was then examined for the effect on cell migration in the following section 4.4.1.2.2.2 - 0.1 and 0.2 µM for MDA-MB-231; 0.02 and 0.04 µM for T47D cells.

4.4.1.2.2.2 Effects of cytochalasin D on cell migration

Scratch-wound migration assays were performed in breast cancer cells treated with cytochalasin D at low doses that had minimal, if any, effect on cell proliferation, i.e., 0.1 and 0.2 µM for MDA-MB-231 and 0.02 and 0.04 µM for T47D cells (section 4.4.1.2.2.1). Figure 4.18-A and -B show that MDA-MB-231 cells migrated faster than T47D cells. Within 24 hours, the parental MDA-MB-231 cell wound was almost completely closed, by 80.34 ± 5.34%, while only 29.66 ± 3.18% wound closure was observed in T47D cells. Cytochalasin D at the chosen concentrations had no effect in reducing the migration of either cell line. At 24-hour post-scratch, wounds of cytochalasin D-treated MDA-MB-231

cells were closed by ~82% for both 0.1 and 0.2 µM. For T47D, 0.02 and 0.04 µM cytochalasin D caused 24-25% and 27-28% wound closure at 18 and 24 hours post-scratch, respectively. At 48 hours post-wounding, assessment of wound closure in T47D cell monolayers could not be extended longer than 24 hours post-scratch due to significant cytotoxicity becoming apparent in controls, with lots of floating cells evident.

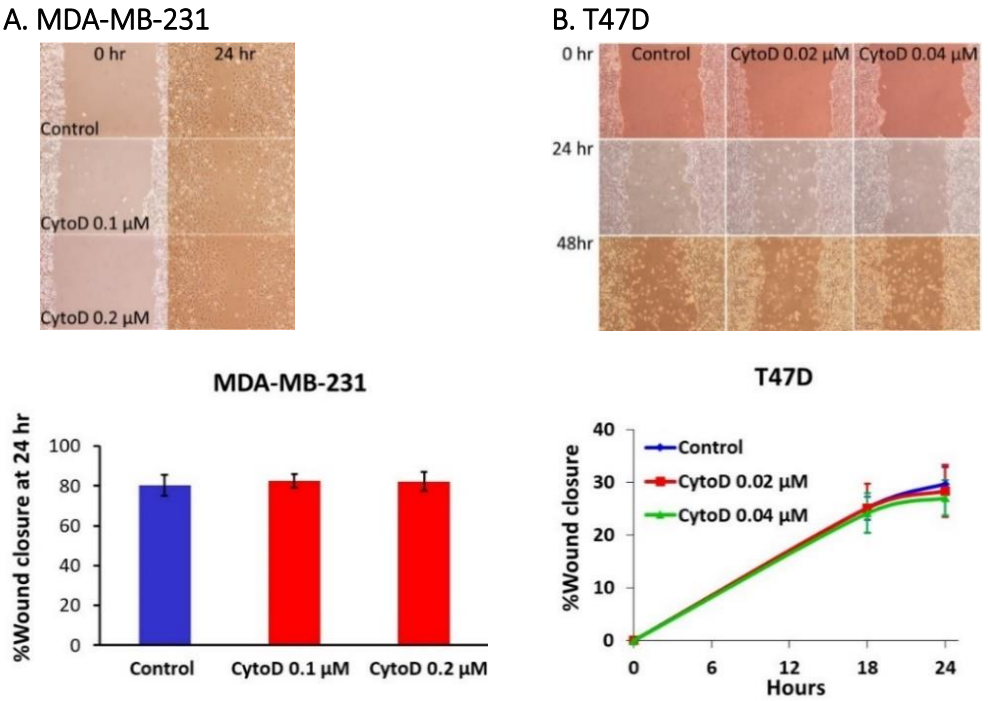


Figure 4.18 Effect of cytochalasin D on breast cancer cell migration detected by scratch-wound assay. (A) MDA-MB-231 and (B) T47D cells were treated with cytochalasin D (CytoD) at the indicated concentrations for 24 hours before wounding, followed by the addition of mitomycin C to inhibit cell proliferation. Representative images of wounds at indicated time points are shown (100x magnification). Wound closure (%) was calculated relative to the initial wound area. Data represent the average ± SD of two independent experiments, each in triplicate.

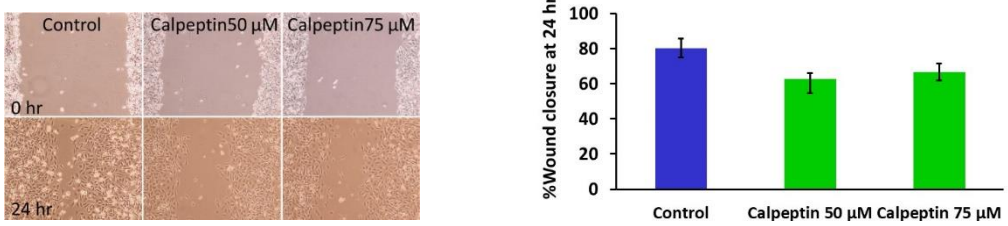
Due to inactive ability of PP2 and cytochalasin D in inhibiting migration of MDA-MB-231 or T47D cell lines, calpeptin was then considered as a potential positive control if it could be demonstrated that non-toxic concentrations were able to significantly inhibit breast cancer cell migration (section 4.4.1.2.3).

4.4.1.2.3 Calpeptin

Calpeptin at 50 and 75 µM, which showed no or little effect, respectively, on MDA-MB-231 and T47D cell proliferation (section 4.2.1), had a parallel ability in inhibiting wound healing in each cell line, as shown in Figure 4.19. At 24 hours

after wounding, 50 and 75 µM calpeptin suppressed MDA-MB-231 cell migration by 21.78 ± 2.86 and 16.88 ± 6.89% relative to the untreated group, respectively but had no effect on T47D cell migration. Wound closure of the untreated group at 24 hours (35.49 ± 10.57%) was similar to that of the calpeptin-treated T47D cell monolayers (42.22 ± 5.77% and 35.21 ± 9.31% for 50 and 75 µM calpeptin, respectively). As indicated above, T47D wound closure at 48 hours could not be assessed due to cellular toxicity in controls (Figure 4.19-B).

A. MDA-MB-231



B. T47D

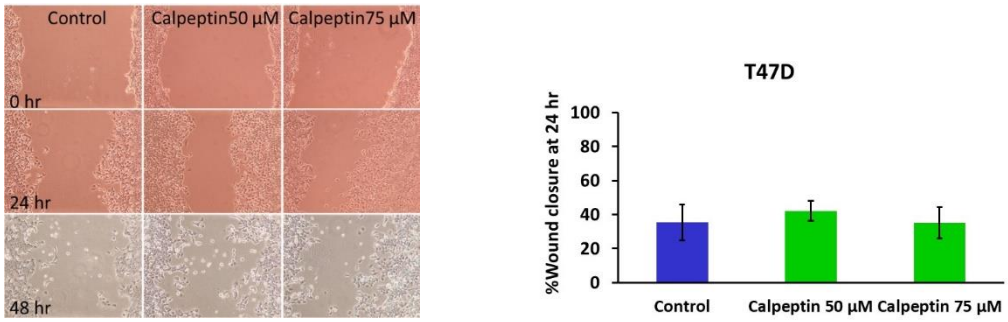


Figure 4.19 Effect of calpeptin on breast cancer cell migration detected by scratch-wound assay. (A) MDA-MB-231 and (B) T47D cells were treated with calpeptin (50 and 75 µM) for 24 hours before wound-scratch, followed by the addition of mitomycin C to inhibit cell proliferation. Representative images of wounds at indicated time points are shown (100x magnification). %Wound closure was calculated relative to the initial wound area. Data represent the average ± SD of two independent experiments, each in triplicate.

It may be that the significant effect of calpeptin was present on the migration of MDA-MB-231 but not on T47D's because T47D cells migrated slowly and much more slowly than MDA-MB-231 cells; if cells are not moving fast then obvious changes will not be seen. However, 50 µM calpeptin was used as a positive control in subsequent migration experiments.

4.4.1.3 Effects of 0.5% DBS culture medium on cell proliferation

As T47D cell migration may be affected by the anti-proliferative agent mitomycin C, an alternate strategy was used, i.e., low serum conditions. Thus, instead of using mitomycin C to inhibit cell proliferation after wounding, 0.5% DBS culture medium was used for T47D cell migration assessment. To ensure that wound healing of parental and transfected T47D cell lines was not influenced by cell growth, the effect of 0.5% DBS-containing culture medium on cell proliferation was examined in comparison to the routine used complete culture medium containing 10% DBS. Cell proliferation of T47D, T47DCtrl and T47DCAST1 cells at 24, 48, and 72 hours post-medium refreshment was analysed as the percentages of cell number relative to the cell number at a 24-hour time point, as shown in Figure 4.20.

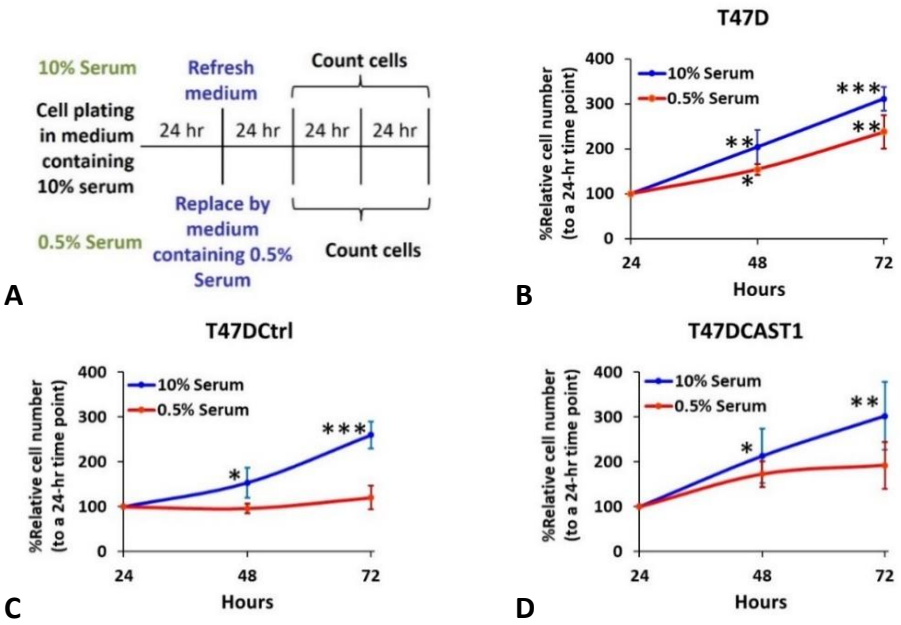


Figure 4.20 Effects of 0.5% DBS culture medium on the proliferation of parental and transfected T47D cells. As indicated in (A) a study flow diagram, (B) parental T47D, (C) mock-transfected T47DCtrl and (D) T47DCAST1 cells were plated and incubated with 10% DBS culture medium for 24 hours before being refreshed with the culture medium containing 10% or 0.5% DBS. Cell proliferation at 24, 48, and 72 hours post-medium refreshment was presented as the percentage cell number relative to that of a 24-hour time point. Data represent the average ± SD of three independent experiments, each in triplicate. *P*-values were assessed for showing the statistical differences between the groups at 48 or 72 hours and a 24-hour time point group; **P*< 0.05, ***P*< 0.01, ****P*<0.001.

While culturing cells in 10% DBS culture medium allowed the growth of all cell lines, 0.5% DBS culture medium slowed the proliferation of either parental

T47D or transfected cell lines (T47DCtrl and T47DCAST1). By culturing cells with 0.5% DBS culture medium, the cell number of T47DCtrl and T47DCAST1 cells was stable over 24, 48 and 72 hours post-medium refreshment, indicating that no cell proliferation occurred throughout the experimental period. Although the growth of T47D parental cells was decreased by the use of 0.5% DBS culture medium, significant increases in cell number over 48 (P = 0.0487) and 72 hours of investigation (P = 0.0012) were observed in comparison to the 24-hour time point.

Based upon no influencing effect of low-serum medium on wound healing through enhancing the growth of T47DCAST1 and mock-transfected T47DCtrl cells over 72 hours of investigation, the effect of calpastatin Type 1 on T47D cell migration, therefore, could be interpreted from the difference of migration ability between T47DCAST1 cells and the respective mock-transfected cells. The 0.5% DBS culture medium was therefore used to inhibit the proliferation of T47D cell lines after producing wounds in subsequent migration assays.

4.4.1.4 Effects of calpastatin isoform overexpression on cell migration

Migration ability of breast cancer cells, which overexpressed calpastatin Type 1 (231CAST1 and T47DCAST1) or Type 2 (231CAST2), was assessed using scratch-wound migration assay in comparison with their mock-transfected controls. Calpeptin at 50 µM optimised from section 4.4.1.2.3 was used as a positive control to show the effect of calpain inhibition on breast cancer cell migration. As shown in Figure 4.21, calpeptin evidently inhibited the migration of mock-transfected 231Ctrl cells at all time-points as well as it could in the parental MDA-MB-231 (section 4.4.1.2.3). Wound closures of calpeptin-treated cells vs untreated cells were 3.11% vs 4.30% (P = 0.0495), 5.66% vs 8.78% (P = 0.1663), 8.97% vs 12.09% (P = 0.4055), and 36.40% vs 46.37% (P = 0.0836) for 2, 4, 6, and 24 hours post-scratch, respectively. However, the significant effect of calpeptin was only present at a 2-hour time point. In comparison, calpeptin had no effect on the migration of mock-transfected T47DCtrl cell over 72 hours of investigation.

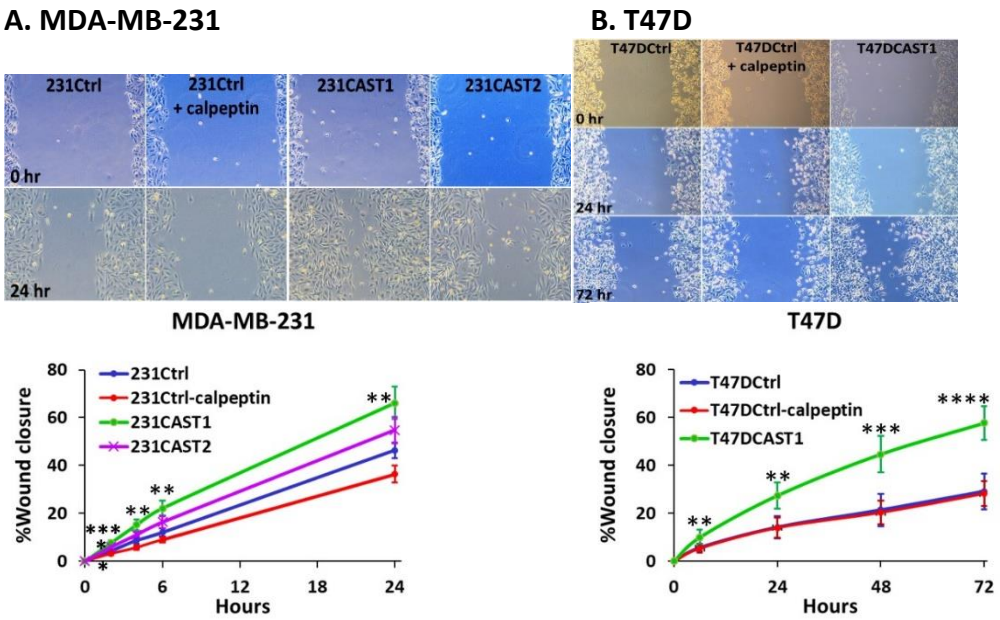


Figure 4.21 Effect of calpastatin isoform overexpression on breast cancer cell migration detected by scratch-wound assay. Monolayers of MDA-MB-231, T47D, their respective transfected cells overexpressing calpastatin Type 1 (231CAST1 & T47DCAST1) or Type 2 (231CAST2), and mock-transfected controls (231Ctrl & T47DCtrl) were scratch-wounded. After wounding, mitomycin C and 0.5% DBS culture medium were used to inhibit the proliferation of MDA-MB-231 and T47D cells, respectively. Wound closure was measured at (A) 2, 4, 6 and 24 hours post-scratch for MDA-MB-231 cells, and (B) 6, 24, 48 and 72 hours post-scratch for T47D cells. Pre-treatment with 50 µM calpeptin for 24 hours was used to show the effect of calpain inhibition. Representative images of wounds at indicated time points are shown (100x magnification). %Wound closure was calculated relative to the initial wound area. Data represent the average ± SD of three independent experiments, each performed in triplicate. P-values were assessed for showing the statistical differences between each group and the non-treated mock-transfected control;*P <0.05, ** P < 0.01, *** P < 0.001, and ****P < 0.0001.

Type 1 overexpression, in either T47D luminal or MDA-MB-231 basal-like breast cancer cells, unexpectedly demonstrated the opposing effect to the activity of calpeptin. Both 231CAST1 and T47DCAST1 cells exhibited a significantly higher migratory activity compared to the respective mock-transfected controls at all time-points. Wound closures of 231CAST1 vs 231Ctrl were 7.61% vs 4.30% (P = 0.0001), 15.22% vs 8.78%, (P = 0.0072), 22.16% vs 12.09%, (P = 0.0047), and 66.13% vs 46.37%, (P = 0.0026) at 2, 4, 6, and 24 hours post-scratch, respectively. T47DCAST1 cells also migrated significantly faster than the mock-transfected T47DCtrl cells at all investigated time points (6, 24, 48 and 72 hours post-scratch). Wound closures of T47DCAST1 vs T47Ctrl were 9.92% vs 5.68% (P = 0.0048), 27.41% vs 14.18% (P = 0.0054), 44.67% vs 21.33% (P = 0.0002), and 57.68% vs 29.09% (P <0.0001), respectively, for each time point.

Likewise, calpastatin Type 2 overexpression increased 231CAST2 cell migration at all time-points; however, a significant increase of 231CAST2 cell migration relative to the mock-transfected cells was only present at 2 hours after wounding (P = 0.0120). At each time point, 231CAST2 cells migrated to close the cell-free area by 5.91%, 11.07%, 16.37%, and 54.79%. Migratory abilities between 231CAST1 and 231CAST2 cells were significantly different only at 2 hours post-scratch (P = 0.0182).

4.4.1.5 Effects of A23187 calcium ionophore on cell migration

The role of calpastatin isoform overexpression in regulating breast cancer cell migration was also examined whether it could be altered by the presence of A23187 calcium ionophore. Figure 4.22 shows the effect of A23187 or calpeptin on cell migration in the parental and transfected MDA-MB-231 cells.

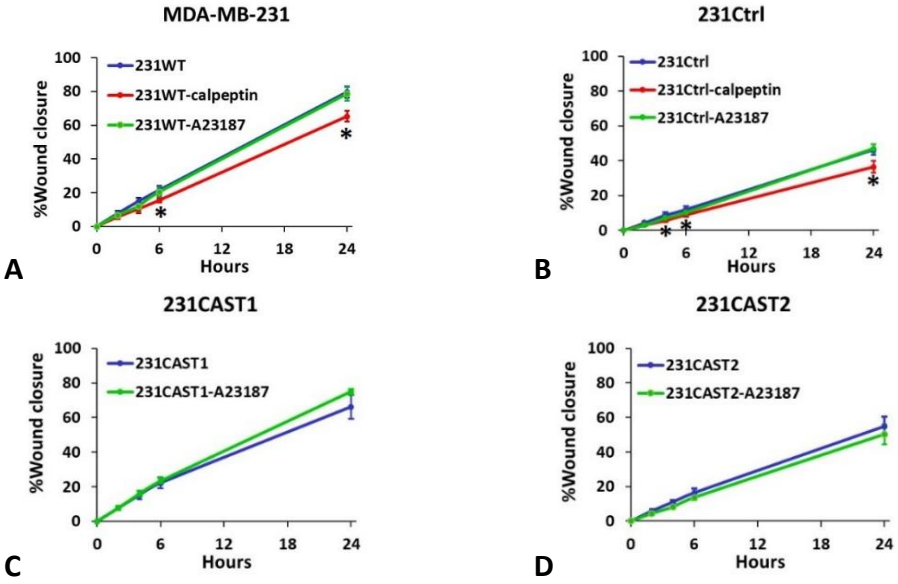


Figure 4.22 Effect of A23187 or calpeptin on cell migration in MDA-MB-231 cells overexpressing calpastatin isoforms detected by scratch-wound assay. (A) parental MDA-MB-231, (B) mock-transfected 231Ctrl, (C) the stably transfected cells overexpressing calpastatin Type 1 (231CAST1), and (D) Type 2 (231CAST2) were treated with 0.5 µM A23187 or 50 µM calpeptin for 24 hours. Mitomycin C was used for the inhibition of cell proliferation after wounding. Wound closure was measured at 2, 4, 6 and 24 hours post-scratch. Data represent the average ± SD of three independent experiments, each performed in triplicate. P-values were assessed to show the statistical differences between the treatment groups and no-treatment controls at each time-point; * $P < 0.05$.

Figure 4.22-A and -B show that the migration rate of the mock-transfected 231Ctrl cells was significantly slower than that of the parental cells. At each time point (2, 4, 6, and 24 hours post wound creation), wound closures of

parental cells vs 231Ctrl cells were 7.65% vs 4.30% (P = 0.0581), 14.84% vs 8.78% (P = 0.0122), 21.51% vs 12.09% (P = 0.0089), and 79.60% vs 46.37% (P = 0.0004), respectively. As both 231Ctrl and parental cells migrated under the same condition, the slower migration of 231Ctrl cells might be a result of the empty vector transfection. Calpeptin at 50 µM inhibited migration of both 231Ctrl and MDA-MB-231 cells by a similar effect. In comparison with an untreated group, calpeptin significantly reduced wound healing of parental cells at 6- and 24-hour time points by 27.89% (15.51 vs 21.51 %wound closure, P = 0.0235) and 18.02% (65.26 vs 79.60 %wound closure, P = 0.0344), respectively. Meanwhile, significant decreases of calpeptin-treated 231Ctrl cell migration were detected at 4, 6 and 24 hours after wounding with 35.54% (5.66 vs 8.78 %wound closure, P = 0.0326), 25.81% (8.97 vs 12.09 %wound closure, P = 0.0403), and 21.50% (36.40 vs 46.37 %wound closure, P = 0.0486), respectively, relative to wound closure of untreated cells.

Treatment with 0.5 µM A23187 for 24 hours did not alter the migration in either parental MDA-MB-231 or mock-transfected 231Ctrl cells at any time-point (Figure 4.22-A and -B). Wound closures at 24 hours post-scratch of A23187-treated groups in MDA-MB-231 or 231Ctrl vs the respective controls were 78.50% vs 79.60% (P = 0.9586) and 46.97% vs 46.37% (P = 0.9782), respectively. For CAST-transfected MDA-MB-231 cells, A23187 also had no significant effect on cell migration at any time-point. Although there was no statistical significance, A23187 seemed to increase the migration of treated 231CAST1 cells relative to the untreated cells by 13.53% (75.08% vs 66.13% wound closure, P = 0.1598) (Figure 4.22-C) but slightly decrease cell migration in 231CAST2 cells by 8.19% (50.30% vs 54.79% wound closure, P = 0.4630) at 24 hours post-scratch (Figure 4.22-D).

For T47D cell clones, T47DCtrl mock-transfected cells also significantly migrated slower than the parental T47D cell line (Figure 4.23-A and -B). Wound closures of T47D vs T47DCtrl cells were 24.41% vs 5.68% (P = 0.0002), 56.03% vs 14.18% (P = 0.0002), 76.65% vs 21.33% (P = 0.0001), and 95.85% vs 29.09% (P < 0.0001), at 6, 24, 48, and 72 hours post-scratch, respectively. Such data is strongly

suggestive of the empty vector reducing the migratory ability of breast cancer cells if 0.5% DBS did not affect the proliferation of both parental and mock-transfected T47DCtrl cells. The mock-transfected T47DCtrl and parental cells responded similarly to calpeptin and A23187 (Figure 4.23-A and -B). Calpeptin could not inhibit the migration of either cell line; at 72 hours post-scratch, wound closures of calpeptin-treated groups in T47D or T47DCtrl vs the respective controls were 90.30% vs 95.85% (*P* = 0.0833) and 28.20% vs 29.09% (*P* = 0.8748), respectively. A23187, generally, seemed to have no effect on the migration of either cell line at all time points although a 5.55% decrease of cell migration was significantly observed in A23187-treated T47D group at 72 hours post-scratch (87.61 %wound closure, *P* = 0.0186). Wound closure of A23187-treated T47DCtrl (27.23%, *P* = 0.5926) at the same time-point was similar to the control.

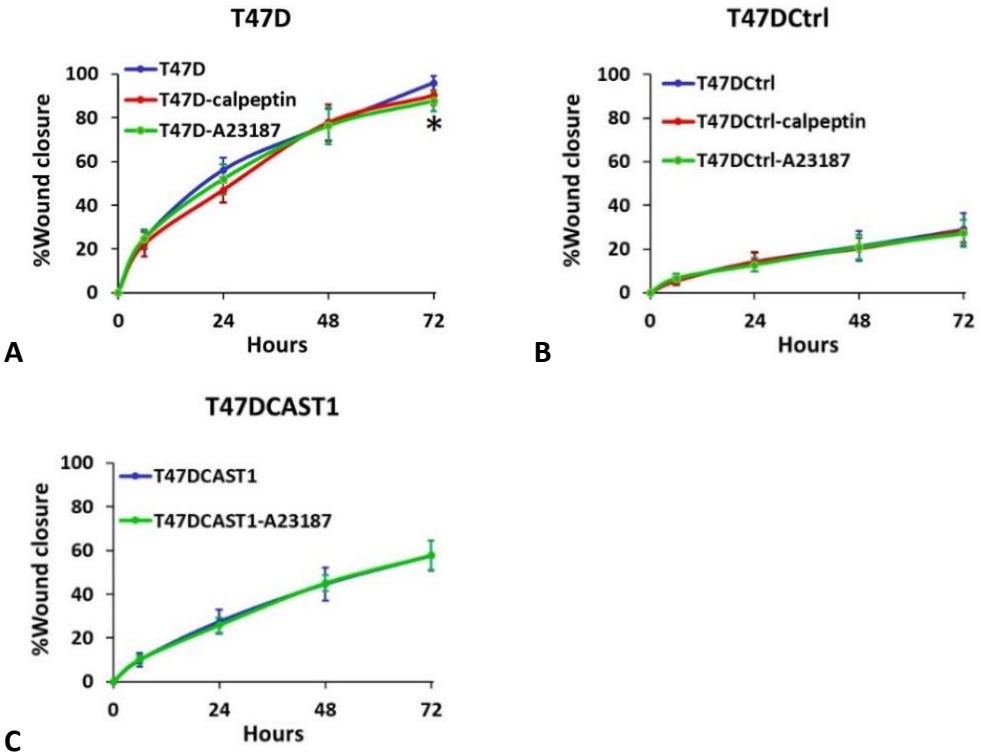


Figure 4.23 Effect of A23187 or calpeptin on cell migration in T47D cells overexpressing calpastatin isoform detected by scratch-wound assay. (A) parental T47D, (B) mock-transfected T47DCtrl, and (C) the transfected cells overexpressing calpastatin Type 1 (T47DCAST1) were treated with 0.5 µM A23187 or 50 µM calpeptin for 24 hours before wounding. Culture medium containing 0.5% DBS was used for the inhibition of cell proliferation after wound-scratch. Wound closure was measured at 6, 24, 48 and 72 hours post-scratch. Data represent the average ± SD of three independent experiments, each performed in triplicate. P-values were assessed for showing the statistical differences between the treatment groups and no-treatment controls at each time-point; * *P*< 0.05.

Also, A23187 did not cause any changes in the migration of calpastatin Type 1-overexpressing T47DCAST1 cells over 72 hours of investigation (Figure 4.23-C). Wound closures of A23187-treated T47DCAST1 cells vs no-treatment group were 10.06% vs 9.92% (P = 0.8727), 25.87% vs 27.41% (P = 0.5755), 45.08% vs 44.67% (P = 0.9099), and 57.79% vs 57.68% (P = 0.9632), at 6, 24, 48, and 72 hours post-scratch, respectively.

Such data suggest that, in terms of migratory effects, calpastatin isoform (1 or 2) overexpression may play a role in promoting breast cancer progression and LVI through enhancing cell migration. A23187 used as a calpain regulator seemed not to have any effect on calpastatin isoform overexpression in influencing cell migration.

4.4.2 Endothelial cell interactions

The adhesive ability of breast cancer cells to blood vessel vs lymphatic endothelial cells (BECs vs LECs) in response to overexpression of calpastatin Type 1 or Type 2 was investigated in the current study using a static cell adhesion assay protocol. In the assay, CellTracker Green CMFDA Dye was used to detect the number of tumour cell adhered to the confluent monolayers of hMEC-1 blood vascular or hTERT-LEC lymphatic ECs (section 2.11).

4.4.2.1 Effects of CellTracker Green CMFDA labelling on cell proliferation

MDA-MB-231 cells labelled with 1 µM CellTracker Green have previously shown a comparable proliferative rate to the unlabelled cells over 72 hours (Safuan, 2012). In the current study, the effect of CellTracker Green CMFDA labelling on T47D cell proliferation was examined by cell counting with a haemocytometer (section 2.3). Figure 4.24 shows no difference between the proliferation of T47D cells with and without labelling with 1 µM CellTracker Green at 24 hours (P = 0.3050), 48 hours (P = 0.8509) or 72 hours (P = 0.3089) following labelling. CellTracker Green CMFDA at 1 µM was therefore used for labelling MDA-MB-231 and T47D tumour cells in subsequent adhesion experiments.

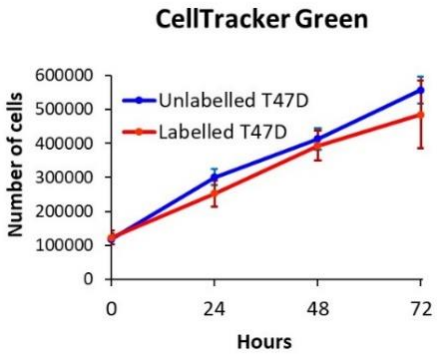


Figure 4.24 Effect of CellTracker Green CMFDA labelling on T47D cell proliferation. T47D cells were incubated with 1 µM CellTracker Green CMFDA at 37°C for 30 minutes before being plated and determined cell number over 72 hours. Data represent the average ± SD of three independent experiments, each performed in triplicate.

4.4.2.2 Optimisation of endothelial cell plating density

Optimisation of hMEC-1 or hTERT-LEC endothelial cell plating density to form confluent cell monolayer (90-100%) was performed before conducting any static adhesion assessment of PBMC or breast cancer cells. Figure 4.25 shows representative images of cell monolayers formed at 24 hours post-cell seeding in a 24-well culture plate at various cell plating densities. After 24 hours of incubation, $3x10^5$ hMEC-1 cells/mL and $2x10^5$ hTERT-LEC cells/mL produced >90% confluent monolayers. Therefore, these densities were used in subsequent adhesion assays.

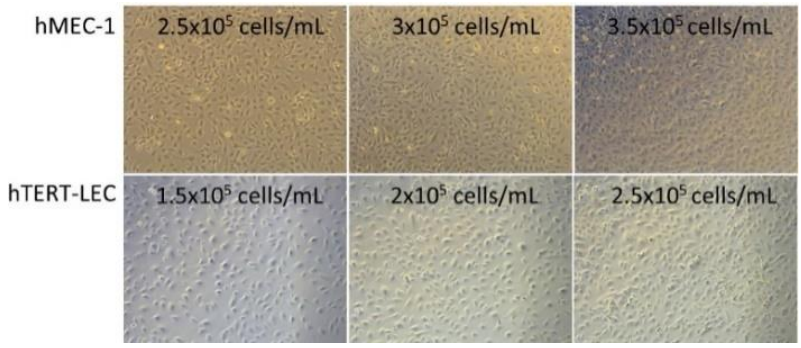


Figure 4.25 Optimisation of endothelial cell plating density for static adhesion assay. Representative images of hMEC-1 and hTERT-LEC endothelial cells (100x magnification) at 24 hours after plating cells at the indicated cell densities.

4.4.2.3 Effects of calpastatin isoform overexpression on cell adhesion

Before performing each experimental assessment of the role of calpastatin isoform overexpression on breast tumour cell adhesion to hTERT-LEC lymphatic

or hMEC-1 blood vascular ECs, PBMC adhesion onto TNF-α-treated ECs was initially assessed and used as a positive control to ensure that ECs were appropriately responsive and behaved as expected. Figure 4.26 shows a significant increase of PBMC adhesion to both TNF-α-stimulated hMEC-1 and hTERT-LEC ECs compared to the unstimulated control cells ($P < 0.0001$ and $P = 0.0066$ respectively).

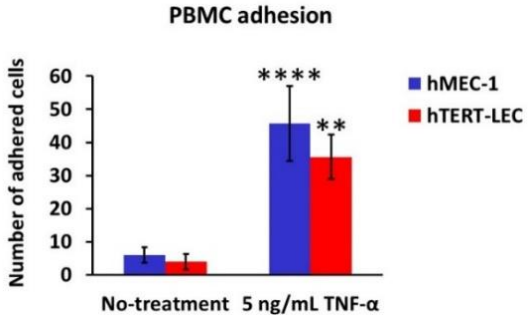


Figure 4.26 PBMC adhesion to endothelial cells. hMEC-1 and hTERT-LEC endothelial cell monolayers were pre-treated by 5 ng/mL TNF-α before being performed static PBMC cells adhesion studies. Data represent the average PBMC adhered cell number (per two 100x fields) ± SD of independent experiments (n = 5 for hMEC-1 and n= 3 for hTERT-LEC), each in triplicate; n is the number of experiment. P-values were assessed for showing the statistical differences between the treatment groups and no-treatment controls; ** $P < 0.01$ and **** $P < 0.0001$.

The number of PBMC adhered on hMEC-1 cells increased by 7.6 fold from 6.00 ± 2.33 to 45.67 ± 11.35 cells by stimulating hMEC-1 cells with 5 ng/mL TNF-α, while the stimulated hTERT-LEC cells by the same treatment caused an approximately 9-fold increase of the number of adhered PBMC from 3.89 ± 2.33 to 35.56 ± 6.74 cells. Such results confirm previous findings reported in PhD theses from the current group (Safuan, 2012; Ahmad, 2016).

The effects of calpastatin isoform overexpression on MDA-MB-231 cell adhesion to ECs were assessed using 231CAST1 and 231CAST2 clones overexpressing Type 1 and Type 2 calpastatin, respectively, as *in vitro* cell models. Figure 4.27 presents the absolute number of tumour cells adhering towards EC monolayers, and Table 4.3 shows percentages of adhered tumour cell relative to the number of adhered mock-transfected 231Ctrl control.

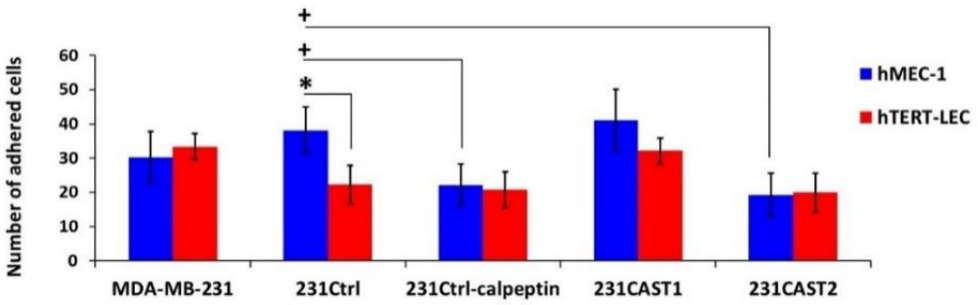


Figure 4.27 Adhesion to endothelial cells of MDA-MB-231 cell overexpressing calpastatin isoforms. Static adhesion assays were performed on MDA-MB-231 cells overexpressing calpastatin Type 1 (231CAST1) and Type 2 (231CAST2), mock-transfected 231Ctrl and parental MDA-MB-231 cells. 231Ctrl cells pre-treated with 50 µM calpeptin for 24 hours were used to show the effect of calpain inhibition. The adhered tumour cell number (per two 400x fields) to hMEC-1 and hTERT-LEC was assessed. Data represent the average ± SD of independent experiments (n = 5 for hMEC-1 and n= 3 for hTERT-LEC), each in triplicate; n is the number of experiment. P-values were assessed for showing the statistical differences between each cell line and the mock-transfected control (+ $P < 0.05$ and ++ $P < 0.01$) and between adhesion to hMEC1 and hTERT-LEC within a group (* $P < 0.05$).

Table 4.3 Percentage of adhered MDA-MB-231 cells overexpressing calpastatin isoforms to endothelial cells.

Endothelial cells	Percentage of adhered cell number to endothelial cells (relative to the number of adhered 231Ctrl control cells)				
	MDA-MB-231	231Ctrl	231Ctrl + calpeptin	231CAST1	231CAST2
hMEC-1	94.31 ± 36.67	100	67.79 ± 24.27	108.91 ± 30.62	50.20* ± 23.25
hTERT-LEC	149.38** ± 9.31	100	93.83 ± 16.90	141.47** ± 18.77	90.80 ± 8.47

Percentages of adhered cells were calculated relative to the number of adhered 231Ctrl cells. Data represent the average ± SD of independent experiments (n = 5 for hMEC-1; n= 3 for hTERT-LEC), each performed in triplicate; n is the number of experiment. P-values were assessed for showing the statistical differences between each group and 231Ctrl cells; * $P < 0.05$ and ** $P < 0.01$.

As demonstrated in Figure 4.27, higher affinity towards hMEC-1 cells relative to hTERT-LEC cells was observed significantly in 231Ctrl cells (38.10 ± 6.89 vs 22.22 ± 5.59 cells, $P = 0.0171$), and also detected markedly in 231CAST1 cell (41.03 ± 9.05 vs 32.11 ± 3.79 cells, $P = 0.3367$). Meanwhile, the comparable numbers of adhered tumour cells to both EC types were observed in parental MDA-MB-231 (30.20 ± 7.51 vs 33.33 ± 3.73 cells, $P = 0.6552$) and 231CAST2 cells (19.20 ± 6.29 vs 19.89 ± 5.73, $P = 0.9075$). To compare adhesion ability to ECs between the mock-transfected 231Ctrl control and the parental cells, Figure 4.27 shows that the absolute number of adhered 231Ctrl cells to both hMEC-1 (38.10 ± 6.89 vs 30.20 ± 7.51 cells, $P = 0.4658$) and hTERT-LEC monolayers (22.22 ± 5.59 vs 33.33

± 3.73 cells, *P* = 0.3050) was not statistically different from that of MDA-MB-231 cells. However, as presented in Table 4.3, the percentage adhesion ability towards hTERT-LEC of parental cells was significantly higher relative to 231Ctrl cells (*P* = 0.0025), but not different in adhesion to hMEC-1 cells. As with previous endpoints mentioned earlier, such data is suggestive of the empty vector affecting MDA-MB-231 cell adhesion to LECs. Although there was a difference of adhesion ability between 231Ctrl and the parental cells, the role of calpastatin isoform overexpression on endothelial interactions was interpreted from the adhesion ability of breast cancer cells overexpressing calpastatin isoforms relative to that of the mock-transfected 231Ctrl control.

Treatment with 50 µM calpeptin for 24 hours used as a comparator to the effect of calpastatin isoform overexpression was found to significantly impede the number of the mock-transfected 231Ctrl control cells adhering to hMEC-1 cells from 38.10 ± 6.89 cells to 22.13 ± 6.01 cells (*P* = 0.0381) (Figure 4.27), accounting for a 32.21% decrease (Table 4.3). Although the calpain inhibitor caused a 6.17% decrease of the adhesive ability of 231Ctrl cells to LECs, a statistical significance was not detected (*P* = 0.9307).

For CAST-transfected cells, calpastatin Type 1 overexpression seemed to increase the affinity of 231CAST1 cells to both hMEC-1 and hTERT-LEC cells in comparison to mock-transfected control. The adhesion of 231CAST1 cells to hMEC-1 was only 8.91% greater than that of mock-transfected cells (*P* = 0.9522). On the other hand, the adhesive ability of 231CAST1 to hTERT-LEC was significantly higher than the adhesion of mock-transfected cells by 41.47% (*P* = 0.0080). In comparison, Type 2 overexpression seemed to suppress the adhesiveness of 231CAST2 cells to both ECs. Adhesion of 231CAST2 cells towards hMEC-1 was significantly less relative to 231Ctrl cells, represented by 49.80% decrease in adhered cell number (*P* = 0.0232). Meanwhile, adhesion of 231CAST2 cells to hTERT-LEC was 9.20% lower than the number of adhered 231Ctrl cells (*P* = 0.7846). Together, the higher affinity of 231CAST1 cells or lower affinity of 231CAST2 cells to ECs might suggest a differential role for calpastatin Type 1 and Type 2, respectively, in breast cancer cell-endothelial

interactions – inductive and suppressive effects, respectively. Overexpression of Type 1 was more likely to affect LEC interaction, whereas Type 2 overexpression seems to be more involved with adhesion to BECs.

The adhesive ability of parental T47D to hMEC-1 and hTERT-LEC was investigated using the same experimental design as used for MDA-MB-231 cells. In this study, static adhesion assays of PBMCs and MDA-MB-231 cells to both ECs were performed prior and in parallel, respectively, to the study of T47D cell adhesion. The consistent adhesion to hMEC-1 and hTERT-LEC ECs by PBMC (7- and 5-fold increase, respectively) (Figure 4.28-A) and MDA-MB-231 (24.67 ± 6.03 and 34.33 ± 4.93 cells, respectively) (Figure 4.28-B) indicated that the ECs responded as expected, and the technique in performing the adhesion assay was reliable. However, T47D cells could not firmly adhere to either EC model after being incubated for 35 minutes, 1, 2, 3, 12, 15, or 20 hours. At each time of the washing in the protocol, the adhered T47D cells were substantially washed away from the endothelial monolayers (Figure 4.28-C).

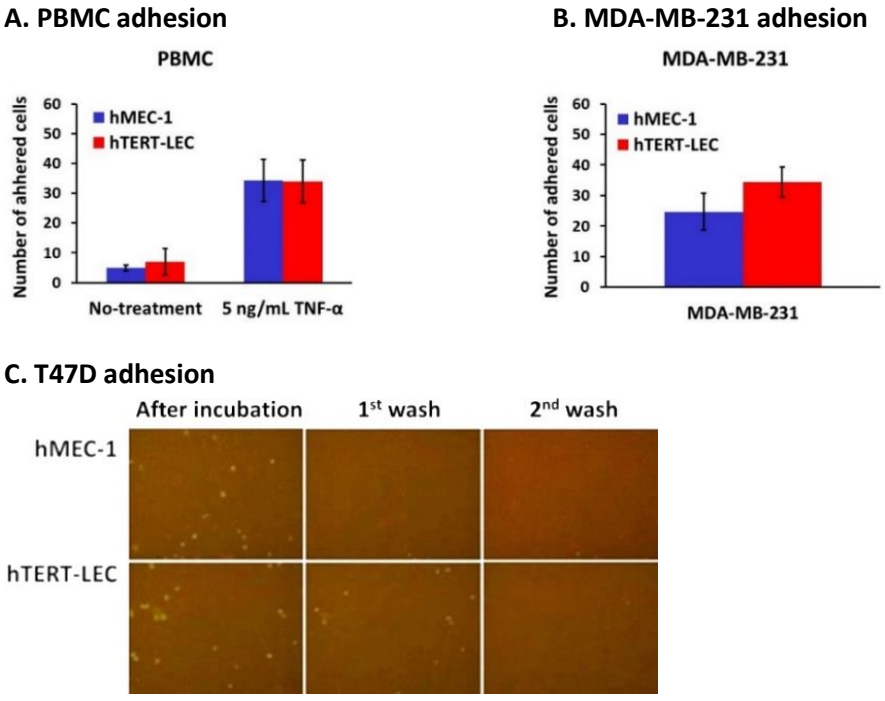


Figure 4.28 T47D cell adhesion to endothelial cells. Static adhesion assays of (A) PBMC and (B) MDA-MB-231 cells to hMEC-1 and hTERT-LEC ECs were performed prior and in parallel, respectively, to the study of (C) T47D cell adhesion. Data represent the average of adhered cell number (per two 100x fields for PBMCs or 400x fields for tumour cells) ± SD of triplicate wells of one experiment. (C) Representative images of fluorescent labelled T47D cells adhered to hMEC-1 or hTERT-LEC monolayers (400x magnification). T47D cells were incubated with hMEC-1 (for 20 hours) or hTERT-LEC monolayers (for 15 hours) before washing and removing unattached tumour cells twice.

After the second wash, cells were almost entirely removed. T47DCAST1 cells, therefore, could not be used to ascertain the role of calpastatin Type 1 overexpression in endothelial cell interactions by using the current static adhesion protocol.

4.4.2.4 Effects of A23187 calcium ionophore on cell adhesion

The effect of A23187 on endothelial interactions of the MDA-MB-231 lines overexpressing calpastatin Type 1 and Type 2 was assessed in the current study. Figure 4.29 shows percentages of tumour cells adhering to hMEC-1 or hTERT-LEC cells in response to A23187 or calpeptin treatment calculated relative to untreated controls.

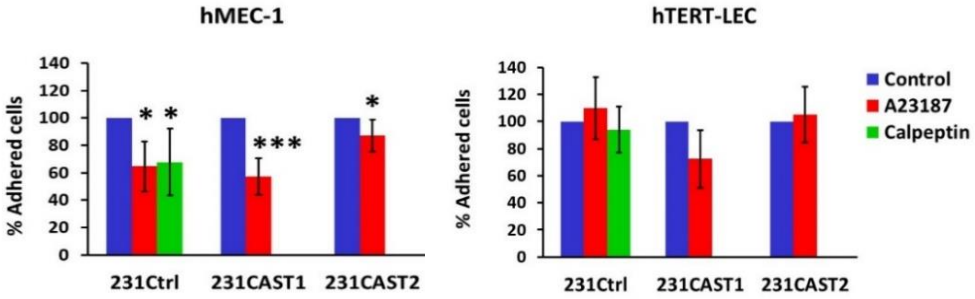


Figure 4.29 Effect of A23187 or calpeptin on adhesion of MDA-MB-231 cells overexpressing calpastatin isoforms to endothelial cells. MDA-MB-231 cells overexpressing calpastatin Type 1 (231CAST1) and Type 2 (231CAST2) and the mock-transfected cells (231Ctrl) were pre-treated by 0.5 µM A23187 for 24 hours before being examined adhesion activity to hMEC-1 and hTERT-LEC. Percentage of adhered cells (per two 400x fields) was calculated relative to a no-treatment control. Data represent the average ± SD of independent experiments (n = 5 for hMEC-1 and n = 3 for hTERT-LEC), each in triplicate; n is the number of experiment. P-values were assessed for showing the level of statistical differences between drug treatment groups and no-treatment control within each cell line; * $P < 0.05$ and *** $P < 0.001$.

Treatment of 231Ctrl mock-transfected control, 231CAST1 and 231CAST2 cells with 0.5 µM A23187 for 24 hours significantly inhibited their adhesion to hMEC-1 cells but did not show any significant effect on tumour cell adhesion to hTERT-LEC cells (Figure 4.29-A and -B). A23187 significantly reduced the adherence of mock-transfected 231Ctrl cells to hMEC-1 monolayers (35.42% inhibition, P = 0.0144) by a similar level as the inhibitory effect of 50 µM calpeptin (32.21% inhibition, P = 0.0244). However, A23187 seemed to have no effect on the adhesion of 231Ctrl to hTERT-LEC cells (109.78 ± 22.95% adhered cells, P = 0.7036). Although calpeptin showed an inhibitory effect on 231Ctrl-hTERT-LEC

cell interaction, its activity was not statistically significant (6.17% inhibition, *P* = 0.8624).

As shown in Figure 4.29-A, 231CAST1 or 231CAST2 cells overexpressing calpastatin Type 1 and 2, respectively, treated with A23187 also had a significantly lower affinity to hMEC-1 relative to untreated controls; they exhibited 57.17 ± 13.50% (*P* = 0.0001) or 87.14 ± 11.65% cell adhesion (*P* = 0.0388) relative to the activity of non-treated cells. In term of adhesion to LECs (Figure 4.29-B), no significant effect of A23187 was detected in either 231CAST1 (72.21 ± 21.48% adhered cells, *P* = 0.0886) or 231CAST2 cells (105.25 ± 20.58% adhered cells, *P* = 0.6817), although a decrease in adhered cell number was observed by 27.79% in the treated 231CAST1 cells.

4.5 Summary

1. Calpain activity in MDA-MB-231 cells was significantly increased following overexpression of calpastatin Type 1 and Type 2 in MDA-MB-231, while calpeptin significantly caused calpain inhibition in the parental cells.

2. Calpastatin Type 1 overexpression seemed to shorten cell doubling times in either MDA-MB-231 or T47D cells, while overexpression of Type 2 and Type 3 had no such effect in MDA-MB-231 and T47D cells, respectively.

3. Overexpression of calpastatin Type 1 and Type 2 had no effect in regulating clonogenicity of MDA-MB-231 cells.

4. Overexpression of calpastatin Type 1 in both MDA-MB-231 and T47D cells, as well as Type 2 in MDA-MB-231 line, increased cell migration. In comparison, calpeptin inhibited cell migration in either parental or mock-transfected cell lines of MDA-MB-231 cells but had no such effect on that of T47D lines.

5. Calpastatin Type 1 overexpression seemed to increase the adhesiveness of MDA-MB-231 cells to BECs and LECs, while Type 2 overexpression and calpeptin tended to suppress adhesion of the tumour cells to both ECs. Type 1

overexpression was more likely to affect LEC interactions, whereas overexpression of Type 2 seemed to be more involved with BEC interactions.

6. A23187 at 0.5 μM 1) induced calpain activity in MDA-MB-231 cells overexpressing Type 1 and Type 2 and the wild type cells; 2) did not affect cell proliferation, clonogenic survival, and migration in all parental and transfected MDA-MB-231 cells; and 3) significantly suppressed adhesion to hMEC-1 cells but not to hTERT-LEC cells in all parental and transfected MDA-MB-231 cells.

Chapter 5 Discussion, limitations and conclusion

5.1 Discussion

Currently, breast cancer is the most common female cancer in the UK and globally, and it is also the leading cause of female cancer death worldwide (Global Cancer Observatory, 2019c; Global Cancer Observatory, 2019e; Global Cancer Observatory, 2019f). Approximately 30% of women with early disease will develop distant dissemination (O'Shaughnessy, 2005), and the mean survival of the metastatic stage is as short as 18-24 months (Gennari *et al.*, 2005; Martino *et al.*, 2013). LVI, an early and crucial step in the metastasis process, has been suggested to help to identify who is at increased risk for axillary lymph node metastasis, local recurrence, or distant dissemination (Ejlertsen *et al.*, 2009). Although rich in blood vasculature, LI (96%) is the predominant type of breast cancer LVI (Lauria *et al.*, 1995; Mohammed *et al.*, 2011). LVI, LI and BVI have been reported as being associated with poor survival in operable breast cancer patients, either with or without axillary lymph node involvement, who are undergoing adjuvant treatment (section 1.2.3.2.1).

Calpastatin is a specific endogenous inhibitor of calpain, a Ca^{2+}-dependent cysteine protease. To our knowledge, the current group published the first report of calpastatin being involved in breast cancer progression, in particular LI. The previous IHC and gene expression studies suggested that calpastatin may negatively be implicated in breast cancer progression, lymph-node and distant metastases through regulating LI (Storr *et al.*, 2011b; Storr *et al.*, 2011c; Storr *et al.*, 2012a). In addition to its correlation with lymph-node status (Storr *et al.*, 2011c), calpastatin expression is negatively associated with the presence of LI (Storr *et al.*, 2011b; Storr *et al.*, 2012a). High calpastatin significantly associated with the absence of intratumoural LI as well as clinicopathological features of the low-risk group for breast cancer recurrence, including older patients (≥40 years), small tumours (<2 cm), low grade, low NPI, ER-positive, PR-positive, and non-basal phenotypic breast cancer (Storr *et al.*, 2012a). Meanwhile, decreased expression of calpastatin protein and the exon 3-

containing variant have been found to associate with the existence of LI and clinicopathological variations of the high-risk group for breast cancer recurrence. Low calpastatin exon 3-containing mRNA expression was significantly associated with tumour size, and NPI, while low calpastatin was associated with negative ER and PR statuses, and basal phenotype (Storr *et al.*, 2011b). In other tumours, for instance, bile duct and ampullary carcinomas, low nuclear calpastatin expression was also found to be associated with the presence of LVI and increased tumour stage (Storr *et al.*, 2012d). Paradoxically, high calpastatin was reported to be preferentially expressed in endometrial cancer than benign tissue (Salehin *et al.*, 2010), and also associated with serous ovarian cancer, the most common form of epithelial ovarian tumours (Storr *et al.*, 2012c). Associations between calpastatin expression and clinical outcomes were also present. Adverse breast cancer-specific survival was associated with high calpastatin in large but operable non-inflammatory breast cancer patients, but with low calpastatin in large but operable inflammatory cases (Storr *et al.*, 2016). Low cytoplasmic expression of calpastatin was also associated with poor overall survival in patients with bile duct and ampullary carcinomas (Storr *et al.*, 2012d). However, calpastatin expression was not associated with clinical outcomes in early-stage invasive breast cancer patients (Storr *et al.*, 2011b; Storr *et al.*, 2012a; Storr *et al.*, 2016), triple-negative/basal cases (Storr *et al.*, 2012a), and ovarian carcinomas (Storr *et al.*, 2012c).

m-Calpain and μ-calpain are conventional heterodimeric calpains consisting of a common, smaller regulatory subunit (calpain-4) and a distinct, larger catalytic calpain subunit (calpain-1 or calpain-2, respectively). They are strictly regulated by Ca^{2+} concentration and interaction with calpastatin (section 1.3). Both proteases are recognised as important regulators of various cellular pathways, and dysregulation of the calpain-calpastatin system, such as an imbalance between the level of calpain and calpastatin, is associated with a wide range of pathologies, including cancer progression and metastasis (section 1.3). Although various calpastatin isoforms originate from a single gene, the mechanism whereby each regulates calpain activity is mostly unknown, with

nothing previously examined regarding their ability to regulate cancer progression and LVI. It was therefore of interest to determine the role that individual calpastatin isoforms, encoded by exon 3-containing CAST mRNA, play in regulating breast cancer cell proliferation and clonogenicity as well as cell migration and endothelium interactions. Results would help to understand the processes involved in regulating breast cancer progression and LVI. Also, intracellular localisation of different isoforms was explored. Stably transfected breast cancer cells overexpressing calpastatin Type 1, Type 2 or Type 3 were established in the current project from two cell lines representing different breast cancer subtypes before being used as *in vitro* cell models.

5.1.1 Expression of calpain and calpastatin system proteins and CAST mRNA in different breast cancer phenotypes *in vitro*

Previous IHC analyses, conducted by the current group, revealed that expression of calpain family members, specifically calpain-1, -2, -9 and calpastatin, were associated with the chemotherapy response or clinical outcomes in particular subtypes of breast cancers, including basal-like, triple-negative and HER2-enriched (Storr *et al.*, 2011c; Storr *et al.*, 2012a; Davis *et al.*, 2014; Pu *et al.*, 2016; Pu, 2016). Such data suggested a heterogeneous expression of the calpain-calpastatin system in different breast cancer cell types. To select breast cancer cell lines with low calpastatin/CAST mRNA but high calpains levels for overexpressing calpastatin isoforms, the current study first screened the protein expression levels of calpastatin and conventional calpain subunits using fluorescent Western blotting in seven breast cancer cell lines representing different types of breast cancer, including basal-like (MDA-MB-231, MDA-MB-468 and SUM149), luminal (MCF-7 and T47D), and HER2-enriched (JIMT-1 and SKBR3). In addition to assessing calpastatin/calpain levels, CAST mRNA levels were studied by RT-qPCR, respectively (section 3.2). Also, cell growth characteristics assessed in the current project, as well as clonogenicity and cell motility demonstrated in the published literature, were used as supporting information.

Diverse expression of the calpain-calpastatin system proteins (calpain-1, -2, - 4 and calpastatin) (section3.2.1.2), as well as the levels of CAST mRNA (total CAST, CASTexon3, CAST1, CAST2 and CAST3) (section 3.2.1.3), was observed across seven cells. Besides, it seemed that there was no direct effect of the breast cancer cell phenotype on the expression of calpain, calpastatin, and CAST mRNA. Calpastatin was detected at the lowest level in T47D cells followed by all three basal-like cells, MCF-7, SKBR3 and JIMT-1, respectively, however, with no statistical significance. Similar results were also reported in the study by Pu (2016). Both HER2-enriched cell lines were the top-ranked cells expressing the highest calpastatin. Such data corresponded to the findings of breast cancer studies demonstrating a positive correlation of HER2 level with the expression of calpastatin protein (r = 0.350, *P* = 0.001) (Storr *et al.*, 2011c) or with exon 3-containing variant (χ^2 = 4.127, d.f. = 1, *P* = 0.042) (Storr *et al.*, 2011b). A correlation between calpastatin level and HER2 gene amplification ratio was also observed (r = 0.258, *P* = 0.027) (Storr *et al.*, 2011c). In the current study, calpain-1, -2, and -4 were expressed across all seven breast cancer cell lines with the relatively highest levels of calpain-1 and -4 in SKBR3 cells and calpain-2 in MDA-MB-231 and SUM149 basal-like cells. The lowest levels of calpain-1 in MDA-MB-231 and calpain-2 in MCF-7 were also previously observed by the current group, conducted by chemiluminescent Western blotting across six cell lines (except SUM149) (Pu, 2016). Wu and colleagues also found that MCF-7 cells had a deficient level of calpain-2 (Wu *et al.*, 2006).

The RT-qPCR analysis of total CAST and CASTexon3 mRNA expression supported the phenomenon presenting the relatively lower expression of calpastatin protein in T47D and the basal-like cells. The lowest expression of both total CAST and CASTexon3 mRNA was also detected in T47D, followed by the basal-like cells except for MDA-MB-231 in the case of CASTexon3 mRNA. MDA-MB-231 had a relatively higher CASTexon3 mRNA level amongst all seven cells. Considering the expression of individual CAST1, CAST2 and CAST3, T47D showed the relatively low-to-lowest levels of all mRNA compared to the rest of

breast cancer cells. Meanwhile, all basal-like cells had a relatively high CAST1 and CAST3 mRNA, but low CAST2 mRNA (section 3.2.1.3).

The low expression of the calpastatin protein and mRNA observed in T47D luminal and three basal-like cells, suggesting to select two cells from them as *in vitro* cell models for overexpressing calpastatin isoforms. The T47D cell line was first designated due to its promisingly supportive characteristics to accomplish the creation of transfected monoclonal cells, including its relatively medium-to-high expression of all calpains (section 3.2.1.2), its second shortest doubling time (29.53 hours) amongst seven cell lines (section 3.2.1.1), and its clonogenic ability (~20% PE in three weeks; Abdullah, 2019).

Three basal-like cell lines expressed comparable levels of calpain-1 and -4, while the highest calpain-2 amongst all seven cells was observed in MDA-MB-231 and SUM149 cells (section 3.2.1.2). Within 14 days, MDA-MB-231 cells showed a high capability to form colonies with 69.07 ± 6.74% PE (section 4.3.2.1), which was comparable to the previous results observed by the current group - 52.89 ± 13.69% in 14 days by Abdullah (2019) and 52.83 ± 7.43 in 18 days by Zhang (2014). SUM149 cells could also form colonies with 40-60% PE within a similar period (14 days) (Rahal *et al.*, 2018). Although the clonogenic abilities of MDA-MB-231 and SUM149 cells were comparable, MDA-MB-231 cells proliferated with the shortest doubling time (~19 hours) compared to the other six cells, and more than two times faster than SUM149 cells (~43 hours) (section 3.2.1.1), suggesting a superior property of MDA-MB-231 over SUM149 to establish the transfected monoclonal clones successfully. As calpastatin has been reported to inhibit calpain-mediated cell proliferation (section 1.3.5.1), calpastatin overexpression in more rapidly proliferating cells, therefore, might show the expected results more clearly.

In addition, calpastatin has also been found to inhibit calpain-mediated cell migration and adhesion (section 1.3.5.2). Higher cell migration activity or adhesion ability towards BECs and LECs were considered as the other superior quality for the cells to be selected as a cell model to overexpress calpastatin

isoforms. MDA-MB-231 cells, by scratch-wound assay, were able to migrate two times faster (24 hours) (section 4.4.1; Ahmad, 2016; Pu, 2016) than SUM149 cells (48 hours) (Novikov *et al.*, 2016), to almost wholly close cell-free gaps. This was considered as an advantage as the expected calpain inhibitory effects on cell migration following calpastatin overexpression in MDA-MB-231 could be clearly detected compared to SUM149 cells. To our knowledge to date, there is no evidence of SUM149 adherent ability to ECs, while MDA-MB-231 exhibited a higher adhesion ability to both BECs and LECs compared to MCF-7, a luminal cell line (Safuan *et al.*, 2012). Thus, the basal-like MDA-MB-231 and the luminal T47D cell lines were selected to generate the stably transfected monoclonal cells overexpressing HA-tagged full-length calpastatin isoforms.

5.1.2 Establishment of stably transfected breast cancer cells overexpressing calpastatin isoforms

In an attempt to stably transfect cells with DNA constructs containing cDNA encoding HA-tagged full-length calpastatin isoforms or the empty vector (section 3.2.2), cationic nanomeric complexes were applied in the current study, regarding their properties that are stable enough for creating their bound nucleic acids from degradation and are capable of entering cells regularly by endocytosis (Scherer *et al.*, 2002). Instead of using the viral or other nonviral delivery methods, cationic nonviral delivery systems were used in the present project, due to several advantages compared to those methods, such as low toxicity and antigenicity, because they are produced only from biological lipids, as well as a long-term expression with fewer risk of insertional oncogenesis. However, lower efficiency remains the disadvantage of this system (Nayerossadat *et al.*, 2012). The transfection efficiency of vectors, generally, is associated with cell types, type of DNA, and medium conditions, while the optimal amount of DNA used in transfection varies widely, depending on the type of DNA and target cell line (Yamano *et al.*, 2010).

As mentioned in section 2.6.2, FuGENE®HD is recognised as the most preferred transfection reagent, as indicated by its maximal transfection efficiency for

several cell lines compared to other commercially available reagents, including jetPEI® (a formulation of polyethylenimine) and Lipofectamine®2000 (Yamano *et al.*, 2010). To our knowledge, transfection efficiency comparison between FuGENE®HD and Lipofectamine®3000 reagents used in this study has not been tested. In the current study, the relatively smaller DNA constructs of CAST2 (6306 bp), CAST3 (6102 bp) or the empty vector (4018 bp) were efficiently delivered into MDA-MB-231 or T47D cells by FuGENE®HD (cationic micelle). In comparison, CAST1 constructs containing the most extensive DNA sequence (6351 bp) seemed to be more challenging for being delivered into both breast cancer cells compared to the other constructs, and Lipofectamine®3000 seemed to be more effective in delivering the CAST1 constructs into the cells compared to FuGENE®HD and Viromer®Red (a formulation of polyethylenimine).

Amongst all transfections, the generation of CAST1- or CAST2-transfected T47D populations was the most challenging work and took more attempts to accomplish. Although dense, small colonies of the transfected cells were apparent in several experiments, the single cells separated from them by trypsinisation could not survive or proliferate. This might be due to G418 selective reagent, which was reported to extend the doubling time of various transfected cells (Yallop & Svendsen, 2001), in parallel with the area of a multiple well culture plate used in transfection experiments that might be too large for a small number of T47D cells to survive and expand. As suggested by T47D growth curve (Appendix C Figure C3.2), the high density of cells as $6.1x10^5$cells/well in a six-well plate were required for T47D to initiate log phase of cell growth at 24 hours post-cell seeding, while 2- to 4-fold lesser cell densities were required for the other six breast cancer cell lines, including MDA-MB-231 (4-fold lesser) (Appendix C Figure C3.1). In addition, only approximately 20% of single T47D cells could survive and form colonies containing at least 50 cells in a T25cm^2 culture flask within 21 days (Abdullah, 2019). In comparison, MDA-MB-231 cells had more competency to form colonies (2- to 3-fold higher PE) within a shorter period (14 or 18 days) in the same culture containers

(section 4.3.2.1; Abdullah, 2019; Zhang, 2014). Transfections of CAST1 and CAST2 constructs in T47D cells were successful after being performed in a 96-well plate instead of using a plate comprised of a larger surface area. In short, the generation of stable CAST-overexpressing cells may require careful consideration of the size of the DNA constructs as well as the proliferating rates and clonogenic abilities of the parental cells.

The current project successfully established stable MDA-MB-231 clones overexpressing calpastatin Type 1 (231CAST1) and Type 2 (231CAST1), as well as T47D clones overexpressing Type 1 (T47DCAST1) and Type 3 (T47DCAST3), and their respective mock-transfected control cells (231Ctrl and T47DCtrl). Multiclonal 231CAST3 cells and their established monoclonal clones made in section 3.2.2.1 did not express HA tag and, therefore, were not used in this study. Similarly, monoclonal population selection of T47DCAST2 clone remained unaccomplished after several attempts (section 3.2.2.2). Due to time constraints, it was not possible to produce 231CAST3 and T47DCAST2 clones, and they were dismissed from this study. Therefore, the series of stably transfected cells overexpressing calpastatin Type 1, Type 2 or Type 3 could not be completely made from either the MDA-MB-231 or T47D cell lines by this study. However, 231CAST1 and 231CAST2 clones were principally used as *in vitro* cell models in the current project to investigate and compare the roles of calpastatin Type 1 and Type 2 with each other in regulating phenotypic characteristics related to breast cancer progression and LVI due to their mRNA sequences differing by only one exon. As T47DCAST1 clone overexpressed Type 1 calpastatin, it was also considered as another cell model of the study. All of these clones were used as cell models if their overexpression of calpastatin isoform protein or mRNA was present.

5.1.3 Expression of the calpain-calpastatin system proteins and CAST mRNA in transfected cells models

The CAST1- or CAST2-transfected monoclonal breast cancer cells were quantitatively analysed to ascertain the overexpression of HA-tagged

calpastatin isoforms and total calpastatin using Western blotting analysis (section 3.3.1), and/or the particular CAST mRNA expression (CAST1 or CAST2 mRNA) using RT-qPCR method (section 3.3.2). The ultimate aim was to select clones for studying the effects of calpastatin isoform upregulation on phenotypic endpoints related to breast cancer progression and LVI *in vitro*.

In transfected MDA-MB-231 cells, total calpastatin levels were significantly higher than the mock-transfected 231Ctrl cells by 3.44 fold in 231CAST1 cells ($P < 0.0001$) and 2.61 fold in 231CAST2 cells ($P = 0.0035$). The generic calpastatin antibody used in this study identified the expression of total calpastatin as duplicate bands migrated between 100 and 120 kDa, indicating the detection of multiple calpastatin isoforms. The duplicate bands of calpastatin were also observed previously in Pu (2016)'s and Zhang (2018)'s PhD theses. The molecular diversity of calpastatin appears in human and other species. In humans, according to differences in mobility on SDS-PAGE, calpastatins are classified into the tissue type (100-120 kDa) and the erythrocyte type (70 kDa) which lacks the amino-terminal domains (domains L and I). Takano *et al.* (1993) described that diversity amongst the tissue type calpastatins is caused by alternative splicing and post-translational processing while conversion from the tissue type to the erythrocyte type is a consequence of proteolytic processing. Human T98G Glioblastoma and WI-38 fibroblast cell lines have been evaluated for the expression of the non-deleted, the exon 3-deleted and the exon 3- and 5-deleted calpastatin mRNA types, corresponding to 117, 114 and 110 kDa calpastatin proteins. In human hematopoietic cells, human erythrocytes showed the 110-kDa form (the tissue type) in addition to the predominant 70-kDa form (the erythrocyte type), whereas the mononuclear and polymorphonuclear cells expressed the tissue type (110 and 114 kDa) (Takano *et al.*, 1993).

HA-tagged calpastatin expression significantly increased in both 231CAST1 and 231CAST2 cells relative to the mock-transfected 231Ctrl cells ($P < 0.0001$ and $= 0.0005$, respectively) and the parental cells ($P < 0.0001$ and $= 0.0005$,

respectively). Such results indicate overexpression of calpastatin Type 1 in 231CAST1 clone and Type 2 in 231CAST2 clone. Both cells overexpressed similar levels of HA-tagged calpastatin (*P* = 0.1096). Interestingly, by using the HA-tag antibody, duplicate bands of HA-tagged calpastatin located at 100-120 kDa (a major band migrated at the higher position) were shown in 231CAST2 cell line (section 3.4.1, Figure 3.15-B), whereas a single band was detected in 231CAST1 clone slightly above 120 kDa (section 3.4.1, Figure 3.15-A). The duplicate bands of HA-tagged calpastatin observed in 231CAST2 cells can be explained by the study of Parr *et al.* (2004). Parr *et al.* (2004) revealed that in porcine skeletal tissues the 145-kDa full-length calpastatin Type 1 could be detected by the anti-1xa peptide antibody and the 135-kDa band was the translation product of Type 3 mRNA presumably originating from the AUG codon in exon 2. Interestingly, the 135-kDa peptide could be translated from Type 1 mRNA by starting the translation at the downstream AUG codon in exon 2 or from the upstream AUG codon in exon 1xa before subsequently being cleaved to a truncated protein (Parr *et al.*, 2004). Cong *et al.* (1998) also described the presence of a doublet of peptide bands translated from bovine calpastatin Type 2 mRNA in a similar way, and that can be used to explain the duplicate bands of HA-tagged calpastatin observed in 231CAST2 cells. The peptides originated mainly from the upstream AUG codon in exon 1xb of the HA-tagged Type 2 mRNA (a major band), and a minority of them was then subsequently cleaved to a truncated protein (a minor band).

CAST1 mRNA was significantly overexpressed in both 231CAST1 (2.60 fold, *P* = 0.0020) and T47DCAST1 cell lines (6.22 fold, *P* < 0.0001) relative to the mock-transfected counterparts. The PCR protocol for analysing CAST2 mRNA expression in the current study, however, was not optimal according to its poor PCR efficiency (27.44 %E). Theoretically, the number of templates should double after each cycle of PCR reaction, resulting in E = 2 or 100% (Booth *et al.*, 2010). The PCR with amplification efficiency between 90% and 110% is considered an acceptable method for quantitative analysis (Broeders *et al.*, 2014). The poor amplification efficiency of PCR could be a consequence of

several parameters, such as non-optimal primer sequence or inappropriate primer concentration, resulting in a small amount of product (amplicon) or no product due to non-specific amplification or primer-dimer formation (Abd-Elsalam, 2003; Green & Sambrook, 2018). The other factors for the poor PCR efficiency include poor reaction conditions, inaccurate sample and reagent pipetting, improper analysis of standard (Green & Sambrook, 2018), and a presence of PCR inhibitors originated from the sample or introduced during sample preparation (such as cell debris, bacterial cells, immunoglobulin, polysaccharides, contaminants from the nucleic acid extraction phase) (Schrader *et al.*, 2012).

The poor efficiency of the PCR analysis for CAST2 mRNA expression indicated that the PCR condition used in this study was not optimal for evaluating CAST2 expression in 231CAST2 cells and required modification and optimisation. By using a Primer-Blast tool (https://www.ncbi.nlm.nih.gov/tools/primer-blast/) and a Primer 3 tool (http://primer3.ut.ee/), it has been found that the forward primer for the CAST2 expression analysis has no site to align against the CAST2 cDNA sequence constructed in the plasmid. The CAST2 cDNA sequence used in this study starts with the first ATG start codon appeared in the natural CAST mRNA sequence, leading to an absence of a forward primer binding site from the CAST2 cDNA sequence, in which normally shown at the early region of the natural CAST mRNA sequence. Amplification of CAST2 cDNA by only reverse primers, therefore, could not double the number of templates after each cycle. Ideally, by use of both forward and reverse primers, the number of amplicons formed after a given number of cycles is 2^n (E=2 or 100%), where n is the number of cycles (Kralik & Ricchi, 2017).

Due to time constraints, primer redesign, PCR protocol optimisation or CAST2 expression analysis seemed impossible to be completed by the current project; however, it can be continued in future projects by our group. Although there was no confirmation of CAST2 mRNA overexpression in 231CAST2 cells, they significantly showed upregulation of HA-tagged and total calpastatin, as well as

the signal of HA-tagged calpastatin detected under a confocal microscope (section 3.5), leading to consideration of 231CAST2 clone as another *in vitro* cell model for the current project in addition to 231CAST1 and T47DCAST1 cell lines.

The effect of calpastatin isoform overexpression on the expression levels of calpain-1, -2 and -4 was also explored in 231CAST1 and 231CAST2 cells compared to that in the mock-transfected 231Ctrl control (section 3.3.1). The expression levels of all investigated proteins (calpastatin, calpain-1, -2 and -4) were comparable in between the mock-transfected and the parental cell lines ($P > 0.9999$, 0.7788, 0.9848 and 0.9964, respectively). Such results suggest that there was no effect of the empty vector and G418 on the expression of the calpain-calpastatin system proteins. While the empty vector was not likely to alter the expression level of any conventional calpain subunits, only calpain-1 expression significantly increased in calpastatin isoform-overexpressing MDA-MB-231 clones, including 231CAST1 (1.40 fold, $P = 0.0188$) and 231CAST2 cells (1.33 fold, $P = 0.0446$), relative to that detected in the mock-transfected control (section 3.3.1). This suggests that the increase of calpastatin in MDA-MB-231 might induce the expression of calpain-1, as supported by a correlation observed between the expression of calpain-1 and calpastatin in various studies. In a cohort of large but operable breast tumours, treated with neoadjuvant chemotherapy, calpastatin expression significantly correlated with the expression of calpain-1 but not with calpain-2 (Storr *et al.*, 2016). Paradoxically, in early-stage breast cancer cohorts, the expression of calpastatin correlated with the expression of calpain-9 (Davis *et al.*, 2014), calpain-2, but not calpain-1 (Storr *et al.*, 2011c). In addition to breast cancer, Liu *et al.* (2017) indicated that in normal-appearing peritumoural gastric mucosa, calpastatin expression strongly correlated with the expression of calpain-1 ($r = 0.741$; $P < 0.0001$) but weakly correlated with calpain-2 ($r = 0.535$; $P < 0.0001$). In gastric cancer tissues, the expression of calpain-1, -2, and calpastatin significantly correlated with each other ($P < 0.05$), although the correlations were weak ($r = 0.342$, 0.553 and 0.441 for calpastatin correlation with calpain-1, or-2 and calpain-1 correlation with calpain-2, respectively) (Liu

et al., 2017). In both endometrial and ovarian cancers, calpastatin expression has been observed to correlate with calpain-1 (endometrial cancers: r = 0.579, *P* = 0.001, Salehin *et al.*, 2010; ovarian cancer: r = 0.602, *P* < 0.001, Storr *et al.*, 2012c; r = 0.512, *P* < 0.001, Zhang *et al.*, 2019) but not with calpain-2 (Salehin *et al.*, 2010; Storr *et al.*, 2012c; Zhang *et al.*, 2019). These phenomena could be explained by the possibility of balancing feedback within the calpain-calpastatin system to promote an equilibrium between calpain and calpastatin levels and minimise the effects of perturbations.

5.1.4 Effects of cell culture factors on calpastatin expression and migration of transfected cells models

Persistent expression of HA-tagged and total calpastatin was confirmed in 231CAST1 and 231CAST2 cell lines after being serially subcultured from the master cells (passage number 0) for ten times (section 3.4.1). There was no difference in the expression of the HA-tagged and total calpastatin between passage number 2 and 10 of both 231CAST1 (*P* = 0.8279 and 0.6724, respectively) and 231CAST2 cells (*P* = 0.9996 and 0.9839, respectively), indicating stable transfection in both clones. Thus, all stably transfected cells were routinely cultured in selection medium (750 µg/mL G418) and used in routine experiments up to passage number 10.

As the mock-transfected 231Ctrl cells cultured in the selection medium significantly proliferated slower than the parental cells (38.41 vs 19.07 hours, *P* = 0.0018; section 4.3.1.1), G418 contained in the selection medium might affect the phenotypic endpoints of the transfected cells. Yallop and Svendsen (2001) stated that G418 affected the growth and metabolism in baby hamster kidney BHK 570 cells transfected with the human gastric inhibitory peptide (h-GIP). G418 slowed down the cell growth and increased utilisation of glutamine. In the transfected Chinese Hamster Ovary (CHO) 679 cells by glucagon receptor, G418 affected the cell metabolism by that the flux of glucose was directed away from lactate production and towards both the TCA cycle to provide energy and biosynthetic pathways (Yallop & Svendsen, 2001). In addition, Kung and

colleagues reported the G418-associated reduction of cell-associated glycosylphosphatidylinositol (GPI)-anchored alkaline phosphatase (AP) in either transfected or wild-type COS-1 monkey kidney epithelial cells (Kung *et al.*, 1997).

To avoid the effects of G418 on phenotypic endpoints of interest, G418-free culture medium was used in the following experiments. Short-term removal of G418 from the culture medium for seven days had no effect on the expression levels of HA-tagged and total calpastatin in 231CAST1 (P = 0.8031 and 0.1893, respectively) and 231CAST2 cell lines (P > 0.9999 and >0.9999, respectively) compared to the cells cultured in parallel in the selection medium. By comparing with the cells of day 0, HA-tagged and total calpastatin expression in both 231CAST1 (P = 0.3476 and 0.8809) and 231CAST2 cell lines (P = 0.9998 and 0.9479) remained unchanged after the cells were cultured in the G418-free medium for seven days. As concluded in the study of Yallop and Svendsen (2001), the expression of the proteins of interest in the transfected CHO 679 and BHK 570 cells remained stable without selection by G418 over six months. The CHO cells transfected with plasmid DNA encoding both GFP and neomycin phosphotransferase (neo) cassettes maintained high-level green fluorescence after removal of G418 from the growth medium for 12 weeks (Gubin *et al.*, 1997). This suggests that the stably G418-resistant transfectants are able to maintain expression of the proteins of interests in the non-selective medium.

The transfected 231CAST1, 231CAST2 and mock-transfected 231Ctrl cells were pre-incubated with G418-free medium for up to 14 days before being examined migratory activity using scratch-wound assay (section 3.4.2.2). The migration abilities of such cells were not different from that of the respective control groups cultured and performed the migration assay in the selection medium. The absence of differences in cell migration characteristics might be a consequence of unchanged levels of HA-tagged and total calpastatin at different culture conditions and suggested stable transfection of 231CAST1, 231CAST2 and 231Ctrl cells. Although 231Ctrl cells were pre-treated with the

G418-removed medium for up to 14 days, their migration remained to be significantly slower than the parental cells, suggesting that G418 was not a factor inhibiting 231Ctrl cell migration. Thus, the slower migration ability of 231Ctrl cells compared to the parental cells might be a consequence of plasmid transfection or overexpression of the resistance protein produced from Neo^r resistant gene (Yallop & Svendsen, 2001). Although G418 did not affect the migration of the transfected MDA-MB-231, it might affect other phenotypic endpoints. Thus, to recover from and avoid the effect of G418 on phenotypic features, complete G418-free culture medium was then used to culture all transfected cells, including MDA-MB-231 and T47D clones, for two days before performing and while conducting the experiments.

5.1.5 Intracellular localisation of calpastatin isoforms

The full-length forms of each calpastatin Type 1, Type 2 or Type 3 seemed to have similar patterns of intracellular distribution, detected by IF confocal microscopy, in comparison to the respective truncated (only XL and L domains) forms encoded by cDNA containing exon3 (investigated by Dr Sarah Storr, unpublished data) in both MDA-MB-231 and T47D cell models (section 3.5). In addition, an exon 3-deleted version of the truncated calpastatin isoforms also distributed similarly to both truncated and full-length forms, encoded by exon3-containing CAST in MDA-MB-231 cells (investigated by Dr Sarah Storr, unpublished data). In consideration of the CAST mRNA structure, both calpastatin Type 1 and Type 2 contain the XL and L domain but possess different N-terminal sequences generated from tandem promoters, which are associated with exons 1xa and 1xb, respectively. Calpastatin Type 3 is generated from a promoter that is associated with the untranslated exon 1u, resulting in a protein that lacks XL region (section 1.3.2; Takano *et al.*, 2000; review in Storr *et al.*, 2011a). Together, the Leader domain excluded exon 3 may play a role as a crucial component in regulating intracellular localisation of calpastatin Type 1, Type 2 and Type 3.

Calpastatin Type 1 and Type 3 localised principally throughout the cytoplasm and partially in the nuclei in both MDA-MB-231 and T47D lines. Consistent with previous *in vitro* observation in large cell lung cancer-103H cell line, calpastatin homogeneously distributed in the cytoplasm, with a slight multitude around the nuclear region, and it was also found to accumulate in the nuclei (Gil-Parrado *et al.*, 2003). In breast cancer tissue, the distribution of calpastatin investigated by IHC using the generic calpastatin antibody has also been observed predominantly in the cytoplasm but infrequently in the nucleus (Storr *et al.*, 2011c; Storr *et al.*, 2012a; Storr *et al.*, 2016)). Paradoxically, De Tullio *et al.* (1999) revealed that calpastatin distributed as an aggregation that was almost completely confined in two granule-like structures without surrounding membranes, and it was nearly absent in the nucleus and cytosol. Such data suggest that most of the calpastatin intracellularly distributed in specific structures rather than localised in a diffused form throughout the cytosol. The unique localisation of calpastatin aggregation has been similarly observed in various human or murine cell types, such as murine erythroleukemia MEL cells and pheochromocytoma PC12 cells, as well as human neuroblastoma LAN-5 cells and aortic smooth muscle AoSMC cells (De Tullio *et al.*, 1999). Such calpastatin aggregations were affected by an increase of the intracellular Ca^{2+}, which resulted in calpastatin gradually becoming a soluble protein (De Tullio *et al.*, 1999). Although calpastatin Type 2 did not distribute definitely in two-granule-like structure, this isoform was also found unique localisation in the cytoplasm with a predominant perinuclear expression, i.e., visible spots in MDA-MB-231 cells and fibre-like aggregations in T47D cell line.

Calpain and calpastatin co-localise in the cytoplasm, with a slight multitude around the nuclear region (Gil-Parrado *et al.*, 2003). Dissociation of calpain from calpastatin is crucial for calpain activation under calcium-stimulating conditions, resulting in calpain re-localises to the plasma membrane where it cleaves and regulates downstream targets including cell migration- or adhesion-enhancing effectors, while calpastatin remains in the cytoplasm (Gil-Parrado *et al.*, 2003; Stifanese *et al.*, 2010). Calpains can reside in or translocate

to the cell nucleus (Tremper-Wells & Vallano, 2005). Several studies have suggested calpains as one of the DNA process-regulating proteins (Baek *et al.*, 2016), and nuclear or translocated calpains has been shown to play a role in promoting cell survival via several signalling pathways, including Ku80, NF-κB and PI-3K/Akt (Baek *et al.*, 2016; Baghdiguian *et al.*, 1999; Tremper-Wells & Vallano, 2005; Burchett *et al.*, 2019).

Ku80, a subunit of the Ku protein complex, is an initiator of the non-homologous, end-joining (NHEJ), double-strand breaks (DSBs) repair pathway. The nuclear Ku80 can be cleaved in a calcium concentration-dependent manner by m-calpain but not by μ-calpain, and the cleaved Ku80 still forms a Ku heterodimer, leading to DNA DSB repair. Thus, translocated or nuclear m-calpain promotes the NHEJ pathway through the cleavage of Ku80 (Baek *et al.*, 2016). Calpain 3-dependent IκBα degradation has been demonstrated to take place in a co-expression cell system. IκBα overexpression causes depletion of nuclear accumulation of NF-κB, leading to apoptosis. Calpain 3, present in healthy muscle as sarcoplasmic and nuclear forms, controls IκBα turnover and indirectly regulates NF-κB-dependent expression of survival genes (Baghdiguian *et al.*, 1999). Ca^{2+}/calmodulin-dependent protein kinase Type IV (CaMKIV) is highly enriched in the nucleus and thought to be critical for improved survival. Under conditions of sustained Ca^{2+} influx, nuclear calpain regulates Ca^{2+}-dependent signallings, including PI-3K/Akt pathway, via proteolysis of nuclear CaMKIV and subsequently resulting in an improved long-term cell survival (Tremper-Wells & Vallano, 2005).

The phenomenon of perinuclear localisation of calpastatin Type 2 observed in this study could potentially be a consequence of accumulated aggregation of calpastatin after disassociation from binding to calpain (Averna *et al.*, 2003) and possibly results in driving cell migration but antagonising the pro-survival effects mediated by nuclear calpain, as described by Burchett *et al.* (2019). Besides, the distribution of calpastatin Type 1 and Type 3 in the nuclei may

promote cell death through suppressing the pro-survival effects mediated by nuclear calpain (Burchett *et al.*, 2019).

Intracellular localisation of calpastatin in human malignant glioma (MG) cells has been found to be regulated by hypophosphorylated nuclear factor I (NFIs) through the usage of an alternative CAST promoter located upstream of exon4 (Burchett *et al.*, 2019). Binding of hypophosphorylated NFI to CAST intron3 increased utilisation of the alternative promoter, resulting in a higher ratio of class 2 CAST variant (translating to ~135-kDa XL-less calpastatin isoforms by the alternative promoter) to class 1 variant (translating to ~145-kDa full-length calpastatin by the canonical promoter). Class 1 variant encodes full-length human calpastatin, which contains domains XL, L, and four inhibitory repeats, shares homology with the ~145 kDa bovine calpastatin Type II. Depletion of NFIs in U251 MG cells was observed together with a reduction of class 2 CAST variant but an increase of class 1 CAST variants. In NFI-hypophosphorylated U251 MG cells, calpastatin was primarily distributed in the nucleus and cytoplasm, with increased immunostaining in the perinuclear region. On the other hand, depletion of NFIs resulted in increased accumulation of calpastatin at the plasma membrane (Burchett *et al.*, 2019). In addition, *in vivo* phosphorylation of calpastatin by protein kinase A (PKA) has been found to cause a 5-fold elevated level of membrane-associated calpastatin (from 6% to 30%) (Adachi *et al.*, 1988). In support of that, three PKA phosphorylation sites were located within the XL domain (Cong *et al.*, 1998). Hence, phosphorylation by PKA may cause calpastatin containing the XL domain to be more likely to localise to and suppress calpain activity at the plasma membrane, resulting in inhibiting cell migration, compared to the XL-less isoforms. Calpastatin containing the XL domain could be Type 1 and Type 2 calpastatin of the current study or calpastatin encoded by class 1 variants in the study of Burchett *et al.* (2019), and the XL-less isoforms could be the translational product of class 2 variants (Burchett *et al.*, 2019) or Type 3 of the current project.

The different intracellular localisation between calpastatin Type 1 and Type 2 (section 3.5) suggested to study and compare their effect on calpain activity and phenotypic endpoints related to breast cancer progression (cell proliferation and clonogenicity) and LVI (cell migration and adhesion to ECs) *in vitro*. Therefore, the breast cancer cells transfected with CAST1 cDNA (231CAST1 and T47DCAST1) and CAST 2 cDNA (231CAST2) were used as principal cell models for the current project. All cellular functions were assessed in the presence/absence of A23187 calcium ionophore, used to ensure calpain activation. Calpeptin, a calpain inhibitor, was used as a comparator to the effect of calpastatin isoform overexpression.

5.1.6 Role of calpastatin isoform overexpression in regulating calpain activity *in vitro*

Calpain activity, which is strictly regulated by Ca^{2+}, has been implicated in cancer progression and metastasis, by facilitating various related physiological pathways, such as cell cycle redistribution, growth, survival, migration, adhesion, and invasion, through interacting with crucial regulators of those pathways (sections 1.3.5.1 and 1.3.5.2). Depletion of calpain activity by upregulation of calpastatin, pharmacological calpain inhibitors (e.g., calpeptin) or genetic disruption of calpain contribute to inhibition of calpain-dependent cellular functions. This indicates that calpain is a positive regulator of cancer progression and metastasis, whereas calpastatin is an inhibitor of these processes. The opposing effects of calpain or calpastatin on cancer progression and metastasis have also been shown in several *in vitro* or *in vivo* studies (Carragher *et al.*, 2001; Lokuta *et al.*, 2003; Cortesio *et al.*, 2011; Raimbourg *et al.*, 2013; Machado *et al.*, 2015; Machado *et al.*, 2017).

In this study, the role that calpastatin isoform overexpression plays in regulating calpain activity in breast cancer cells was explored and compared to that of calpeptin (section 4.2). Calpeptin treatment conditions causing minimal cytotoxicity but maximal inhibition of calpain activity in MDA-MB-231 and T47D cells were identified. Calpeptin at 50 and 75 µM had no or slightly anti-

proliferative effect in MDA-MB-231 and T47D cells, respectively, after 24 hours of exposure (section 4.2.1). Both concentrations exhibited similar capabilities to reduce calpain activity in both cells for all incubation periods (0.5, 1, 2, and 24 hours) (section 4.2.2). Consistent with the previous publications, the inhibitory effect of calpeptin was not in a dose-dependent manner in breast cancer cells (Pu, 2016). In ovarian cancer cells, calpain inhibitory effects were not different between calpeptin at 50 µM and higher concentrations in PEO1, PEO4 and SKOV3 cells (Zhang, 2018) but reduced with concentrations >25 µM in OV2008 cells (Woo *et al.*, 2012).

Calpain activity could not be significantly inhibited following treatment with calpeptin for 1 or 2 hours in MDA-MB-231 and 1 hour for T47D cells, and the inhibitory effects of calpeptin at the indicated time-points were decreased compared to the 0.5-hour treatment (section 4.2.2). The reduction of calpain inhibition by calpeptin observed when the breast cancer cells exposed to the calpain inhibitor for longer than 30 minutes might be due to cellular compensation of calpain activity occurring shortly before recovery of calpain inhibitory effect by calpeptin significantly re-detected, or it might be a result of the sensitivity of the t-boc assay. By considering the differences between controls and treated cells, it could be that the assay was not sensitive enough to show significant differences at all time points. Wide variations of calpain activity detected by the t-boc assay were also observed in the studies of Pu (2016) and Zhang (2018). However, as the non-cytotoxic concentration of calpeptin (50 µM) caused a significant calpain inhibition following cell treatment for 24 hours in both MDA-MB-231 and T47D cells, calpeptin was used as a comparator to the effect of calpastatin isoform overexpression in the subsequent phenotypic endpoint assessments.

Several *in vitro* or *in vivo* studies demonstrated that calpastatin overexpression prevented calpain activity or calpain-mediated proteolysis (Lu *et al.*, 2002; Vaisid *et al.*, 2007; Schoch *et al.*, 2012; Diepenbroek *et al.*, 2014; Ye *et al.*, 2015). On the other hand, a deficiency/decrease in calpastatin enhanced calpain

activity/upregulation (Carragher *et al.*, 2002; Diepenbroek *et al.*, 2014). In the current study, although 231CAST1 and 231CAST2 clones significantly overexpressed both HA-tagged calpastatin isoforms and total calpastatin (section 3.3.1), higher calpain activity was unexpectedly detected in both CAST-transfected cells relative to that in their mock-transfected cells (39.82% increase, P = 0.0157; and 70.78% increase, P = 0.0009, respectively) (section 4.2.4.1). Such increased calpain activity in the calpastatin isoform-overexpressing MDA-MB-231 clones might be due to an increased ratio of calpains to calpastatin, which could be a result of the significantly-increased calpain-1 levels detected in both 231CAST1 and 231CAST2 cells (section 3.3.1). As overexpression of HA-tagged calpastatin (sections 3.2.2.2 and 3.5) and CAST1 mRNA (section 3.3.2) was detected in T47DCAST1 cells, calpain-1 expression and calpain activity in T47DCAST1 clone might also increase. Furthermore, increased calpain activity might also be a consequence of the L-domain contained in calpastatin Type 1, 2 and 3, as described by the studies of De Tullio *et al.* (2014) and De Tullio *et al.* (2018).

Calpastatin domain L recognises a site at domain II of calpain not coincident with the catalytic cleft and which possibly directs the first downstream inhibitory unit to the substrate cleft (De Tullio *et al.*, 2014). In other words, the existence of the L-domain is able to increase the affinity of the downstream inhibitory unit for the active cleft, and when this complex is formed, calpain is inhibited. De Tullio *et al.* (2014), however, demonstrated that the L-domain of calpastatin is responsible for the decrease in inhibitory efficiency at high calpastatin concentration and calpain is never fully inhibited even in the presence of an excess of calpastatin. At this condition, the association of the inhibitor with calpain occurs at the other sites in the EF-hands located in domains IV and VI of the protease (De Tullio *et al.*, 2014; De Tullio *et al.*, 2018). In the presence of Ca^{2+}, the interaction of calpastatin containing the L-domain with the EF-hands creates a steric hindrance that obstructs the binding of another calpastatin molecule at the catalytic site. In this complex, calpain is therefore active and able to digest substrates including other calpastatin

molecules (De Tullio *et al.*, 2014) that are primarily digested to 15 kD active inhibitory units before being shortened into inactive fragments (De Tullio *et al.*, 2000). De Tullio *et al.* (2014) reported that calpastatin Type 1, 2 and 3 at the concentration as high as 7 nM caused a loss of efficiency in inhibiting calpain activity. Therefore, in addition to the increase of calpain-1 level, the increased calpain activity in both 231CAST1 and 231CAST2 cells might be a consequence of L-domain-containing calpastatin isoforms overexpressed in their cells.

5.1.7 Role of calpastatin isoform overexpression in *in vitro* models of breast cancer progression (cell proliferation and clonogenicity)

Calpain activity is involved with a variety of cellular functions related with cancer progression, such as inducing cell cycle progression (Carragher *et al.*, 2002; Honda *et al.*, 2004; Jánossy *et al.*, 2004; Ho *et al.*, 2012; Ma *et al.*, 2011; Kovács & Su, 2014), suspending cancer cell death, and inducing cancer cell survival (Conacci-Sorrell *et al.*, 2014; Gonen *et al.*, 1997; Kubbutat & Vousden, 1997). Calpain inhibition, including inhibition mediated by calpastatin overexpression, however, prevented those processes (section 1.3.5.1). The current study evaluated the role that overexpression of individual calpastatin isoforms plays in regulating breast cancer cell proliferation and clonogenicity, to understand processes involved in regulating breast cancer progression *in vitro*.

5.1.7.1 Calpastatin isoform overexpression and cell proliferation

Growth curve analyses of all transfected cells were performed with the selection medium containing G418 (section 4.3.1.1). The mock-transfected 231Ctrl and T47DCtrl cells proliferated with longer doubling times compared to their respective parental cells (38.41 vs 19.07 hours, $P = 0.0018$ for MDA-MB-231; 41.97 vs 29.53 hours, $P = 0.0822$ for T47D), suggesting possible effects of the empty vector transfection or G418 on the proliferation of the mock-transfected cells. As mentioned in section 5.1.4, G418 has been reported to slow down cell growth and extend doubling time of the transfected CHO 679 cells and BHK 570 cells; metabolism of those cells was also affected by G418

(Yallop & Svendsen, 2001). However, the effect of G418 on cell proliferation may be cell type dependent, and the mechanism still needs to be explained by further studies.

Calpain inhibition following the treatment with 50 µM calpeptin for 24 hours had no effect on the proliferation of MDA-MB-231 and T47D wild type cell lines (section 4.2.1), as well as on the clonogenicity of MDA-MB-231 cells (section 4.3.2.1; ND for T47D). Calpeptin at various concentrations, however, reduced the proliferation of both cells in a time- and dose-dependent manner (section 4.2.1). Upregulation of Type 1 calpastatin unexpectedly accelerated the proliferation of both MDA-MB-231 and T47D cells by shortening the population doubling time from 38.41 to 29.13 hours and from 41.97 to 33.11 hours, respectively (section 4.3.1.1), however, such effect was not statistically significant. In comparison, overexpression of Type 2 in MDA-MB-231 and Type 3 in T47D cells had no effect on cell proliferation. The doubling times of 231CAST2 (35.63 hours) and T47DCAST3 cells (37.09 hours) were similar to that of the respective mock-transfected cells (38.41 and 41.97 hours, respectively).

Generally, calpain activity acts as a positive inducer on cell proliferation, while calpastatin impedes the effect of calpain (section 1.3.5.1). Calpain was found to induce hyperphosphorylation of the retinoblastoma protein (pRb) and increase the level of cell cycle proteins (cyclin-dependent kinase 2, cyclins A, and D), leading to facilitating the progression of transformed cells through the G1 stage of the cell cycle (Carragher *et al.*, 2002). Calpain inhibition by calpastatin overexpression or calpain inhibitors was found to decrease such effect of calpain (Carragher *et al.*, 2002). Jánossy *et al.* (2004) reported calpain as a requirement for promoting the cell cycle at the G1 checkpoint, as well as in the S and G2M phase progression. Honda *et al.* (2004) also stated that calpain was involved in mitosis. Silencing of calpain-2 expression, but not calpain-1, using specific siRNA and/or inhibiting the calpain activity by specific peptidyl calpain inhibitors resulted in abnormal mitosis, which was accompanied by chromosome misalignment. Also, calpain inhibition delayed the prometaphase

and repressed the generation of polar ejection force on chromosomes. Calpain 2 was demonstrated to mediate the proliferation of mammary cancer cells via Akt-FoxO-p27Kip1 signalling pathway (Ho *et al.*, 2012). Knockdown of calpain-2 caused an increase in protein phosphatase 2A (PP2A) level and a reduction in Akt activation, contributing to the activation and nuclear translocation of FoxO3a transcription factor that was associated with the elevated level of cyclin-dependent kinase inhibitor p27Kip1 and a reduction in the breast carcinoma cell proliferation (Ho *et al.*, 2012). Incubation of the pulmonary artery smooth muscle cells (PASMCs) with epidermal growth factor (EGF) and platelet-derived growth factor (PDGF) significantly increased the calpain activity and cell proliferation. The effects of the growth factors could be decreased using specific calpain inhibitor MDL28170 or siRNAs against calpain-1 and -2 (Ma *et al.*, 2011). In murine models of melanoma, calpain inhibition through overexpressing calpastatin in both tumour and transgenic mice diminished tumour growth. Calpastatin overexpression only in B16-F10 melanoma cell also reduced the tumour growth either *in vitro* or *in vivo* but enhanced tumour dissemination through enlarging cell resistance to apoptosis (Raimbourg *et al.*, 2013).

Paradoxically, in some cases, such as in colon carcinoma cells, calpain decreased proliferation and anchorage-independent growth of cancer cells (Benetti *et al.*, 2005) through facilitating the degradation of β-catenin, a substrate of calpain (Li & Iyengar, 2002). In the adult murine models, lack of calpastatin and the consequently increased calpain activity reduced the proliferation of neural stem cells (NSC) in the subgranular zone of the hippocampus (Machado *et al.*, 2015), whereas calpastatin overexpression enhanced the proliferation of such NSC (Machado *et al.*, 2017). In MDA-MB-231-Luc-D3H1 xenograft mouse models of breast cancer, disulfiram-induced calpain activation suppressed tumour growth and lung nodule growth (Kim *et al.*, 2017). In addition, calpain can play a role to cooperate with either caspase-dependent or caspase-independent apoptosis, and the calpain-mediated apoptosis resulted in amplification of cell resistance to cell death (section

1.3.5.1; Chua *et al.*, 2000; Tan *et al.*, 2006 ; Gafni *et al.*, 2009 ; Polster *et al.*, 2005 ; Liu *et al.*, 2009).

Although both 231CAST1 and 231CAST2 clones were observed the increases of calpastatin expression (3.44- and 2.61-fold increase respectively; section 3.3.1) and calpain activity (39.82 and 70.78 % increase respectively; section 4.2.4.1) relative to the mock-transfected control, only calpastatin Type 1 overexpression seemed to show an effect on cell proliferation. This suggested that Type 1 calpastatin might act as a stronger regulator that mediated MDA-MB-231 cell proliferation compared to Type 2 calpastatin. Although the shortened doubling time observed in Type 1-overexpressing cells was an unexpected result, it corresponded to the increased calpain activity detected in the cells. Calpain activity assessment in T47DCAST1 cells should be assessed in future work to investigate whether their shorter doubling time in comparison with the mock-transfected cells is as a result of increased calpain activity or a unique role of calpastatin Type 1.

5.1.7.2 Calpastatin isoform overexpression and clonogenicity

To investigate the role of calpastatin isoform overexpression in breast cancer cells clonogenicity (section 4.3.2.1), transfected MDA-MB-231 models were cultured in the regular medium, without G418, for two days before being used in and during performing the clonogenic survival assays. Thus, G418 was not the factor for any alterations in the clonogenic survival of breast cancer cells. In comparison to parental MDA-MB-231 cells, significant colony inhibition was observed in the mock-transfected 231Ctrl cells (SF = 0.68 ± 0.05, P <0.0001), perhaps indicating that the empty vector is having an effect on cell clonogenecity. In term of plating efficiency, a PE value of the mock-transfected cells was significantly lower than that of the parental cells (PE = 46.85 ± 4.37% vs 69.07 ± 6.74%, P = 0.0009). Such PE of the parental cells was similar to the previous result evaluated by the current group using the same protocol (52.89 ± 13.69; Abdullah, 2019), suggesting the reliability of the present results. However, there was no significant effect of either calpeptin or calpastatin

isoform overexpression on MDA-MB-231 clonogenic survival (SF = 0.99 ± 0.17, 1.04 ± 0.20, and 0.96 ± 0.23 for calpeptin-treated parental cells, 231CAST1, and 231CAST2, respectively). Due to time limitations, T47DCAST1 clone, which was successfully made in the late period of the project, were not assessed for their clonogenic survival by the present project. However, T47DCAST1 clonogenic survival will be studied in the future project of the current group.

Although overexpression of calpastatin Type 1 and Type 2 had no effect on clonogenicity of MDA-MB-231 cells, overexpression of total calpastatin has mostly been reported to impede calpain-mediated clonogenicity in various *in vitro* cell models. In the establishment of Caco-2 cell line overexpressing calpastatin by Potter *et al.* (2003), calpastatin overexpression level was limited (up to 2.5-fold) due to decreased clonogenicity related to increasing calpastatin overexpression. Calpastatin overexpression levels, as low as 2.4-fold, hindered the recovery of the calpastatin-overexpressing Caco-2 clones determined by MTT assay compared with the mock-transfected cells. The Caco-2 cells expressing higher calpastatin levels were nearly absent (Potter *et al.*, 2003). Xu and Mellgren (2002) explored the effect of calpastatin overexpression on the growth of isolated colonies of CHO cell lines and found a decreased growth of the colonies adhering to tissue culture plates (2D) but no different effect on the clonogenicity in soft agar (3D) compared to the mock-transfected cells. Generally, a 3D tissue culture model more closely mimics the native environment in *vivo* and provides better conditions for the cells compared to traditional culture on a 2D surface (Kapałczyńska *et al.*, 2018). The 3D and *in vivo* studies, therefore, are suggested to confirm the role of calpastatin overexpression on colony formation. Calpain inhibition using calpain inhibitors (10 µM ALLN or 30 µM Calpain Inhibitor III) was also found to reduce the clonogenic survival of Kasumi-1 leukemic cells significantly but showed no effect on the clonogenicity of HL-60 leukemic cells (Osman *et al.*, 2009). Conversely, the high level of calpastatin overexpression in MCF-7 breast cancer cells was reported to delay β-lap-mediated apoptosis and showed higher ability to increase clonogenic survival of the cells at the presence of 1.5 µM β-lap

compared to the MCF-7 cells that overexpressed calpastatin at the lower level and the wild-type cells (Tagliarino *et al.*, 2003).

5.1.8 Role of calpastatin isoform overexpression on *in vitro* models of breast cancer LVI (cell migration and endothelial interactions)

Before entering into the lumina of lymphatic or blood vessels, tumour cells detach from the growing tumour mass, followed by invasion and migration through the ECM before adhering to the vascular walls. These phenomena are considered prerequisites for the LVI event (Pantel & Brakenhoff, 2004; Aleskandarany *et al.*, 2015). Calpastatin expression level was found to be negatively associated specifically with LI (Storr *et al.*, 2011b; Storr *et al.*, 2012a), the predominant form of breast cancer LVI (Mohammed *et al.*, 2007; Mohammed *et al.*, 2011). This raised the question if different calpastatin isoforms play a differential role in regulating the LVI-related breast cancer cell phenotypic features. The current study, therefore, assessed the roles of calpastatin Type 1 and Type 2 in regulating breast cancer cell migration by the haptotaxis scratch-wound assay (section 4.4.1.4) and vascular endothelial interactions by static adhesion assay (section 4.4.2.3).

5.1.8.1 Calpastatin isoform overexpression and cell migration

For cell migration assessment, MDA-MB-231 inherently migrated faster than T47D under control conditions. Within 24 hours, scratched wounds of MDA-MB-231 and T47D cell monolayers could be closed by approximately 70-80% and 40-50%, respectively (section 4.4.1.4). The haptotaxis scratch-wound assay was therefore performed over a 24-hour interval for MDA-MB-231 parental and the respective transfected cells or over a 72-hour interval for T47D parental and the respective transfected cells.

Both mock-transfected 231Ctrl and T47DCtrl cells migrated largely slower than their respective parental cells at all investigated time points (2, 4, 6, and 24 hours for MDA-MB-231; 6, 24, 48, and 72 hours for T47D). For instance, at 24-hour post-scratch, wound closures of 231Ctrl or T47DCtrl vs the respective

parental cell lines were 46.37% vs 79.60% (*P* = 0.0004) and 14.18% vs 56.03% (*P* = 0.0002), respectively. As all transfected cells were treated with the non-selective medium two days before being used in the assays and during experimentation, G418 was not the factor interfering cell migration of the transfected cells (supported by section 3.4.2.2). Such data is suggestive of the empty vector reducing the migratory ability of breast cancer cells.

The empty vector was a potential factor causing a reduction in the migration rate of mock-transfected T47DCtrl cells in comparison to the parental cells. Moreover, the current study was considerate of the differential effects of the low-serum culture medium (0.5% DBS), used as a proliferative inhibitor after wound-scratch, on the wound healing of both cells. As described in section 4.4.1.3, by culturing cells in 0.5% DBS culture medium, the numbers of transfected T47DCtrl and T47DCAST1 cells were stable over 72 hours of growth curves analyses. In comparison, parental T47D cells remained to significantly proliferate in the low-serum medium, although at a slower rate compared to being cultured with the regular medium (10% DBS). This suggests that in addition to the effect of the empty vector, the slower wound healing in T47DCtrl cells compared to T47D parental cells might be a result of the low-serum medium significantly inducing the proliferation of the parental cells but lacking the effect on T47DCtrl proliferation.

Unexpectedly and unlike the effect of calpeptin, overexpression of Type 1 in both MDA-MB-231 and T47D cells, as well as Type 2 in MDA-MB-231 cells, increased cell migration. In comparison, calpeptin significantly inhibited migration of either parental or mock-transfected MDA-MB-231 cells (18.02 and 21.50 % inhibition, respectively, at 24-hour post-scratch; section 4.5.1.5). Although significant downregulation of calpain activity was detected by the t-boc assay following calpeptin treatment (section 4.2.2), calpeptin could not induce any alteration to the migration of either parental or mock-transfected T47D cells. As the 24-hour treatment with 50 µM calpeptin did not have any effect on cell proliferation in MDA-MB-231 and T47D (section 4.2.1), the

changes in cell migration influenced by such agent were not a result of different cell proliferation rates between the experimental and no-treatment groups. Calpastatin Type 1 overexpression significantly induced the migration of both 231CAST1 and T47DCAST1 cells at all investigated time points. For instance, at 24 hours post-wounding, both cells migrated significantly faster relative to their respective mock-transfected controls by 42.61% for 231CAST1 cells, and 93.30% for T47DCAST1 cells. Type 2-overexpressing 231CAST2 also seemed to have higher migratory activity relative to the mock-transfected cells at all time-point, but a significant effect of Type 2 overexpression was only observed at 2 hours after producing wound (37.44% increase) (section 4.4.1.4).

Conventional calpain-1 and -2, generally, have been positively implicated in regulating cell motility by several mechanisms, including destabilising cell adhesion to ECM, promoting rear detachment, cell spreading, membrane protrusion, chemotaxis, and adhesion complex turnover. Calpains regulate such processes through their proteolytic substrates, including components of adhesion complex and migration-related proteins (section 1.3.5.2). Calpain inhibition, by calpastatin upregulation, pharmacological calpain inhibitors (e.g., calpeptin) or genetic disruption of calpain, can prevent the calpain-mediated cleavage of substrates related to cell migration, leading to the inhibition of *in vitro* or *in vivo* migration of various cell types, including breast cancer MDA-MB-231 and MCF-7 cells (Rodriguez-Fernandez *et al.*, 2016). For instance, calpain inhibitors I and II altered the amount of integrin receptor that detached from the cell and remained on the substratum at the rear of the CHO cells during migration, resulting in stabilising cytoskeletal linkages and reducing the rate of rear cell detachment and cell migration (Huttenlocher *et al.*, 1997). Also, the CHO cells expressing low calpain-1 level showed the reduced migration rates and the altered morphology (Huttenlocher *et al.*, 1997). Potter *et al.* (1998) revealed that wild-type NIH-3T3 fibroblasts extended lamellae within 30 minutes after plating, and the spreading of the cells on culture plates could be inhibited by calpastatin overexpression and treatment with calpain inhibitors (calpeptin and MDL 28, 170). In addition, fibroblast cells overexpressing

calpastatin encoded by a full-length cDNA lacking only exon 3 were unable to assemble actin-rich processes and presented a decrease in calpain activity, causing an increase of the ERM protein ezrin but not radixin and moesin (Potter *et al.*, 1998). Calpastatin-overexpressing myoblasts could not migrate due to their rounded morphology, loss of membrane extensions, and disorganisation of stress fibres, leading to a significant defect in new adhesion formation. Myristoylated alanine-rich C kinase substrate (MARCKS) level was accumulated in the myoblast cells having a decreased calpain activity, suggesting that calpain is involved with either migration or adhesion of myoblast cells through regulating this actin-binding protein (Dedieu *et al.*, 2004). Calpastatin overexpression also caused a reduction of neuroblast migration in the dentate gyrus (DG) of the hippocampus in adult murine models (Machado et al., 2017), while the absence of calpastatin and the consequently increased calpain activity resulted in the opposing outcome (Machado *et al.*, 2015).

In breast cancer, as defined in section 1.3.5.2, a growing body of evidence indicates the roles of calpain in regulating breast tumour cell migration and invasion through a variety of pathways, contributing to disease progression and metastasis. In a similar vein, calpain inhibition either by overexpressing calpastatin, silencing calpain expression or using inhibitors has provided evidence to support that the calpain/calpastatin system is a potential target for anti-metastasis therapy. For instance, Rodriguez-Fernandez *et al.* (2016) showed that calpain is a potential target in regulating disease progression and metastasis of breast cancer. Calpain inhibitors (calpeptin, calpain inhibitor VI, and ALLN) suppressed calpain 1-, and calpain 2-mediated cleavage of lactating mammary gland adhesion proteins (E-cadherin, β-catenin, δ-catenin, and talin-1), indicating that both proteases could precisely recognise and cleave adhesion proteins from mammary gland epithelia. Knockdown of calpain-1 significantly suppressed calpain-mediated cleavage of those adhesion proteins and reduced the migration ability of MCF-7 and MDA-MB-231 breast cancer cell lines (Rodriguez-Fernandez *et al.*, 2016). However, a previous study of the current group showed that knockdown of calpastatin had no significant effect on MDA-

MB-231 and MCF-7 cell migration either with or without the treatment of A23187 calcium ionophore (Pu, 2016).

As defined, the role of Type 1 and Type 2 calpastatin overexpression in increasing breast cancer cell migration was an unexpected finding since most reports show that calpastatin overexpression is much more likely to reduce calpain-associated cell migration. However, there are studies reporting the opposing role of calpain inhibition in cell migration and cancer metastasis. Raimbourg *et al.* (2013) showed a contradictory role of the calpain-calpastatin system to what has been published before in metastatic dissemination in a murine model of melanoma. Calpain inhibition through overexpressing calpastatin in both tumour and host impeded tumour growth but paradoxically increased metastatic dissemination to regional lymph nodes. Calpastatin overexpression in B16-F10 melanoma cell line also reduced the tumour growth both *in vitro* and *in vivo* but enhanced tumour dissemination through increasing cell resistance to apoptosis and accelerating migration. Besides, calpastatin transgene expression restricted to host cells decreased immune cell infiltration in the tumour as well as angiogenesis required for antitumor immunity, allowing tumour cells to escape tumour niche and disseminate (Raimbourg *et al.*, 2013). Lokuta *et al.* (2003) also reported the negative regulatory effect of calpain activity on cell migration; calpain inhibition in neutrophil caused increased cell polarisation, rapid chemokinesis in the absence of exogenous activators, and altered morphology. High calpain activity detected in resting neutrophils was assumed to repress neutrophil adhesion and migration as well as to maintain their unstimulated spherical morphology (Lokuta *et al.*, 2003). Raimbourg *et al.* (2013) hypothesised that cells exhibiting high calpain activity may have low focal adhesion dynamics since focal adhesion components are targets for calpains; inhibition of calpain activity, therefore, support migration. Furthermore, as mentioned in section 1.3.5.2, cell migration requires a subtle balance between cellular focal adhesions and detachment from the ECM, both of which can be regulated by calpain activity. Calpain-dependent proteolysis of paxillin, for example, has been shown to generate proteolytic fragment, called

paxillin delta, which functioned as a paxillin antagonist. Paxillin delta was found to negatively regulate focal adhesion dynamics by reducing focal adhesion disassembly and decrease migration in HeLa and HEK 293 cell lines (Cortesio *et al.*, 2011). Kim *et al.* (2017) reported that disulfiram/Cu-induced calpain activation in MDA-MB-231 cells could cause the degradation of focal adhesion molecules (talin and vimentin), the collapse of vimentin filaments, and eventually the reduction of cell migration and invasion.

Although the inductive effect of calpastatin Type 1- or Type 2-overexpression on the migration of 231CAST1 or 231CAST2 cells, respectively, was contradictive to the inhibitory effect of calpain inhibition reported in most published studies, the increased migration ability corresponded to the increased calpain activity detected in both cells (section 4.2.4.1). Zhang (2018) stated that ovarian cancer cell lines, including SKOV3, PEO1 and PEO4 ranked from high to low, seemed to show a positive linear correlation between calpain activity level and migratory ability, similar to what was reported in non-tumour human myoblasts cells and rhabdomyosarcoma cells (Roumes *et al.*, 2010). In the current study, the migration ability of the basal-like cell clones from high to low was 231CAST1, 231CAST2 and mock-transfected 231Ctrl (section 4.4.1.4), while ranking 231CAST2, 231CAST1, and 231Ctrl clones from high to low calpain activity levels (section 4.2.4.1). Between 231CAST1 and 231CAST2, however, their calpain activity (39.82 vs 70.78 % relative increase) and ability to migrate (42.61 vs 18.16 %relative increase) were not statistically different. The presumption that the increased migration activities of calpastatin isoform 1- or 2-overexpressing breast cancer cells might be due to the increased calpain activity or the specific property of each isoform on cell migration had no firm supportive information obtained from the present study. Therefore, in a future study conducted by the current group, calpain activity assessments in T47DCAS1 clone should be considerate. Monoclonal T47DCAST2 clone is also suggested to be completely established and used to prove the presumption, mentioned above.

5.1.8.2 Calpastatin isoform overexpression and endothelial interactions

To our knowledge, this is the first report whereby the role of the calpain-calpastatin system on tumour cell-endothelial interactions was verified. Static adhesion assays revealed that the mock-transfected 231Ctrl cells (P = 0.0171) showed significantly preferential adhesion towards BECs (i.e., hMEC-1) as opposed to LECs (i.e., hTERT-LEC). Such preferential adhesion of tumour cells has also been previously reported in MDA-MB-231 and MCF-7 breast cancer cells by the studies of the current group (Safuan, 2012; Safuan *et al.*, 2012; Ahmad, 2016). Although the *in vitro* studies seemed to suggest that BVI was a preference for breast cancer cells, the IHC study of the current group has demonstrated that LI (96%), detected by D2-40, is a predominant form of breast cancer LVI (Mohammed *et al.*, 2007; Mohammed *et al.*, 2011). However, evidence to explain the preference of LI in breast cancer remains sparse. The anatomical and physiological properties of lymphatic vessels, which promote LI over BVI, have been described in section 1.2.2. More active processes inducing tumour cells to interact with LECs and enter the lumen of lymphatic capillaries have been suggested, such as the cellular cross-talk involving a large number of molecules, including macrophage and associated cytokines, as well as chemokine gradients (section 1.2.3.2.2).

The data obtained from the current study is suggestive of the empty vector affecting MDA-MB-231 cell adhesion to LECs. The percentage adhesion ability to hTERT-LEC of the mock-transfected 231Ctrl cells was significantly lower relative to parental cell line (P = 0.0025), but not different in adhesion to hMEC-1 cells. Although there was a difference of adhesion ability between the mock-transfected 231Ctrl and parental MDA-MB-231 cells, the role of calpastatin isoform overexpression on endothelial interactions was interpreted from the adhesion ability of breast cancer cells overexpressing calpastatin isoforms relative to that of the mock-transfected 231Ctrl cells.

Type 1 and Type 2 calpastatin seemed to have differential roles in regulating tumour cell-endothelial interactions (section 4.4.2.3). Type 2 overexpression

preferentially reduced the adhesiveness of MDA-MB-231 cells to hMEC-1 cells (49.80% inhibition, *P* = 0.0232) as opposed to hTERT-LEC cells (9.20% inhibition, *P* = 0.7846), consistent with the effect of calpain inhibition by calpeptin to the mock-transfected cell adhesion (32.21% inhibition, *P* = 0.0244 to hMEC-1; 6.17% inhibition, *P* = 0.9307 to hTERT-LEC). Conversely, Type 1 overexpression played a different role by preferentially causing an increased affinity of the tumour cells to the hTERT-LEC cells (41.47% induction, *P* = 0.0080) rather than to hMEC-1 cells (8.91% induction, *P* = 0.9522). Although an increase of calpain activity was detected in both 231CAST1 and 231CAST2 cells, they had opposing roles in tumour cell adhesion to ECs and different preferences on the type of ECs to interact with, suggesting a unique effect of each calpastatin Type 1 and Type 2 on tumour cell-endothelial interactions. Differential subcellular localisation between both isoforms may be involved with their opposing roles in regulating tumour cell adhesion.

The number of studies showing the implication of calpain on cell-endothelial interactions is limited, and calpain activity has been found to positively regulate such processes. In a genetic Zucker rat model of type 2 diabetes, proteolytic activity of μ-calpain was increased in parallel with the increased expression of vascular cell adhesion molecule-1 (VCAM-1) and intracellular adhesion molecule-1 (ICAM-1) (Stalker *et al.*, 2005). Leukocyte-mesenteric endothelial interactions and such increased expression of those two cell adhesion molecules could be suppressed by calpain inhibition using benzyloxycarbonyl-leucyl-leucinal (ZLLal) (Stalker *et al.*, 2005). Also, calpain has been discovered to enhance leukocyte cell-endothelial interaction through angiotensin II (Ang II) type 1 receptor (AT(1)R) signalling (Scalia *et al.*, 2011). Ang II-induced calpain activation can cause endothelial dysfunction with disruption of the EC barrier and increased leukocyte-blood vessel endothelial interactions in both *in vivo* studies with mesenteric postcapillary venules and *ex vivo* studies with aortas of murine models. While leukocyte adhesion was hindered by the calpain inhibitor ZLLal, the study has verified that calpain-expressed endothelium rather than leukocyte-expressed calpain was the target of Ang II (Scalia *et al.*, 2011).

Collectively, higher calpain-expressing LECs or BECs may lead to a higher possibility of lymphatic or blood vessel invasion, respectively, through Ang II/AT1R signalling and an increased level of cell adhesion molecules.

However, calpain activation is also associated with suppression of cell-cell or cell-ECM interactions, but calpain inhibition stabilises cell adhesion (section 1.3.5.2). For the role of calpain activity in cell-cell adhesion, knockdown of calpain-1 significantly suppressed calpain-mediated cleavage of the lactating mammary gland proteins (E-cadherin, β-catenin, and δ-catenin) and reduced disruption of cell adhesion in MCF-7 and MDA-MB-231 breast cancer cells (Rodriguez-Fernandez *et al.*, 2016). By calpain activation, integrins, which are heterodimeric cell-surface receptors and fundamental in cell-cell and cell-matrix adhesion, could be negatively regulated their functions in mediating adhesion, signalling, and cytoskeleton association during apoptosis of human umbilical vein ECs (Meredith *et al.*, 1998). Calpain can also shift the functional outcome of integrin signalling from cell spreading to retraction in CHO cells by mediating cleavage of integrin β3 subunit at C-terminal Tyr(759) (Flevaris *et al.*, 2007). Calpain-mediated disassembly of focal adhesions results in a reduction in the strength of cell adhesion to ECM (section 1.3.5.2). In primary chicken embryo fibroblasts (CEF), calpain-dependent proteolysis of FAK was observed accompanied by v-Src-induced disassembly of focal adhesions. Calpain inhibitors I and II, however, suppressed v-Src-induced focal adhesion disruption, loss of substrate adhesion, and cell migration (Carragher *et al.*, 2001). In CHO cell line, calpain inhibition using calpain inhibitors I and II have been shown to specifically stabilise peripheral focal adhesion, decrease the rate of cell detachment, increase cell adhesiveness, and modify the fate of integrin receptors at the rear of the cell during migration (Huttenlocher *et al.*, 1997). In neutrophil, calpain inhibition increased cell adhesion, polarisation, chemokinesis in an absence of exogenous activators and altered neutrophil morphology. High calpain activity with μ-calpain being the predominant active isoform detected in resting neutrophils may act as a negative regulator of

neutrophil adhesion, protrusion, and migration and may also function to maintain their unstimulated spherical morphology (Lokuta *et al.*, 2003).

The effect of calpastatin Type 1 overexpression in enhancing cell adhesion to ECs as observed in MDA-MB-231 cells could not be assessed in the T47D luminal A cell model by the same experimental design. With extending the adhesion period of the assay from 35 minutes, as used in the experiment of MDA-MB-231 cells, to 20 hours, T47D parental cells did not firmly adhere to both hMEC-1 and hTERT-LEC monolayers (section 4.4.2.3). Almost entirely adhered T47D cells detached from EC monolayers after the washing step. Together with results from scratch-wound assays, T47D cells had a relatively lower migration ability, as opposed to MDA-MB-231 cells; at a 24-hour time point, MDA-MB-231 and T47D cells migrated under the same condition (10 µg/mL mitomycin C in complete medium) to cover approximately 80% and 35%, respectively, of the cell-free area (section 4.4.1.2.3). These findings suggest lower abilities of the luminal cells in LVI and metastasis, in comparison with the basal-like triple-negative cells. Consistent with previous studies of the current group, MCF-7 luminal A breast cancer cells showed lower affinities to both hMEC-1 and hTERT-LEC models compared to the basal-like triple-negative MDA-MB-231 cells (Safuan, 2012; Safuan *et al.*, 2012, and Ahmad, 2016). The cohort study of invasive breast cancer patients, however, showed no statistic difference of the prevalence of LI, detected by D2-40, amongst all four main subtypes, including triple-negative (22.5%), luminal A (20.9%), luminal B (27.7%), and HER2-enriched cases (31.7%) (He *et al.*, 2017).

5.1.9 Effects of A23187 calcium ionophore on calpain activity and phenotypic characteristics

Efficient control of intracellular Ca^{2+} concentration is critical for mediating fundamental cell physiology, including cell cycle, proliferation, apoptosis, motility and invasion (Cui *et al.*, 2017), via regulating calpains (Croall and DeMartino 1991; Ono and Sorimachi 2012; Cui *et al.*, 2017), and other intracellular downstream effectors, such as calmodulin (CaM), calmodulin-

dependent protein kinase II (CaMKII), nuclear factor of activated T-cells (NFAT), and NF-κB (Farfariello *et al.*, 2015; Cui *et al.*, 2017). In the calpain-calpastatin system, Ca^{2+} flux plays a significant role in both activating calpain and enhancing calpastatin inhibition of calpains, suggesting that calpastatin might attenuate activated calpains, rather than prevent activation (Wells & Leloup, 2010). A23187 calcium ionophore, used in the current study, has been reported to enormously enhance a Ca^{2+} influx into MCF-7 breast cancer cells after being exposed to 0.01-10 µM A23187 for 24 hours (Journé *et al.*, 2004). A23187 promotes the release of intracellular Ca^{2+} stores and the influx of extracellular Ca^{2+} (Mtango *et al.*, 2008), before subsequently increasing calpain activity.

A23187 has demonstrated the inductive effect on calpain activity in a variety of cell types. In SH-SY5Y neuroblastoma cells, cleavage of caspase-7 and -9, the direct substrates of calpains, was activated by pre-incubation with 1 µM A23187 for 5, 10, and 30 minutes but inhibited by 5 µM calpain inhibitor II (Chua *et al.*, 2000). Exposure of human T lymphocyte Jurkat cells to 1 µM A23187 for 0.5, 1, 2 or 3 hours induced calpain-dependent cleavage of cain/cabin1 during apoptosis as well as Rhodamine-110-based substrate. Such A23187-induced calpain activities could be suppressed by calpeptin and zLLY calpain inhibitors (Kim *et al.*, 2002). Heterodimeric calpains, for another example, in erythrocytes could be rapidly activated by 3 µM A23187 (Molinari *et al.*, 1994). In breast cancer cells, calpain activity in MDA-MB-231 cells could be enhanced after 30 minutes of exposure to 0.1 µM (10% increase detected by t-Boc assay) and 2 µM A23187 (94% increase detected by Suc-LLVY-AMC assay) (Pu, 2016). In the current study, by using t-Boc assay, calpain activity in MDA-MB-231 cells pre-treated with 2 µM A23187 for 30 minutes was enhanced by approximately 10%, which could be normalised towards the basal level after exposure to 50 µM calpeptin for another 30 minutes. In comparison, 0.5 µM A23187 treatment for 24 hours exhibited the higher inductive effect on calpain activity by increasing 58% calpain activity, which was attenuated to 28% by a 30-minute treatment of calpeptin (section 4.2.3). Although the prolonged treatment of 0.5 µM A23187 for 24 hours contributed to the largely increased calpain activity in

parental cells (58% increase), no similar effect on the activity was observed in 231Ctrl mock-transfected cells (section 4.2.4.2). This might be an impact of the empty vector on calpain activity. For calpastatin-overexpressing cells, A23187 seemed to enhance calpain activity in both 231CAST1 (35.39% increase) and 231CAST2 cell lines (10.12% increase) (section 4.2.4.2).

With limited upregulation of calpain activity explored by the t-Boc assay in the transfected 231CAST1, 231CAST2 and 231Ctrl cell lines by the 24-hour treatment with 0.5 µM A23187 (section 4.2.4.2), no significant alteration to proliferation (section 4.3.1.2), clonogenic survival (section 4.3.2.2), and migration was observed (section 4.4.1.5). Consistently, such unchanged phenotypic features also appeared in MDA-MB-231 parental cells although upregulated calpain activity by A23187 was evidently detected (section 4.2.3). However, A23187 at a higher concentration (1 µM) or prolonged treatment (>24 hours) significantly inhibit proliferation and colony formation in all MDA-MB-231 cell clones (sections 4.3.1.2 and 4.3.2.2).

An increase in intracellular Ca^{2+} has been reported in either suppressing or enhancing cell proliferation through regulating calpain activity or other pathways. For instance, in LNCaP prostate cancer cells, increased intracellular Ca^{2+} using A23187 was found to enhance the degradation of androgen receptor (AR) (Pelley *et al.*, 2006), a substrate of calpain (Libertini *et al.*, 2007). Such A23187-mediated degradation of AR has been found to be associated with either activating or suppressing cell proliferation in prostate cancer *in vitro* and *in vivo* (Yang *et al.*, 2016). In human myelo-erythroid CD34+ leukaemia cells (TF-1), increased intracellular calcium levels was found to induce cell survival and proliferation through the activation of the MAPK pathway. Moderate elevation of Ca^{2+} concentration by cyclopiasonic acid protected TF1 cells from apoptosis, whereas a higher, but transiently, increased Ca^{2+} level by ionomycin enhanced cell proliferation. In both cases, caspase-3 activity was attenuated, and Bcl-2 was up-regulated. The higher elevation of Ca^{2+} by ionomycin induced MEK-dependent biphasic ERK1/2 activation, leading to transferring the cells from

G0/G1 to S/M phases (Apáti *et al.*, 2003). However, Hipfner and Cohen (2004) stated that signals that trigger cell proliferation also could trigger programmed cell death. In the case of Ca^{2+}, when the alteration of intracellular Ca^{2+} level exceeds the normal spatial and temporal boundaries, Ca^{2+} is able to contribute to cell death through both necrosis and apoptosis (Berridge *et al.*, 2000).

The anti-proliferative effect of A23187 in MDA-MB-231 clones at the higher concentration (1 µM) and the prolonged treatment (> 24 hours; section 4.3.1.2) might be a consequence of calcium alteration exceeding the normal spatial and temporal variation of cellular Ca^{2+} levels or the ability of A23187 in inducing cell apoptosis through enhancing calpain activity or other factors, such as calmodulin, NFAT, and NF-κB (Cui et al., 2017). Calpain activity is involved with both caspase-dependent/independent apoptosis (section 1.3.5.1) and can be induced by A23187, other calcium ionophores or calcium influx in various cancer cells, such as pheochromocytorna PC12 (Ray *et al.*, 2000), intestinal CaCo-2 (Chakrabarti & McClane, 2005), hepatocellular carcinoma HCC (Shi, Zhang et al. 2013), large cell lung carcinoma LCLC 103H (Gil-Parrado *et al.*, 2002), hepatic stellate (HSCs) (Li, Yan et al. 2018), breast cancer MDA-MB-231 and MCF-7 cell lines, and xenograft mouse models of breast cancer (Sareen *et al.*, 2007). A23187 may also decrease the clonogenicity of the MDA-MB-231 clones (section 4.3.2.2) through enhancing calpain-mediated apoptosis. However, Vara-Ciruelos and co-workers revealed that pre-treatment with 10 µM A23187 for 6 hours exhibited a protective effect against etoposide (100 and 250 nM) in impeding clonogenic survival of HeLa human cervical cancer and G361 human Caucasian malignant melanoma cells (Vara-Ciruelos *et al.*, 2018).

Without a statistic significance, migration of 231CAST1 cells seemed to be increased by A23187 (from 66.13 to 75.08 %wound closure, $P = 0.1598$ at 24 hours post-scratch), indicating an effect of A23187-mediated calpain activity on cell migration (section 4.4.1.5). By contrast, a significant reduction of cell migration was observed in A23187-treated T47D parental cells at 72 hours post-scratch (from 95.85 to 87.61 %wound closure, $P = 0.0186$, section 4.4.1.5). The

study in ovarian cancer cells by Zhang (2018) also found that A23187 significantly contributed to increased calpain activity detected by the t-Boc assay and the inhibition of SKOV3 cell migration detected by the scratch-wound assay. The reduced migratory ability of A23187-treated cells might be due to the Ca^{2+}-inducing effect of A23187 in inducing calpain-mediated proteolysis of adhesion complex components and migration-related proteins, such as paxillin (Cortesio *et al.*, 2011) or talin and vimentin (Kim *et al.*, 2017), which subsequently cause a suppression of cell migration, as discussed in section 5.1.8.1. Elevated Ca^{2+} induced by A23187 may also downregulate tumour cell migration through other pathways, such as calcineurin-mediated signalling in cell chemotaxis to type IV collagen, as observed in A2058 human melanoma cells (Hodgson & Dong, 2001). Moreover, it is possible that A23187-induced Ca^{2+} concentrations can initiate cell death through necrosis or apoptosis (Berridge *et al.*, 2000). Apoptosis could be induced by A23187 or initiated spontaneously to maintain the homeostatic cellular balance (Gavrilescu & Denkers, 2003). Amongst all T47D cell clones, parental cells were the only type of cells remaining proliferative in 0.5% DBS medium, used in inhibiting cell proliferation post-scratch, throughout 72 hours of experimentation (section 4.4.1.3). Thus, apoptosis might be responsible for overgrowth of the wild type cells at the 72-hour time point, leading to a reduction of cell migration.

Amongst all phenotypic endpoints assessed in all MDA-MB-231 clones, treatment with A23187 at 0.5 µM for 24 hours only significantly affected tumour cell-BEC interactions (section 4.4.2.4), suggesting that tumour adhesion to BECs might be relatively more sensitive to the effect of Ca^{2+} influx compared to the other phenotypic characteristics investigated in the current project. Although overexpression of calpastatin Type 1 and Type 2 seemed to have contradictory roles on MDA-MB-231 cell adhesion to both hMEC-1 and hTERT-LEC models (i.e., inductive and suppressive, respectively), A23187 was able to significantly suppress the interactions between either 231CAST1 or 231CAST2 and the hMEC-1 models but did not cause any significant alteration on the adhesion to hTERT-LEC cells (section 4.4.2.4). With a potential to induce calpain

activity detected by t-Boc assay (section 4.2.4.2), A23187 significantly reduced the adhesion to hMEC-1 cells in 231CAST1 and 231CAST2 (57.17 and 87.14 %inhibition, respectively). Although there was no statistical significance, LEC interactions were reduced by A23187 in 231CAST1 cells (27.79% inhibition) but increased in 231CAST2 cells (5.25% induction). A23187 or increased cytosolic Ca^{2+} have been reported to either increase or decrease cell adhesion, as will be discussed further. Although A23187-upregulated calpain activity in 231Ctrl mock-transfected cells seemed not to be detected by the t-Boc assay, A23187 significantly suppressed 231Ctrl cell adhesion to hMEC-1 cells (35.42% inhibition) but seemingly increased the adherence to the hTERT-LEC model (9.78% induction). These findings suggest that A23187 might regulate 231Ctrl cell adhesion through other pathways, as discussed further below, rather than via controlling the calpain system.

A23187, generally, has been reported to induce tumour-endothelial cell interactions through influencing pro-adhesive molecules, which are lipoxygenase products of arachidonic acid (AA) metabolism. Treatment of human umbilical vein ECs (HUVECs) and bovine aortic ECs (BAECs) with inflammatory stimuli, including A23187, significantly increased the numbers of MCF-7 breast cancer cells and JEG-3 choriocarcinoma cells adherent to the ECs compared to GH-3 non-metastatic pituitary cell. Upon stimulation, while GH-3 cells preferentially generated prostaglandins, MCF-7 and JEG-3 carcinoma cells produced lipoxygenase products (LTB4 and 5-HETE). The lipoxygenase inhibitor nordihydroguiaretic acid partially inhibited adhesion of MCF-7 and JEG-3 to ECs, suggesting that lipoxygenase products of AA play a role in tumour-EC interaction and metastasis (Damtew & Spagnuolo, 1997). Increasing cytosolic Ca^{2+} by oxidised low-density lipoprotein (LDL) or A23187 induced a phosphatidylserine-dependent adhesion of Jurkat T cells to HUVECs (Qu *et al.*, 2000). Although to our knowledge, there is no publication showing the effect of A23187 on calpain-mediated endothelial interactions, A23187 may increase the interactions through influencing calpain activity, as calpain activity has been found to positively regulate such processes (discussed in section 5.1.8.2).

A23187 also dramatically enhanced AA-mediated adhesion of metastatic human breast carcinoma MDA-MB-435 cells to various ECM protein substrates, such as vitronectin and type IV collagen (Palmantier *et al.*, 1996; Kennett *et al.*, 2004). AA-mediated adhesion of MDA-MB-435 cells to collagen type IV depended on the PKC pathways and was associated with the translocation of PKCμ from the cytoplasm to the membrane (Kennett *et al.*, 2004). As PKC is a substrate for μ-calpain- and m-calpain-mediated cleavage to produce a catalytically active PKC fragment (Mikawa, 1990), inhibition of calpain activity by calpeptin or MDL-28170 has been shown to repressed the production of the truncated PKCμ and attenuated the increased AA-mediated adhesion of the breast cancer cells (Kennett *et al.*, 2004). These studies revealed the evidence for calpain cleavage of a non-structural protein causing an increase of tumour cell adhesion. Treatment with A23187 also enabled the rapid induction of integrin-dependent T cell adhesion to three distinct ligands: the ECM protein fibronectin, and the cell surface molecules VCAM-1 and ICAM-1 (Shimizu *et al.*, 1992). Moreover, the calcium-sensing receptor (CaSR), a family C G protein-coupled receptor, that can be activated by raising the levels of extracellular divalent cations, has been reported to promote cell adhesion and migration through coupling to members of the integrin family of ECM-binding proteins in medullary thyroid carcinoma cells (Tharmalingam *et al.*, 2011).

Although the effects of A23187 or increased cytosolic Ca^{2+} mostly have been described to increase cell adhesion, the effects of A23187 in suppressing the interactions previously observed between tumour cells and the EC models (section 4.4.2.4) might be due to an increase in calpain-mediated cell detachment (discussed in section 5.1.8.2) through A23187-induced calcium ion influx. For instance, the ion channel kinase TRPM7 was reported to be implicated in focal adhesion disassembly and cell detachment through regulating m-calpain activity by mediating the local influx of Ca^{2+} into peripheral adhesion complexes. While silencing of TRPM7 by siRNA strengthened cell adhesiveness and elevated the number of peripheral adhesion complexes in HEK 293 cells, knockdown of m-calpain prevented TRPM7-induced cell

rounding and loss of cell adhesion (Su *et al.*, 2006). In addition, the observed decrease in the adhesive ability of transfected MDA-MB-231 cells to ECs might be a result of A23187-induced apoptosis, as mentioned previously that calcium ionophores (i.e., A23187) or calcium influx were able to induce apoptosis through regulating calpain activity or different pathways. There are publications illuminating the association between apoptosis and loss of cell adhesion. Loss of cell–ECM adhesion or unligated integrin leads to activation of anoikis, a form of apoptosis, which is an important mechanism for preventing detached cells surviving in inappropriate places and growing dysplastically (Suzanne & Steller, 2009), through both major signalling routes for cell death, i.e., the intrinsic (mitochondria) and extrinsic (death receptor) pathways (Zhong & Rescorla, 2012). For instance, in hepatocellular carcinoma cells, the reduction of adhesion signal molecules (i.e., FAK, ILK, PKB, and β-catenin) has been found to induce apoptosis (Su *et al.*, 2005). Whereas alterations in cell adhesion are known to regulate caspases, they are also able to regulate cell adhesion (Suzanne & Steller, 2009). Disassembly of adherens junctions during apoptosis in Drosophila has been found to be progressive and require the amino-terminal cleavage of the β-catenin Armadillo, a major regulator of cadherin-mediated adhesion, by the apoptotic effector caspase DrICE (Kessler & Muller, 2009; Suzanne & Steller, 2009).

As treatment with 0.5 µM A23187 for 24 hours had no effect on the proliferation (section 4.3.1.2) and clonogenic survival (section 4.3.2.2) of all transfected MDA-MB-231 clones, their decreased adhesive ability towards ECs was not a result of the cytotoxicity of such treatment.

5.2 Limitations and suggestions for future work

5.2.1 Cell lines, other models and related phenotypic assays

Breast cancer is a complex and heterogeneous disease with multiple distinctive characteristics, different morphological features and clinical behaviours (Badve *et al.*, 2011). Molecular stratification based on protein or gene expression profiling allows breast cancers to be subdivided into several distinct subtypes.

Five common intrinsic subtypes (luminal A and B, HER2-enriched, basal-like, and normal-like), however, are typically considered for differentially planning breast cancer management, assessing prognosis, and predicting patient outcomes (Perou *et al.*, 2000; Sorlie *et al.*, 2001; Sotiriou *et al.*, 2003; Desmedt *et al.*, 2009; Russnes *et al.*, 2017). In the *in vitro* settings, the current study found that calpastatin Type 1 and Type 2 potentially play a role in regulating cellular functions related to breast cancer progression and LVI. However, this is mainly generated from only one cell representative of basal-like breast cancer (MDA-MB-231) and partly in one cell representative of luminal A subtype (T47D). It would be insightful to explore the full differential functions of all calpastatin Type 1, Type 2 and Type 3, encoded by exon3-containing cDNA, in regulating breast cancer progression and LVI of both MDA-MB-231 and T47D lines, as well as other cell models. Further study, therefore, is required to confirm the role of calpastatin Type 1 and Type 2 as regulators of cancer progression and LVI in more representative cell lines of various breast cancer subtypes, i.e., luminal A (e.g., MCF-7 and BT483), luminal–B (e.g., BT474 and UACC812), HER2-enriched (e.g., JIMT-1 and SKBR3), and basal-like (e.g., MDA-MB-468 and SUM149). Moreover, it would be useful to confirm how calpastatin Type 1 and Type 2 modulate calpain activity and the phenotypic endpoints by the specific knockdown of Type 1 or Type 2 using shRNA or CRISPR-Cas9, or knockdown of the basal calpastatin expression followed by upregulation of each calpastatin isoform in breast cancer cell lines. For future breast cancer research, IHC or *in vivo* xenograft studies are suggested, to examine the association between calpastatin Type 1 or Type 2 and pathological variations related to breast cancer LVI, progression, or metastasis. In addition, it is interesting to investigate whether calpastatin isoforms retain their unique subcellular localisation in cell line-derived xenograft murine models and human breast cancer tissues.

All the *in vitro* investigations in the current study were performed in a two-dimensional (2D) model, which does not adequately mimic the *in vivo* microenvironment (Huh *et al.*, 2011). Although the traditional 2D cell culture

has been demonstrated to be a valuable technique for cell-based studies to improve our understanding of cell biology, tissue morphology, mechanisms of diseases, protein production, the development of tissue engineering, and drug action, limitations of 2D models have been increasingly recognised. In focusing on drug discovery and cell-based biosensors, 2D cell culture examinations sometimes deliver nonpredictive and misleading information for *in vivo* responses (Birgersdotter *et al.*, 2005; Weaver *et al.*, 1997; Bhadriraju & Chen, 2002), and only 10% of the compounds successfully progress through clinical development (Edmondson *et al.*, 2014). To provide more physiologically-relevant data and more predictive/promising information for *in vivo* studies, growing cells as three-dimensional (3D) models, consisting of cell aggregates/spheroids within/on a biologically derived matrix (e.g., matrigel, collagen and hyaluronic acid), is more reflective to their existence *in vivo* (Edmondson *et al.*, 2014; Kapałczyńska *et al.*, 2018) and being feasibly co-cultured with other cell types (Breslin & O'Driscoll, 2013). Cellular components naturally occurring in 3D models' microenvironment may be more likely to translate into clinical outcomes (Breslin & O'Driscoll, 2013). As noted in the literature, 3D models altered cell proliferation, adhesion, invasion and the related protein expression in comparison to 2D models and could resemble the *in vivo* structural and oxygen conditions, as well as the gradients of immune factor, growth factor, and cytokine of the tumour microenvironment (Weaver *et al.*, 1997; Fuller & Howell, 2014). Thus, it would be of interest to additionally determine if the overexpression of calpastatin Type 1, Type 2 or Type 3 act as key players in regulating breast cancer cells to grow, form colonies, migrate, and adhere to ECs in 3D or co-culture models.

All data of cell motilities obtained from the current project was based on static assays. It, therefore, would be worthy to investigate the effect of calpastatin isoforms on tumour cell migration, and tumour cell-endothelial interactions under the presence of dynamic flow, as the flow-based assays are more reflective of the environment of the *in vivo* processes (Florey & Haskard, 2007; Shetty *et al.*, 2014). Furthermore, the role that calpastatin isoforms play in

modulating tumour cell invasion, another crucial cellular function involved in LVI, assessed either with 2D or 3D models and with/without flow could also be carried out.

5.2.2 Regulation of calpain activity

Calpain activity is strictly regulated by calcium and endogenous calpain inhibitor calpastatin. A23187 calcium ionophore was supposed to be used in the current project as a calpain activator; however, it seemed to demonstrate the opposite effect to calpain activation, including the suppressing of cell proliferation, clonogenic survival, migration and endothelial interaction (with BECs in particular), although a statistical significance was not observed in some cases. As mentioned in section 5.1.9, efficient control of intracellular Ca^{2+} concentration is critical for mediating various normal cellular physiology (e.g., cell proliferation, apoptosis, migration, adhesion and invasion), and complexity of Ca^{2+}-signalling, regulating intracellular Ca^{2+} concentration, regulates such cellular processes not only through calpain system but also via various mechanisms (Farfariello *et al.*, 2015; Cui *et al.*, 2017). A23187-mediated apoptosis was suspected as a primary underlying mechanism of those suppressed phenotypic endpoints (e.g., cell proliferation, clonogenic survival, migration and BEC interactions); treatment with A23187 might induce programmed cell death via regulating other factors, such as calmodulin, NFAT, and NF-κB (Cui *et al.*, 2017), in addition to activating calpain.

In addition to Ca^{2+}, A23187 as a mobile ion-carrier also forms stable complexes with other divalent cations, such as Mn^{2+}, Mg^{2+} and Zn^{2+}. A rise in intracellular cytosolic of Mn^{2+} has been found to inhibit cell growth and induce apoptosis of various *in vitro* cells, such as Epstein Barr virus (EBV)-negative Burkitt's lymphoma (BL-CL), EBV-transformed B (EBV-BCL) (Schrantz *et al.*, 1999), and prostate cancer cells (Hernroth *et al.*, 2018). Moreover, Mn^{2+}levels in patients with breast cancer was lower compared to healthy controls (Shen *et al.*, 2015). A reduction in intracellular concentration of Mg^{2+} was observed, along with increased apoptosis in HT29 colon cancer cell (Cappadone *et al.*, 2012). TRPM7-

mediated Mn^{2+} influx has been shown to stimulate migration in human vascular smooth muscle (Callera *et al.*, 2009), osteoblastic (Abed & Moreau, 2009; Abed *et al.*, 2011), and pancreatic adenocarcinoma cell lines (Rybarczyk *et al.*, 2012). Human breast cancer MDA-MB-231 cells illustrated Mg^{2+}-dependent migration on fibronectin that could be inhibited by Zn^{2+}; however, Zn^{2+} could not exhibit identical activity when the migration was modulated by Mn^{2+} exposure (Lymburner *et al.*, 2013). Thus, it was difficult to draw a firm conclusion that the phenotypic endpoints of breast cancer cell lines, observed in the current study, were definitely influenced by Ca^{2+} influx-induced calpain activity.

A wide variety of studies reported calpain activation by other factors besides Ca^{2+}. Dibucaine, a sodium channel blockade and local amide anaesthetic, has been recognised and used as a calpain activator in several studies, for more than two decades (Fox *et al.*, 1991; Rutledge & Whiteheart, 2002; Zhang *et al.*, 2011; Zhang *et al.*, 2013b). High-energy compounds, such as adenosine triphosphate (ATP), guanosine triphosphate (GTP), phosphoenolpyruvate, pyrophosphate, phosphocreatine, and acetyl coenzyme A, were also reported to induce intracellular calpain activity (Nguyen & Chen, 2014). These compounds, however, have also been involved with cell physiology via other pathways, such as enhancing apoptosis via inducing caspase-3 activity by ATP (Zamaraeva *et al.*, 2005), caspase-3, -6, -8, and -9 (-like) but not caspase-1 (-like) activity by dibucaine (Arita *et al.*, 2000). Surprisingly, 19-mer oligopeptide calpastatin subdomains A (SGKSGMDAALDDLIDTLGG) and C (SKPIGPDDAIDALSSDFTS) can strongly activate μ- and m-calpain and increase the Ca^{2+} sensitivity of both proteases *in vitro* (Tompa *et al.*, 2002; Banoczi *et al.*, 2007; Vilagi *et al.*, 2008; Toke *et al.*, 2009). As calpastatin is a specific inhibitor of calpain, subdomains A or C or their derivatives may be able to act as a specific calpain activator. Vilagi *et al.* (2008) synthesised a membrane-permeable calpain activator, by conjugating an oligo-arginine tail to both 19-mer peptides, the conjugates of which could enhance neuronal excitability on rat brain slices *ex vivo* without additional Ca^{2+} requirement. This literature proposed that the synthesised activator can be used with any mammalian cells to specifically

challenge the calpain system without a rise of cytoplasmic Ca^{2+} (Vilagi *et al.*, 2008).

To continue examining whether calpain activation is involved in specific phenomena in future studies, it is suggested that: 1) further optimisation of A23187 working concentrations lacking apoptosis inductive effect is required, or 2) more specific calpain activators would be interesting, or 3) different types of activators are necessary to determine whether calpains are involved in specific phenomena. A lack of specificity in activating calpain activity by pharmacological calpain activators might cause an insufficiency in altering phenotypic characteristics of cells or provide misleading information regarding the involvement of calpain activity in the investigated cellular physiology.

Likewise, since all pharmacological calpain inhibitors are not specific but only selective to calpain, the inhibitory effect might be deficient in showing significant changes in cellular functions, such as no effect of calpeptin presented in regulating cell migration of T47D parental and mock-transfected cells (section 4.4.1.5). Therefore, it is necessary to use various inhibitors to determine whether inhibition of calpain activity is involved in this specific phenomena. Calpeptin (benzyloxycarbonyl-Leu-norLeu-H) has been recognised as a synthesised cell-penetrative peptide inhibitor against μ- and m-calpain since 1988 (Tsujinaka *et al.*, 1988). It shows more selectivity to inhibit calpain activity over the chymotrypsin-like activity of the eukaryotic proteasome compared to calpain inhibitors I (ALLN) and II (ALLM) (Figueiredo-Pereira *et al.*, 1994), which more preferentially inhibit μ- and m-calpains, respectively, than others (Zimmerman *et al.*, 1995). Comparing with leupeptin, calpeptin has more sensitivity to μ-calpain, yet is less active against papain, a proteolytic enzyme (Tsujinaka *et al.*, 1988). Besides proteases, calpeptin also inhibits the Ca^{2+}-activated mitochondrial K channel in murine models, resulting in the inductive activation of the permeability transition pore of inner mitochondrial membranes, the opening of which is responsible for ion equilibration and loss of membrane potential in apoptosis (Derksen *et al.*, 2016). In the case of

investigating calpain-mediated apoptosis, use of calpeptin may lead to an incorrect conclusion of calpain activity, if there is no awareness of the other targets for calpeptin.

Although a variety of calpain inhibitors are commercially available, it remains that the discovery of novel calpain inhibitors, driven primarily by improvements in the specificity for calpains and bioavailability of calpain inhibitors, is required (Ono *et al.*, 2016). As differential functions in pathophysiological mechanisms between μ- and m-calpains are present (Prangsaengtong *et al.*, 2012; Santos *et al.*, 2012; Wang *et al.*, 2016), specific inhibition of each protease may potentially provide more information regarding the role of such proteases, and also improve the therapeutic efficacy of the inhibitors on the target pathologies. Although, to date, a μ-calpain-specific inhibitor has not been yet established (PD151746, an α-mercaptoacrylate derivative, has only ~20-fold selectivity for μ-calpain over m-calpain (Wang *et al.*, 1996), mCalp-I, a peptidyl α-ketoamide derivative, has been reported to be >100-fold more selective for m-calpain than for μ-calpain (Li *et al.*, 1996; Wang *et al.*, 2014). Moreover, the observed differential effects of different calpastatin isoforms on the investigated phenotypic endpoints might be due to their different selectivity in inhibiting different types of calpain. Therefore, the use of various specific/selective calpain inhibitors as a comparator to the effects of calpastatin isoforms is suggested for future projects.

5.2.3 Expression of calpastatin mRNA and proteins

CAST2 mRNA expression in the CAST2-transfected cell model could not be assessed due to poor PCR efficiency. Thus, PCR protocol optimisation and CAST2 mRNA expression analysis are required for the future study of the current group. Although there is no commercially available antibody for specific detection of calpain isoforms expression, HA-tag antibodies could be responsible for detecting the expression of HA-tagged full-length calpastatin Type 1, Type 2 or Type 3. For future projects, it would be useful to produce the

specific antibodies for each isoform by the current group, collaborators, or the professional company.

Differential subcellular localisation between calpastatin Type 1 and Type 2 may be involved with their opposing role in regulating tumour cell adhesion to ECs. In the presence of A23187, localisation of both isoforms was not changed (investigated by Dr Sarah Storr, unpublished data). It would be interesting to investigate the intracellular co-localisation of each calpastatin isoform and calpain in the presence /absence of Ca^{2+} influx.

5.3 Conclusion

The current study presents the first evidence for the roles of calpastatin isoform overexpression in regulating breast cancer progression and LVI. The data suggest that modulating calpain activity via upregulation of calpastatin isoform 1 and 2, encoded by exon3-containing CAST cDNA, contributes to the promotion of breast cancer progression and LVI differentially *in vitro*. This project sheds light on calpastatin Type 1 overexpression in inducing breast tumour cell proliferation, migration, and endothelial interactions, in particular that of LECs. Although calpastatin Type 2 upregulation enhanced breast tumour cell migration, it prevented tumour cell adhesion, specifically to BECs. The current study, therefore, presents an important *in vitro* preliminary evidence supporting that both calpastatin isoforms 1 and 2 may play a role in promoting tumour progression but are opposingly involved in LVI. The opposing roles in regulating LVI may be related to their differential subcellular localisation: Type 1 localised mostly throughout the cytoplasm and slightly in the nuclei may enhance LI, and Type 2 cytoplasmically distributed with a predominant perinuclear expression may prevent BVI. Further study, therefore, is valuable to investigate and conclude the role of calpastatin Type 1 and Type 2 as regulators of breast cancer progression and LVI.

References

Abd-Elsalam, K. A. (2003). Bioinformatic tools and guideline for PCR primer design. *african Journal of biotechnology, 2*(5), 91-95.

Abdullah, N. A. (2019). *The role of redox proteins in the radiotherapeutic response of breast cancer (Doctoral thesis).* University of Nottingham.

Abed, E., Martineau, C. & Moreau, R. (2011). Role of melastatin transient receptor potential 7 channels in the osteoblastic differentiation of murine MC3T3 cells. *Calcif Tissue Int, 88*(3), 246-253. doi:10.1007/s00223-010-9455-z

Abed, E. & Moreau, R. (2009). Importance of melastatin-like transient receptor potential 7 and magnesium in the stimulation of osteoblast proliferation and migration by platelet-derived growth factor. *Am J Physiol Cell Physiol, 297*(2), C360-368. doi:10.1152/ajpcell.00614.2008

Adachi, Y., Takano, E., Murachi, T. & Hatanaka, M. (1988). Distribution and expression of calpastatin in human hematopoietic system cells. *Biol Chem Hoppe Seyler, 369 Suppl*, 223-227.

Ahmad, N. (2016). *Role of macrophage and associated cytokines in the regulation of breast tumour lymphovascular invasion (Doctoral thesis).* University of Nottingham.

Ahmad, N., Ammar, A., Storr, S. J., Green, A. R., Rakha, E., Ellis, I. O. & Martin, S. G. (2018). IL-6 and IL-10 are associated with good prognosis in early stage invasive breast cancer patients. *Cancer Immunol Immunother, 67*(4), 537-549. doi:10.1007/s00262-017-2106-8

Ahn, H. J., Jung, S. J., Kim, T. H., Oh, M. K. & Yoon, H.-K. (2015). Differences in clinical outcomes between Luminal A and B type breast cancers according to the St. Gallen Consensus 2013. *J Breast Cancer, 18*(2), 149-159.

Aleskandarany, M. A., Sonbul, S. N., Mukherjee, A. & Rakha, E. A. (2015). Molecular Mechanisms Underlying Lymphovascular Invasion in Invasive Breast Cancer. *Pathobiology, 82*(3-4), 113-123. doi:10.1159/000433583

Allemani, C., Weir, H. K., Carreira, H., Harewood, R., Spika, D., Wang, X. S., . . . &Coleman, M. P. (2015). Global surveillance of cancer survival 1995-2009: analysis of individual data for 25,676,887 patients from 279 population-based registries in 67 countries (CONCORD-2). *Lancet, 385*(9972), 977-1010. doi:10.1016/s0140-6736(14)62038-9

Alluri, P. & Newman, L. A. (2014). Basal-like and triple-negative breast cancers: searching for positives among many negatives. *Surg Oncol Clin N Am, 23*(3), 567-577. doi:10.1016/j.soc.2014.03.003

Ambrosini, E., Ceccherini-Silberstein, F., Erfle, V., Aloisi, F. & Levi, G. (1999). Gene transfer in astrocytes: comparison between different delivering methods and expression of the HIV-1 protein Nef. *J Neurosci Res, 55*(5), 569-577. doi:10.1002/(sici)1097-4547(19990301)55:5<569::aid-jnr4>3.0.co;2-f

Apáti, A., Jánossy, J., Brózik, A., Bauer, P. I. & Magócsi, M. (2003). Calcium induces cell survival and proliferation through the activation of the MAPK pathway in a human hormone-dependent leukemia cell line, TF-1. *J Biol Chem, 278*(11), 9235-9243. doi:10.1074/jbc.m205528200

Arita, K., Utsumi, T., Kato, A., Kanno, T., Kobuchi, H., Inoue, B., . . . &Utsumi, K. (2000). Mechanism of dibucaine-induced apoptosis in promyelocytic leukemia cells (HL-60). *Biochem Pharmacol, 60*(7), 905-915. doi:10.1016/s0006-2952(00)00406-8

Aroui, S., Ram, N., Appaix, F., Ronjat, M., Kenani, A., Pirollet, F. & De Waard, M. (2009). Maurocalcine as a non toxic drug carrier overcomes doxorubicin resistance in

the cancer cell line MDA-MB 231. *Pharm Res, 26*(4), 836-845. doi:10.1007/s11095-008-9782-1

Asada, K., Ishino, Y., Shimada, M., Shimojo, T., Endo, M., Kimizuka, F., . . . &Murachi, T. (1989). cDNA cloning of human calpastatin: sequence homology among human, pig, and rabbit calpastatins. *J Enzyme Inhib, 3*(1), 49-56.

Asangani, I. A., Rasheed, S. A., Nikolova, D. A., Leupold, J. H., Colburn, N. H., Post, S. & Allgayer, H. (2008). MicroRNA-21 (miR-21) post-transcriptionally downregulates tumor suppressor Pdcd4 and stimulates invasion, intravasation and metastasis in colorectal cancer. *Oncogene, 27*(15), 2128-2136. doi:10.1038/sj.onc.1210856

Asioli, S., Eusebi, V., Gaetano, L., Losi, L. & Bussolati, G. (2008). The pre-lymphatic pathway, the rooths of the lymphatic system in breast tissue: a 3D study. *Virchows Arch, 453*(4), 401-406. doi:10.1007/s00428-008-0657-y

Atencio, I. A., Ramachandra, M., Shabram, P. & Demers, G. W. (2000). Calpain inhibitor 1 activates p53-dependent apoptosis in tumor cell lines. *Cell Growth Differ, 11*(5), 247-253.

Averna, M., De Tullio, R., Capini, P., Salamino, F., Pontremoli, S. & Melloni, E. (2003). Changes in calpastatin localization and expression during calpain activation: a new mechanism for the regulation of intracellular Ca(2+)-dependent proteolysis. *Cell Mol Life Sci, 60*(12), 2669-2678. doi:10.1007/s00018-003-3288-0

Badve, S., Dabbs, D. J., Schnitt, S. J., Baehner, F. L., Decker, T., Eusebi, V., . . . &Reis-Filho, J. S. (2011). Basal-like and triple-negative breast cancers: a critical review with an emphasis on the implications for pathologists and oncologists. *Mod Pathol, 24*(2), 157-167. doi:10.1038/modpathol.2010.200

Baek, K. H., Yu, H. V., Kim, E., Na, Y. & Kwon, Y. (2016). Calcium influx-mediated translocation of m-calpain induces Ku80 cleavage and enhances the Ku80-related DNA repair pathway. *Oncotarget, 7*(21), 30831-30844. doi:10.18632/oncotarget.8791

Baghdiguian, S., Martin, M., Richard, I., Pons, F., Astier, C., Bourg, N., . . . &Lefranc, G. (1999). Calpain 3 deficiency is associated with myonuclear apoptosis and profound perturbation of the IkappaB alpha/NF-kappaB pathway in limb-girdle muscular dystrophy type 2A. *Nat Med, 5*(5), 503-511. doi:10.1038/8385

Banerjee, S., Reis-Filho, J. S., Ashley, S., Steele, D., Ashworth, A., Lakhani, S. R. & Smith, I. E. (2006). Basal-like breast carcinomas: clinical outcome and response to chemotherapy. *J Clin Pathol, 59*(7), 729-735. doi:10.1136/jcp.2005.033043

Banoczi, Z., Tantos, A., Farkas, A., Tompa, P., Friedrich, P. & Hudecz, F. (2007). Synthesis of cell-penetrating conjugates of calpain activator peptides. *Bioconjug Chem, 18*(1), 130-137. doi:10.1021/bc0601976

Barbero, S., Mielgo, A., Torres, V., Teitz, T., Shields, D. J., Mikolon, D., . . . &Stupack, D. G. (2009). Caspase-8 association with the focal adhesion complex promotes tumor cell migration and metastasis. *Cancer Res, 69*(9), 3755-3763. doi:10.1158/0008-5472.can-08-3937

Barnabas, N. & Cohen, D. (2013). Phenotypic and molecular characterization of MCF10DCIS and SUM breast cancer cell lines. *Int J Breast Cancer, 2013*.

Bartscht, T., Lehnert, H., Gieseler, F. & Ungefroren, H. (2012). The Src family kinase inhibitors PP2 and PP1 effectively block TGF-beta1-induced cell migration and invasion in both established and primary carcinoma cells. *Cancer Chemother Pharmacol, 70*(2), 221-230. doi:10.1007/s00280-012-1904-0

Barzegar, E., Fouladdel, S., Movahhed, T. K., Atashpour, S., Ghahremani, M. H., Ostad, S. N. & Azizi, E. (2015). Effects of berberine on proliferation, cell cycle

distribution and apoptosis of human breast cancer T47D and MCF7 cell lines. *Iran J Basic Med Sci, 18*(4), 334-342.

Baudry, M., Chou, M. M. & Bi, X. (2013). Targeting calpain in synaptic plasticity. *Expert Opin Ther Targets, 17*(5), 579-592. doi:10.1517/14728222.2013.766169

Benetti, R., Copetti, T., Dell'Orso, S., Melloni, E., Brancolini, C., Monte, M. & Schneider, C. (2005). The calpain system is involved in the constitutive regulation of beta-catenin signaling functions. *J Biol Chem, 280*(23), 22070-22080. doi:10.1074/jbc.M501810200

Benetti, R., Del Sal, G., Monte, M., Paroni, G., Brancolini, C. & Schneider, C. (2001). The death substrate Gas2 binds m-calpain and increases susceptibility to p53-dependent apoptosis. *Embo j, 20*(11), 2702-2714. doi:10.1093/emboj/20.11.2702

Beral, V. (2003). Breast cancer and hormone-replacement therapy in the Million Women Study. *Lancet, 362*(9382), 419-427.

Berridge, M. J., Lipp, P. & Bootman, M. D. (2000). The versatility and universality of calcium signalling. *Nat Rev Mol Cell Biol, 1*(1), 11-21. doi:10.1038/35036035

Bertucci, F., Finetti, P., Cervera, N., Esterni, B., Hermitte, F., Viens, P. & Birnbaum, D. (2008). How basal are triple-negative breast cancers? *Int J Cancer, 123*(1), 236-240. doi:10.1002/ijc.23518

Bhadriraju, K. & Chen, C. S. (2002). Engineering cellular microenvironments to improve cell-based drug testing. *Drug Discov Today, 7*(11), 612-620. doi:10.1016/s1359-6446(02)02273-0

Birgersdotter, A., Sandberg, R. & Ernberg, I. (2005). Gene expression perturbation in vitro--a growing case for three-dimensional (3D) culture systems. *Semin Cancer Biol, 15*(5), 405-412. doi:10.1016/j.semcancer.2005.06.009

Blanchard, H., Grochulski, P., Li, Y., Arthur, J. S., Davies, P. L., Elce, J. S. & Cygler, M. (1997). Structure of a calpain Ca(2+)-binding domain reveals a novel EF-hand and Ca(2+)-induced conformational changes. *Nat Struct Biol, 4*(7), 532-538.

Bollet, M. A., Savignoni, A., Pierga, J. Y., Lae, M., Fourchotte, V., Kirova, Y. M., . . . &Vincent-Salomon, A. (2008). High rates of breast conservation for large ductal and lobular invasive carcinomas combining multimodality strategies. *Br J Cancer, 98*(4), 734-741. doi:10.1038/sj.bjc.6604229

Booth, C. S., Pienaar, E., Termaat, J. R., Whitney, S. E., Louw, T. M. & Viljoen, H. J. (2010). Efficiency of the Polymerase Chain Reaction. *Chem Eng Sci, 65*(17), 4996-5006. doi:10.1016/j.ces.2010.05.046

Branca, D. (2004). Calpain-related diseases. *Biochem Biophys Res Commun, 322*(4), 1098-1104. doi:10.1016/j.bbrc.2004.07.126

Breast Cancer Expert Advisory Group. (2016). *Clinical guidelines for the management of breast cancer*. Retrieved from https://www.england.nhs.uk/mids-east/wp-content/uploads/sites/7/2018/02/guidelines-for-the-management-of-breast-cancer-v1.pdf.

Brenton, J. D., Carey, L. A., Ahmed, A. A. & Caldas, C. (2005). Molecular classification and molecular forecasting of breast cancer: ready for clinical application? *J Clin Oncol, 23*(29), 7350-7360. doi:10.1200/jco.2005.03.3845

Breslin, S. & O'Driscoll, L. (2013). Three-dimensional cell culture: the missing link in drug discovery. *Drug Discov Today, 18*(5-6), 240-249. doi:10.1016/j.drudis.2012.10.003

Briz, V., Hsu, Y. T., Li, Y., Lee, E., Bi, X. & Baudry, M. (2013). Calpain-2-mediated PTEN degradation contributes to BDNF-induced stimulation of dendritic protein synthesis. *J Neurosci, 33*(10), 4317-4328. doi:10.1523/jneurosci.4907-12.2013

Brody, L. C. & Biesecker, B. B. (1998). Breast cancer susceptibility genes. BRCA1 and BRCA2. *Medicine (Baltimore), 77*(3), 208-226.

Broeders, S., Huber, I., Grohmann, L., Berben, G., Taverniers, I., Mazzara, M., . . . &Morisset, D. (2014). Guidelines for validation of qualitative real-time PCR methods. *Trends in Food Science & Technology, 37*(2), 115-126.

Bubendorf, L., Schopfer, A., Wagner, U., Sauter, G., Moch, H., Willi, N., . . . &Mihatsch, M. J. (2000). Metastatic patterns of prostate cancer: an autopsy study of 1,589 patients. *Hum Pathol, 31*(5), 578-583.

Burchett, R., Brun, M., Monckton, E. A., Poon, H.-Y. & Godbout, R. (2019). Effects of nuclear factor I phosphorylation on calpastatin (CAST) gene variant expression and subcellular distribution in malignant glioma cells. *Journal of Biological Chemistry, 294*(4), 1173-1188.

Cai, J. J., Qi, Z. X., Hua, W., Zhu, J. J., Zhang, X., Yao, Y. & Mao, Y. (2014). Increased expression of Capn4 is associated with the malignancy of human glioma. *CNS Neurosci Ther, 20*(6), 521-527. doi:10.1111/cns.12248

Callera, G. E., He, Y., Yogi, A., Montezano, A. C., Paravicini, T., Yao, G. & Touyz, R. M. (2009). Regulation of the novel Mg2+ transporter transient receptor potential melastatin 7 (TRPM7) cation channel by bradykinin in vascular smooth muscle cells. *J Hypertens, 27*(1), 155-166. doi:10.1097/hjh.0b013e3283190582

Campbell, P. M. & Der, C. J. (2004). Oncogenic Ras and its role in tumor cell invasion and metastasis. *Semin Cancer Biol, 14*(2), 105-114. doi:10.1016/j.semcancer.2003.09.015

Cancer Research UK. (2017). Risk factors. Retrieved from https://www.cancerresearchuk.org/about-cancer/breast-cancer/risks-causes/risk-factors

Cancer Research UK. (2018). Breast cancer statistics. Retrieved from https://www.cancerresearchuk.org/health-professional/cancer-statistics/statistics-by-cancer-type/breast-cancer

Cappadone, C., Merolle, L., Marraccini, C., Farruggia, G., Sargenti, A., Locatelli, A., . . . &Iotti, S. (2012). Intracellular magnesium content decreases during mitochondria-mediated apoptosis induced by a new indole-derivative in human colon cancer cells. *Magnes Res, 25*(3), 104-111. doi:10.1684/mrh.2012.0319

Cardoso, F., Harbeck, N., Fallowfield, L., Kyriakides, S. & Senkus, E. (2012). Locally recurrent or metastatic breast cancer: ESMO Clinical Practice Guidelines for diagnosis, treatment and follow-up. *Ann Oncol, 23 Suppl 7*, vii11-19. doi:10.1093/annonc/mds232

Cardoso, F., Kyriakides, S., Ohno, S., Penault-Llorca, F., Poortmans, P., Rubio, I., . . . &Senkus, E. (2019). Early breast cancer: ESMO Clinical Practice Guidelines for diagnosis, treatment and follow-up. *Annals of Oncology, 30*(8), 1194-1220.

Carragher, N. O. (2006). Calpain inhibition: a therapeutic strategy targeting multiple disease states. *Curr Pharm Des, 12*(5), 615-638.

Carragher, N. O., Fincham, V. J., Riley, D. & Frame, M. C. (2001). Cleavage of focal adhesion kinase by different proteases during SRC-regulated transformation and apoptosis. Distinct roles for calpain and caspases. *J Biol Chem, 276*(6), 4270-4275. doi:10.1074/jbc.M008972200

Carragher, N. O., Fonseca, B. D. & Frame, M. C. (2004). Calpain activity is generally elevated during transformation but has oncogene-specific biological functions. *Neoplasia, 6*(1), 53-73.

Carragher, N. O. & Frame, M. C. (2002). Calpain: a role in cell transformation and migration. *Int J Biochem Cell Biol, 34*(12), 1539-1543.

Carragher, N. O., Westhoff, M. A., Riley, D., Potter, D. A., Dutt, P., Elce, J. S., . . . &Frame, M. C. (2002). v-Src-induced modulation of the calpain-calpastatin proteolytic system regulates transformation. *Mol Cell Biol, 22*(1), 257-269. doi:10.1128/mcb.22.1.257-269.2002

Casar, B., Rimann, I., Kato, H., Shattil, S. J., Quigley, J. P. & Deryugina, E. I. (2014). In vivo cleaved CDCP1 promotes early tumor dissemination via complexing with activated beta1 integrin and induction of FAK/PI3K/Akt motility signaling. *Oncogene, 33*(2), 255-268. doi:10.1038/onc.2012.547

Catsburg, C., Miller, A. B. & Rohan, T. E. (2015). Active cigarette smoking and risk of breast cancer. *Int J Cancer, 136*(9), 2204-2209. doi:10.1002/ijc.29266

Cayman Chemical. (2015, 25 February 2015). Product information: PP2. Retrieved from https://www.caymanchem.com/pdfs/13198.pdf

Cecchini, R. S., Costantino, J. P., Cauley, J. A., Cronin, W. M., Wickerham, D. L., Land, S. R., . . . &Wolmark, N. (2012). Body mass index and the risk for developing invasive breast cancer among high-risk women in NSABP P-1 and STAR breast cancer prevention trials. *Cancer Prev Res (Phila), 5*(4), 583-592. doi:10.1158/1940-6207.capr-11-0482

Cerniglia, G. J., Pore, N., Tsai, J. H., Schultz, S., Mick, R., Choe, R., . . . &Maity, A. (2009). Epidermal growth factor receptor inhibition modulates the microenvironment by vascular normalization to improve chemotherapy and radiotherapy efficacy. *PLoS One, 4*(8), e6539. doi:10.1371/journal.pone.0006539

Chakrabarti, G. & McClane, B. A. (2005). The importance of calcium influx, calpain and calmodulin for the activation of CaCo-2 cell death pathways by Clostridium perfringens enterotoxin. *Cell Microbiol, 7*(1), 129-146. doi:10.1111/j.1462-5822.2004.00442.x

Chan, K. T., Bennin, D. A. & Huttenlocher, A. (2010). Regulation of adhesion dynamics by calpain-mediated proteolysis of focal adhesion kinase (FAK). *J Biol Chem, 285*(15), 11418-11426. doi:10.1074/jbc.M109.090746

Cheang, M. C., Chia, S. K., Voduc, D., Gao, D., Leung, S., Snider, J., . . . &Nielsen, T. O. (2009). Ki67 index, HER2 status, and prognosis of patients with luminal B breast cancer. *J Natl Cancer Inst, 101*(10), 736-750. doi:10.1093/jnci/djp082

Chen, W., Chen, M., Liao, Z., Wang, Y., Zhan, Q. & Cai, G. (2009). Lymphatic vessel density as predictive marker for the local recurrence of rectal cancer. *Dis Colon Rectum, 52*(3), 513-519.

Chetty, C., Lakka, S. S., Bhoopathi, P. & Rao, J. S. (2010). MMP-2 alters VEGF expression via alphaVbeta3 integrin-mediated PI3K/AKT signaling in A549 lung cancer cells. *Int J Cancer, 127*(5), 1081-1095. doi:10.1002/ijc.25134

Chiang, S. P., Cabrera, R. M. & Segall, J. E. (2016). Tumor cell intravasation. *Am J Physiol Cell Physiol, 311*(1), C1-c14. doi:10.1152/ajpcell.00238.2015

Chua, B. T., Guo, K. & Li, P. (2000). Direct cleavage by the calcium-activated protease calpain can lead to inactivation of caspases. *J Biol Chem, 275*(7), 5131-5135.

Coleman, R. E. & Rubens, R. D. (1987). The clinical course of bone metastases from breast cancer. *Br J Cancer, 55*(1), 61-66.

Collaborative Group on Hormonal Factors in Breast, C. (2012). Menarche, menopause, and breast cancer risk: individual participant meta-analysis, including 118 964 women with breast cancer from 117 epidemiological studies. *The lancet oncology, 13*(11), 1141-1151. doi:http://dx.doi.org/10.1016/S1470-2045(12)70425-4

Conacci-Sorrell, M., Ngouenet, C., Anderson, S., Brabletz, T. & Eisenman, R. N. (2014). Stress-induced cleavage of Myc promotes cancer cell survival. *Genes Dev, 28*(7), 689-707. doi:10.1101/gad.231894.113

Cong, J., Goll, D. E., Peterson, A. M. & Kapprell, H. P. (1989). The role of autolysis in activity of the Ca2+-dependent proteinases (mu-calpain and m-calpain). *J Biol Chem, 264*(17), 10096-10103.

Cong, M., Thompson, V. F., Goll, D. E. & Antin, P. B. (1998). The bovine calpastatin gene promoter and a new N-terminal region of the protein are targets for cAMP-dependent protein kinase activity. *J Biol Chem, 273*(1), 660-666.

Cortesio, C. L., Boateng, L. R., Piazza, T. M., Bennin, D. A. & Huttenlocher, A. (2011). Calpain-mediated proteolysis of paxillin negatively regulates focal adhesion dynamics and cell migration. *J Biol Chem, 286*(12), 9998-10006. doi:10.1074/jbc.M110.187294

Cortesio, C. L., Chan, K. T., Perrin, B. J., Burton, N. O., Zhang, S., Zhang, Z. Y. & Huttenlocher, A. (2008). Calpain 2 and PTP1B function in a novel pathway with Src to regulate invadopodia dynamics and breast cancer cell invasion. *J Cell Biol, 180*(5), 957-971. doi:10.1083/jcb.200708048

Cory, G. (2011). Scratch-wound assay. *Methods Mol Biol, 769*, 25-30. doi:10.1007/978-1-61779-207-6_2

Cristofanilli, M., Gonzalez-Angulo, A., Sneige, N., Kau, S. W., Broglio, K., Theriault, R. L., . . . &Hortobagyi, G. N. (2005). Invasive lobular carcinoma classic type: response to primary chemotherapy and survival outcomes. *J Clin Oncol, 23*(1), 41-48. doi:10.1200/jco.2005.03.111

Croall, D. E. & DeMartino, G. N. (1991). Calcium-activated neutral protease (calpain) system: structure, function, and regulation. *Physiol Rev, 71*(3), 813-847. doi:10.1152/physrev.1991.71.3.813

Croall, D. E. & McGrody, K. S. (1994). Domain structure of calpain: mapping the binding site for calpastatin. *Biochemistry, 33*(45), 13223-13230.

Cui, C., Merritt, R., Fu, L. & Pan, Z. (2017). Targeting calcium signaling in cancer therapy. *Acta Pharm Sin B, 7*(1), 3-17. doi:10.1016/j.apsb.2016.11.001

da Costa Vieira, R. A., Biller, G., Uemura, G., Ruiz, C. A. & Curado, M. P. (2017). Breast cancer screening in developing countries. *Clinics (Sao Paulo, Brazil), 72*(4), 244-253. doi:10.6061/clinics/2017(04)09

Damtew, B. & Spagnuolo, P. J. (1997). Tumor cell-endothelial cell interactions: evidence for roles for lipoxygenase products of arachidonic acid in metastasis. *Prostaglandins Leukot Essent Fatty Acids, 56*(4), 295-300.

Dang, C. V. (2012). MYC on the path to cancer. *Cell, 149*(1), 22-35. doi:10.1016/j.cell.2012.03.003

Davis, B. W., Gelber, R., Goldhirsch, A., Hartmann, W. H., Hollaway, L., Russell, I. & Rudenstam, C. M. (1985). Prognostic significance of peritumoral vessel invasion in clinical trials of adjuvant therapy for breast cancer with axillary lymph node metastasis. *Hum Pathol, 16*(12), 1212-1218.

Davis, J., Martin, S. G., Patel, P. M., Green, A. R., Rakha, E. A., Ellis, I. O. & Storr, S. J. (2014). Low calpain-9 is associated with adverse disease-specific survival following endocrine therapy in breast cancer. *BMC Cancer, 14*, 995. doi:10.1186/1471-2407-14-995

de Azambuja, E., Cardoso, F., de Castro, G., Jr., Colozza, M., Mano, M. S., Durbecq, V., . . . &Paesmans, M. (2007). Ki-67 as prognostic marker in early breast cancer: a meta-analysis of published studies involving 12,155 patients. *Br J Cancer, 96*(10), 1504-1513. doi:10.1038/sj.bjc.6603756

de Mascarel, I., Bonichon, F., Durand, M., Mauriac, L., MacGrogan, G., Soubeyran, I., . . . &Trojani, M. (1998). Obvious peritumoral emboli: an elusive prognostic factor reappraised. Multivariate analysis of 1320 node-negative breast cancers. *Eur J Cancer, 34*(1), 58-65. doi:10.1016/s0959-8049(97)00344-4

De Tullio, R., Averna, M., Pedrazzi, M., Sparatore, B., Salamino, F., Pontremoli, S. & Melloni, E. (2014). Differential regulation of the calpain-calpastatin complex by the L-domain of calpastatin. *Biochim Biophys Acta, 1843*(11), 2583-2591. doi:10.1016/j.bbamcr.2014.07.002

De Tullio, R., Averna, M., Salamino, F., Pontremoli, S. & Melloni, E. (2000). Differential degradation of calpastatin by mu- and m-calpain in Ca(2+)-enriched human neuroblastoma LAN-5 cells. *FEBS Lett, 475*(1), 17-21. doi:10.1016/s0014-5793(00)01613-6

De Tullio, R., Cantoni, C., Broggio, C., Prato, C., Stifanese, R., Averna, M., . . . &Melloni, E. (2009). Involvement of exon 6-mediated calpastatin intracellular movements in the modulation of calpain activation. *Biochim Biophys Acta, 1790*(3), 182-187. doi:10.1016/j.bbagen.2008.11.002

De Tullio, R., Franchi, A., Martines, A., Averna, M., Pedrazzi, M., Melloni, E. & Sparatore, B. (2018). Unexpected role of the L-domain of calpastatin during the autoproteolytic activation of human erythrocyte calpain. *Biosci Rep, 38*(2). doi:10.1042/bsr20180147

De Tullio, R., Passalacqua, M., Averna, M., Salamino, F., Melloni, E. & Pontremoli, S. (1999). Changes in intracellular localization of calpastatin during calpain activation. *Biochem J, 343 Pt 2*, 467-472.

De Tullio, R., Sparatore, B., Salamino, F., Melloni, E. & Pontremoli, S. (1998). Rat brain contains multiple mRNAs for calpastatin. *FEBS Lett, 422*(1), 113-117.

Dedieu, S., Poussard, S., Mazeres, G., Grise, F., Dargelos, E., Cottin, P. & Brustis, J. J. (2004). Myoblast migration is regulated by calpain through its involvement in cell attachment and cytoskeletal organization. *Exp Cell Res, 292*(1), 187-200. doi:10.1016/j.yexcr.2003.08.014

Dent, R., Trudeau, M., Pritchard, K. I., Hanna, W. M., Kahn, H. K., Sawka, C. A., . . . &Narod, S. A. (2007). Triple-negative breast cancer: clinical features and patterns of recurrence. *Clin Cancer Res, 13*(15 Pt 1), 4429-4434. doi:10.1158/1078-0432.ccr-06-3045

Derksen, M., Vorwerk, C. & Siemen, D. (2016). Calpeptin, not calpain, directly inhibits an ion channel of the inner mitochondrial membrane. *Protoplasma, 253*(3), 835-843. doi:10.1007/s00709-015-0846-x

Deryugina, E. I. & Quigley, J. P. (2015). Tumor angiogenesis: MMP-mediated induction of intravasation- and metastasis-sustaining neovasculature. *Matrix Biol, 44-46*, 94-112. doi:10.1016/j.matbio.2015.04.004

Desjardins, P. & Conklin, D. (2010). NanoDrop microvolume quantitation of nucleic acids. *J Vis Exp*(45), 2565. doi:10.3791/2565

Desmedt, C., Sotiriou, C. & Piccart-Gebhart, M. J. (2009). Development and validation of gene expression profile signatures in early-stage breast cancer. *Cancer Invest, 27*(1), 1-10. doi:10.1080/07357900802574710

Dieckgraefe, B. K., Weems, D. M., Santoro, S. A. & Alpers, D. H. (1997). ERK and p38 MAP kinase pathways are mediators of intestinal epithelial wound-induced signal transduction. *Biochem Biophys Res Commun, 233*(2), 389-394. doi:10.1006/bbrc.1997.6469

Diepenbroek, M., Casadei, N., Esmer, H., Saido, T. C., Takano, J., Kahle, P. J., . . . &Nuber, S. (2014). Overexpression of the calpain-specific inhibitor calpastatin reduces human alpha-Synuclein processing, aggregation and synaptic impairment in [A30P]alphaSyn transgenic mice. *Hum Mol Genet, 23*(15), 3975-3989. doi:10.1093/hmg/ddu112

Dillekas, H., Transeth, M., Pilskog, M., Assmus, J. & Straume, O. (2014). Differences in metastatic patterns in relation to time between primary surgery and first

relapse from breast cancer suggest synchronized growth of dormant micrometastases. *Breast Cancer Res Treat, 146*(3), 627-636. doi:10.1007/s10549-014-3057-9

Dowsett, M., Nielsen, T. O., A'Hern, R., Bartlett, J., Coombes, R. C., Cuzick, J., . . . &Hayes, D. F. (2011). Assessment of Ki67 in breast cancer: recommendations from the International Ki67 in Breast Cancer working group. *J Natl Cancer Inst, 103*(22), 1656-1664. doi:10.1093/jnci/djr393

Dunn, B. K., Wagner, P. D., Anderson, D. & Greenwald, P. (2010). Molecular markers for early detection. *Semin Oncol, 37*(3), 224-242. doi:10.1053/j.seminoncol.2010.05.007

Edge, S. B., Byrd, D. R., Compton, C. C., Fritz, A. G., Greene, F. L. & Trotti, A. (2010). Breast *AJCC Cancer Staging Manual* (7th ed., pp. 347–376). New York: Springer.

Edmondson, R., Broglie, J. J., Adcock, A. F. & Yang, L. (2014). Three-dimensional cell culture systems and their applications in drug discovery and cell-based biosensors. *Assay Drug Dev Technol, 12*(4), 207-218. doi:10.1089/adt.2014.573

Ejlertsen, B., Jensen, M. B., Rank, F., Rasmussen, B. B., Christiansen, P., Kroman, N., . . . &Mouridsen, H. T. (2009). Population-based study of peritumoral lymphovascular invasion and outcome among patients with operable breast cancer. *J Natl Cancer Inst, 101*(10), 729-735. doi:10.1093/jnci/djp090

Elkind, E., Vaisid, T., Kornspan, J. D., Barnoy, S., Rottem, S. & Kosower, N. S. (2011). Neuroprotective effects of Mycoplasma hyorhinis against amyloid-beta-peptide toxicity in SH-SY5Y human neuroblastoma cells are mediated by calpastatin upregulation in the mycoplasma-infected cells. *Neurochem Int, 58*(4), 497-503. doi:10.1016/j.neuint.2011.01.005

Emori, Y., Kawasaki, H., Imajoh, S., Minami, Y. & Suzuki, K. (1988). All four repeating domains of the endogenous inhibitor for calcium-dependent protease independently retain inhibitory activity. Expression of the cDNA fragments in Escherichia coli. *J Biol Chem, 263*(5), 2364-2370.

Evangelou, E., Kyzas, P. A. & Trikalinos, T. A. (2005). Comparison of the diagnostic accuracy of lymphatic endothelium markers: Bayesian approach. *Mod Pathol, 18*(11), 1490-1497. doi:10.1038/modpathol.3800457

Ewing, J. (1928). Neoplastic Diseases (3rd). *Ed. Philadelphia, W. B. Saunders Co*, 825.

Farfariello, V., Iamshanova, O., Germain, E., Fliniaux, I. & Prevarskaya, N. (2015). Calcium homeostasis in cancer: A focus on senescence. *Biochim Biophys Acta, 1853*(9), 1974-1979. doi:10.1016/j.bbamcr.2015.03.005

Fei, B., Yu, S. & Geahlen, R. L. (2013). Modulation by Syk of Bcl-2, calcium and the calpain-calpastatin proteolytic system in human breast cancer cells. *Biochim Biophys Acta, 1833*(10), 2153-2164. doi:10.1016/j.bbamcr.2013.05.010

Felgner, J. H., Kumar, R., Sridhar, C. N., Wheeler, C. J., Tsai, Y. J., Border, R., . . . &Felgner, P. L. (1994). Enhanced gene delivery and mechanism studies with a novel series of cationic lipid formulations. *J Biol Chem, 269*(4), 2550-2561.

Figueiredo-Pereira, M. E., Banik, N. & Wilk, S. (1994). Comparison of the effect of calpain inhibitors on two extralysosomal proteinases: the multicatalytic proteinase complex and m-calpain. *J Neurochem, 62*(5), 1989-1994. doi:10.1046/j.1471-4159.1994.62051989.x

Filippini, S. E. & Vega, A. (2013). Breast cancer genes: beyond BRCA1 and BRCA2. *Front Biosci (Landmark Ed), 18*, 1358-1372.

Flevaris, P., Stojanovic, A., Gong, H., Chishti, A., Welch, E. & Du, X. (2007). A molecular switch that controls cell spreading and retraction. *J Cell Biol, 179*(3), 553-565. doi:10.1083/jcb.200703185

Florey, O. & Haskard, D. O. (2007). Analysis of flow-based adhesion in vitro. *Methods Mol Med, 135*, 323-331.

Fox, J. E., Austin, C. D., Reynolds, C. C. & Steffen, P. K. (1991). Evidence that agonist-induced activation of calpain causes the shedding of procoagulant-containing microvesicles from the membrane of aggregating platelets. *J Biol Chem, 266*(20), 13289-13295.

Franco, S., Perrin, B. & Huttenlocher, A. (2004a). Isoform specific function of calpain 2 in regulating membrane protrusion. *Exp Cell Res, 299*(1), 179-187. doi:10.1016/j.yexcr.2004.05.021

Franco, S. J. & Huttenlocher, A. (2005). Regulating cell migration: calpains make the cut. *J Cell Sci, 118*(Pt 17), 3829-3838. doi:10.1242/jcs.02562

Franco, S. J., Rodgers, M. A., Perrin, B. J., Han, J., Bennin, D. A., Critchley, D. R. & Huttenlocher, A. (2004b). Calpain-mediated proteolysis of talin regulates adhesion dynamics. *Nat Cell Biol, 6*(10), 977-983. doi:10.1038/ncb1175

Friberg, S. & Nystrom, A. (2015). Cancer metastases: early dissemination and late recurrences. *Cancer growth and metastasis, 8*, CGM. S31244.

Fuller, E. S. & Howell, V. M. (2014). Culture models to define key mediators of cancer matrix remodeling. *Front Oncol, 4*, 57. doi:10.3389/fonc.2014.00057

Gafni, J., Cong, X., Chen, S. F., Gibson, B. W. & Ellerby, L. M. (2009). Calpain-1 cleaves and activates caspase-7. *J Biol Chem, 284*(37), 25441-25449. doi:10.1074/jbc.M109.038174

Gao, P., Zhou, G. Y., Zhang, Q. H., Su, Z. X., Zhang, T. G., Xiang, L., . . . &Mu, K. (2009). Lymphangiogenesis in gastric carcinoma correlates with prognosis. *J Pathol*.

Garcia-Dorado, D., Ruiz-Meana, M., Inserte, J., Rodriguez-Sinovas, A. & Piper, H. M. (2012). Calcium-mediated cell death during myocardial reperfusion. *Cardiovasc Res, 94*(2), 168-180. doi:10.1093/cvr/cvs116

Gasco, M., Shami, S. & Crook, T. (2002). The p53 pathway in breast cancer. *Breast Cancer Res, 4*(2), 70-76.

Gaudet, M. M., Gapstur, S. M., Sun, J., Diver, W. R., Hannan, L. M. & Thun, M. J. (2013). Active smoking and breast cancer risk: original cohort data and meta-analysis. *J Natl Cancer Inst, 105*(8), 515-525. doi:10.1093/jnci/djt023

Gavrilescu, L. C. & Denkers, E. Y. (2003). Apoptosis and the balance of homeostatic and pathologic responses to protozoan infection. *Infection and immunity, 71*(11), 6109-6115. doi:10.1128/iai.71.11.6109-6115.2003

Gemignani, M. L. & Armstrong, D. K. (2014). Breast cancer. *Gynecol Oncol, 132*(2), 264-267. doi:10.1016/j.ygyno.2014.01.022

Gennari, A., Conte, P., Rosso, R., Orlandini, C. & Bruzzi, P. (2005). Survival of metastatic breast carcinoma patients over a 20-year period: a retrospective analysis based on individual patient data from six consecutive studies. *Cancer, 104*(8), 1742-1750. doi:10.1002/cncr.21359

Gil-Parrado, S., Fernández-Montalván, A., Assfalg-Machleidt, I., Popp, O., Bestvater, F., Holloschi, A., . . . &Machleidt, W. (2002). Ionomycin-activated calpain triggers apoptosis. A probable role for Bcl-2 family members. *J Biol Chem, 277*(30), 27217-27226. doi:10.1074/jbc.m202945200

Gil-Parrado, S., Popp, O., Knoch, T. A., Zahler, S., Bestvater, F., Felgentrager, M., . . . &Spiess, E. (2003). Subcellular localization and in vivo subunit interactions of ubiquitous mu-calpain. *J Biol Chem, 278*(18), 16336-16346. doi:10.1074/jbc.M208657200

Giuliano, A. E., Connolly, J. L., Edge, S. B., Mittendorf, E. A., Rugo, H. S., Solin, L. J., . . . &Hortobagyi, G. N. (2017). Breast cancer—major changes in the American Joint

Committee on Cancer eighth edition cancer staging manual. *CA Cancer J Clin, 67*(4), 290-303.

Giuliano, A. E., Edge, S. B. & Hortobagyi, G. N. (2018). Eighth Edition of the AJCC Cancer Staging Manual: Breast Cancer. *Annals of surgical oncology, 25*(7), 1783-1785. doi:10.1245/s10434-018-6486-6

Glenn, H. L., Messner, J. & Meldrum, D. R. (2016). A simple non-perturbing cell migration assay insensitive to proliferation effects. *Sci Rep, 6*, 31694. doi:10.1038/srep31694

Global Cancer Observatory. (2019a). Estimated number of deaths in 2018, Thailand, all cancers, females, all ages. Available from International Agency for Research on Cancer, WHO. Cancer Today Retrieved 9 June 2019 http://gco.iarc.fr/today/online-analysis-pie?v=2018&mode=cancer&mode_population=continents&population=900&populations=764&key=total&sex=2&cancer=39&type=1&statistic=5&prevalence=0&population_group=0&ages_group%5B%5D=0&ages_group%5B%5D=17&nb_items=7&group_cancer=1&include_nmsc=1&include_nmsc_other=1&half_pie=0&donut=0&population_group_globocan_id=

Global Cancer Observatory. (2019b). Estimated number of deaths in 2018, United Kingdom, all cancers, females, all ages. Available from International Agency for Research on Cancer, WHO. Cancer Today Retrieved 2019 http://gco.iarc.fr/today/online-analysis-pie?v=2018&mode=cancer&mode_population=continents&population=900&populations=826&key=total&sex=2&cancer=39&type=1&statistic=5&prevalence=0&population_group=0&ages_group%5B%5D=0&ages_group%5B%5D=17&nb_items=7&group_cancer=1&include_nmsc=1&include_nmsc_other=1&half_pie=0&donut=0&population_group_globocan_id=

Global Cancer Observatory. (2019c). Estimated number of deaths in 2018, worldwide, all cancers, females, all ages. Available from International Agency for Research on Cancer, WHO. Cancer today Retrieved 9 June, 2019 http://gco.iarc.fr/today/online-analysis-table?v=2018&mode=cancer&mode_population=continents&population=900&populations=900&key=asr&sex=2&cancer=39&type=1&statistic=5&prevalence=0&population_group=0&ages_group%5B%5D=0&ages_group%5B%5D=17&nb_items=5&group_cancer=1&include_nmsc=1&include_nmsc_other=1

Global Cancer Observatory. (2019d). Estimated number of new cases in 2018, Thailand. Available from International Agency for Research on Cancer, WHO. Cancer Today Retrieved 9 June 2019 http://gco.iarc.fr/today/online-analysis-table?v=2018&mode=cancer&mode_population=continents&population=900&populations=764&key=asr&sex=2&cancer=39&type=0&statistic=5&prevalence=0&population_group=0&ages_group%5B%5D=0&ages_group%5B%5D=17&nb_items=5&group_cancer=1&include_nmsc=1&include_nmsc_other=1

Global Cancer Observatory. (2019e). Estimated number of new cases in 2018, United Kingdom. Available from International Agency for Research on Cancer, WHO. Cancer Today Retrieved 9 June 2019 http://gco.iarc.fr/today/online-analysis-table?v=2018&mode=cancer&mode_population=continents&population=900&populations=764&key=asr&sex=0&cancer=39&type=0&statistic=5&prevalence=0&population_group=0&ages_group%5B%5D=0&ages_group%5B%5D=17&nb_items=5&group_cancer=1&include_nmsc=1&include_nmsc_other=1

Global Cancer Observatory. (2019f). Estimated number of new cases in 2018, worldwide. Available from International Agency for Research on Cancer, WHO. Cancer today Retrieved 9 June, 2019 http://gco.iarc.fr/today/online-analysis-

table?v=2018&mode=cancer&mode_population=continents&population=900&populations=900&key=asr&sex=2&cancer=39&type=0&statistic=5&prevalence=0&population_group=0&ages_group%5B%5D=0&ages_group%5B%5D=17&nb_items=5&group_cancer=1&include_nmsc=1&include_nmsc_other=1

Goll, D. E., Thompson, V. F., Li, H., Wei, W. & Cong, J. (2003). The calpain system. *Physiol Rev, 83*(3), 731-801. doi:10.1152/physrev.00029.2002

Gonen, H., Shkedy, D., Barnoy, S., Kosower, N. S. & Ciechanover, A. (1997). On the involvement of calpains in the degradation of the tumor suppressor protein p53. *FEBS Lett, 406*(1-2), 17-22.

Gouaze-Andersson, V., Yu, J. Y., Kreitenberg, A. J., Bielawska, A., Giuliano, A. E. & Cabot, M. C. (2007). Ceramide and glucosylceramide upregulate expression of the multidrug resistance gene MDR1 in cancer cells. *Biochim Biophys Acta, 1771*(12), 1407-1417. doi:10.1016/j.bbalip.2007.09.005

Green, M. R. & Sambrook, J. (2018). Constructing a standard curve for real-time polymerase chain reaction (PCR) experiments. *Cold Spring Harbor Protocols, 2018*(10), pdb. prot095026.

Gu, J., Xu, F. K., Zhao, G. Y., Lu, C. L., Lin, Z. W., Ding, J. Y. & Ge, D. (2015). Capn4 promotes non-small cell lung cancer progression via upregulation of matrix metalloproteinase 2. *Med Oncol, 32*(3), 51. doi:10.1007/s12032-015-0500-7

Gubin, A. N., Reddy, B., Njoroge, J. M. & Miller, J. L. (1997). Long-term, stable expression of green fluorescent protein in mammalian cells. *Biochem Biophys Res Commun, 236*(2), 347-350. doi:10.1006/bbrc.1997.6963

Gujam, F. J., Going, J. J., Edwards, J., Mohammed, Z. M. & McMillan, D. C. (2014a). The role of lymphatic and blood vessel invasion in predicting survival and methods of detection in patients with primary operable breast cancer. *Crit Rev Oncol Hematol, 89*(2), 231-241. doi:10.1016/j.critrevonc.2013.08.014

Gujam, F. J., Going, J. J., Mohammed, Z. M., Orange, C., Edwards, J. & McMillan, D. C. (2014b). Immunohistochemical detection improves the prognostic value of lymphatic and blood vessel invasion in primary ductal breast cancer. *BMC Cancer, 14*, 676. doi:10.1186/1471-2407-14-676

Gurlo, T., Costes, S., Hoang, J. D., Rivera, J. F., Butler, A. E. & Butler, P. C. (2016). beta Cell-specific increased expression of calpastatin prevents diabetes induced by islet amyloid polypeptide toxicity. *JCI Insight, 1*(18), e89590. doi:10.1172/jci.insight.89590

Hamajima, N., Hirose, K., Tajima, K., Rohan, T., Calle, E. E., Heath, C. W., Jr., . . . &Meirik, O. (2002). Alcohol, tobacco and breast cancer--collaborative reanalysis of individual data from 53 epidemiological studies, including 58,515 women with breast cancer and 95,067 women without the disease. *Br J Cancer, 87*(11), 1234-1245. doi:10.1038/sj.bjc.6600596

Han, Y., Weinman, S., Boldogh, I., Walker, R. K. & Brasier, A. R. (1999). Tumor necrosis factor-alpha-inducible IkappaBalpha proteolysis mediated by cytosolic m-calpain. A mechanism parallel to the ubiquitin-proteasome pathway for nuclear factor-kappab activation. *J Biol Chem, 274*(2), 787-794.

Hanahan, D. & Weinberg, R. A. (2011). Hallmarks of cancer: the next generation. *Cell, 144*(5), 646-674. doi:10.1016/j.cell.2011.02.013

Hance, K. W., Anderson, W. F., Devesa, S. S., Young, H. A. & Levine, P. H. (2005). Trends in inflammatory breast carcinoma incidence and survival: the surveillance, epidemiology, and end results program at the National Cancer Institute. *J Natl Cancer Inst, 97*(13), 966-975. doi:10.1093/jnci/dji172

Hanna, R. A., Campbell, R. L. & Davies, P. L. (2008). Calcium-bound structure of calpain and its mechanism of inhibition by calpastatin. *Nature, 456*(7220), 409-412. doi:10.1038/nature07451

Hanna, R. A., Garcia-Diaz, B. E. & Davies, P. L. (2007). Calpastatin simultaneously binds four calpains with different kinetic constants. *FEBS Lett, 581*(16), 2894-2898. doi:10.1016/j.febslet.2007.05.035

Harbeck, N. & Jakesz, R. (2007). St. Gallen 2007: breast cancer treatment consensus report. *Breast care, 2*(3), 130-134.

Hartveit, E. (1990). Attenuated cells in breast stroma: the missing lymphatic system of the breast. *Histopathology, 16*(6), 533-543.

Hata, S., Abe, M., Suzuki, H., Kitamura, F., Toyama-Sorimachi, N., Abe, K., . . . &Sorimachi, H. (2010). Calpain 8/nCL-2 and calpain 9/nCL-4 constitute an active protease complex, G-calpain, involved in gastric mucosal defense. *PLoS Genet, 6*(7), e1001040. doi:10.1371/journal.pgen.1001040

Haybittle, J. L., Blamey, R. W., Elston, C. W., Johnson, J., Doyle, P. J., Campbell, F. C., . . . &Griffiths, K. (1982). A prognostic index in primary breast cancer. *Br J Cancer, 45*(3), 361-366.

He, K. W., Sun, J. J., Liu, Z. B., Zhuo, P. Y., Ma, Q. H., Liu, Z. Y. & Yu, Z. Y. (2017). Prognostic significance of lymphatic vessel invasion diagnosed by D2-40 in Chinese invasive breast cancers. *Medicine (Baltimore), 96*(44), e8490. doi:10.1097/md.0000000000008490

Hernroth, B., Holm, I., Gondikas, A. & Tassidis, H. (2018). Manganese Inhibits Viability of Prostate Cancer Cells. *Anticancer Res, 38*(1), 137-145. doi:10.21873/anticanres.12201

Higuchi, M., Iwata, N., Matsuba, Y., Takano, J., Suemoto, T., Maeda, J., . . . &Saido, T. C. (2012). Mechanistic involvement of the calpain-calpastatin system in Alzheimer neuropathology. *Faseb j, 26*(3), 1204-1217. doi:10.1096/fj.11-187740

Hipfner, D. R. & Cohen, S. M. (2004). Connecting proliferation and apoptosis in development and disease. *Nat Rev Mol Cell Biol, 5*(10), 805-815. doi:10.1038/nrm1491

Ho, A. Y., Gupta, G., King, T. A., Perez, C. A., Patil, S. M., Rogers, K. H., . . . &Robson, M. E. (2012). Favorable prognosis in patients with T1a/T1bN0 triple-negative breast cancers treated with multimodality therapy. *Cancer, 118*(20), 4944-4952. doi:10.1002/cncr.27480

Hodgson, L. & Dong, C. (2001). [Ca2+]i as a potential downregulator of alpha2beta1-integrin-mediated A2058 tumor cell migration to type IV collagen. *Am J Physiol Cell Physiol, 281*(1), C106-113. doi:10.1152/ajpcell.2001.281.1.C106

Hoffmann, D. B., Williams, S. K., Bojcevski, J., Muller, A., Stadelmann, C., Naidoo, V., . . . &Fairless, R. (2013). Calcium influx and calpain activation mediate preclinical retinal neurodegeneration in autoimmune optic neuritis. *J Neuropathol Exp Neurol, 72*(8), 745-757. doi:10.1097/NEN.0b013e31829c7370

Honda, S., Marumoto, T., Hirota, T., Nitta, M., Arima, Y., Ogawa, M. & Saya, H. (2004). Activation of m-calpain is required for chromosome alignment on the metaphase plate during mitosis. *Journal of Biological Chemistry, 279*(11), 10615-10623.

Hong, Y. K., Shin, J. W. & Detmar, M. (2004). Development of the lymphatic vascular system: a mystery unravels. *Dev Dyn, 231*(3), 462-473. doi:10.1002/dvdy.20179

Hortobagyi, G. N., Connolly, J. L., D'Orsi, C. J., Edge, S. B., Mittendorf, E. A., Rugo, H. S., . . . &Giuliano, A. (2017). Breast. In M. B. e. a. Amin (Ed.), *AJCC Cancer Staging Manual* (8th ed., pp. 587-636): The American College of Surgeons.

Hortobagyi, G. N., de la Garza Salazar, J., Pritchard, K., Amadori, D., Haidinger, R., Hudis, C. A., . . . &Albain, K. S. (2005). The global breast cancer burden: variations in epidemiology and survival. *Clin Breast Cancer, 6*(5), 391-401.

Hosfield, C. M., Elce, J. S., Davies, P. L. & Jia, Z. (1999). Crystal structure of calpain reveals the structural basis for Ca(2+)-dependent protease activity and a novel mode of enzyme activation. *Embo j, 18*(24), 6880-6889. doi:10.1093/emboj/18.24.6880

Hoskin, V., Szeto, A., Ghaffari, A., Greer, P. A., Cote, G. P. & Elliott, B. E. (2015). Ezrin regulates focal adhesion and invadopodia dynamics by altering calpain activity to promote breast cancer cell invasion. *Mol Biol Cell, 26*(19), 3464-3479. doi:10.1091/mbc.E14-12-1584

Huang, E. H., Singh, B., Cristofanilli, M., Gelovani, J., Wei, C., Vincent, L., . . . &Lucci, A. (2009). A CXCR4 antagonist CTCE-9908 inhibits primary tumor growth and metastasis of breast cancer. *J Surg Res, 155*(2), 231-236. doi:10.1016/j.jss.2008.06.044

Huber, M. C., Mall, R., Braselmann, H., Feuchtinger, A., Molatore, S., Lindner, K., . . . &Aubele, M. (2016). uPAR enhances malignant potential of triple-negative breast cancer by directly interacting with uPA and IGF1R. *BMC Cancer, 16*, 615-615. doi:10.1186/s12885-016-2663-9

Huh, D., Hamilton, G. A. & Ingber, D. E. (2011). From 3D cell culture to organs-on-chips. *Trends Cell Biol, 21*(12), 745-754. doi:10.1016/j.tcb.2011.09.005

Huttenlocher, A., Palecek, S. P., Lu, Q., Zhang, W., Mellgren, R. L., Lauffenburger, D. A., . . . &Horwitz, A. F. (1997). Regulation of cell migration by the calcium-dependent protease calpain. *J Biol Chem, 272*(52), 32719-32722.

Imajoh, S., Kawasaki, H. & Suzuki, K. (1986a). The amino-terminal hydrophobic region of the small subunit of calcium-activated neutral protease (CANP) is essential for its activation by phosphatidylinositol. *J Biochem, 99*(4), 1281-1284.

Imajoh, S., Kawasaki, H. & Suzuki, K. (1986b). Limited autolysis of calcium-activated neutral protease (CANP): reduction of the Ca2+-requirement is due to the NH2-terminal processing of the large subunit. *J Biochem, 100*(3), 633-642.

Imajoh, S., Kawasaki, H. & Suzuki, K. (1987). The COOH-terminal E-F hand structure of calcium-activated neutral protease (CANP) is important for the association of subunits and resulting proteolytic activity. *J Biochem, 101*(2), 447-452.

Ioachim, E., Charchanti, A., Briasoulis, E., Karavasilis, V., Tsanou, H., Arvanitis, D. L., . . . &Pavlidis, N. (2002). Immunohistochemical expression of extracellular matrix components tenascin, fibronectin, collagen type IV and laminin in breast cancer: their prognostic value and role in tumour invasion and progression. *Eur J Cancer, 38*(18), 2362-2370.

Ishida, S., Emori, Y. & Suzuki, K. (1991). Rat calpastatin has diverged primary sequence from other mammalian calpastatins but retains functionally important sequences. *Biochim Biophys Acta, 1088*(3), 436-438.

Jang, H. S., Lal, S. & Greenwood, J. A. (2010). Calpain 2 is required for glioblastoma cell invasion: regulation of matrix metalloproteinase 2. *Neurochem Res, 35*(11), 1796-1804. doi:10.1007/s11064-010-0246-8

Jánossy, J., Ubezio, P., Apáti, Á., Magócsi, M., Tompa, P. & Friedrich, P. (2004). Calpain as a multi-site regulator of cell cycle. *Biochem Pharmacol, 67*(8), 1513-1521.

Jegatheeswaran, S., Mason, J. M., Hancock, H. C. & Siriwardena, A. K. (2013). The liver-first approach to the management of colorectal cancer with synchronous hepatic metastases: a systematic review. *JAMA Surg, 148*(4), 385-391. doi:10.1001/jamasurg.2013.1216

Jemal, A., Siegel, R., Xu, J. & Ward, E. (2010). Cancer statistics, 2010. *CA Cancer J Clin, 60*(5), 277-300. doi:10.3322/caac.20073

Jensen, A. O., Jacobsen, J. B., Norgaard, M., Yong, M., Fryzek, J. P. & Sorensen, H. T. (2011). Incidence of bone metastases and skeletal-related events in breast cancer patients: a population-based cohort study in Denmark. *BMC Cancer, 11*, 29. doi:10.1186/1471-2407-11-29

Ji, R. C. (2016). Lymph Nodes and Cancer Metastasis: New Perspectives on the Role of Intranodal Lymphatic Sinuses. *Int J Mol Sci, 18*(1). doi:10.3390/ijms18010051

Ji, R. C., Eshita, Y. & Kato, S. (2007). Investigation of intratumoural and peritumoural lymphatics expressed by podoplanin and LYVE-1 in the hybridoma-induced tumours. *Int J Exp Pathol, 88*(4), 257-270. doi:10.1111/j.1365-2613.2007.00532.x

Jones, M. E., Schoemaker, M. J., Wright, L. B., Ashworth, A. & Swerdlow, A. J. (2017). Smoking and risk of breast cancer in the Generations Study cohort. *Breast Cancer Res, 19*(1), 118. doi:10.1186/s13058-017-0908-4

Jotzu, C., Alt, E., Welte, G., Li, J., Hennessy, B. T., Devarajan, E., . . . &Song, Y. H. (2011). Adipose tissue derived stem cells differentiate into carcinoma-associated fibroblast-like cells under the influence of tumor derived factors. *Cell Oncol (Dordr), 34*(1), 55-67. doi:10.1007/s13402-011-0012-1

Journé, F., Dumon, J.-C., Kheddoumi, N., Fox, J., Laïos, I., Leclercq, G. & Body, J.-J. (2004). Extracellular calcium downregulates estrogen receptor alpha and increases its transcriptional activity through calcium-sensing receptor in breast cancer cells. *Bone, 35*(2), 479-488.

Juncker-Jensen, A., Deryugina, E. I., Rimann, I., Zajac, E., Kupriyanova, T. A., Engelholm, L. H. & Quigley, J. P. (2013). Tumor MMP-1 activates endothelial PAR1 to facilitate vascular intravasation and metastatic dissemination. *Cancer Res, 73*(14), 4196-4211. doi:10.1158/0008-5472.can-12-4495

Jutzy, J. M. S., Lemons, J. M., Luke, J. J. & Chmura, S. J. (2018). The Evolution of Radiation Therapy in Metastatic Breast Cancer: From Local Therapy to Systemic Agent. *Int J Breast Cancer, 2018*, 4786819. doi:10.1155/2018/4786819

Kang, S.-H., Cheung, K.-Y. & Kim, Y.-S. (2003a). Correlation between hormonal receptor status and clinicopathologic factors with prognostic assesment in breast cancer. *Annals of Surgical Treatment and Research, 65*(3), 198-204.

Kang, Y., Siegel, P. M., Shu, W., Drobnjak, M., Kakonen, S. M., Cordon-Cardo, C., . . . &Massague, J. (2003b). A multigenic program mediating breast cancer metastasis to bone. *Cancer Cell, 3*(6), 537-549.

Kapałczyńska, M., Kolenda, T., Przybyła, W., Zajączkowska, M., Teresiak, A., Filas, V., . . . &Lamperska, K. (2018). 2D and 3D cell cultures - a comparison of different types of cancer cell cultures. *Archives of medical science : AMS, 14*(4), 910-919. doi:10.5114/aoms.2016.63743

Kapprell, H. P. & Goll, D. E. (1989). Effect of Ca2+ on binding of the calpains to calpastatin. *J Biol Chem, 264*(30), 17888-17896.

Kawasaki, H., Emori, Y., Imajoh-Ohmi, S., Minami, Y. & Suzuki, K. (1989). Identification and characterization of inhibitory sequences in four repeating domains of the endogenous inhibitor for calcium-dependent protease. *J Biochem, 106*(2), 274-281.

Kawasaki, H., Imajoh, S., Kawashima, S., Hayashi, H. & Suzuki, K. (1986). The small subunits of calcium dependent proteases with different calcium sensitivities are identical. *J Biochem, 99*(5), 1525-1532.

Kawasaki, H. & Kawashima, S. (1996). Regulation of the calpain-calpastatin system by membranes (review). *Mol Membr Biol, 13*(4), 217-224.

Kennecke, H., Yerushalmi, R., Woods, R., Cheang, M. C., Voduc, D., Speers, C. H., . . . &Gelmon, K. (2010). Metastatic behavior of breast cancer subtypes. *J Clin Oncol, 28*(20), 3271-3277. doi:10.1200/jco.2009.25.9820

Kennett, S. B., Roberts, J. D. & Olden, K. (2004). Requirement of protein kinase C micro activation and calpain-mediated proteolysis for arachidonic acid-stimulated adhesion of MDA-MB-435 human mammary carcinoma cells to collagen type IV. *J Biol Chem, 279*(5), 3300-3307. doi:10.1074/jbc.M305734200

Keshamouni, V. G., Jagtap, P., Michailidis, G., Strahler, J. R., Kuick, R., Reka, A. K., . . . &Omenn, G. S. (2009). Temporal quantitative proteomics by iTRAQ 2D-LC-MS/MS and corresponding mRNA expression analysis identify post-transcriptional modulation of actin-cytoskeleton regulators during TGF-beta-Induced epithelial-mesenchymal transition. *J Proteome Res, 8*(1), 35-47. doi:10.1021/pr8006478

Kessler, T. & Muller, H. A. (2009). Cleavage of Armadillo/beta-catenin by the caspase DrICE in Drosophila apoptotic epithelial cells. *BMC Dev Biol, 9*, 15. doi:10.1186/1471-213x-9-15

Key, J., Hodgson, S., Omar, R. Z., Jensen, T. K., Thompson, S. G., Boobis, A. R., . . . &Elliott, P. (2006). Meta-analysis of studies of alcohol and breast cancer with consideration of the methodological issues. *Cancer Causes Control, 17*(6), 759-770. doi:10.1007/s10552-006-0011-0

Keyomarsi, K., Tucker, S. L., Buchholz, T. A., Callister, M., Ding, Y., Hortobagyi, G. N., . . . &Bacus, S. S. (2002). Cyclin E and survival in patients with breast cancer. *N Engl J Med, 347*(20), 1566-1575. doi:10.1056/NEJMoa021153

Kim, H. S., Park, I., Cho, H. J., Gwak, G., Yang, K., Bae, B. N., . . . &Kim, Y. D. (2012). Analysis of the potent prognostic factors in luminal-type breast cancer. *J Breast Cancer, 15*(4), 401-406. doi:10.4048/jbc.2012.15.4.401

Kim, J. Y., Lee, N., Kim, Y. J., Cho, Y., An, H., Oh, E., . . . &Seo, J. H. (2017). Disulfiram induces anoikis and suppresses lung colonization in triple-negative breast cancer via calpain activation. *Cancer Lett, 386*, 151-160. doi:10.1016/j.canlet.2016.11.022

Kim, M.-Y., Oskarsson, T., Acharyya, S., Nguyen, D. X., Zhang, X. H. F., Norton, L. & Massagué, J. (2009). Tumor self-seeding by circulating cancer cells. *Cell, 139*(7), 1315-1326. doi:10.1016/j.cell.2009.11.025

Kim, M. J., Jo, D. G., Hong, G. S., Kim, B. J., Lai, M., Cho, D. H., . . . &Jung, Y. K. (2002). Calpain-dependent cleavage of cain/cabin1 activates calcineurin to mediate calcium-triggered cell death. *Proc Natl Acad Sci U S A, 99*(15), 9870-9875. doi:10.1073/pnas.152336999

Kondo, Y., Higa, S., Iwasaki, T., Matsumoto, T., Maehara, K., Harada, A., . . . &Ohkawa, Y. (2018). Sensitive detection of fluorescence in western blotting by merging images. *PLoS One, 13*(1), e0191532. doi:10.1371/journal.pone.0191532

Kopp, T. I., Vogel, U., Dragsted, L. O., Tjonneland, A. & Ravn-Haren, G. (2017). Association between single nucleotide polymorphisms in the antioxidant genes CAT, GR and SOD1, erythrocyte enzyme activities, dietary and life style factors and breast cancer risk in a Danish, prospective cohort study. *Oncotarget, 8*(38), 62984-62997. doi:10.18632/oncotarget.18062

Kovács, L. & Su, Y. (2014). The critical role of calpain in cell proliferation. *J Biomol Res Ther, 3*(112), 2.

Kralik, P. & Ricchi, M. (2017). A Basic Guide to Real Time PCR in Microbial Diagnostics: Definitions, Parameters, and Everything. *Front Microbiol, 8*, 108. doi:10.3389/fmicb.2017.00108

Kubbutat, M. H. & Vousden, K. H. (1997). Proteolytic cleavage of human p53 by calpain: a potential regulator of protein stability. *Mol Cell Biol, 17*(1), 460-468.

Kulkarni, S., Reddy, K. B., Esteva, F. J., Moore, H. C., Budd, G. T. & Tubbs, R. R. (2010). Calpain regulates sensitivity to trastuzumab and survival in HER2-positive breast cancer. *Oncogene, 29*(9), 1339-1350. doi:10.1038/onc.2009.422

Kulkarni, S., Saju, L., Farver, C. & Tubbs, R. (2012). Calpain4 is required for activation of HER2 in breast cancer cells exposed to trastuzumab and its suppression decreases survival and enhances response. *Int J Cancer, 131*(10), 2420-2432. doi:10.1002/ijc.27510

Kumar, V., Abbas, A. K. & Aster, J. C. (2018). Neoplasia *Robbins basic pathology; tenth edition* (pp. 189-242). Philadelphia, PA: Elsevier Health Sciences.

Kumar, V., Abbas, A. K., Aster, J. C., Robbins, S. L., Perkins, J. A. & Ebrary, I. (2013). *Robbins basic pathology*. Philadelphia, PA: Elsevier Saunders.

Kung, M., Stadelmann, B., Brodbeck, U. & Butikofer, P. (1997). Addition of G418 and other aminoglycoside antibiotics to mammalian cells results in the release of GPI-anchored proteins. *FEBS Lett, 409*(3), 333-338. doi:10.1016/s0014-5793(97)00452-3

Kwak, H.-I., Kang, H., Dave, J. M., Mendoza, E. A., Su, S.-C., Maxwell, S. A. & Bayless, K. J. (2012). Calpain-mediated vimentin cleavage occurs upstream of MT1-MMP membrane translocation to facilitate endothelial sprout initiation. *Angiogenesis, 15*(2), 287-303. doi:10.1007/s10456-012-9262-4

Lakshmikuttyamma, A., Selvakumar, P., Kanthan, R., Kanthan, S. C. & Sharma, R. K. (2004). Overexpression of m-calpain in human colorectal adenocarcinomas. *Cancer Epidemiol Biomarkers Prev, 13*(10), 1604-1609.

Lauria, R., Perrone, F., Carlomagno, C., De Laurentiis, M., Morabito, A., Gallo, C., . . . &et al. (1995). The prognostic value of lymphatic and blood vessel invasion in operable breast cancer. *Cancer, 76*(10), 1772-1778. doi:10.1002/1097-0142(19951115)76:10<1772::aid-cncr2820761014>3.0.co;2-o

Lebart, M. C. & Benyamin, Y. (2006). Calpain involvement in the remodeling of cytoskeletal anchorage complexes. *Febs j, 273*(15), 3415-3426. doi:10.1111/j.1742-4658.2006.05350.x

Lee, A. H. & Ellis, I. O. (2008). The Nottingham prognostic index for invasive carcinoma of the breast. *Pathol Oncol Res, 14*(2), 113-115. doi:10.1007/s12253-008-9067-3

Lee, A. H., Pinder, S. E., Macmillan, R. D., Mitchell, M., Ellis, I. O., Elston, C. W. & Blamey, R. W. (2006). Prognostic value of lymphovascular invasion in women with lymph node negative invasive breast carcinoma. *Eur J Cancer, 42*(3), 357-362. doi:10.1016/j.ejca.2005.10.021

Lee, W. J., Hatanaka, M. & Maki, M. (1992a). Multiple forms of rat calpastatin cDNA in the coding region of functionally unknown amino-terminal domain. *Biochim Biophys Acta, 1129*(2), 251-253.

Lee, W. J., Ma, H., Takano, E., Yang, H. Q., Hatanaka, M. & Maki, M. (1992b). Molecular diversity in amino-terminal domains of human calpastatin by exon skipping. *J Biol Chem, 267*(12), 8437-8442.

Leloup, L. & Wells, A. (2011). Calpains as potential anti-cancer targets. *Expert Opin Ther Targets, 15*(3), 309-323. doi:10.1517/14728222.2011.553611

Leupold, J. H., Yang, H. S., Colburn, N. H., Asangani, I., Post, S. & Allgayer, H. (2007). Tumor suppressor Pdcd4 inhibits invasion/intravasation and regulates urokinase receptor (u-PAR) gene expression via Sp-transcription factors. *Oncogene, 26*(31), 4550-4562. doi:10.1038/sj.onc.1210234

Li, C. L., Yang, D., Cao, X., Wang, F., Hong, D. Y., Wang, J., . . . &Chen, Y. (2017a). Fibronectin induces epithelial-mesenchymal transition in human breast cancer MCF-7 cells via activation of calpain. *Oncol Lett, 13*(5), 3889-3895. doi:10.3892/ol.2017.5896

Li, G. & Iyengar, R. (2002). Calpain as an effector of the Gq signaling pathway for inhibition of Wnt/beta -catenin-regulated cell proliferation. *Proc Natl Acad Sci U S A, 99*(20), 13254-13259. doi:10.1073/pnas.202355799

Li, H., Nepal, R. M., Martin, A. & Berger, S. A. (2012). Induction of apoptosis in Emu-myc lymphoma cells in vitro and in vivo through calpain inhibition. *Exp Hematol, 40*(7), 548-563.e542. doi:10.1016/j.exphem.2012.02.002

Li, S. & Goldberg, E. (2000). A Novel N-Terminal Domain Directs Membrane Localization of Mouse Testis-Specific Calpastatin1. *Biology of Reproduction, 63*(6), 1594-1600. doi:10.1095/biolreprod63.6.1594

Li, S., Liang, Z.-G., Wang, G.-Y., Yavetz, B., Kim, E. D. & Goldberg, E. (2000). Molecular Cloning and Characterization of Functional Domains of a Human Testis-Specific Isoform of Calpastatin1. *Biology of Reproduction, 63*(1), 172-178. doi:10.1095/biolreprod63.1.172

Li, X., Luo, R., Chen, R., Song, L., Zhang, S., Hua, W. & Chen, H. (2014). Cleavage of IkappaBalpha by calpain induces myocardial NF-kappaB activation, TNF-alpha expression, and cardiac dysfunction in septic mice. *Am J Physiol Heart Circ Physiol, 306*(6), H833-843. doi:10.1152/ajpheart.00893.2012

Li, X., Sun, S., Li, N., Gao, J., Yu, J., Zhao, J., . . . &Zhao, Z. (2017b). High Expression of CCR7 Predicts Lymph Node Metastasis and Good Prognosis in Triple Negative Breast Cancer. *Cell Physiol Biochem, 43*(2), 531-539. doi:10.1159/000480526

Li, Z., Ortega-Vilain, A. C., Patil, G. S., Chu, D. L., Foreman, J. E., Eveleth, D. D. & Powers, J. C. (1996). Novel peptidyl alpha-keto amide inhibitors of calpains and other cysteine proteases. *J Med Chem, 39*(20), 4089-4098. doi:10.1021/jm950541c

Libertini, S. J., Robinson, B. S., Dhillon, N. K., Glick, D., George, M., Dandekar, S., . . . &Mudryj, M. (2005). Cyclin E both regulates and is regulated by calpain 2, a protease associated with metastatic breast cancer phenotype. *Cancer Res, 65*(23), 10700-10708. doi:10.1158/0008-5472.can-05-1666

Libertini, S. J., Tepper, C. G., Rodriguez, V., Asmuth, D. M., Kung, H. J. & Mudryj, M. (2007). Evidence for calpain-mediated androgen receptor cleavage as a mechanism for androgen independence. *Cancer Res, 67*(19), 9001-9005. doi:10.1158/0008-5472.can-07-1072

Liede, A., Jerzak, K. J., Hernandez, R. K., Wade, S. W., Sun, P. & Narod, S. A. (2016). The incidence of bone metastasis after early-stage breast cancer in Canada. *Breast Cancer Res Treat, 156*(3), 587-595. doi:10.1007/s10549-016-3782-3

Limame, R., Wouters, A., Pauwels, B., Fransen, E., Peeters, M., Lardon, F., . . . &Pauwels, P. (2012). Comparative analysis of dynamic cell viability, migration and invasion assessments by novel real-time technology and classic endpoint assays. *PLoS One, 7*(10), e46536. doi:10.1371/journal.pone.0046536

Liotta, L. A., Steeg, P. S. & Stetler-Stevenson, W. G. (1991). Cancer metastasis and angiogenesis: an imbalance of positive and negative regulation. *Cell, 64*(2), 327-336.

Liu, B., Zhou, Y., Lu, D., Liu, Y., Zhang, S. Q., Xu, Y., . . . &Gu, X. (2017). Comparison of the protein expression of calpain-1, calpain-2, calpastatin and calmodulin between gastric cancer and normal gastric mucosa. *Oncol Lett, 14*(3), 3705-3710. doi:10.3892/ol.2017.6617

Liu, L., Xing, D. & Chen, W. R. (2009). Micro-calpain regulates caspase-dependent and apoptosis inducing factor-mediated caspase-independent apoptotic pathways

in cisplatin-induced apoptosis. *Int J Cancer, 125*(12), 2757-2766. doi:10.1002/ijc.24626

Liu, T. L., Shimada, H., Ochiai, T., Shiratori, T., Lin, S. E., Kitagawa, M., . . . &Hiwasa, T. (2006). Enhancement of chemosensitivity toward peplomycin by calpastatin-stabilized NF-kappaB p65 in esophageal carcinoma cells: possible involvement of Fas/Fas-L synergism. *Apoptosis, 11*(6), 1025-1037. doi:10.1007/s10495-006-6353-y

Lokuta, M. A., Nuzzi, P. A. & Huttenlocher, A. (2003). Calpain regulates neutrophil chemotaxis. *Proc Natl Acad Sci U S A, 100*(7), 4006-4011. doi:10.1073/pnas.0636533100

Louwman, W. J., Voogd, A. C., van Dijck, J. A., Nieuwenhuijzen, G. A., Ribot, J., Pruijt, J. F. & Coebergh, J. W. (2008). On the rising trends of incidence and prognosis for breast cancer patients diagnosed 1975-2004: a long-term population-based study in southeastern Netherlands. *Cancer Causes Control, 19*(1), 97-106. doi:10.1007/s10552-007-9075-8

Lu, T., Xu, Y., Mericle, M. T. & Mellgren, R. L. (2002). Participation of the conventional calpains in apoptosis. *Biochim Biophys Acta, 1590*(1-3), 16-26. doi:10.1016/s0167-4889(02)00193-3

Lymburner, S., McLeod, S., Purtzki, M., Roskelley, C. & Xu, Z. (2013). Zinc inhibits magnesium-dependent migration of human breast cancer MDA-MB-231 cells on fibronectin. *J Nutr Biochem, 24*(6), 1034-1040. doi:10.1016/j.jnutbio.2012.07.013

Ma, H., Yang, H. Q., Takano, E., Hatanaka, M. & Maki, M. (1994). Amino-terminal conserved region in proteinase inhibitor domain of calpastatin potentiates its calpain inhibitory activity by interacting with calmodulin-like domain of the proteinase. *J Biol Chem, 269*(39), 24430-24436.

Ma, W., Han, W., Greer, P. A., Tuder, R. M., Toque, H. A., Wang, K. K. W., . . . &Su, Y. (2011). Calpain mediates pulmonary vascular remodeling in rodent models of pulmonary hypertension, and its inhibition attenuates pathologic features of disease. *The Journal of clinical investigation, 121*(11), 4548-4566. doi:10.1172/JCI57734

Machado, V. M., Lourenço, A. S., Florindo, C., Fernandes, R., Carvalho, C. M. & Araújo, I. M. (2017). Calpastatin Overexpression Preserves Cognitive Function Following Seizures, While Maintaining Post-Injury Neurogenesis. *Frontiers in molecular neuroscience, 10*, 60-60. doi:10.3389/fnmol.2017.00060

Machado, V. M., Morte, M. I., Carreira, B. P., Azevedo, M. M., Takano, J., Iwata, N., . . . &Araujo, I. M. (2015). Involvement of calpains in adult neurogenesis: implications for stroke. *Front Cell Neurosci, 9*, 22. doi:10.3389/fncel.2015.00022

Maki, M., Bagci, H., Hamaguchi, K., Ueda, M., Murachi, T. & Hatanaka, M. (1989). Inhibition of calpain by a synthetic oligopeptide corresponding to an exon of the human calpastatin gene. *J Biol Chem, 264*(32), 18866-18869.

Maki, M., Takano, E., Mori, H., Kannagi, R., Murachi, T. & Hatanaka, M. (1987a). Repetitive region of calpastatin is a functional unit of the proteinase inhibitor. *Biochem Biophys Res Commun, 143*(1), 300-308.

Maki, M., Takano, E., Mori, H., Sato, A., Murachi, T. & Hatanaka, M. (1987b). All four internally repetitive domains of pig calpastatin possess inhibitory activities against calpains I and II. *FEBS Lett, 223*(1), 174-180.

Maki, M., Takano, E., Osawa, T., Ooi, T., Murachi, T. & Hatanaka, M. (1988). Analysis of structure-function relationship of pig calpastatin by expression of mutated cDNAs in Escherichia coli. *J Biol Chem, 263*(21), 10254-10261.

Maldonado, E. M., Svensson, D., Oredsson, S. M. & Sterner, O. (2014). Cytotoxic Sesquiterpene Lactones from Kauna lasiophthalma Griseb. *Sci Pharm, 82*(1), 147-160. doi:10.3797/scipharm.1310-18

Mamoune, A., Luo, J. H., Lauffenburger, D. A. & Wells, A. (2003). Calpain-2 as a target for limiting prostate cancer invasion. *Cancer Res, 63*(15), 4632-4640.

Mao, K., Yang, Y., Wu, W., Liang, S., Deng, H. & Liu, J. (2017). Risk of second breast cancers after lobular carcinoma in situ according to hormone receptor status. *PLoS One, 12*(5), e0176417. doi:10.1371/journal.pone.0176417

Marciel, M. P. & Hoffmann, P. R. (2017). Selenoproteins and Metastasis. *Adv Cancer Res, 136*, 85-108. doi:10.1016/bs.acr.2017.07.008

Martin, T. A., Ye, L., Sanders, A. J., Lane, J. & Jiang, W. G. (2013). Cancer invasion and metastasis: molecular and cellular perspective.

Martinez, J. A., Zhang, Z., Svetlov, S. I., Hayes, R. L., Wang, K. K. & Larner, S. F. (2010). Calpain and caspase processing of caspase-12 contribute to the ER stress-induced cell death pathway in differentiated PC12 cells. *Apoptosis, 15*(12), 1480-1493. doi:10.1007/s10495-010-0526-4

Martino, M., Ballestrero, A., Zambelli, A., Secondino, S., Aieta, M., Bengala, C., . . . &Pedrazzoli, P. (2013). Long-term survival in patients with metastatic breast cancer receiving intensified chemotherapy and stem cell rescue: data from the Italian registry. *Bone Marrow Transplant, 48*(3), 414-418. doi:10.1038/bmt.2012.149

Mazars, R., Spinardi, L., BenCheikh, M., Simony-Lafontaine, J., Jeanteur, P. & Theillet, C. (1992). p53 mutations occur in aggressive breast cancer. *Cancer Res, 52*(14), 3918-3923.

McMahon, S. B. (2014). MYC and the control of apoptosis. *Cold Spring Harb Perspect Med, 4*(7), a014407. doi:10.1101/cshperspect.a014407

Medina, P. J. & Shord, S. S. (2011). Cancer Treatment and Chemotherapy. In J. T. DiPiro, R. L. Talbert, G. C. Yee, M. G. R., B. G. L. Wells, & M. Posey (Eds.), *Pharmacotherapy: A Pathophysiologic Approach* (8th ed., pp. 2191-2228): McGraw-Hill Medical.

Menezes, M. E., Das, S. K., Minn, I., Emdad, L., Wang, X. Y., Sarkar, D., . . . &Fisher, P. B. (2016). Detecting Tumor Metastases: The Road to Therapy Starts Here. *Adv Cancer Res, 132*, 1-44. doi:10.1016/bs.acr.2016.07.001

Meng, X. N., Jin, Y., Yu, Y., Bai, J., Liu, G. Y., Zhu, J., . . . &Fu, S. B. (2009). Characterisation of fibronectin-mediated FAK signalling pathways in lung cancer cell migration and invasion. *Br J Cancer, 101*(2), 327-334. doi:10.1038/sj.bjc.6605154

Menon, R., Im, H., Zhang, E. Y., Wu, S. L., Chen, R., Snyder, M., . . . &Omenn, G. S. (2014). Distinct splice variants and pathway enrichment in the cell-line models of aggressive human breast cancer subtypes. *J Proteome Res, 13*(1), 212-227. doi:10.1021/pr400773v

Meredith, J., Jr., Mu, Z., Saido, T. & Du, X. (1998). Cleavage of the cytoplasmic domain of the integrin beta3 subunit during endothelial cell apoptosis. *J Biol Chem, 273*(31), 19525-19531. doi:10.1074/jbc.273.31.19525

Michaud, L. B., Barnett, C. M. & Esteva, F. J. (2011). Breast cancer. In J. T. DiPiro, R. L. Talbert, G. C. Yee, G. R. Matzke, B. G. L. Wells, & M. Posey (Eds.), *Pharmacotherapy: A Pathophysiologic Approach: A Pathophysiologic Approach* (8th ed.). New York: McGraw-Hill.

Mikawa, K. (1990). Studies on proteolysis of protein kinase C with calpain I and II. *Kobe J Med Sci, 36*(1-2), 55-69.

Minami, Y., Emori, Y., Kawasaki, H. & Suzuki, K. (1987). E-F hand structure-domain of calcium-activated neutral protease (CANP) can bind Ca2+ ions. *J Biochem, 101*(4), 889-895.

Minn, A. J., Gupta, G. P., Siegel, P. M., Bos, P. D., Shu, W., Giri, D. D., . . . &Massague, J. (2005). Genes that mediate breast cancer metastasis to lung. *Nature, 436*(7050), 518-524. doi:10.1038/nature03799

Minn, A. J. & Massave, J. (2011). Invasion and metastases. In V. T. DeVita, S. Hellman, & S. A. Rosenberg (Eds.), *Cancer: Principles and Practice of Oncology* (9th ed.). Philadelphia, PA: Lippincott Williams & Wilkins.

Minobe, E., Hao, L. Y., Saud, Z. A., Xu, J. J., Kameyama, A., Maki, M., . . . &Kameyama, M. (2006). A region of calpastatin domain L that reprimes cardiac L-type Ca2+ channels. *Biochem Biophys Res Commun, 348*(1), 288-294. doi:10.1016/j.bbrc.2006.07.052

Miyazaki, T. & Miyazaki, A. (2018). Dysregulation of Calpain Proteolytic Systems Underlies Degenerative Vascular Disorders. *J Atheroscler Thromb, 25*(1), 1-15. doi:10.5551/jat.RV17008

Mlynarczuk-Bialy, I., Roeckmann, H., Kuckelkorn, U., Schmidt, B., Umbreen, S., Golab, J., . . . &Seifert, U. (2006). Combined effect of proteasome and calpain inhibition on cisplatin-resistant human melanoma cells. *Cancer Res, 66*(15), 7598-7605. doi:10.1158/0008-5472.can-05-2614

Mohammed, R. A., Ellis, I. O., Elsheikh, S., Paish, E. C. & Martin, S. G. (2009a). Lymphatic and angiogenic characteristics in breast cancer: morphometric analysis and prognostic implications. *Breast Cancer Res Treat, 113*(2), 261-273. doi:10.1007/s10549-008-9936-1

Mohammed, R. A., Ellis, I. O., Lee, A. H. & Martin, S. G. (2009b). Vascular invasion in breast cancer; an overview of recent prognostic developments and molecular pathophysiological mechanisms. *Histopathology, 55*(1), 1-9. doi:10.1111/j.1365-2559.2008.03169.x

Mohammed, R. A., Martin, S. G., Gill, M. S., Green, A. R., Paish, E. C. & Ellis, I. O. (2007). Improved methods of detection of lymphovascular invasion demonstrate that it is the predominant method of vascular invasion in breast cancer and has important clinical consequences. *Am J Surg Pathol, 31*(12), 1825-1833. doi:10.1097/PAS.0b013e31806841f6

Mohammed, R. A., Martin, S. G., Mahmmod, A. M., Macmillan, R. D., Green, A. R., Paish, E. C. & Ellis, I. O. (2011). Objective assessment of lymphatic and blood vascular invasion in lymph node-negative breast carcinoma: findings from a large case series with long-term follow-up. *J Pathol, 223*(3), 358-365. doi:10.1002/path.2810

Mohammed, R. A., Menon, S., Martin, S. G., Green, A. R., Paish, E. C. & Ellis, I. O. (2014). Prognostic significance of lymphatic invasion in lymph node-positive breast carcinoma: findings from a large case series with long-term follow-up using immunohistochemical endothelial marker. *Mod Pathol, 27*(12), 1568-1577. doi:10.1038/modpathol.2014.60

Moldoveanu, T., Gehring, K. & Green, D. R. (2008). Concerted multi-pronged attack by calpastatin to occlude the catalytic cleft of heterodimeric calpains. *Nature, 456*(7220), 404-408. doi:10.1038/nature07353

Moldoveanu, T., Hosfield, C. M., Lim, D., Elce, J. S., Jia, Z. & Davies, P. L. (2002a). A Ca 2+ switch aligns the active site of calpain. *Cell, 108*(5), 649-660.

Moldoveanu, T., Hosfield, C. M., Lim, D., Elce, J. S., Jia, Z. & Davies, P. L. (2002b). A Ca(2+) switch aligns the active site of calpain. *Cell, 108*(5), 649-660.

Moldoveanu, T., Jia, Z. & Davies, P. L. (2004). Calpain activation by cooperative Ca2+ binding at two non-EF-hand sites. *J Biol Chem, 279*(7), 6106-6114. doi:10.1074/jbc.M310460200

Molinari, M., Anagli, J. & Carafoli, E. (1994). Ca (2+)-activated neutral protease is active in the erythrocyte membrane in its nonautolyzed 80-kDa form. *Journal of Biological Chemistry, 269*(45), 27992-27995.

Morch, L. S., Hannaford, P. C. & Lidegaard, O. (2018). Contemporary Hormonal Contraception and the Risk of Breast Cancer. *N Engl J Med, 378*(13), 1265-1266. doi:10.1056/NEJMc1800054

Moretti, D., Del Bello, B., Allavena, G. & Maellaro, E. (2014). Calpains and cancer: friends or enemies? *Arch Biochem Biophys, 564*, 26-36. doi:10.1016/j.abb.2014.09.018

Mosly, D., Turnbull, A., Sims, A., Ward, C. & Langdon, S. (2018). Predictive markers of endocrine response in breast cancer. *World journal of experimental medicine, 8*(1), 1.

Mota, A. L., Evangelista, A. F., Macedo, T., Oliveira, R., Scapulatempo-Neto, C., Vieira, R. A. & Marques, M. M. C. (2017). Molecular characterization of breast cancer cell lines by clinical immunohistochemical markers. *Oncol Lett, 13*(6), 4708-4712. doi:10.3892/ol.2017.6093

Moutasim, K. A., Nystrom, M. L. & Thomas, G. J. (2011). Cell migration and invasion assays. *Methods Mol Biol, 731*, 333-343. doi:10.1007/978-1-61779-080-5_27

Mtango, N. R., Potireddy, S. & Latham, K. E. (2008). Oocyte quality and maternal control of development. *Int Rev Cell Mol Biol, 268*, 223-290. doi:10.1016/s1937-6448(08)00807-1

Mukherjee, A. (2004). *AW64 a novel thioredoxin inhibitor.* University of Nottingham.

Murachi, T. (1989). Intracellular regulatory system involving calpain and calpastatin. *Biochem Int, 18*(2), 263-294.

Musolino, A., Ciccolallo, L., Panebianco, M., Fontana, E., Zanoni, D., Bozzetti, C., . . . &Ardizzoni, A. (2011). Multifactorial central nervous system recurrence susceptibility in patients with HER2-positive breast cancer: epidemiological and clinical data from a population-based cancer registry study. *Cancer, 117*(9), 1837-1846. doi:10.1002/cncr.25771

Nagao, T., Kinoshita, T., Hojo, T., Tsuda, H., Tamura, K. & Fujiwara, Y. (2012). The differences in the histological types of breast cancer and the response to neoadjuvant chemotherapy: the relationship between the outcome and the clinicopathological characteristics. *Breast, 21*(3), 289-295. doi:10.1016/j.breast.2011.12.011

Nakagawa, K., Masumoto, H., Sorimachi, H. & Suzuki, K. (2001). Dissociation of m-calpain subunits occurs after autolysis of the N-terminus of the catalytic subunit, and is not required for activation. *J Biochem, 130*(5), 605-611.

Narod, S., Ford, D., Devilee, P., Barkardottir, R. B., Eyfjord, J., Lenoir, G., . . . &Goldgar, D. (1995). Genetic heterogeneity of breast-ovarian cancer revisited. Breast Cancer Linkage Consortium. *Am J Hum Genet, 57*(4), 957-958.

Nathanson, S. D., Kwon, D., Kapke, A., Alford, S. H. & Chitale, D. (2009). The role of lymph node metastasis in the systemic dissemination of breast cancer. *Ann Surg Oncol, 16*(12), 3396-3405. doi:10.1245/s10434-009-0659-2

National Center for Biotechnology Information, U. (2019, 12 May 2019). CAST calpastatin [Homo sapiens (human)]. Retrieved from https://www.ncbi.nlm.nih.gov/gene?Db=gene&Cmd=DetailsSearch&Term=831

Nayerossadat, N., Maedeh, T. & Ali, P. A. (2012). Viral and nonviral delivery systems for gene delivery. *Advanced biomedical research, 1*, 27-27. doi:10.4103/2277-9175.98152

Nelson, M., Millican-Slater, R., Forrest, L. C. & Brackenbury, W. J. (2014). The sodium channel beta1 subunit mediates outgrowth of neurite-like processes on breast cancer cells and promotes tumour growth and metastasis. *Int J Cancer, 135*(10), 2338-2351. doi:10.1002/ijc.28890

Ngeow, J., Sesock, K. & Eng, C. (2017). Breast cancer risk and clinical implications for germline PTEN mutation carriers. *Breast Cancer Res Treat, 165*(1), 1-8. doi:10.1007/s10549-015-3665-z

Nguyen, D. X., Bos, P. D. & Massague, J. (2009). Metastasis: from dissemination to organ-specific colonization. *Nat Rev Cancer, 9*(4), 274-284. doi:10.1038/nrc2622

Nguyen, H. T. & Chen, M. (2014). High-energy compounds mobilize intracellular Ca2+ and activate calpain in cultured cells: is calpain an energy-dependent protease? *Brain Res Bull, 102*, 9-14. doi:10.1016/j.brainresbull.2014.01.006

Niapour, M., Yu, Y. & Berger, S. A. (2008). Regulation of calpain activity by c-Myc through calpastatin and promotion of transformation in c-Myc-negative cells by calpastatin suppression. *J Biol Chem, 283*(31), 21371-21381. doi:10.1074/jbc.M801462200

NIHR Innovation Observatory. (2015). The Nottingham Prognostic Index Plus test for breast cancer management. Retrieved from NIHR Innovation Observatory website: http://www.io.nihr.ac.uk/wp-content/uploads/migrated/2751.b7628239.FINALNPItestforbreastcancer.pdf

Nikfarjam, L. & Farzaneh, P. (2012). Prevention and detection of Mycoplasma contamination in cell culture. *Cell J, 13*(4), 203-212.

Nime, F. A., Rosen, P. P., Thaler, H. T., Ashikari, R. & Urban, J. A. (1977). Prognostic significance of tumor emboli in intramammary lymphatics in patients with mammary carcinoma. *Am J Surg Pathol, 1*(1), 25-30. doi:10.1097/00000478-197701010-00003

Nims, R. W., Sykes, G., Cottrill, K., Ikonomi, P. & Elmore, E. (2010). Short tandem repeat profiling: part of an overall strategy for reducing the frequency of cell misidentification. *In Vitro Cell Dev Biol Anim, 46*(10), 811-819. doi:10.1007/s11626-010-9352-9

Novikov, O., Wang, Z., Stanford, E. A., Parks, A. J., Ramirez-Cardenas, A., Landesman, E., . . . &Sherr, D. H. (2016). An Aryl Hydrocarbon Receptor-Mediated Amplification Loop That Enforces Cell Migration in ER-/PR-/Her2- Human Breast Cancer Cells. *Mol Pharmacol, 90*(5), 674-688. doi:10.1124/mol.116.105361

O'Shaughnessy, J. (2005). Extending survival with chemotherapy in metastatic breast cancer. *Oncologist, 10 Suppl 3*, 20-29. doi:10.1634/theoncologist.10-90003-20

Ohtani, O. & Ohtani, Y. (2012). Recent developments in morphology of lymphatic vessels and lymph nodes. *Ann Vasc Dis, 5*(2), 145-150. doi:10.3400/avd.ra.11.00099

Oliver, G. & Alitalo, K. (2005). The lymphatic vasculature: recent progress and paradigms. *Annu Rev Cell Dev Biol, 21*, 457-483. doi:10.1146/annurev.cellbio.21.012704.132338

Ono, Y., Saido, T. C. & Sorimachi, H. (2016). Calpain research for drug discovery: challenges and potential. *Nat Rev Drug Discov, 15*(12), 854-876. doi:10.1038/nrd.2016.212

Ono, Y. & Sorimachi, H. (2012). Calpains: an elaborate proteolytic system. *Biochim Biophys Acta, 1824*(1), 224-236. doi:10.1016/j.bbapap.2011.08.005

Osman, D., Gobert, V., Ponthan, F., Heidenreich, O., Haenlin, M. & Waltzer, L. (2009). A Drosophila model identifies calpains as modulators of the human leukemogenic fusion protein AML1-ETO. *Proc Natl Acad Sci U S A, 106*(29), 12043-12048. doi:10.1073/pnas.0902449106

Pachmayr, E., Treese, C. & Stein, U. (2017). Underlying Mechanisms for Distant Metastasis - Molecular Biology. *Visc Med, 33*(1), 11-20. doi:10.1159/000454696

Paget, S. (1989). The distribution of secondary growths in cancer of the breast. 1889. *Cancer Metastasis Rev, 8*(2), 98-101.

Pal, G. P., Elce, J. S. & Jia, Z. (2001). Dissociation and aggregation of calpain in the presence of calcium. *J Biol Chem, 276*(50), 47233-47238. doi:10.1074/jbc.M105149200

Palmantier, R., Roberts, J. D., Glasgow, W. C., Eling, T. & Olden, K. (1996). Regulation of the adhesion of a human breast carcinoma cell line to type IV collagen and vitronectin: roles for lipoxygenase and protein kinase C. *Cancer Res, 56*(9), 2206-2212.

Palmieri, D., Bronder, J. L., Herring, J. M., Yoneda, T., Weil, R. J., Stark, A. M., . . . &Steeg, P. S. (2007). Her-2 overexpression increases the metastatic outgrowth of breast cancer cells in the brain. *Cancer Res, 67*(9), 4190-4198. doi:10.1158/0008-5472.can-06-3316

Pantel, K. & Brakenhoff, R. H. (2004). Dissecting the metastatic cascade. *Nat Rev Cancer, 4*(6), 448-456. doi:10.1038/nrc1370

Pariat, M., Carillo, S., Molinari, M., Salvat, C., Debussche, L., Bracco, L., . . . &Piechaczyk, M. (1997). Proteolysis by calpains: a possible contribution to degradation of p53. *Mol Cell Biol, 17*(5), 2806-2815.

Parkin, D. & Boyd, L. (2011). 8. Cancers attributable to overweight and obesity in the UK in 2010. *Br J Cancer, 105*(S2), S34.

Parkin, D. M., Bray, F., Ferlay, J. & Pisani, P. (2005). Global cancer statistics, 2002. *CA Cancer J Clin, 55*(2), 74-108.

Parr, T., Jewell, K. K., Sensky, P. L., Brameld, J. M., Bardsley, R. G. & Buttery, P. J. (2004). Expression of calpastatin isoforms in muscle and functionality of multiple calpastatin promoters. *Arch Biochem Biophys, 427*(1), 8-15. doi:10.1016/j.abb.2004.04.001

Parr, T., Sensky, P. L., Bardsley, R. G. & Buttery, P. J. (2001a). Calpastatin expression in porcine cardiac and skeletal muscle and partial gene structure. *Arch Biochem Biophys, 395*(1), 1-13. doi:10.1006/abbi.2001.2546

Parr, T., Sensky, P. L., Bardsley, R. G. & Buttery, P. J. (2001b). Calpastatin expression in porcine cardiac and skeletal muscle and partial gene structure. *Arch Biochem Biophys, 395*(1), 1-13.

Pasqualini, R. & Ruoslahti, E. (1996). Organ targeting in vivo using phage display peptide libraries. *Nature, 380*(6572), 364-366. doi:10.1038/380364a0

Pelley, R. P., Chinnakannu, K., Murthy, S., Strickland, F. M., Menon, M., Dou, Q. P., . . . &Reddy, G. P. (2006). Calmodulin-androgen receptor (AR) interaction: calcium-dependent, calpain-mediated breakdown of AR in LNCaP prostate cancer cells. *Cancer Res, 66*(24), 11754-11762. doi:10.1158/0008-5472.can-06-2918

Peng, P., Min, L., Song, S., Zhao, J., Li, L., Yang, C., . . . &Gu, J. (2016a). Elevated Expression of Calpain-4 Predicts Poor Prognosis in Patients with Gastric Cancer after Gastrectomy. *Int J Mol Sci, 17*(10). doi:10.3390/ijms17101612

Peng, P., Wu, W., Zhao, J., Song, S., Wang, X., Jia, D., . . . &Gu, J. (2016b). Decreased expression of Calpain-9 predicts unfavorable prognosis in patients with gastric cancer. *Sci Rep, 6*, 29604. doi:10.1038/srep29604

Pepper, M. S. & Skobe, M. (2003). Lymphatic endothelium: morphological, molecular and functional properties. *J Cell Biol, 163*(2), 209-213. doi:10.1083/jcb.200308082

Pepper, M. S., Tille, J. C., Nisato, R. & Skobe, M. (2003). Lymphangiogenesis and tumor metastasis. *Cell Tissue Res, 314*(1), 167-177. doi:10.1007/s00441-003-0748-7

Perou, C. M., Sorlie, T., Eisen, M. B., van de Rijn, M., Jeffrey, S. S., Rees, C. A., . . . &Botstein, D. (2000). Molecular portraits of human breast tumours. *Nature, 406*(6797), 747-752. doi:10.1038/35021093

Perrin, B. J., Amann, K. J. & Huttenlocher, A. (2006). Proteolysis of cortactin by calpain regulates membrane protrusion during cell migration. *Mol Biol Cell, 17*(1), 239-250. doi:10.1091/mbc.e05-06-0488

Pestalozzi, B. C., Zahrieh, D., Price, K. N., Holmberg, S. B., Lindtner, J., Collins, J., . . . &Goldhirsch, A. (2006). Identifying breast cancer patients at risk for Central Nervous System (CNS) metastases in trials of the International Breast Cancer Study Group (IBCSG). *Ann Oncol, 17*(6), 935-944. doi:10.1093/annonc/mdl064

Pharoah, P. D., Day, N. E. & Caldas, C. (1999). Somatic mutations in the p53 gene and prognosis in breast cancer: a meta-analysis. *Br J Cancer, 80*(12), 1968-1973. doi:10.1038/sj.bjc.6690628

Pianetti, S., Arsura, M., Romieu-Mourez, R., Coffey, R. J. & Sonenshein, G. E. (2001). Her-2/neu overexpression induces NF-kappaB via a PI3-kinase/Akt pathway involving calpain-mediated degradation of IkappaB-alpha that can be inhibited by the tumor suppressor PTEN. *Oncogene, 20*(11), 1287-1299. doi:10.1038/sj.onc.1204257

Pichot, C. S., Hartig, S. M., Xia, L., Arvanitis, C., Monisvais, D., Lee, F. Y., . . . &Corey, S. J. (2009). Dasatinib synergizes with doxorubicin to block growth, migration, and invasion of breast cancer cells. *Br J Cancer, 101*(1), 38-47. doi:10.1038/sj.bjc.6605101

Pilco-Ferreto, N. & Calaf, G. M. (2016). Influence of doxorubicin on apoptosis and oxidative stress in breast cancer cell lines. *Int J Oncol, 49*(2), 753-762. doi:10.3892/ijo.2016.3558

Pinder, S. E., Ellis, I. O., Galea, M., O'Rouke, S., Blamey, R. W. & Elston, C. W. (1994). Pathological prognostic factors in breast cancer. III. Vascular invasion: relationship with recurrence and survival in a large study with long-term follow-up. *Histopathology, 24*(1), 41-47. doi:10.1111/j.1365-2559.1994.tb01269.x

Piva, R., Belardo, G. & Santoro, M. G. (2006). NF-kappaB: a stress-regulated switch for cell survival. *Antioxid Redox Signal, 8*(3-4), 478-486. doi:10.1089/ars.2006.8.478

Polster, B. M., Basanez, G., Etxebarria, A., Hardwick, J. M. & Nicholls, D. G. (2005). Calpain I induces cleavage and release of apoptosis-inducing factor from isolated mitochondria. *J Biol Chem, 280*(8), 6447-6454. doi:10.1074/jbc.M413269200

Popp, O., Heidinger, M., Ruiz-Heinrich, L., Ries, C., Jochum, M. & Gil-Parrado, S. (2003). The calpastatin-derived calpain inhibitor CP1B reduces mRNA expression of matrix metalloproteinase-2 and -9 and invasion by leukemic THP-1 cells. *Biol Chem, 384*(6), 951-958. doi:10.1515/bc.2003.107

Porn-Ares, M. I., Samali, A. & Orrenius, S. (1998). Cleavage of the calpain inhibitor, calpastatin, during apoptosis. *Cell Death Differ, 5*(12), 1028-1033. doi:10.1038/sj.cdd.4400424

Poste, G. & Fidler, I. J. (1980). The pathogenesis of cancer metastasis. *Nature, 283*(5743), 139-146.

Postovit, L. M., Dutt, P., Dourdin, N., Park, M., Greer, P. A., Graham, C. H. & Elce, J. S. (2002). Calpain is required for MMP-2 and u-PA expression in SV40 large T-antigen-immortalized cells. *Biochem Biophys Res Commun, 297*(2), 294-301.

Potter, D. A., Srirangam, A., Fiacco, K. A., Brocks, D., Hawes, J., Herndon, C., . . . &Herman, I. M. (2003). Calpain regulates enterocyte brush border actin assembly and pathogenic Escherichia coli-mediated effacement. *J Biol Chem, 278*(32), 30403-30412. doi:10.1074/jbc.M304616200

Potter, D. A., Tirnauer, J. S., Janssen, R., Croall, D. E., Hughes, C. N., Fiacco, K. A., . . . &Herman, I. M. (1998). Calpain regulates actin remodeling during cell spreading. *J Cell Biol, 141*(3), 647-662. doi:10.1083/jcb.141.3.647

Potz, B. A., Abid, M. R. & Sellke, F. W. (2016). Role of Calpain in Pathogenesis of Human Disease Processes. *J Nat Sci, 2*(9).

Prangsaengtong, O., Senda, K., Doki, Y., Park, J. Y., Jo, M., Sakurai, H., . . . &Koizumi, K. (2012). Calpain 1 and -2 play opposite roles in cord formation of lymphatic endothelial cells via eNOS regulation. *Hum Cell, 25*(2), 36-44. doi:10.1007/s13577-012-0042-7

Prat, A., Adamo, B., Cheang, M. C., Anders, C. K., Carey, L. A. & Perou, C. M. (2013). Molecular characterization of basal-like and non-basal-like triple-negative breast cancer. *Oncologist, 18*(2), 123-133. doi:10.1634/theoncologist.2012-0397

Prat, A., Bianchini, G., Thomas, M., Belousov, A., Cheang, M. C., Koehler, A., . . . &Baselga, J. (2014). Research-based PAM50 subtype predictor identifies higher responses and improved survival outcomes in HER2-positive breast cancer in the NOAH study. *Clin Cancer Res, 20*(2), 511-521. doi:10.1158/1078-0432.ccr-13-0239

Prat, A., Pascual, T. & Adamo, B. (2017). Intrinsic molecular subtypes of HER2+ breast cancer. *Oncotarget, 8*(43), 73362-73363. doi:10.18632/oncotarget.20629

Prat, A., Pineda, E., Adamo, B., Galvan, P., Fernandez, A., Gaba, L., . . . &Munoz, M. (2015). Clinical implications of the intrinsic molecular subtypes of breast cancer. *Breast, 24 Suppl 2*, S26-35. doi:10.1016/j.breast.2015.07.008

Pu, X. (2016). *Role of calpain in breast cancer and regulation of therapeutic response to targeted treatment (Doctoral thesis).* University of Nottingham.

Pu, X., Storr, S. J., Ahmad, N. S., Chan, S. Y., Moseley, P. M., Televantou, D., . . . &Martin, S. G. (2016). Calpain-1 is associated with adverse relapse free survival in breast cancer: a confirmatory study. *Histopathology, 68*(7), 1021-1029. doi:10.1111/his.12896

Punglia, R. S., Bifolck, K., Golshan, M., Lehman, C., Collins, L., Polyak, K., . . . &Schnitt, S. J. (2018). Epidemiology, Biology, Treatment, and Prevention of Ductal Carcinoma In Situ (DCIS). *JNCI cancer spectrum, 2*(4), pky063.

Putri, H., Jenie, R. I., Handayani, S., Kastian, R. F. & Meiyanto, E. (2016). Combination of Potassium Pentagamavunon-0 and Doxorubicin Induces Apoptosis and Cell Cycle Arrest and Inhibits Metastasis in Breast Cancer Cells. *Asian Pac J Cancer Prev, 17*(5), 2683-2688.

Pylayeva-Gupta, Y., Grabocka, E. & Bar-Sagi, D. (2011). RAS oncogenes: weaving a tumorigenic web. *Nat Rev Cancer, 11*(11), 761-774. doi:10.1038/nrc3106

Qu, J., Adam, J., Bloxham, D. M., Bruckdorfer, K. R., Miller, N. G., Parkinson, N. A. & Lucy, J. A. (2000). Phosphatidylserine-dependent adhesion of T cells to endothelial cells. *Biochim Biophys Acta, 1501*(2-3), 99-115. doi:10.1016/s0925-4439(00)00022-3

Rahal, O. M., Wolfe, A. R., Mandal, P. K., Larson, R., Tin, S., Jimenez, C., . . . &Woodward, W. A. (2018). Blocking Interleukin (IL)4- and IL13-Mediated Phosphorylation of

STAT6 (Tyr641) Decreases M2 Polarization of Macrophages and Protects Against Macrophage-Mediated Radioresistance of Inflammatory Breast Cancer. *Int J Radiat Oncol Biol Phys, 100*(4), 1034-1043. doi:10.1016/j.ijrobp.2017.11.043

Raica, M., Jitariu, A. A. & Cimpean, A. M. (2016). Lymphangiogenesis and Anti-lymphangiogenesis in Cutaneous Melanoma. *Anticancer Res, 36*(9), 4427-4435. doi:10.21873/anticanres.10986

Raimbourg, Q., Perez, J., Vandermeersch, S., Prignon, A., Hanouna, G., Haymann, J. P., . . . &Letavernier, E. (2013). The calpain/calpastatin system has opposing roles in growth and metastatic dissemination of melanoma. *PLoS One, 8*(4), e60469. doi:10.1371/journal.pone.0060469

Rakha, E. A., Reis-Filho, J. S. & Ellis, I. O. (2008). Basal-like breast cancer: a critical review. *J Clin Oncol, 26*(15), 2568-2581. doi:10.1200/jco.2007.13.1748

Rakha, E. A., Soria, D., Green, A. R., Lemetre, C., Powe, D. G., Nolan, C. C., . . . &Ellis, I. O. (2014). Nottingham Prognostic Index Plus (NPI+): a modern clinical decision making tool in breast cancer. *Br J Cancer, 110*(7), 1688-1697. doi:10.1038/bjc.2014.120

Rao, S., Morales, A. A. & Pearse, D. D. (2015). The Comparative Utility of Viromer RED and Lipofectamine for Transient Gene Introduction into Glial Cells. *Biomed Res Int, 2015*, 458624. doi:10.1155/2015/458624

Ravulapalli, R., Campbell, R. L., Gauthier, S. Y., Dhe-Paganon, S. & Davies, P. L. (2009). Distinguishing between calpain heterodimerization and homodimerization. *Febs j, 276*(4), 973-982. doi:10.1111/j.1742-4658.2008.06833.x

Ray, S. K., Fidan, M., Nowak, M. W., Wilford, G. G., Hogan, E. L. & Banik, N. L. (2000). Oxidative stress and Ca2+ influx upregulate calpain and induce apoptosis in PC12 cells. *Brain Res, 852*(2), 326-334. doi:10.1016/s0006-8993(99)02148-4

Reid, Y., Storts, D., Riss, T. & Minor, L. (2013). Authentication of human cell lines by STR DNA profiling analysis.

Reverter, D., Strobl, S., Fernandez-Catalan, C., Sorimachi, H., Suzuki, K. & Bode, W. (2001). Structural basis for possible calcium-induced activation mechanisms of calpains. *Biol Chem, 382*(5), 753-766. doi:10.1515/bc.2001.091

Ribatti, D., Mangialardi, G. & Vacca, A. (2006). Stephen Paget and the 'seed and soil' theory of metastatic dissemination. *Clin Exp Med, 6*(4), 145-149. doi:10.1007/s10238-006-0117-4

Rios-Doria, J., Kuefer, R., Ethier, S. P. & Day, M. L. (2004). Cleavage of beta-catenin by calpain in prostate and mammary tumor cells. *Cancer Res, 64*(20), 7237-7240. doi:10.1158/0008-5472.can-04-1048

Risinger, A. L., Dybdal-Hargreaves, N. F. & Mooberry, S. L. (2015). Breast Cancer Cell Lines Exhibit Differential Sensitivities to Microtubule-targeting Drugs Independent of Doubling Time. *Anticancer Res, 35*(11), 5845-5850.

Rivera-Franco, M. M. & Leon-Rodriguez, E. (2018). Delays in Breast Cancer Detection and Treatment in Developing Countries. *Breast Cancer (Auckl), 12*, 1178223417752677. doi:10.1177/1178223417752677

Rodriguez-Fernandez, L., Ferrer-Vicens, I., Garcia, C., Oltra, S. S., Zaragoza, R., Vina, J. R. & Garcia-Trevijano, E. R. (2016). Isoform-specific function of calpains in cell adhesion disruption: studies in postlactational mammary gland and breast cancer. *Biochem J, 473*(18), 2893-2909. doi:10.1042/bcj20160198

Ross, R. K., Paganini-Hill, A., Wan, P. C. & Pike, M. C. (2000). Effect of hormone replacement therapy on breast cancer risk: estrogen versus estrogen plus progestin. *J Natl Cancer Inst, 92*(4), 328-332.

Rosser, B. G., Powers, S. P. & Gores, G. J. (1993). Calpain activity increases in hepatocytes following addition of ATP. Demonstration by a novel fluorescent approach. *J Biol Chem, 268*(31), 23593-23600.

Rothbarth, J. & van de Velde, C. J. (2005). Treatment of liver metastases of colorectal cancer. *Ann Oncol, 16 Suppl 2*, ii144-149. doi:10.1093/annonc/mdi702

Roumes, H., Leloup, L., Dargelos, E., Brustis, J. J., Daury, L. & Cottin, P. (2010). Calpains: markers of tumor aggressiveness? *Exp Cell Res, 316*(9), 1587-1599. doi:10.1016/j.yexcr.2010.02.017

Russnes, H. G., Lingjaerde, O. C., Borresen-Dale, A. L. & Caldas, C. (2017). Breast Cancer Molecular Stratification: From Intrinsic Subtypes to Integrative Clusters. *Am J Pathol, 187*(10), 2152-2162. doi:10.1016/j.ajpath.2017.04.022

Rutledge, T. W. & Whiteheart, S. W. (2002). SNAP-23 is a target for calpain cleavage in activated platelets. *J Biol Chem, 277*(40), 37009-37015. doi:10.1074/jbc.M204526200

Ryan, B. M. & Faupel-Badger, J. M. (2016). The hallmarks of premalignant conditions: a molecular basis for cancer prevention. *Semin Oncol, 43*(1), 22-35. doi:10.1053/j.seminoncol.2015.09.007

Rybarczyk, P., Gautier, M., Hague, F., Dhennin-Duthille, I., Chatelain, D., Kerr-Conte, J., . . . &Ouadid-Ahidouch, H. (2012). Transient receptor potential melastatin-related 7 channel is overexpressed in human pancreatic ductal adenocarcinomas and regulates human pancreatic cancer cell migration. *Int J Cancer, 131*(6), E851-861. doi:10.1002/ijc.27487

Ryu, Y. J., Kang, S. J., Cho, J. S., Yoon, J. H. & Park, M. H. (2018). Lymphovascular invasion can be better than pathologic complete response to predict prognosis in breast cancer treated with neoadjuvant chemotherapy. *Medicine (Baltimore), 97*(30), e11647. doi:10.1097/md.0000000000011647

Saez, M. E., Ramirez-Lorca, R., Moron, F. J. & Ruiz, A. (2006). The therapeutic potential of the calpain family: new aspects. *Drug Discov Today, 11*(19-20), 917-923. doi:10.1016/j.drudis.2006.08.009

Safuan, S. (2012). *Lymphovascular invasion in melanoma and breast cancer (Doctoral thesis).* University of Nottingham.

Safuan, S., Storr, S. J., Patel, P. M. & Martin, S. G. (2012). A comparative study of adhesion of melanoma and breast cancer cells to blood and lymphatic endothelium. *Lymphatic research and biology, 10*(4), 173-181.

Salehin, D., Fromberg, I., Haugk, C., Dohmen, B., Georg, T., Bohle, R. M., . . . &Friedrich, M. (2010). Immunhistochemical analysis for expression of calpain 1, calpain 2 and calpastatin in endometrial cancer. *Anticancer Res, 30*(7), 2837-2843.

Salehin, D., Fromberg, I., Haugk, C., Dohmen, B., Georg, T., Bohle, R. M., . . . &Friedrich, M. (2011). Immunhistochemical analysis for expression of calpain 1, calpain 2 and calpastatin in ovarian cancer. *Eur J Gynaecol Oncol, 32*(6), 628-635.

Samame Perez-Vargas, J. C., Biondani, P., Maggi, C., Gariboldi, M., Gloghini, A., Inno, A., . . . &Pietrantonio, F. (2013). Role of cMET in the development and progression of colorectal cancer. *Int J Mol Sci, 14*(9), 18056-18077. doi:10.3390/ijms140918056

Sandmann, S., Yu, M. & Unger, T. (2001). Transcriptional and translational regulation of calpain in the rat heart after myocardial infarction--effects of AT(1) and AT(2) receptor antagonists and ACE inhibitor. *Br J Pharmacol, 132*(3), 767-777. doi:10.1038/sj.bjp.0703860

Santos, D. M., Xavier, J. M., Morgado, A. L., Sola, S. & Rodrigues, C. M. (2012). Distinct regulatory functions of calpain 1 and 2 during neural stem cell self-renewal and differentiation. *PLoS One, 7*(3), e33468. doi:10.1371/journal.pone.0033468

Sareen, D., Darjatmoko, S. R., Albert, D. M. & Polans, A. S. (2007). Mitochondria, calcium, and calpain are key mediators of resveratrol-induced apoptosis in breast cancer. *Mol Pharmacol, 72*(6), 1466-1475. doi:10.1124/mol.107.039040

Scalia, R., Gong, Y., Berzins, B., Freund, B., Feather, D., Landesberg, G. & Mishra, G. (2011). A novel role for calpain in the endothelial dysfunction induced by activation of angiotensin II type 1 receptor signaling. *Circ Res, 108*(9), 1102-1111. doi:10.1161/circresaha.110.229393

Schad, E., Farkas, A., Jekely, G., Tompa, P. & Friedrich, P. (2002). A novel human small subunit of calpains. *Biochem J, 362*(Pt 2), 383-388.

Scherer, F., Anton, M., Schillinger, U., Henke, J., Bergemann, C., Kruger, A., . . . &Plank, C. (2002). Magnetofection: enhancing and targeting gene delivery by magnetic force in vitro and in vivo. *Gene Ther, 9*(2), 102-109. doi:10.1038/sj.gt.3301624

Schnitt, S. J. & Guidi, A. J. (2004). Pathology of invasive breast cancer. In J. R. Harris, M. E. Lippman, M. Morrow, & C. K. Osborne (Eds.), *Diseases of the Breast* (3th ed., pp. 541–584). Philadelphia, PA: Lippincott Williams & Wilkins.

Schoch, K. M., Evans, H. N., Brelsfoard, J. M., Madathil, S. K., Takano, J., Saido, T. C. & Saatman, K. E. (2012). Calpastatin overexpression limits calpain-mediated proteolysis and behavioral deficits following traumatic brain injury. *Exp Neurol, 236*(2), 371-382. doi:10.1016/j.expneurol.2012.04.022

Schoemaker, M. J., Nichols, H. B., Wright, L. B., Brook, M. N., Jones, M. E., O'Brien, K. M., . . . &Swerdlow, A. J. (2018). Association of Body Mass Index and Age With Subsequent Breast Cancer Risk in Premenopausal Women. *JAMA Oncol, 4*(11), e181771. doi:10.1001/jamaoncol.2018.1771

Schrader, C., Schielke, A., Ellerbroek, L. & Johne, R. (2012). PCR inhibitors - occurrence, properties and removal. *J Appl Microbiol, 113*(5), 1014-1026. doi:10.1111/j.1365-2672.2012.05384.x

Schrantz, N., Blanchard, D. A., Mitenne, F., Auffredou, M. T., Vazquez, A. & Leca, G. (1999). Manganese induces apoptosis of human B cells: caspase-dependent cell death blocked by bcl-2. *Cell Death Differ, 6*(5), 445-453. doi:10.1038/sj.cdd.4400508

Shah, N. R. & Wong, T. (2006). Current breast cancer risks of hormone replacement therapy in postmenopausal women. *Expert opinion on pharmacotherapy, 7*(18), 2455-2463.

Shakes, D. C., Miller, D. M., 3rd & Nonet, M. L. (2012). Immunofluorescence microscopy. *Methods Cell Biol, 107*, 35-66. doi:10.1016/b978-0-12-394620-1.00002-3

Sharma, G. N., Dave, R., Sanadya, J., Sharma, P. & Sharma, K. K. (2010). Various types and management of breast cancer: an overview. *J Adv Pharm Technol Res, 1*(2), 109-126.

Shen, F., Cai, W.-S., Li, J.-L., Feng, Z., Cao, J. & Xu, B. (2015). The association between deficient manganese levels and breast cancer: a meta-analysis. *International journal of clinical and experimental medicine, 8*(3), 3671-3680.

Shetty, S., Weston, C. J., Adams, D. H. & Lalor, P. F. (2014). A flow adhesion assay to study leucocyte recruitment to human hepatic sinusoidal endothelium under conditions of shear stress. *J Vis Exp*(85), 51330. doi:10.3791/51330

Shimizu, Y., van Seventer, G. A., Ennis, E., Newman, W., Horgan, K. J. & Shaw, S. (1992). Crosslinking of the T cell-specific accessory molecules CD7 and CD28 modulates T cell adhesion. *J Exp Med, 175*(2), 577-582. doi:10.1084/jem.175.2.577

Shiovitz, S. & Korde, L. A. (2015). Genetics of breast cancer: a topic in evolution. *Ann Oncol, 26*(7), 1291-1299. doi:10.1093/annonc/mdv022

Shord, S. S. & Cordes, L. M. (2017). Cancer Treatment and Chemotherapy. In J. T. DiPiro, R. L. Talbert, G. C. Yee, M. G. R., B. G. L. Wells, & M. Posey (Eds.),

Pharmacotherapy: A Pathophysiologic Approach (10th ed.): McGraw-Hill Education.

Shumway, S. D., Maki, M. & Miyamoto, S. (1999). The PEST domain of IkappaBalpha is necessary and sufficient for in vitro degradation by mu-calpain. *J Biol Chem, 274*(43), 30874-30881.

Shuster, C. B., Lin, A. Y., Nayak, R. & Herman, I. M. (1996). Beta cap73: a novel beta actin-specific binding protein. *Cell Motil Cytoskeleton, 35*(3), 175-187. doi:10.1002/(sici)1097-0169(1996)35:3<175::aid-cm1>3.0.co;2-8

SIB. (2019). Cellosaurus SUM149PT (CVCL_3422). Available from Swiss Institute of Bioinformatics SIB Bioinformatics Resource Portal Retrieved 30 Nov 2019 https://web.expasy.org/cellosaurus/CVCL_3422

Silva, T. M., Andersson, S., Sukumaran, S. K., Marques, M. P., Persson, L. & Oredsson, S. (2013). Norspermidine and novel Pd(II) and Pt(II) polynuclear complexes of norspermidine as potential antineoplastic agents against breast cancer. *PLoS One, 8*(2), e55651. doi:10.1371/journal.pone.0055651

Smakman, N., Borel Rinkes, I. H., Voest, E. E. & Kranenburg, O. (2005). Control of colorectal metastasis formation by K-Ras. *Biochim Biophys Acta, 1756*(2), 103-114. doi:10.1016/j.bbcan.2005.07.001

Smid, M., Wang, Y., Zhang, Y., Sieuwerts, A. M., Yu, J., Klijn, J. G., . . . &Martens, J. W. (2008). Subtypes of breast cancer show preferential site of relapse. *Cancer Res, 68*(9), 3108-3114. doi:10.1158/0008-5472.can-07-5644

Sogaard, K. K., Cronin-Fenton, D. P., Pedersen, L., Sorensen, H. T. & Lash, T. L. (2008). Survival in Danish patients with breast cancer and inflammatory bowel disease: a nationwide cohort study. *Inflamm Bowel Dis, 14*(4), 519-525. doi:10.1002/ibd.20341

Song, X., Voronov, E., Dvorkin, T., Fima, E., Cagnano, E., Benharroch, D., . . . &Apte, R. N. (2003). Differential effects of IL-1 alpha and IL-1 beta on tumorigenicity patterns and invasiveness. *J Immunol, 171*(12), 6448-6456. doi:10.4049/jimmunol.171.12.6448

Song, Y., Liu, X., Zhang, G., Song, H., Ren, Y., He, X., . . . &Pang, D. (2013). Unique clinicopathological features of metaplastic breast carcinoma compared with invasive ductal carcinoma and poor prognostic indicators. *World J Surg Oncol, 11*, 129. doi:10.1186/1477-7819-11-129

Song, Y. J., Shin, S. H., Cho, J. S., Park, M. H., Yoon, J. H. & Jegal, Y. J. (2011). The role of lymphovascular invasion as a prognostic factor in patients with lymph node-positive operable invasive breast cancer. *J Breast Cancer, 14*(3), 198-203. doi:10.4048/jbc.2011.14.3.198

Sorimachi, H., Hata, S. & Ono, Y. (2010). Expanding members and roles of the calpain superfamily and their genetically modified animals. *Exp Anim, 59*(5), 549-566.

Sorimachi, H., Hata, S. & Ono, Y. (2011a). Calpain chronicle--an enzyme family under multidisciplinary characterization. *Proc Jpn Acad Ser B Phys Biol Sci, 87*(6), 287-327.

Sorimachi, H., Hata, S. & Ono, Y. (2011b). Impact of genetic insights into calpain biology. *J Biochem, 150*(1), 23-37. doi:10.1093/jb/mvr070

Sorimachi, H., Ishiura, S. & Suzuki, K. (1993). A novel tissue-specific calpain species expressed predominantly in the stomach comprises two alternative splicing products with and without Ca(2+)-binding domain. *J Biol Chem, 268*(26), 19476-19482.

Sorimachi, H. & Ono, Y. (2012). Regulation and physiological roles of the calpain system in muscular disorders. *Cardiovasc Res, 96*(1), 11-22. doi:10.1093/cvr/cvs157

Sorlie, T., Perou, C. M., Tibshirani, R., Aas, T., Geisler, S., Johnsen, H., . . . &Borresen-Dale, A. L. (2001). Gene expression patterns of breast carcinomas distinguish tumor subclasses with clinical implications. *Proc Natl Acad Sci U S A, 98*(19), 10869-10874. doi:10.1073/pnas.191367098

Sotiriou, C., Neo, S. Y., McShane, L. M., Korn, E. L., Long, P. M., Jazaeri, A., . . . &Liu, E. T. (2003). Breast cancer classification and prognosis based on gene expression profiles from a population-based study. *Proc Natl Acad Sci U S A, 100*(18), 10393-10398. doi:10.1073/pnas.1732912100

Span, P. N., Tjan-Heijnen, V. C., Manders, P., Beex, L. V. & Sweep, C. G. (2003). Cyclin-E is a strong predictor of endocrine therapy failure in human breast cancer. *Oncogene, 22*(31), 4898-4904. doi:10.1038/sj.onc.1206818

Stacker, S. A., Achen, M. G., Jussila, L., Baldwin, M. E. & Alitalo, K. (2002). Lymphangiogenesis and cancer metastasis. *Nat Rev Cancer, 2*(8), 573-583. doi:10.1038/nrc863

Stalker, T. J., Gong, Y. & Scalia, R. (2005). The calcium-dependent protease calpain causes endothelial dysfunction in type 2 diabetes. *Diabetes, 54*(4), 1132-1140. doi:10.2337/diabetes.54.4.1132

Stengl, A., Horl, D., Leonhardt, H. & Helma, J. (2017). A Simple and Sensitive High-Content Assay for the Characterization of Antiproliferative Therapeutic Antibodies. *SLAS Discov, 22*(3), 309-315. doi:10.1177/1087057116677821

Stifanese, R., Averna, M., De Tullio, R., Pedrazzi, M., Beccaria, F., Salamino, F., . . . &Melloni, E. (2010). Adaptive modifications in the calpain/calpastatin system in brain cells after persistent alteration in Ca2+ homeostasis. *J Biol Chem, 285*(1), 631-643. doi:10.1074/jbc.M109.031674

Storr, S. J., Carragher, N. O., Frame, M. C., Parr, T. & Martin, S. G. (2011a). The calpain system and cancer. *Nat Rev Cancer, 11*(5), 364-374. doi:10.1038/nrc3050

Storr, S. J., Lee, K. W., Woolston, C. M., Safuan, S., Green, A. R., Macmillan, R. D., . . . &Martin, S. G. (2012a). Calpain system protein expression in basal-like and triple-negative invasive breast cancer. *Ann Oncol, 23*(9), 2289-2296. doi:10.1093/annonc/mds176

Storr, S. J., Mohammed, R. A., Woolston, C. M., Green, A. R., Parr, T., Spiteri, I., . . . &Martin, S. G. (2011b). Calpastatin is associated with lymphovascular invasion in breast cancer. *Breast, 20*(5), 413-418. doi:10.1016/j.breast.2011.04.002

Storr, S. J., Safuan, S., Mitra, A., Elliott, F., Walker, C., Vasko, M. J., . . . &Martin, S. G. (2012b). Objective assessment of blood and lymphatic vessel invasion and association with macrophage infiltration in cutaneous melanoma. *Mod Pathol, 25*(4), 493-504. doi:10.1038/modpathol.2011.182

Storr, S. J., Safuan, S., Woolston, C. M., Abdel-Fatah, T., Deen, S., Chan, S. Y. & Martin, S. G. (2012c). Calpain-2 expression is associated with response to platinum based chemotherapy, progression-free and overall survival in ovarian cancer. *J Cell Mol Med, 16*(10), 2422-2428. doi:10.1111/j.1582-4934.2012.01559.x

Storr, S. J., Thompson, N., Pu, X., Zhang, Y. & Martin, S. G. (2015). Calpain in Breast Cancer: Role in Disease Progression and Treatment Response. *Pathobiology, 82*(3-4), 133-141. doi:10.1159/000430464

Storr, S. J., Woolston, C. M., Barros, F. F., Green, A. R., Shehata, M., Chan, S. Y., . . . &Martin, S. G. (2011c). Calpain-1 expression is associated with relapse-free survival in breast cancer patients treated with trastuzumab following adjuvant chemotherapy. *Int J Cancer, 129*(7), 1773-1780. doi:10.1002/ijc.25832

Storr, S. J., Zaitoun, A. M., Arora, A., Durrant, L. G., Lobo, D. N., Madhusudan, S. & Martin, S. G. (2012d). Calpain system protein expression in carcinomas of the

pancreas, bile duct and ampulla. *BMC Cancer, 12*, 511. doi:10.1186/1471-2407-12-511

Storr, S. J., Zhang, S., Perren, T., Lansdown, M., Fatayer, H., Sharma, N., . . . &Martin, S. G. (2016). The calpain system is associated with survival of breast cancer patients with large but operable inflammatory and non-inflammatory tumours treated with neoadjuvant chemotherapy. *Oncotarget, 7*(30), 47927.

Strobl, S., Fernandez-Catalan, C., Braun, M., Huber, R., Masumoto, H., Nakagawa, K., . . . &Bode, W. (2000). The crystal structure of calcium-free human m-calpain suggests an electrostatic switch mechanism for activation by calcium. *Proc Natl Acad Sci U S A, 97*(2), 588-592.

Strong, A. L., Semon, J. A., Strong, T. A., Santoke, T. T., Zhang, S., McFerrin, H. E., . . . &Bunnell, B. A. (2012). Obesity-associated dysregulation of calpastatin and MMP-15 in adipose-derived stromal cells results in their enhanced invasion. *Stem Cells, 30*(12), 2774-2783. doi:10.1002/stem.1229

Su, J.-M., Wang, L.-Y., Liang, Y.-L. & Zha, X.-L. (2005). Role of cell adhesion signal molecules in hepatocellular carcinoma cell apoptosis. *World journal of gastroenterology, 11*(30), 4667-4673. doi:10.3748/wjg.v11.i30.4667

Su, L. T., Agapito, M. A., Li, M., Simonson, W. T., Huttenlocher, A., Habas, R., . . . &Runnels, L. W. (2006). TRPM7 regulates cell adhesion by controlling the calcium-dependent protease calpain. *J Biol Chem, 281*(16), 11260-11270. doi:10.1074/jbc.M512885200

Subik, K., Lee, J. F., Baxter, L., Strzepek, T., Costello, D., Crowley, P., . . . &Tang, P. (2010). The Expression Patterns of ER, PR, HER2, CK5/6, EGFR, Ki-67 and AR by Immunohistochemical Analysis in Breast Cancer Cell Lines. *Breast Cancer (Auckl), 4*, 35-41.

Sun, J. G., Wang, Y., Chen, Z. T., Zhuo, W. L., Zhu, B., Liao, R. X. & Zhang, S. X. (2009). Detection of lymphangiogenesis in non-small cell lung cancer and its prognostic value. *J Exp Clin Cancer Res, 28*, 21.

Sundquist, M., Thorstenson, S., Klintenberg, C., Brudin, L. & Nordenskjold, B. (2000). Indicators of loco-regional recurrence in breast cancer. The South East Swedish Breast Cancer Group. *Eur J Surg Oncol, 26*(4), 357-362. doi:10.1053/ejso.1999.0898

Suzanne, M. & Steller, H. (2009). Letting go: modification of cell adhesion during apoptosis. *Journal of biology, 8*(5), 49-49. doi:10.1186/jbiol152

Suzuki, K., Hata, S., Kawabata, Y. & Sorimachi, H. (2004). Structure, activation, and biology of calpain. *Diabetes, 53 Suppl 1*, S12-18.

Suzuki, K., Sorimachi, H., Yoshizawa, T., Kinbara, K. & Ishiura, S. (1995). Calpain: novel family members, activation, and physiologic function. *Biol Chem Hoppe Seyler, 376*(9), 523-529.

Suzuki, K., Tsuji, S., Kubota, S., Kimura, Y. & Imahori, K. (1981). Limited autolysis of Ca2+-activated neutral protease (CANP) changes its sensitivity to Ca2+ ions. *J Biochem, 90*(1), 275-278.

Tagliarino, C., Pink, J. J., Reinicke, K. E., Simmers, S. M., Wuerzberger-Davis, S. M. & Boothman, D. A. (2003). Mu-calpain activation in beta-lapachone-mediated apoptosis. *Cancer Biol Ther, 2*(2), 141-152. doi:10.4161/cbt.2.2.237

Takano, E., Maki, M., Mori, H., Hatanaka, M., Marti, T., Titani, K., . . . &Murachi, T. (1988). Pig heart calpastatin: identification of repetitive domain structures and anomalous behavior in polyacrylamide gel electrophoresis. *Biochemistry, 27*(6), 1964-1972.

Takano, E., Nosaka, T., Lee, W. J., Nakamura, K., Takahashi, T., Funaki, M., . . . &Maki, M. (1993). Molecular diversity of calpastatin in human erythroid cells. *Arch Biochem Biophys, 303*(2), 349-354. doi:10.1006/abbi.1993.1294

Takano, J., Kawamura, T., Murase, M., Hitomi, K. & Maki, M. (1999). Structure of mouse calpastatin isoforms: implications of species-common and species-specific alternative splicing. *Biochem Biophys Res Commun, 260*(2), 339-345. doi:10.1006/bbrc.1999.0903

Takano, J., Tomioka, M., Tsubuki, S., Higuchi, M., Iwata, N., Itohara, S., . . . &Saido, T. C. (2005). Calpain mediates excitotoxic DNA fragmentation via mitochondrial pathways in adult brains: evidence from calpastatin mutant mice. *J Biol Chem, 280*(16), 16175-16184. doi:10.1074/jbc.M414552200

Takano, J., Watanabe, M., Hitomi, K. & Maki, M. (2000). Four types of calpastatin isoforms with distinct amino-terminal sequences are specified by alternative first exons and differentially expressed in mouse tissues. *J Biochem, 128*(1), 83-92.

Talmadge, J. E. (2007). Clonal selection of metastasis within the life history of a tumor. *Cancer Res, 67*(24), 11471-11475. doi:10.1158/0008-5472.can-07-2496

Talmadge, J. E. & Fidler, I. J. (2010). AACR centennial series: the biology of cancer metastasis: historical perspective. *Cancer Res, 70*(14), 5649-5669. doi:10.1158/0008-5472.can-10-1040

Tan, Y., Dourdin, N., Wu, C., De Veyra, T., Elce, J. S. & Greer, P. A. (2006). Ubiquitous calpains promote caspase-12 and JNK activation during endoplasmic reticulum stress-induced apoptosis. *J Biol Chem, 281*(23), 16016-16024. doi:10.1074/jbc.M601299200

Tang, Z. N., Zhang, F., Tang, P., Qi, X. W. & Jiang, J. (2011). RANKL-induced migration of MDA-MB-231 human breast cancer cells via Src and MAPK activation. *Oncol Rep, 26*(5), 1243-1250. doi:10.3892/or.2011.1368

Tanner, M., Kapanen, A. I., Junttila, T., Raheem, O., Grenman, S., Elo, J., . . . &Isola, J. (2004). Characterization of a novel cell line established from a patient with Herceptin-resistant breast cancer. *Mol Cancer Ther, 3*(12), 1585-1592.

Tharmalingam, S., Daulat, A. M., Antflick, J. E., Ahmed, S. M., Nemeth, E. F., Angers, S., . . . &Hampson, D. R. (2011). Calcium-sensing receptor modulates cell adhesion and migration via integrins. *J Biol Chem, 286*(47), 40922-40933. doi:10.1074/jbc.M111.265454

Tidball, J. G. & Spencer, M. J. (2000). Calpains and muscular dystrophies. *Int J Biochem Cell Biol, 32*(1), 1-5.

Todd, B., Moore, D., Deivanayagam, C. C., Lin, G. D., Chattopadhyay, D., Maki, M., . . . &Narayana, S. V. (2003). A structural model for the inhibition of calpain by calpastatin: crystal structures of the native domain VI of calpain and its complexes with calpastatin peptide and a small molecule inhibitor. *J Mol Biol, 328*(1), 131-146.

Toke, O., Banoczi, Z., Tarkanyi, G., Friedrich, P. & Hudecz, F. (2009). Folding transitions in calpain activator peptides studied by solution NMR spectroscopy. *J Pept Sci, 15*(6), 404-410. doi:10.1002/psc.1131

Tompa, P., Emori, Y., Sorimachi, H., Suzuki, K. & Friedrich, P. (2001). Domain III of calpain is a ca2+-regulated phospholipid-binding domain. *Biochem Biophys Res Commun, 280*(5), 1333-1339. doi:10.1006/bbrc.2001.4279

Tompa, P., Mucsi, Z., Orosz, G. & Friedrich, P. (2002). Calpastatin subdomains A and C are activators of calpain. *J Biol Chem, 277*(11), 9022-9026. doi:10.1074/jbc.C100700200

Tremper-Wells, B. & Vallano, M. L. (2005). Nuclear calpain regulates Ca2+-dependent signaling via proteolysis of nuclear Ca2+/calmodulin-dependent protein kinase type IV in cultured neurons. *J Biol Chem, 280*(3), 2165-2175. doi:10.1074/jbc.M410591200

Tryfonidis, K., Senkus, E., Cardoso, M. J. & Cardoso, F. (2015). Management of locally advanced breast cancer-perspectives and future directions. *Nat Rev Clin Oncol, 12*(3), 147-162. doi:10.1038/nrclinonc.2015.13

Tsuji, T., Shimohama, S., Kimura, J. & Shimizu, K. (1998). m-Calpain (calcium-activated neutral proteinase) in Alzheimer's disease brains. *Neurosci Lett, 248*(2), 109-112.

Tsujinaka, T., Kajiwara, Y., Kambayashi, J., Sakon, M., Higuchi, N., Tanaka, T. & Mori, T. (1988). Synthesis of a new cell penetrating calpain inhibitor (calpeptin). *Biochem Biophys Res Commun, 153*(3), 1201-1208. doi:10.1016/s0006-291x(88)81355-x

Tutunea-Fatan, E., Majumder, M., Xin, X. & Lala, P. K. (2015). The role of CCL21/CCR7 chemokine axis in breast cancer-induced lymphangiogenesis. *Mol Cancer, 14*, 35. doi:10.1186/s12943-015-0306-4

Uehara, H., Kim, S. J., Karashima, T., Shepherd, D. L., Fan, D., Tsan, R., . . . &Fidler, I. J. (2003). Effects of blocking platelet-derived growth factor-receptor signaling in a mouse model of experimental prostate cancer bone metastases. *J Natl Cancer Inst, 95*(6), 458-470.

Uemori, T., Shimojo, T., Asada, K., Asano, T., Kimizuka, F., Kato, I., . . . &et al. (1990). Characterization of a functional domain of human calpastatin. *Biochem Biophys Res Commun, 166*(3), 1485-1493.

Vaisid, T., Kosower, N. S., Katzav, A., Chapman, J. & Barnoy, S. (2007). Calpastatin levels affect calpain activation and calpain proteolytic activity in APP transgenic mouse model of Alzheimer's disease. *Neurochem Int, 51*(6-7), 391-397. doi:10.1016/j.neuint.2007.04.004

Valastyan, S. & Weinberg, R. A. (2011). Tumor metastasis: molecular insights and evolving paradigms. *Cell, 147*(2), 275-292. doi:10.1016/j.cell.2011.09.024

Valderrama-Treviño, A. I., Barrera-Mera, B., Ceballos-Villalva, J. C. & Montalvo-Javé, E. E. (2017). Hepatic metastasis from colorectal cancer. *Euroasian journal of hepato-gastroenterology, 7*(2), 166.

Van den Eynden, G. G., Van der Auwera, I., Van Laere, S. J., Colpaert, C. G., van Dam, P., Dirix, L. Y., . . . &Van Marck, E. A. (2006). Distinguishing blood and lymph vessel invasion in breast cancer: a prospective immunohistochemical study. *Br J Cancer, 94*(11), 1643-1649. doi:10.1038/sj.bjc.6603152

Van Slambrouck, S., Groux-Degroote, S., Krzewinski-Recchi, M. A., Cazet, A., Delannoy, P. & Steelant, W. F. (2014). Carbohydrate-to-carbohydrate interactions between alpha2,3-linked sialic acids on alpha2 integrin subunits and asialo-GM1 underlie the bone metastatic behaviour of LNCAP-derivative C4-2B prostate cancer cells. *Biosci Rep, 34*(5). doi:10.1042/bsr20140096

Vara-Ciruelos, D., Dandapani, M., Gray, A., Egbani, E. O., Evans, A. M. & Hardie, D. G. (2018). Genotoxic Damage Activates the AMPK-alpha1 Isoform in the Nucleus via Ca(2+)/CaMKK2 Signaling to Enhance Tumor Cell Survival. *Mol Cancer Res, 16*(2), 345-357. doi:10.1158/1541-7786.mcr-17-0323

Varga, K., Hollosi, A., Paszty, K., Hegedus, L., Szakacs, G., Timar, J., . . . &Padanyi, R. (2018). Expression of calcium pumps is differentially regulated by histone deacetylase inhibitors and estrogen receptor alpha in breast cancer cells. *BMC Cancer, 18*(1), 1029. doi:10.1186/s12885-018-4945-x

Veronesi, U., Marubini, E., Del Vecchio, M., Manzari, A., Andreola, S., Greco, M., . . . &et al. (1995). Local recurrences and distant metastases after conservative breast cancer treatments: partly independent events. *J Natl Cancer Inst, 87*(1), 19-27. doi:10.1093/jnci/87.1.19

Vilagi, I., Kiss, D. S., Farkas, A., Borbely, S., Tarnok, K., Halasy, K., . . . &Friedrich, P. (2008). Synthetic calpain activator boosts neuronal excitability without extra Ca2+. *Mol Cell Neurosci, 38*(4), 629-636. doi:10.1016/j.mcn.2008.05.012

Voogd, A. C., Nielsen, M., Peterse, J. L., Blichert-Toft, M., Bartelink, H., Overgaard, M., . . . &van Dongen, J. A. (2001). Differences in risk factors for local and distant recurrence after breast-conserving therapy or mastectomy for stage I and II breast cancer: pooled results of two large European randomized trials. *J Clin Oncol, 19*(6), 1688-1697. doi:10.1200/jco.2001.19.6.1688

Vosler, P. S., Brennan, C. S. & Chen, J. (2008). Calpain-mediated signaling mechanisms in neuronal injury and neurodegeneration. *Mol Neurobiol, 38*(1), 78-100. doi:10.1007/s12035-008-8036-x

Vosler, P. S., Sun, D., Wang, S., Gao, Y., Kintner, D. B., Signore, A. P., . . . &Chen, J. (2009). Calcium dysregulation induces apoptosis-inducing factor release: cross-talk between PARP-1- and calpain-signaling pathways. *Exp Neurol, 218*(2), 213-220. doi:10.1016/j.expneurol.2009.04.032

Wang, E., Wang, D., Li, B., Ma, H., Wang, C., Guan, L., . . . &Li, S. (2017). Capn4 promotes epithelial-mesenchymal transition in human melanoma cells through activation of the Wnt/beta-catenin pathway. *Oncol Rep, 37*(1), 379-387. doi:10.3892/or.2016.5247

Wang, K. K., Nath, R., Posner, A., Raser, K. J., Buroker-Kilgore, M., Hajimohammadreza, I., . . . &Yuen, P. (1996). An alpha-mercaptoacrylic acid derivative is a selective nonpeptide cell-permeable calpain inhibitor and is neuroprotective. *Proc Natl Acad Sci U S A, 93*(13), 6687-6692. doi:10.1073/pnas.93.13.6687

Wang, K. K., Posmantur, R., Nadimpalli, R., Nath, R., Mohan, P., Nixon, R. A., . . . &Allen, H. (1998). Caspase-mediated fragmentation of calpain inhibitor protein calpastatin during apoptosis. *Arch Biochem Biophys, 356*(2), 187-196. doi:10.1006/abbi.1998.0748

Wang, X. D., Rosales, J. L., Magliocco, A., Gnanakumar, R. & Lee, K. Y. (2003). Cyclin E in breast tumors is cleaved into its low molecular weight forms by calpain. *Oncogene, 22*(5), 769-774. doi:10.1038/sj.onc.1206166

Wang, Y., Lopez, D., Davey, P. G., Cameron, D. J., Nguyen, K., Tran, J., . . . &Baudry, M. (2016). Calpain-1 and calpain-2 play opposite roles in retinal ganglion cell degeneration induced by retinal ischemia/reperfusion injury. *Neurobiol Dis, 93*, 121-128. doi:10.1016/j.nbd.2016.05.007

Wang, Y., Zhu, G., Briz, V., Hsu, Y.-T., Bi, X. & Baudry, M. (2014). A molecular brake controls the magnitude of long-term potentiation. *Nat Commun, 5*, 3051-3051. doi:10.1038/ncomms4051

Watanabe, N., Okochi, E., Mochizuki, M., Sugimura, T. & Ushijima, T. (2001). The presence of single nucleotide instability in human breast cancer cell lines. *Cancer Res, 61*(21), 7739-7742.

Weaver, V. M., Petersen, O. W., Wang, F., Larabell, C. A., Briand, P., Damsky, C. & Bissell, M. J. (1997). Reversion of the malignant phenotype of human breast cells in three-dimensional culture and in vivo by integrin blocking antibodies. *J Cell Biol, 137*(1), 231-245. doi:10.1083/jcb.137.1.231

Weigand, R. A., Isenberg, W. M., Russo, J., Brennan, M. J. & Rich, M. A. (1982). Blood vessel invasion and axillary lymph node involvement as prognostic indicators

for human breast cancer. *Cancer, 50*(5), 962-969. doi:10.1002/1097-0142(19820901)50:5<962::aid-cncr2820500526>3.0.co;2-x

Weigelt, B., Peterse, J. L. & van 't Veer, L. J. (2005). Breast cancer metastasis: markers and models. *Nat Rev Cancer, 5*(8), 591-602. doi:10.1038/nrc1670

Weiss, L. & Schmid-Schonbein, G. W. (1989). Biomechanical interactions of cancer cells with the microvasculature during metastasis. *Cell Biophys, 14*(2), 187-215. doi:10.1007/bf02797133

Wells, A., Grahovac, J., Wheeler, S., Ma, B. & Lauffenburger, D. (2013). Targeting tumor cell motility as a strategy against invasion and metastasis. *Trends Pharmacol Sci, 34*(5), 283-289. doi:10.1016/j.tips.2013.03.001

Wells, A., Huttenlocher, A. & Lauffenburger, D. A. (2005). Calpain proteases in cell adhesion and motility. *Int Rev Cytol, 245*, 1-16. doi:10.1016/s0074-7696(05)45001-9

Wells, A. & Leloup, L. (2010). Calpain *Handbook of Cell Signaling* (pp. 999-1008): Elsevier.

Wendt, A., Thompson, V. F. & Goll, D. E. (2004). Interaction of calpastatin with calpain: a review. *Biol Chem, 385*(6), 465-472. doi:10.1515/bc.2004.054

Westhoff, C. L. & Pike, M. C. (2018). Hormonal contraception and breast cancer. *Am J Obstet Gynecol, 219*(2), 169.e161-169.e164. doi:10.1016/j.ajog.2018.03.032

Witkowski, J. M., Zmuda-Trzebiatowska, E., Swiercz, J. M., Cichorek, M., Ciepluch, H., Lewandowski, K., . . . &Hellmann, A. (2002). Modulation of the activity of calcium-activated neutral proteases (calpains) in chronic lymphocytic leukemia (B-CLL) cells. *Blood, 100*(5), 1802-1809. doi:10.1182/blood-2001-11-0073

Witte, M. H., Bernas, M. J., Martin, C. P. & Witte, C. L. (2001). Lymphangiogenesis and lymphangiodysplasia: from molecular to clinical lymphology. *Microsc Res Tech, 55*(2), 122-145.

Witte, M. H., Jones, K., Wilting, J., Dictor, M., Selg, M., McHale, N., . . . &Jackson, D. G. (2006). Structure function relationships in the lymphatic system and implications for cancer biology. *Cancer Metastasis Rev, 25*(2), 159-184. doi:10.1007/s10555-006-8496-2

Woo, C. S., Silberman, H., Nakamura, S. K., Ye, W., Sposto, R., Colburn, W., . . . &Silverstein, M. J. (2002). Lymph node status combined with lymphovascular invasion creates a more powerful tool for predicting outcome in patients with invasive breast cancer. *Am J Surg, 184*(4), 337-340.

Woo, M. G., Xue, K., Liu, J., McBride, H. & Tsang, B. K. (2012). Calpain-mediated processing of p53-associated parkin-like cytoplasmic protein (PARC) affects chemosensitivity of human ovarian cancer cells by promoting p53 subcellular trafficking. *J Biol Chem, 287*(6), 3963-3975. doi:10.1074/jbc.M111.314765

Woolston, C. & Martin, S. (2011). Analysis of tumor and endothelial cell viability and survival using sulforhodamine B and clonogenic assays *Mammalian Cell Viability* (pp. 45-56): Springer.

Wright, K. L., Adams, J. R., Liu, J. C., Loch, A. J., Wong, R. G., Jo, C. E., . . . &Egan, S. E. (2015). Ras Signaling Is a Key Determinant for Metastatic Dissemination and Poor Survival of Luminal Breast Cancer Patients. *Cancer Res, 75*(22), 4960-4972. doi:10.1158/0008-5472.can-14-2992

Wu, A., Loutherback, K., Lambert, G., Estevez-Salmeron, L., Tlsty, T. D., Austin, R. H. & Sturm, J. C. (2013). Cell motility and drug gradients in the emergence of resistance to chemotherapy. *Proc Natl Acad Sci U S A, 110*(40), 16103-16108. doi:10.1073/pnas.1314385110

Wu, M., Yu, Z., Fan, J., Caron, A., Whiteway, M. & Shen, S. H. (2006). Functional dissection of human protease mu-calpain in cell migration using RNAi. *FEBS Lett, 580*(13), 3246-3256. doi:10.1016/j.febslet.2006.05.003

Xu, F., Gu, J., Lu, C., Mao, W., Wang, L., Zhu, Q., . . . &Ge, D. (2019). Calpain-2 Enhances Non-Small Cell Lung Cancer Progression and Chemoresistance to Paclitaxel via EGFR-pAKT Pathway. *Int J Biol Sci, 15*(1), 127-137. doi:10.7150/ijbs.28834

Xu, K. P., Ding, Y., Ling, J., Dong, Z. & Yu, F. S. (2004). Wound-induced HB-EGF ectodomain shedding and EGFR activation in corneal epithelial cells. *Invest Ophthalmol Vis Sci, 45*(3), 813-820.

Xu, Y. & Mellgren, R. L. (2002). Calpain inhibition decreases the growth rate of mammalian cell colonies. *J Biol Chem, 277*(24), 21474-21479. doi:10.1074/jbc.M111689200

Yallop, C. A. & Svendsen, I. (2001). The effects of G418 on the growth and metabolism of recombinant mammalian cell lines. *Cytotechnology, 35*(2), 101-114. doi:10.1023/a:1017550902771

Yamano, S., Dai, J. & Moursi, A. M. (2010). Comparison of transfection efficiency of nonviral gene transfer reagents. *Mol Biotechnol, 46*(3), 287-300. doi:10.1007/s12033-010-9302-5

Yang, H. Q., Ma, H., Takano, E., Hatanaka, M. & Maki, M. (1994). Analysis of calcium-dependent interaction between amino-terminal conserved region of calpastatin functional domain and calmodulin-like domain of mu-calpain large subunit. *J Biol Chem, 269*(29), 18977-18984.

Yang, S., Jiang, M., Grabowska, M. M., Li, J., Connelly, Z. M., Zhang, J., . . . &Yu, X. (2016). Androgen receptor differentially regulates the proliferation of prostatic epithelial cells in vitro and in vivo. *Oncotarget, 7*(43), 70404-70419. doi:10.18632/oncotarget.11879

Yang, X., Sun, J., Xia, D., Can, X., Liu, L., Zhang, J., . . . &Xi, X. (2017). Capn4 Enhances Osteopontin Expression through Activation of the Wnt/beta-Catenin Pathway to Promote Epithelial Ovarian Carcinoma Metastasis. *Cell Physiol Biochem, 42*(1), 185-197. doi:10.1159/000477310

Yao, X., Thibodeau, A. & Forte, J. G. (1993). Ezrin-calpain I interactions in gastric parietal cells. *Am J Physiol, 265*(1 Pt 1), C36-46. doi:10.1152/ajpcell.1993.265.1.C36

Ye, T., Wang, Q., Zhang, Y., Song, X., Yang, D., Li, D., . . . &Ma, S. (2015). Over-expression of calpastatin inhibits calpain activation and attenuates post-infarction myocardial remodeling. *PLoS One, 10*(3), e0120178. doi:10.1371/journal.pone.0120178

Yee, G. C. (2005). Oncologic Disorders. In J. T. DiPiro, R. L. Talbert, G. C. Yee, M. G. R., B. G. L. Wells, & M. Posey (Eds.), Pharmacotherapy - A Pathophysiologic Approach (6th ed., pp. 2279-2558).

Yin, J., Xu, K., Zhang, J., Kumar, A. & Yu, F. S. (2007). Wound-induced ATP release and EGF receptor activation in epithelial cells. *J Cell Sci, 120*(Pt 5), 815-825. doi:10.1242/jcs.03389

Youlden, D. R., Cramb, S. M., Dunn, N. A., Muller, J. M., Pyke, C. M. & Baade, P. D. (2012). The descriptive epidemiology of female breast cancer: an international comparison of screening, incidence, survival and mortality. *Cancer Epidemiol, 36*(3), 237-248. doi:10.1016/j.canep.2012.02.007

Yousefi, M., Nosrati, R., Salmaninejad, A., Dehghani, S., Shahryari, A. & Saberi, A. (2018). Organ-specific metastasis of breast cancer: molecular and cellular mechanisms underlying lung metastasis. *Cell Oncol (Dordr), 41*(2), 123-140. doi:10.1007/s13402-018-0376-6

Yue, C. H., Chiu, Y. W., Tung, J. N., Tzang, B. S., Shiu, J. J., Huang, W. H., . . . &Hwang, J. M. (2012). Expression of protein kinase C alpha and the MZF-1 and Elk-1 transcription factors in human breast cancer cells. *Chin J Physiol, 55*(1), 31-36. doi:10.4077/cjp.2012.amm109

Zamaraeva, M. V., Sabirov, R. Z., Maeno, E., Ando-Akatsuka, Y., Bessonova, S. V. & Okada, Y. (2005). Cells die with increased cytosolic ATP during apoptosis: a bioluminescence study with intracellular luciferase. *Cell Death Differ, 12*(11), 1390-1397. doi:10.1038/sj.cdd.4401661

Zhang, C., Bai, D. S., Huang, X. Y., Shi, G. M., Ke, A. W., Yang, L. X., . . . &Fan, J. (2013a). Prognostic significance of Capn4 overexpression in intrahepatic cholangiocarcinoma. *PLoS One, 8*(1), e54619. doi:10.1371/journal.pone.0054619

Zhang, P., Du, J., Zhao, L., Wang, X., Zhang, Y., Yan, R., . . . &Dai, K. (2013b). The role of intraplatelet reactive oxygen species in the regulation of platelet glycoprotein Ibalpha ectodomain shedding. *Thromb Res, 132*(6), 696-701. doi:10.1016/j.thromres.2013.09.034

Zhang, S. (2018). *Calpain in ovarian cancer progression and chemotherapeutic response (Doctoral thesis).* University of Nottingham.

Zhang, S., Deen, S., Storr, S. J., Chondrou, P. S., Nicholls, H., Yao, A., . . . &Martin, S. G. (2019). Calpain system protein expression and activity in ovarian cancer. *J Cancer Res Clin Oncol, 145*(2), 345-361. doi:10.1007/s00432-018-2794-2

Zhang, S. M., Lee, I. M., Manson, J. E., Cook, N. R., Willett, W. C. & Buring, J. E. (2007). Alcohol consumption and breast cancer risk in the Women's Health Study. *Am J Epidemiol, 165*(6), 667-676. doi:10.1093/aje/kwk054

Zhang, W., Liu, J., Sun, R., Zhao, L., Du, J., Ruan, C. & Dai, K. (2011). Calpain activator dibucaine induces platelet apoptosis. *Int J Mol Sci, 12*(4), 2125-2137. doi:10.3390/ijms12042125

Zhang, W. & Mellgren, R. L. (1996). Calpain subunits remain associated during catalysis. *Biochem Biophys Res Commun, 227*(3), 891-896.

Zhang, X., Wu, X., Su, P., Gao, Y., Meng, B., Sun, Y., . . . &Zhou, G. (2012). Doxorubicin influences the expression of glucosylceramide synthase in invasive ductal breast cancer. *PLoS One, 7*(11), e48492. doi:10.1371/journal.pone.0048492

Zhang, Y. (2014). *Redox protein regulation of therapeutic response in breast cancer (Doctoral thesis).* University of Nottingham.

Zhao, X., Moloughney, J. G., Zhang, S., Komazaki, S. & Weisleder, N. (2012). Orai1 mediates exacerbated Ca(2+) entry in dystrophic skeletal muscle. *PLoS One, 7*(11), e49862-e49862. doi:10.1371/journal.pone.0049862

Zheng, P. C., Chen, X., Zhu, H. W., Zheng, W., Mao, L. H., Lin, C., . . . &Zheng, M. (2014). Capn4 is a marker of poor clinical outcomes and promotes nasopharyngeal carcinoma metastasis via nuclear factor-kappaB-induced matrix metalloproteinase 2 expression. *Cancer Sci, 105*(6), 630-638. doi:10.1111/cas.12416

Zhong, X. & Rescorla, F. J. (2012). Cell surface adhesion molecules and adhesion-initiated signaling: understanding of anoikis resistance mechanisms and therapeutic opportunities. *Cell Signal, 24*(2), 393-401. doi:10.1016/j.cellsig.2011.10.005

Zhou, Z., Qutaish, M., Han, Z., Schur, R. M., Liu, Y., Wilson, D. L. & Lu, Z. R. (2015). MRI detection of breast cancer micrometastases with a fibronectin-targeting contrast agent. *Nat Commun, 6*, 7984. doi:10.1038/ncomms8984

Zhuang, Q., Qian, X., Cao, Y., Fan, M., Xu, X. & He, X. (2014). Capn4 mRNA level is correlated with tumour progression and clinical outcome in clear cell renal cell carcinoma. *J Int Med Res, 42*(2), 282-291. doi:10.1177/0300060513505524

Zimmerlin, L., Donnenberg, A. D., Rubin, J. P., Basse, P., Landreneau, R. J. & Donnenberg, V. S. (2011). Regenerative therapy and cancer: in vitro and in vivo studies of the interaction between adipose-derived stem cells and breast cancer cells from clinical isolates. *Tissue Eng Part A, 17*(1-2), 93-106. doi:10.1089/ten.TEA.2010.0248

Zimmerman, U. J., Wang, M. & Liu, L. (1995). Inhibition of secretion from isolated rat alveolar epithelial type II cells by the cell permeant calpain inhibitor II (N-acetyl-leucyl-leucyl-methioninal). *Cell Calcium, 18*(1), 1-8. doi:10.1016/0143-4160(95)90040-3

Zlotnik, A. (2008). New insights on the role of CXCR4 in cancer metastasis. *J Pathol, 215*(3), 211-213. doi:10.1002/path.2350

Appendix

Appendix A: Permission for republishing or display content

Copyright for Table 1.2 NPI prognostic groups and prognosis. Data reproduced from Lee and Ellis (2008).

Springer - License Terms and Conditions

This is a License Agreement between Bhudsaban Sukkarn ("You") and Springer ("Publisher") provided by Copyright Clearance Center ("CCC"). The license consists of your order details, the terms and conditions provided by Springer, and the CCC terms and conditions.
All payments must be made in full to CCC.

Order Date	11-Jan-2020
Order license ID	1013075-1
ISSN	1219-4956
Type of Use	Republish in a thesis/dissertation
Publisher	W.B./SAUNDERS CO. LTD.
Portion	Chapter/article
Publication Title	Pathology oncology research : POR
Date	01/01/1995
Language	English
Country	United Kingdom of Great Britain and Northern Ireland
Rightsholder	Springer
Publication Type	Journal
URL	http://www.harcourt-international.com/journals/
Portion Type	Chapter/article
Page range(s)	1-58
Total number of pages	58
Format (select all that apply)	Print, Electronic
Who will republish the content?	Academic institution
Duration of Use	Life of current edition
Lifetime Unit Quantity	Up to 499
Rights Requested	Main product
Distribution	Worldwide
Translation	Original language of publication
Copies for the disabled?	No
Minor editing privileges?	Yes
Incidental promotional use?	No
Currency	GBP
Title	The role of calpastatin isoform in breast cancer LVI
Instructor name	Bhudsaban Sukkarn
Institution name	University of Nottingham
Expected presentation date	2020-05-31
Order reference number	7
The requesting person / organization to appear on the license	Bhudsaban Sukkarn
Title, description or numeric reference of the portion(s)	Table 1 The prognostic value of the NPI in two eras
Editor of portion(s)	N/A
Volume of serial or monograph	14
Page or page range of portion	113-5
Title of the article/chapter the portion is from	The Nottingham prognostic index for invasive carcinoma of the breast
Author of portion(s)	Lee, A. H. and Ellis, I. O.
Issue, if republishing an article from a serial	2
Publication date of portion	2008-06-11

Copyright for Table 1.5 Summary of calpastatin isoforms identified in tissues. Data adapted from Wendt *et al.* (2004).

Walter de Gruyter and Company LICENSE
TERMS AND CONDITIONS

This is a License Agreement between Miss -- Bhudsaban Sukkarn ("You") and Walter de Gruyter and Company ("Walter de Gruyter and Company") provided by Copyright Clearance Center ("CCC"). The license consists of your order details, the terms and conditions provided by Walter de Gruyter and Company, and the payment terms and conditions.

All payments must be made in full to CCC. For payment instructions, please see information listed at the bottom of this form.

License Number	4594361357921
License date	May 22, 2019
Licensed content publisher	Walter de Gruyter and Company
Licensed content title	Biological chemistry
Licensed content date	Jan 1, 1999
Type of Use	Thesis/Dissertation
Requestor type	Author of requested content
Format	Print, Electronic
Portion	chart/graph/table/figure
Number of charts/graphs/tables/figures	1
The requesting person/organization is:	Bhudsaban Sukkarn
Title or numeric reference of the portion(s)	Summary of calpastatin isoforms that have been identified in tissues
Title of the article or chapter the portion is from	Interaction of calpastatin with calpain: a review
Editor of portion(s)	N/A
Author of portion(s)	Wendt, A., Thompson, V. F., and Goll, D. E.
Volume of serial or monograph.	385
Issue, if republishing an article from a serial	6
Page range of the portion	465-72
Publication date of portion	June 2004
Rights for	Main product
Duration of use	Life of current edition
Creation of copies for the disabled	no
With minor editing privileges	no
For distribution to	Worldwide
In the following language(s)	Original language of publication
With incidental promotional use	no
The lifetime unit quantity of new product	Up to 499
Title	The Role of Calpastatin Isoforms in Breast Cancer Lymphovascular Invasion
Institution name	The University of Nottingham
Expected presentation date	Dec 2019
Order reference number	4
Total (may include CCC user fee)	0.00 USD

Copyright for Figure 1.1 The invasion-metastasis cascade. Reproduced from Valastyan and Weinberg (2011) with permission.

Elsevier Science and Technology Journals LICENSE
TERMS AND CONDITIONS

This is a License Agreement between Miss -- Bhudsaban Sukkarn ("You") and Elsevier Science and Technology Journals ("Elsevier Science and Technology Journals") provided by Copyright Clearance Center ("CCC"). The license consists of your order details, the terms and conditions provided by Elsevier Science and Technology Journals, and the payment terms and conditions.

All payments must be made in full to CCC. For payment instructions, please see information listed at the bottom of this form.

License Number	4575030879274
License date	Apr 23, 2019
Licensed content publisher	Elsevier Science and Technology Journals
Licensed content title	Cell
Licensed content date	Jan 1, 1974
Type of Use	Thesis/Dissertation
Requestor type	Author of requested content
Format	Print, Electronic
Portion	image/photo
Number of images/photos requested	1
The requesting person/organization is:	Bhudsaban Sukkarn
Title or numeric reference of the portion(s)	Figure 1. The Invasion-Metastasis Cascade
Title of the article or chapter the portion is from	Tumor metastasis: molecular insights and evolving paradigms
Editor of portion(s)	N/A
Author of portion(s)	Valastyan, S., & Weinberg, R. A.
Volume of serial or monograph.	147
Page range of the portion	275-92
Publication date of portion	October 14, 2011
Rights for	Main product
Duration of use	Life of current edition
For distribution to	Worldwide
In the following language(s)	Original language of publication
The lifetime unit quantity of new product	Up to 499
Title	The Role of Calpastatin Isoforms in Breast Cancer Lymphovascular Invasion
Institution name	The University of Nottingham
Expected presentation date	Dec 2019
Order reference number	2
Total (may include CCC user fee)	0.00 USD

Copyright for Figure 1.2 Schematic structure of μ-calpain heterodimer and calpain family members, and Figure 1.3 Schematic structure of calpastatin protein, cDNA and gDNA. Reproduced from Storr *et al.* (2011a) with permission.

Nature Publishing Group LICENSE
TERMS AND CONDITIONS

This is a License Agreement between Miss -- Bhudsaban Sukkarn ("You") and Nature Publishing Group ("Nature Publishing Group") provided by Copyright Clearance Center ("CCC"). The license consists of your order details, the terms and conditions provided by Nature Publishing Group, and the payment terms and conditions.

All payments must be made in full to CCC. For payment instructions, please see information listed at the bottom of this form.

License Number	4593021120943
License date	May 20, 2019
Licensed content publisher	Nature Publishing Group
Licensed content title	Nature Reviews Cancer
Licensed content date	Jan 1, 2001
Type of Use	Thesis/Dissertation
Requestor type	Author of requested content
Format	Print, Electronic
Portion	image/photo
Number of images/photos requested	2
The requesting person/organization is:	Bhudsaban Sukkarn
Title or numeric reference of the portion(s)	Chapter 1 Schematic structure of calpastatin, Schematic structure of μ-calpain heterodimer and calpain family members
Title of the article or chapter the portion is from	The calpain system and cancer
Editor of portion(s)	N/A
Author of portion(s)	Storr, S. J., Carragher, N. O., Frame, M. C., Parr, T., and Martin, S. G.
Volume of serial or monograph.	11
Issue, if republishing an article from a serial	5
Page range of the portion	364-74
Publication date of portion	May 2011
Rights for	Main product
Duration of use	Life of current edition
Creation of copies for the disabled	no
With minor editing privileges	yes
For distribution to	Worldwide
In the following language(s)	Original language of publication
With incidental promotional use	no
The lifetime unit quantity of new product	Up to 499
Title	The Role of Calpastatin Isoforms in Breast Cancer Lymphovascular Invasion
Institution name	The University of Nottingham
Expected presentation date	Dec 2019
Order reference number	3
Total (may include CCC user fee)	0.00 USD

Copyright for Figure 1.4 Schematic representation of conventional calpain substrates and major events of tumour cell pathophysiology in which conventional calpains are involved. Reproduced from Moretti *et al.* (2014) with permission.

This is a License Agreement between Bhudsaban Sukkarn ("You") and Elsevier Science & Technology Journals ("Publisher") provided by Copyright Clearance Center ("CCC"). The license consists of your order details, the terms and conditions provided by Elsevier Science & Technology Journals, and the CCC terms and conditions. All payments must be made in full to CCC.

Order Date 18-Sep-2020
Order license ID 1063816-1
ISSN 0003-9861

Type of Use Republish in a thesis/dissertation
Publisher ACADEMIC PRESS
Portion Image/photo/illustration

LICENSED CONTENT

Publication Title Archives of biochemistry and biophysics
Date 01/01/1951
Language English

Country United States of America
Rightsholder Elsevier Science & Technology Journals
Publication Type Journal

REQUEST DETAILS

Portion Type Image/photo/illustration
Number of images / photos / illustrations 1
Format (select all that apply) Print, Electronic
Who will republish the content? Academic institution
Duration of Use Life of current edition
Lifetime Unit Quantity Up to 499
Rights Requested Main product and any product related to main product

Distribution Worldwide
Translation Original language of publication
Copies for the disabled? No
Minor editing privileges? Yes
Incidental promotional use? No
Currency GBP

NEW WORK DETAILS

Title Role of calpastatin isoforms in breast cancer lymphovascular invasion
Instructor name Prof. Stewart Martin

Institution name University of Nottingham
Expected presentation date 2020-10-01

ADDITIONAL DETAILS

Order reference number 180920

The requesting person / organization to appear on the license Bhudsaban Sukkarn

REUSE CONTENT DETAILS

Title, description or numeric reference of the portion(s)
doi:10.1016/j.abb.2014.09.018
Editor of portion(s) N/A
Volume of serial or monograph N/A
Page or page range of portion 26-36

Title of the article/chapter the portion is from
Calpains and cancer: friends or enemies?
Author of portion(s) Moretti, D., Del Bello, B., Allavena, G., & Maellaro, E.
Issue, if republishing an article from a serial N/A
Publication date of portion 2014-12-15

Copyright for Figure 1.5 Calpain and migration. Reproduced from Storr *et al.* (2011a) with permission.

Nature Publishing Group LICENSE
TERMS AND CONDITIONS

This is a License Agreement between Miss -- Bhudsaban Sukkarn ("You") and Nature Publishing Group ("Nature Publishing Group") provided by Copyright Clearance Center ("CCC"). The license consists of your order details, the terms and conditions provided by Nature Publishing Group, and the payment terms and conditions.

All payments must be made in full to CCC. For payment instructions, please see information listed at the bottom of this form.

License Number	4594390812267
License date	May 22, 2019
Licensed content publisher	Nature Publishing Group
Licensed content title	Nature Reviews Cancer
Licensed content date	Jan 1, 2001
Type of Use	Thesis/Dissertation
Requestor type	Author of requested content
Format	Print, Electronic
Portion	image/photo
Number of images/photos requested	1
The requesting person/organization is:	Bhudsaban Sukkarn
Title or numeric reference of the portion(s)	Calpain and migration
Title of the article or chapter the portion is from	The calpain system and cancer
Editor of portion(s)	N/A
Author of portion(s)	Storr, S. J., Carragher, N. O., Frame, M. C., Parr, T., and Martin, S. G.
Volume of serial or monograph.	11
Issue, if republishing an article from a serial	5
Page range of the portion	364-74
Publication date of portion	May 2011
Rights for	Main product
Duration of use	Life of current edition
Creation of copies for the disabled	no
With minor editing privileges	no
For distribution to	Worldwide
In the following language(s)	Original language of publication
With incidental promotional use	no
The lifetime unit quantity of new product	Up to 499
Title	The Role of Calpastatin Isoforms in Breast Cancer Lymphovascular Invasion
Institution name	The University of Nottingham
Expected presentation date	Dec 2019
Order reference number	6
Total (may include CCC user fee)	0.00 USD

Appendix B

Table B2.1 Cell lines and culture media

Cell lines	Components of culture media	Sources	Volume
MDA-MB-231 and MDA-MB-468 Basal-like/ triple-negative (ER^-, PR^-, $HER2^-$)	Minimum Essential Medium Eagle (MEM) (with Earle's salts and sodium bicarbonate, without L-glutamine)	M2279, Sigma-Aldrich, UK	500 mL
	Heat Inactivated Iron Supplemented Donor Bovine Serum	Gibco, Life Technologies, UK	57 mL
	Penicillin/Streptomycin (with 10,000 units penicillin and 10 mg streptomycin/mL)	P4333, Sigma-Aldrich, UK	5.7 mL
	L-glutamine (200 mM)	G7513, Sigma-Aldrich, UK	5.7 mL
	MEM Non-essential amino acids solution (100x)	M7145, Sigma-Aldrich, UK	5.7 mL
SUM149 Basal-like/ triple-negative (ER^-, PR^-, $HER2^-$) and inflammatory type	Ham's F-12 medium	H4878, Sigma-Aldrich, UK	500 mL
	Heat Inactivated Iron Supplemented Donor Bovine Serum	Gibco, Life Technologies, UK	50 mL
	Penicillin/Streptomycin (with 10,000 units penicillin and 10 mg streptomycin/mL)	P4333, Sigma-Aldrich, UK	5 mL
	Insulin (10 mg/mL)	I9278, Sigma-Aldrich, UK	0.25 mL
	Hydrocortisone (5 mg/mL)	H0888, Sigma-Aldrich, UK	0.2 mL
T-47D Luminal (ER^+, PR^+, $HER2^-$)	Dulbecco's Modified Eagle's Medium (DMEM) (with 4500 mg/L glucose, L-glutamine, and sodium bicarbonate, without sodium pyruvate)	D5796, Sigma-Aldrich, UK	500 mL
	Heat Inactivated Iron Supplemented Donor Bovine Serum	Gibco, Life Technologies, UK	56 mL
	Penicillin/Streptomycin (with 10,000 units penicillin and 10 mg streptomycin/mL)	P4333, Sigma-Aldrich, UK	5.6 mL
MCF-7 Luminal (ER^+, PR^+, $HER2^-$)	RPMI-1640 medium	R8758, Sigma-Aldrich, UK	500 mL
	Heat Inactivated Iron Supplemented Donor Bovine Serum	Gibco, Life Technologies, UK	56 mL
	Penicillin/Streptomycin (with 10,000 units penicillin and 10 mg streptomycin/mL)	P4333, Sigma-Aldrich, UK	5.6 mL

Cell lines	Components of culture media	Sources	Volume
JIMT-1 $HER2^+$ (ER^-, PR^-, $HER2^+$)	Dulbecco's Modified Eagle's Medium (DMEM) (with 4500 mg/L glucose, L-glutamine, and sodium bicarbonate, without sodium pyruvate)	D5796, Sigma-Aldrich, UK	500 mL
	Heat Inactivated Iron Supplemented Donor Bovine Serum	Gibco, Life Technologies, UK	56 mL
	Penicillin/Streptomycin (with 10,000 units penicillin and 10 mg streptomycin/mL)	P4333, Sigma-Aldrich, UK	5.6 mL
SKBR3 Luminal/$HER2^+$ (ER^-, PR^-, $HER2^+$)	McCoy's 5A medium (modified, with L-glutamine and sodium bicarbonate)	M9309, Sigma-Aldrich, UK	500 mL
	Heat Inactivated Iron Supplemented Donor Bovine Serum	Gibco, Life Technologies, UK	56 mL
	Penicillin/Streptomycin (with 10,000 units penicillin and 10 mg streptomycin/mL)	P4333, Sigma-Aldrich, UK	5.6 mL
hMEC-1	MCDB131	Gibco, Life Technologies, UK	500 mL
	Heat Inactivated Iron Supplemented Donor Bovine Serum	Gibco, Life Technologies, UK	60 mL
	Penicillin/Streptomycin (with 10,000 units penicillin and 10 mg streptomycin/mL)	P4333, Sigma-Aldrich, UK	6 mL
	Hydrocortisone (5 mg/mL)	H0888, Sigma-Aldrich, UK	0.12 mL
	Endothelial growth factor (100 µg/mL)	AF-100-15, PeproTech, USA	0.06 mL
	L-glutamine (200 mM)	G7513, Sigma-Aldrich, UK	30 mL
hTERT-LEC	Growth Medium MV	C-22020, PromoCell, UK	500 mL
	Growth Medium MV SupplementMix	C-39225, PromoCell, UK	1 mix
	Heat Inactivated Iron Supplemented Donor Bovine Serum	Gibco, Life Technologies, UK	60 mL
	Penicillin/Streptomycin (with 10,000 units penicillin and 10 mg streptomycin/mL)	P4333, Sigma-Aldrich, UK	6 mL

Note: Expression of ER, PR, and HER2 in breast cancer cell lines is reviewed from Tanner *et al.* (2004), Subik *et al.* (2010), Barnabas and Cohen (2013), Menon *et al.* (2014), and Mota *et al.* (2017).

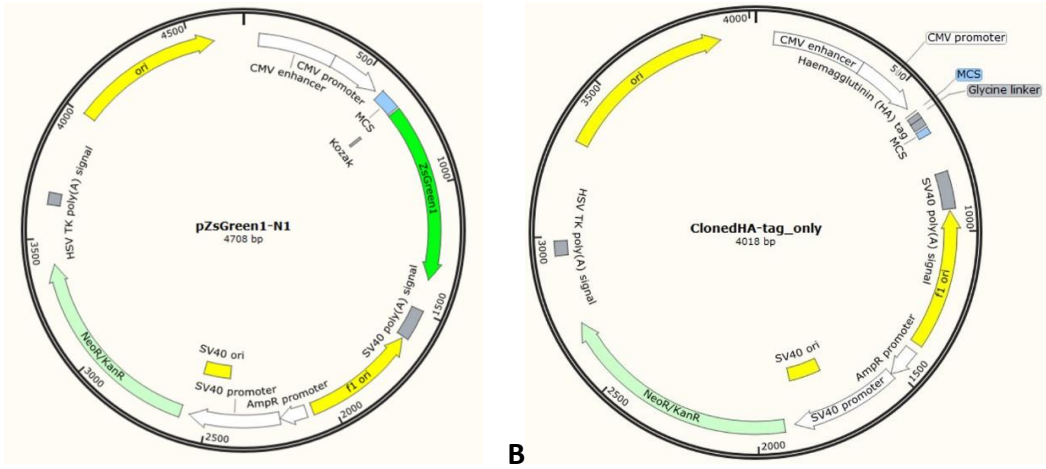


Figure 2B.1 Maps of A) pZsGreen1-N1 plasmid (4708 bp) and B) HA-tagged, GFP-removed, pZsGreen1-N1 plasmid (4018 bp).

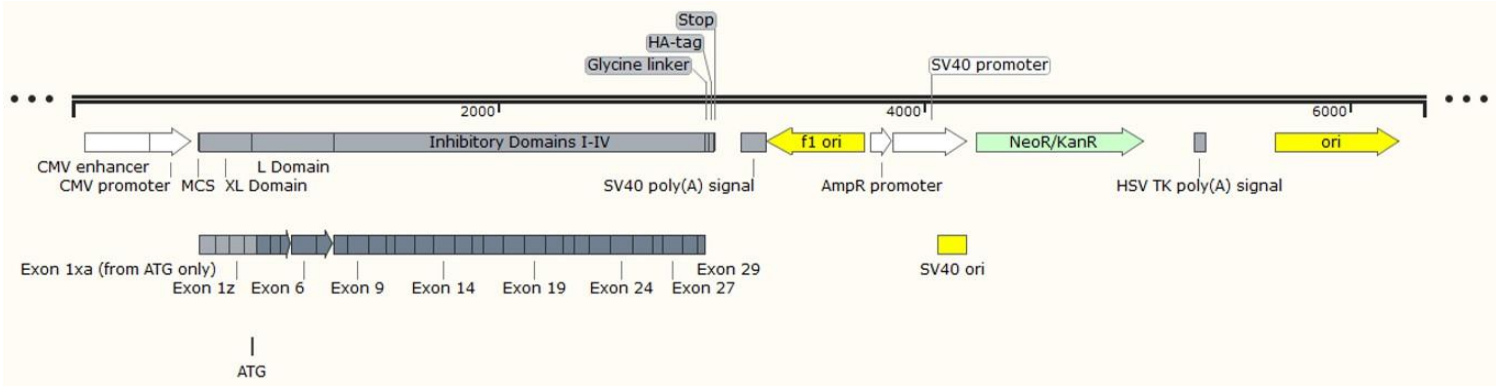


Figure 2B.2 Maps of HA-tagged, GFP-removed, DNA constructs of full-length calpastatin Type 1 (6351 bp)

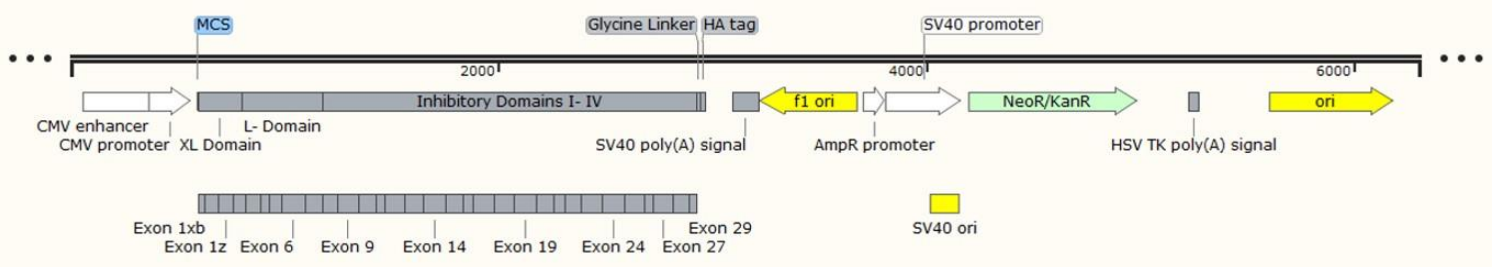


Figure 2B.3 Maps of HA-tagged, GFP-removed, DNA constructs of full-length calpastatin Type 2 (6306 bp).

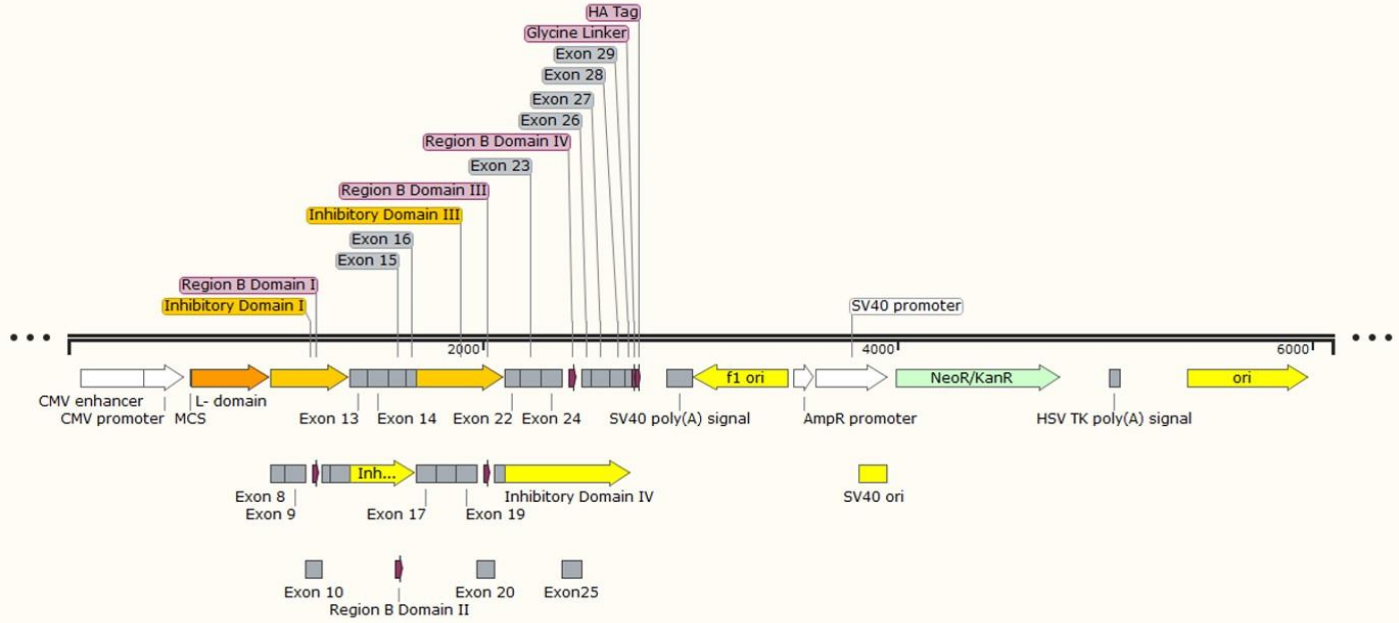


Figure 2B.4 Maps of HA-tagged, GFP-removed, DNA constructs of full-length calpastatin Type 3 (6102 bp).

Sequence of HA-tagged, GFP removed, pZsGreen1-N1 plasmid (4018 bp)

TAGTTATTAATAGTAATCAATTACGGGGTCATTAGTTCATAGCCCATATATGGAGTTCCGCGTTACATAACTT
ACGGTAAATGGCCCGCCTGGCTGACCGCCCAACGACCCCCGCCCATTGACGTCAATAATGACGTATGTTCCC
ATAGTAACGCCAATAGGGACTTTCCATTGACGTCAATGGGTGGAGTATTTACGGTAAACTGCCCACTTGGCA
GTACATCAAGTGTATCATATGCCAAGTACGCCCCCTATTGACGTCAATGACGGTAAATGGCCCGCCTGGCAT
TATGCCCAGTACATGACCTTATGGGACTTTCCTACTTGGCAGTACATCTACGTATTAGTCATCGCTATTACCA
TGGTGATGCGGTTTTGGCAGTACATCAATGGGCGTGGATAGCGGTTTGACTCACGGGGATTTCCAAGTCTC
CACCCCATTGACGTCAATGGGAGTTTGTTTTGGCACCAAAATCAACGGGACTTTCCAAAATGTCGTAACAAC
TCCGCCCCATTGACGCAAATGGGCGGTAGGCGTGTACGGTGGGAGGTCTATATAAGCAGAGCTGGTTTAGT
GAACCGTCAGATCCGCTAGCATGgGTGGTGGTGGTGGTGGTTACCCATACGATGTTCCAGATTACGCTTAA
GGTACCGCGGGCCCGGGATCCACCGGTCGCCACCTAAGCGGCCGCGACTCTAGATCATAATCAGCCATACC
ACATTTGTAGAGGTTTTACTTGCTTTAAAAAACCTCCCACACCTCCCCCTGAACCTGAAACATAAAATGAATG
CAATTGTTGTTGTTAACTTGTTTATTGCAGCTTATAATGGTTACAAATAAAGCAATAGCATCACAAATTTCAC
AAATAAAGCATTTTTTTCACTGCATTCTAGTTGTGGTTTGTCCAAACTCATCAATGTATCTTAAGGCGTAAATT
GTAAGCGTTAATATTTTGTTAAAATTCGCGTTAAATTTTTGTTAAATCAGCTCATTTTTTAACCAATAGGCCGA
AATCGGCAAAATCCCTTATAAATCAAAAGAATAGACCGAGATAGGGTTGAGTGTTGTTCCAGTTTGGAACA
AGAGTCCACTATTAAAGAACGTGGACTCCAACGTCAAAGGGCGAAAAACCGTCTATCAGGGCGATGGCCCA
CTACGTGAACCATCACCCTAATCAAGTTTTTTGGGGTCGAGGTGCCGTAAAGCACTAAATCGGAACCCTAAA
GGGAGCCCCCGATTTAGAGCTTGACGGGGAAAGCCGGCGAACGTGGCGAGAAAGGAAGGGAAGAAAGC
GAAAGGAGCGGGCGCTAGGGCGCTGGCAAGTGTAGCGGTCACGCTGCGCGTAACCACCACACCCGCCGCG
CTTAATGCGCCGCTACAGGGCGCGTCAGGTGGCACTTTTCGGGGAAATGTGCGCGGAACCCCTATTTGTTTA
TTTTTCTAAATACATTCAAATATGTATCCGCTCATGAGACAATAACCCTGATAAATGCTTCAATAATATTGAA
AAAGGAAGAGTCCTGAGGCGGAAAGAACCAGCTGTGGAATGTGTGTCAGTTAGGGTGTGGAAAGTCCCCA
GGCTCCCCAGCAGGCAGAAGTATGCAAAGCATGCATCTCAATTAGTCAGCAACCAGGTGTGGAAAGTCCCC
AGGCTCCCCAGCAGGCAGAAGTATGCAAAGCATGCATCTCAATTAGTCAGCAACCATAGTCCCGCCCCTAAC
TCCGCCCATCCCGCCCCTAACTCCGCCCAGTTCCGCCCATTCTCCGCCCCATGGCTGACTAATTTTTTTTATTT
ATGCAGAGGCCGAGGCCGCCTCGGCCTCTGAGCTATTCCAGAAGTAGTGAGGAGGCTTTTTTGGAGGCCTA
GGCTTTTGCAAAGATCGATCAAGAGACAGGATGAGGATCGTTTCGCATGATTGAACAAGATGGATTGCACG
CAGGTTCTCCGGCCGCTTGGGTGGAGAGGCTATTCGGCTATGACTGGGCACAACAGACAATCGGCTGCTCT
GATGCCGCCGTGTTCCGGCTGTCAGCGCAGGGGCGCCCGGTTCTTTTTGTCAAGACCGACCTGTCCGGTGCC
CTGAATGAACTGCAAGACGAGGCAGCGCGGCTATCGTGGCTGGCCACGACGGGCGTTCCTTGCGCAGCTG
TGCTCGACGTTGTCACTGAAGCGGGAAGGGACTGGCTGCTATTGGGCGAAGTGCCGGGGCAGGATCTCCT
GTCATCTCACCTTGCTCCTGCCGAGAAAGTATCCATCATGGCTGATGCAATGCGGCGGCTGCATACGCTTGA
TCCGGCTACCTGCCCATTCGACCACCAAGCGAAACATCGCATCGAGCGAGCACGTACTCGGATGGAAGCCG
GTCTTGTCGATCAGGATGATCTGGACGAAGAGCATCAGGGGCTCGCGCCAGCCGAACTGTTCGCCAGGCTC
AAGGCGAGCATGCCCGACGGCGAGGATCTCGTCGTGACCCATGGCGATGCCTGCTTGCCGAATATCATGGT
GGAAAATGGCCGCTTTTCTGGATTCATCGACTGTGGCCGGCTGGGTGTGGCGGACCGCTATCAGGACATAG
CGTTGGCTACCCGTGATATTGCTGAAGAGCTTGGCGGCGAATGGGCTGACCGCTTCCTCGTGCTTTACGGTA
TCGCCGCTCCCGATTCGCAGCGCATCGCCTTCTATCGCCTTCTTGACGAGTTCTTCTGAGCGGGACTCTGGG
GTTCGAAATGACCGACCAAGCGACGCCCAACCTGCCATCACGAGATTTCGATTCCACCGCCGCCTTCTATGA
AAGGTTGGGCTTCGGAATCGTTTTCCGGGACGCCGGCTGGATGATCCTCCAGCGCGGGGATCTCATGCTGG
AGTTCTTCGCCCACCCTAGGGGGAGGCTAACTGAAACACGGAAGGAGACAATACCGGAAGGAACCCGCGC
TATGACGGCAATAAAAAGACAGAATAAAACGCACGGTGTTGGGTCGTTTGTTCATAAACGCGGGGTTCGGT
CCCAGGGCTGGCACTCTGTCGATACCCCACCGAGACCCCATTGGGGCCAATACGCCCGCGTTTCTTCCTTTTC
CCCACCCCACCCCCCAAGTTCGGGTGAAGGCCCAGGGCTCGCAGCCAACGTCGGGGCGGCAGGCCCTGCCA
TAGCCTCAGGTTACTCATATATACTTTAGATTGATTTAAAACTTCATTTTTAATTTAAAAGGATCTAGGTGAA
GATCCTTTTTGATAATCTCATGACCAAAATCCCTTAACGTGAGTTTTCGTTCCACTGAGCGTCAGACCCCGTA
GAAAAGATCAAAGGATCTTCTTGAGATCCTTTTTTTCTGCGCGTAATCTGCTGCTTGCAAACAAAAAAACCAC
CGCTACCAGCGGTGGTTTGTTTGCCGGATCAAGAGCTACCAACTCTTTTTCCGAAGGTAACTGGCTTCAGCA
GAGCGCAGATACCAAATACTGTTCTTCTAGTGTAGCCGTAGTTAGGCCACCACTTCAAGAACTCTGTAGCAC
CGCCTACATACCTCGCTCTGCTAATCCTGTTACCAGTGGCTGCTGCCAGTGGCGATAAGTCGTGTCTTACCG
GGTTGGACTCAAGACGATAGTTACCGGATAAGGCGCAGCGGTCGGGCTGAACGGGGGGTTCGTGCACACA
GCCCAGCTTGGAGCGAACGACCTACACCGAACTGAGATACCTACAGCGTGAGCTATGAGAAAGCGCCACGC
TTCCCGAAGGGAGAAAGGCGGACAGGTATCCGGTAAGCGGCAGGGTCGGAACAGGAGAGCGCACGAGG
GAGCTTCCAGGGGGAAACGCCTGGTATCTTTATAGTCCTGTCGGGTTTCGCCACCTCTGACTTGAGCGTCGA
TTTTTGTGATGCTCGTCAGGGGGGCGGAGCCTATGGAAAAACGCCAGCAACGCGGCCTTTTTACGGTTCCT
GGCCTTTTGCTGGCCTTTTGCTCACATGTTCTTTCCTGCGTTATCCCCTGATTCTGTGGATAACCGTATTACCG
CCATGCAT

Note: Glycine linker, HA tag

HA-tagged full-length CAST1 sequence (2418 bp)

HA-tagged CAST1 (2418 bp) constructed in GFP removed, pZsGreen1-N1 plasmid. The whole DNA construct (6351 bp) is consisted of 2373 bp of CAST1 sequence.

ATGTCCCAGCCCGGCCAGAAGCCCGCCGCCTCCCCGCGGCCCCGGCGAGCAGCCGCCGCCCGCCGCACCCA
TGAGCATGTCAGTGAAAAAACCAGTGAATCGCCTTCCAAACCAGGAGAAAAGAAAGGATCAGATGAGAAA
AAAGCAGCAAGCCTCGGCAGCAGTCAATCCTCCAGAACCTATGCTGGTGGAACAGCCTCGGCCACCAAGGT
GTCAGCTTCCTCTGGTGCAACCAGCAAGTCTTCCAGTATGAATCCCACAGAAACCAAGGCCATTCCAGTCAG
CCAACAGATGGAAGGACCACATCTTCCTAACAAGAAAAAACACAAAAAACAGGCTGTAAAAACAGAACCTG
AGAAGAAGTCACAGTCAACCAAGCTGTCTGTGGTTCATGAGAAAAAATCCCAAGAAGGAAAGCCAAAAGA
ACACACAGAGCCAAAAAGCCTACCCAAGCAGGCATCAGATACAGGAAGTAACGATGCTCACAATAAAAAA
GCAGTTTCCAGATCAGCTGAACAGCAGCCATCAGAGAAATCAACAGAACCAAAGACTAAACCACAAGACAT
GATTTCTGCTGGTGGAGAGAGTGTTGCTGGTATCACTGCAATATCTGGCAAGCCGGGTGACAAGAAAAAAG
AAAAGAAATCATTAACCCCAGCTGTGCCAGTTGAATCTAAACCGGATAAACCATCGGGAAAGTCAGGCATG
GATGCTGCTTTGGATGACTTAATAGATACTTTAGGAGGACCTGAAGAAACTGAAGAAGAAAATACAACGTA
TACTGGACCAGAAGTTTCAGATCCAATGAGTTCCACCTACATAGAGGAATTGGGTAAAAGAGAAGTCACAA
TTCCTCCAAAATATAGGGAACTATTGGCTAAAAAGGAAGGGATCACAGGGCCTCCTGCAGACTCTTCGAAA
CCCATAGGGCCAGATGATGCTATAGACGCCTTGTCATCTGACTTCACCTGTGGGTCGCCTACAGCTGCTGGA
AAGAAAACTGAAAAAGAGGAATCTACAGAAGTTTTAAAAGCTCAGTCAGCAGGGACAGTCAGAAGTGCTG
CTCCACCCCAAGAGAAGAAAAGAAAGGTGGAGAAGGATACAATGAGTGATCAAGCACTCGAGGCTCTGTC
GGCTTCACTGGGCACCCGGCAAGCAGAACCTGAGCTCGACCTCCGCTCAATTAAGGAAGTCGATGAGGCAA
AAGCTAAAGAAGAAAAACTAGAGAAGTGTGGTGAGGATGATGAAACAATCCCATCTGAGTACAGATTAAA
ACCAGCCACGGATAAAGATGGAAAACCACTATTGCCAGAGCCTGAAGAAAAACCCAAGCCTCGGAGTGAAT
CAGAACTCATTGATGAACTTTCAGAAGATTTTGACCGGTCTGAATGTAAAGAGAAACCATCTAAGCCAACTG
AAAAGACAGAAGAATCTAAGGCCGCTGCTCCAGCTCCTGTGTCGGAGGCTGTGTGTCGGACCTCCATGTGT
AGTATACAGTCAGCACCCCCTGAGCCGGCTACCTTGAAGGGCACAGTGCCAGATGATGCTGTAGAAGCCTT
GGCTGATAGCCTGGGGAAAAAGGAAGCAGATCCAGAAGATGGAAAACCTGTGATGGATAAAGTCAAGGA
GAAGGCCAAAGAAGAAGACCGTGAAAAGCTTGGTGAAAAAGAAGAAACAATTCCTCCTGATTATAGATTA
GAAGAGGTCAAGGATAAAGATGGAAAGCCACTCCTGCCAAAAGAGTCTAAGGAACAGCTTCCACCCATGA
GTGAAGACTTCCTTCTGGATGCTTTGTCTGAGGACTTCTCTGGTCCACAAAATGCTTCATCTCTTAAATTTGA
AGATGCTAAACTTGCTGCTGCCATCTCTGAAGTGGTTTCCCAAACCCCAGCTTCAACGACCCAAGCTGGAGC
CCCACCCCGTGATACCTCGCAGAGTGACAAAGACCTCGATGATGCCTTGGATAAACTCTCTGACAGTCTAGG
ACAAAGGCAGCCTGACCCAGATGAGAACAAACCAATGGAAGATAAAGTAAAGGAAAAAGCTAAAGCTGAA
CATAGAGACAAGCTTGGAGAAAGAGATGACACTATCCCACCTGAATACAGACATCTCCTGGATGATAATGG
ACAGGACAAACCAGTGAAGCCACCTACAAAGAAATCAGAGGATTCAAAGAAACCTGCAGATGACCAAGAC
CCCATTGATGCTCTCTCAGGAGATCTGGACAGCTGTCCCTCCACTACAGAAACCTCACAGAACACAGCAAAG
GATAAGTGCAAGAAGGCTGCTTCCAGCTCCAAAGCACCTAAGAATGGAGGTAAAGCGAAGGATTCAGCAA
AGACAACAGAGGAAACTTCCAAGCCAAAAGATGACGGTGGTGGTGGTGGTGGTTACCCATACGATGTTCCA
GATTACGCT

Note: Glycine linker, HA tag

Sequence of HA-tagged full-length CAST2 (2373 bp)

HA-tagged CAST2 (2373 bp) constructed in GFP removed, pZsGreen1-N1 plasmid. The whole DNA construct (6306 bp) is consisted of 2328 bp of CAST2 sequence.

ATGGCATTCGCCAGCTGGTGGTACAAGACGCATGTCAGTGAAAAAACCAGTGAATCGCCTTCCAAACCAGG
AGAAAAGAAAGGATCAGATGAGAAAAAAGCAGCAAGCCTCGGCAGCAGTCAATCCTCCAGAACCTATGCT
GGTGGAACAGCCTCGGCCACCAAGGTGTCAGCTTCCTCTGGTGCAACCAGCAAGTCTTCCAGTATGAATCCC
ACAGAAACCAAGGCCATTCCAGTCAGCCAACAGATGGAAGGACCACATCTTCCTAACAAGAAAAAACACAA
AAAACAGGCTGTAAAAACAGAACCTGAGAAGAAGTCACAGTCAACCAAGCTGTCTGTGGTTCATGAGAAAA
AATCCCAAGAAGGAAAGCCAAAAGAACACACAGAGCCAAAAAGCCTACCCAAGCAGGCATCAGATACAGG
AAGTAACGATGCTCACAATAAAAAAGCAGTTTCCAGATCAGCTGAACAGCAGCCATCAGAGAAATCAACAG
AACCAAAGACTAAACCACAAGACATGATTTCTGCTGGTGGAGAGAGTGTTGCTGGTATCACTGCAATATCTG
GCAAGCCGGGTGACAAGAAAAAAGAAAAGAAATCATTAACCCCAGCTGTGCCAGTTGAATCTAAACCGGAT
AAACCATCGGGAAAGTCAGGCATGGATGCTGCTTTGGATGACTTAATAGATACTTTAGGAGGACCTGAAGA
AACTGAAGAAGAAAATACAACGTATACTGGACCAGAAGTTTCAGATCCAATGAGTTCCACCTACATAGAGG
AATTGGGTAAAAGAGAAGTCACAATTCCTCCAAAATATAGGGAACTATTGGCTAAAAAGGAAGGGATCACA
GGGCCTCCTGCAGACTCTTCGAAACCCATAGGGCCAGATGATGCTATAGACGCCTTGTCATCTGACTTCACC
TGTGGGTCGCCTACAGCTGCTGGAAAGAAAACTGAAAAAGAGGAATCTACAGAAGTTTTAAAAGCTCAGTC
AGCAGGGACAGTCAGAAGTGCTGCTCCACCCCAAGAGAAGAAAAGAAAGGTGGAGAAGGATACAATGAG
TGATCAAGCACTCGAGGCTCTGTCGGCTTCACTGGGCACCCGGCAAGCAGAACCTGAGCTCGACCTCCGCT
CAATTAAGGAAGTCGATGAGGCAAAAGCTAAAGAAGAAAAACTAGAGAAGTGTGGTGAGGATGATGAAA
CAATCCCATCTGAGTACAGATTAAAACCAGCCACGGATAAAGATGGAAAACCACTATTGCCAGAGCCTGAA
GAAAAACCCAAGCCTCGGAGTGAATCAGAACTCATTGATGAACTTTCAGAAGATTTTGACCGGTCTGAATGT
AAAGAGAAACCATCTAAGCCAACTGAAAAGACAGAAGAATCTAAGGCCGCTGCTCCAGCTCCTGTGTCGGA
GGCTGTGTGTCGGACCTCCATGTGTAGTATACAGTCAGCACCCCCTGAGCCGGCTACCTTGAAGGGCACAG
TGCCAGATGATGCTGTAGAAGCCTTGGCTGATAGCCTGGGGAAAAAGGAAGCAGATCCAGAAGATGGAAA
ACCTGTGATGGATAAAGTCAAGGAGAAGGCCAAAGAAGAAGACCGTGAAAAGCTTGGTGAAAAAGAAGA
AACAATTCCTCCTGATTATAGATTAGAAGAGGTCAAGGATAAAGATGGAAAGCCACTCCTGCCAAAAGAGT
CTAAGGAACAGCTTCCACCCATGAGTGAAGACTTCCTTCTGGATGCTTTGTCTGAGGACTTCTCTGGTCCACA
AAATGCTTCATCTCTTAAATTTGAAGATGCTAAACTTGCTGCTGCCATCTCTGAAGTGGTTTCCCAAACCCCA
GCTTCAACGACCCAAGCTGGAGCCCCACCCCGTGATACCTCGCAGAGTGACAAAGACCTCGATGATGCCTT
GGATAAACTCTCTGACAGTCTAGGACAAAGGCAGCCTGACCCAGATGAGAACAAACCAATGGAAGATAAA
GTAAAGGAAAAAGCTAAAGCTGAACATAGAGACAAGCTTGGAGAAAGAGATGACACTATCCCACCTGAAT
ACAGACATCTCCTGGATGATAATGGACAGGACAAACCAGTGAAGCCACCTACAAAGAAATCAGAGGATTCA
AAGAAACCTGCAGATGACCAAGACCCCATTGATGCTCTCTCAGGAGATCTGGACAGCTGTCCCTCCACTACA
GAAACCTCACAGAACACAGCAAAGGATAAGTGCAAGAAGGCTGCTTCCAGCTCCAAAGCACCTAAGAATGG
AGGTAAAGCGAAGGATTCAGCAAAGACAACAGAGGAAACTTCCAAGCCAAAAGATGACGGTGGTGGTGGT
GGTGGTTACCCATACGATGTTCCAGATTACGCT

Note: Glycine linker, HA tag

Sequence of HA-tagged full-length CAST3 (2169 bp)

HA-tagged CAST3 (2169 bp) constructed in GFP removed, pZsGreen1-N1 plasmid. The whole DNA construct (6102 bp) is consisted of 2124 bp of CAST3 sequence.

ATGAATCCCACAGAAACCAAGGCCATTCCAGTCAGCCAACAGATGGAAGGACCACATCTTCCTAACAAGAA
AAAACACAAAAAACAGGCTGTAAAAACAGAACCTGAGAAGAAGTCACAGTCAACCAAGCTGTCTGTGGTTC
ATGAGAAAAAATCCCAAGAAGGAAAGCCAAAAGAACACACAGAGCCAAAAAGCCTACCCAAGCAGGCATC
AGATACAGGAAGTAACGATGCTCACAATAAAAAAGCAGTTTCCAGATCAGCTGAACAGCAGCCATCAGAGA
AATCAACAGAACCAAAGACTAAACCACAAGACATGATTTCTGCTGGTGGAGAGAGTGTTGCTGGTATCACT
GCAATATCTGGCAAGCCGGGTGACAAGAAAAAAGAAAAGAAATCATTAACCCCAGCTGTGCCAGTTGAATC
TAAACCGGATAAACCATCGGGAAAGTCAGGCATGGATGCTGCTTTGGATGACTTAATAGATACTTTAGGAG
GACCTGAAGAAACTGAAGAAGAAAATACAACGTATACTGGACCAGAAGTTTCAGATCCAATGAGTTCCACC
TACATAGAGGAATTGGGTAAAAGAGAAGTCACAATTCCTCCAAAATATAGGGAACTATTGGCTAAAAAGGA
AGGGATCACAGGGCCTCCTGCAGACTCTTCGAAACCCATAGGGCCAGATGATGCTATAGACGCCTTGTCATC
TGACTTCACCTGTGGGTCGCCTACAGCTGCTGGAAAGAAAACTGAAAAAGAGGAATCTACAGAAGTTTTAA
AAGCTCAGTCAGCAGGGACAGTCAGAAGTGCTGCTCCACCCCAAGAGAAGAAAAGAAAGGTGGAGAAGG
ATACAATGAGTGATCAAGCACTCGAGGCTCTGTCGGCTTCACTGGGCACCCGGCAAGCAGAACCTGAGCTC
GACCTCCGCTCAATTAAGGAAGTCGATGAGGCAAAAGCTAAAGAAGAAAAACTAGAGAAGTGTGGTGAGG
ATGATGAAACAATCCCATCTGAGTACAGATTAAAACCAGCCACGGATAAAGATGGAAAACCACTATTGCCA
GAGCCTGAAGAAAAACCCAAGCCTCGGAGTGAATCAGAACTCATTGATGAACTTTCAGAAGATTTTGACCG
GTCTGAATGTAAAGAGAAACCATCTAAGCCAACTGAAAAGACAGAAGAATCTAAGGCCGCTGCTCCAGCTC
CTGTGTCGGAGGCTGTGTGTCGGACCTCCATGTGTAGTATACAGTCAGCACCCCCTGAGCCGGCTACCTTGA
AGGGCACAGTGCCAGATGATGCTGTAGAAGCCTTGGCTGATAGCCTGGGGAAAAAGGAAGCAGATCCAGA
AGATGGAAAACCTGTGATGGATAAAGTCAAGGAGAAGGCCAAAGAAGAAGACCGTGAAAAGCTTGGTGA
AAAAGAAGAAACAATTCCTCCTGATTATAGATTAGAAGAGGTCAAGGATAAAGATGGAAAGCCACTCCTGC
CAAAAGAGTCTAAGGAACAGCTTCCACCCATGAGTGAAGACTTCCTTCTGGATGCTTTGTCTGAGGACTTCT
CTGGTCCACAAAATGCTTCATCTCTTAAATTTGAAGATGCTAAACTTGCTGCTGCCATCTCTGAAGTGGTTTC
CCAAACCCCAGCTTCAACGACCCAAGCTGGAGCCCCACCCCGTGATACCTCGCAGAGTGACAAAGACCTCG
ATGATGCCTTGGATAAACTCTCTGACAGTCTAGGACAAAGGCAGCCTGACCCAGATGAGAACAAACCAATG
GAAGATAAAGTAAAGGAAAAAGCTAAAGCTGAACATAGAGACAAGCTTGGAGAAAGAGATGACACTATCC
CACCTGAATACAGACATCTCCTGGATGATAATGGACAGGACAAACCAGTGAAGCCACCTACAAAGAAATCA
GAGGATTCAAAGAAACCTGCAGATGACCAAGACCCCATTGATGCTCTCTCAGGAGATCTGGACAGCTGTCC
CTCCACTACAGAAACCTCACAGAACACAGCAAAGGATAAGTGCAAGAAGGCTGCTTCCAGCTCCAAAGCAC
CTAAGAATGGAGGTAAAGCGAAGGATTCAGCAAAGACAACAGAGGAAACTTCCAAGCCAAAAGATGACGG
TGGTGGTGGTGGTGGTTACCCATACGATGTTCCAGATTACGCT

Note: Glycine linker, HA tag

Table B2.2 Experimental conditions for migration assay

Cell lines	MDA-MB-231 and their stable transfected cells	T47D and their stable transfected cells
Seeding density (cells/well)	3×10^5/well	10×10^5/well
Incubation time to form a monolayer	24 hours	24 hours
Create wound	90° by a 200 µL pipette tip	90° by a 10 µL pipette tip
PP2 (a selective inhibitor of Src-family tyrosine kinases)	1.25, 2.5 and 5 µM	-
Cytochalasin D (a potent inhibitor of actin polymerisation)	0.1 and 0.2 µM (24 hours) treatment only in parental cells	0.02 and 0.04 µM (24 hours) treatment only in parental cells
Calpeptin (a calpain inhibitor used as a positive control)	50 and 75 µM (24 hours) treatment only in parental MDA-MB-231 and 231Ctrl cells	50 and 75 µM (24 hours) treated only in parental T47D and T47DCtrl cells
A23187 (a mobile ion-carrier that increases intracellular Ca^{2+} levels)	0.5 µM (24 hours)	0.5 µM (24 hours)
Cellular proliferation inhibitor	10 µg/mL Mitomycin C	0.5% Serum medium
Post-scratch duration	24 hours	72 hours

Appendix C

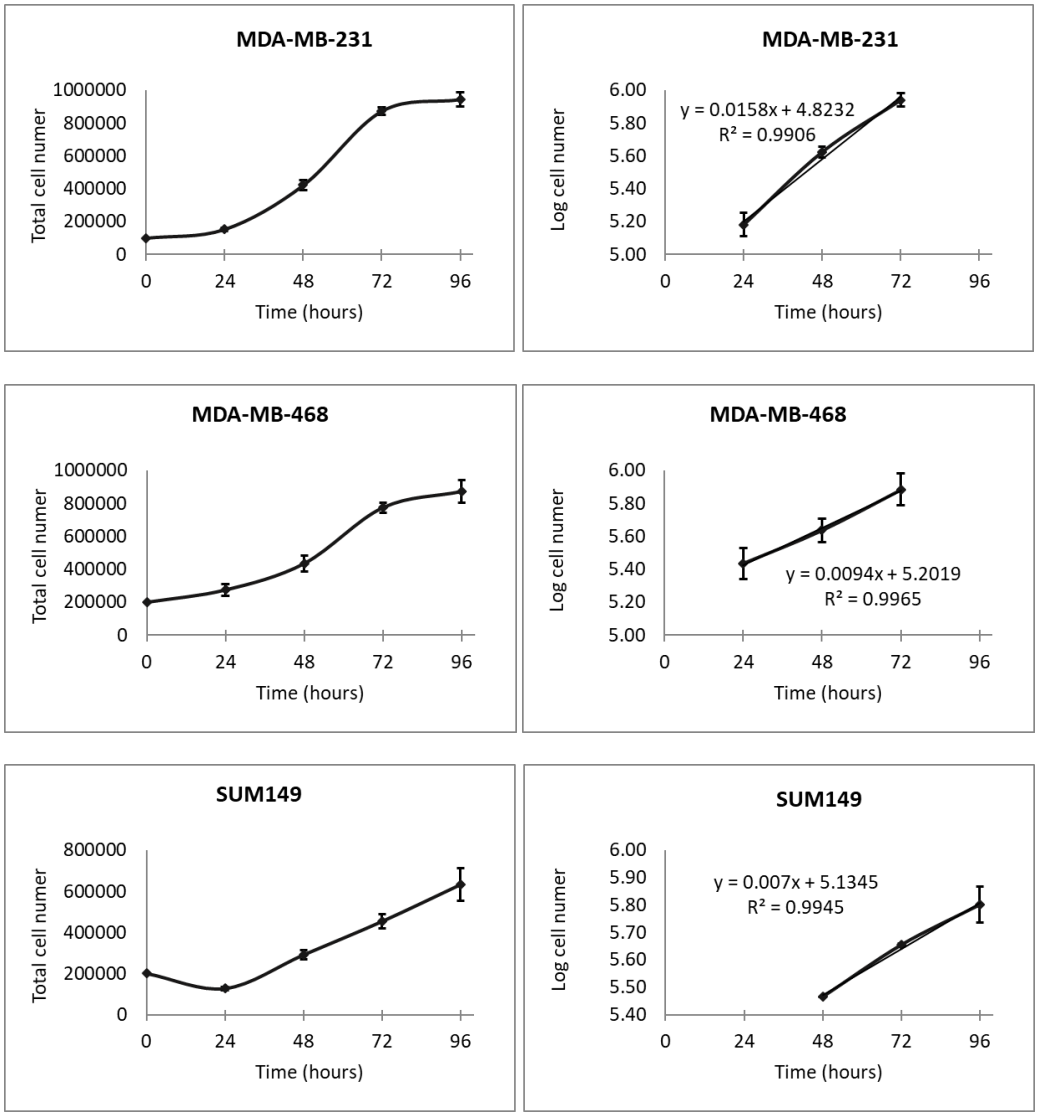


Figure C3.1 Growth curves of basal-like breast cancer cell lines. Figures on the left present total cell number at each time-point while figures on the right present the log cell number at the indicated time-points chosen for population doubling time analysis. Data represent the average ± SD of three independent experiments for MDA-MB-231, and of two independent experiments for MDA-MB-468 and SUM149.

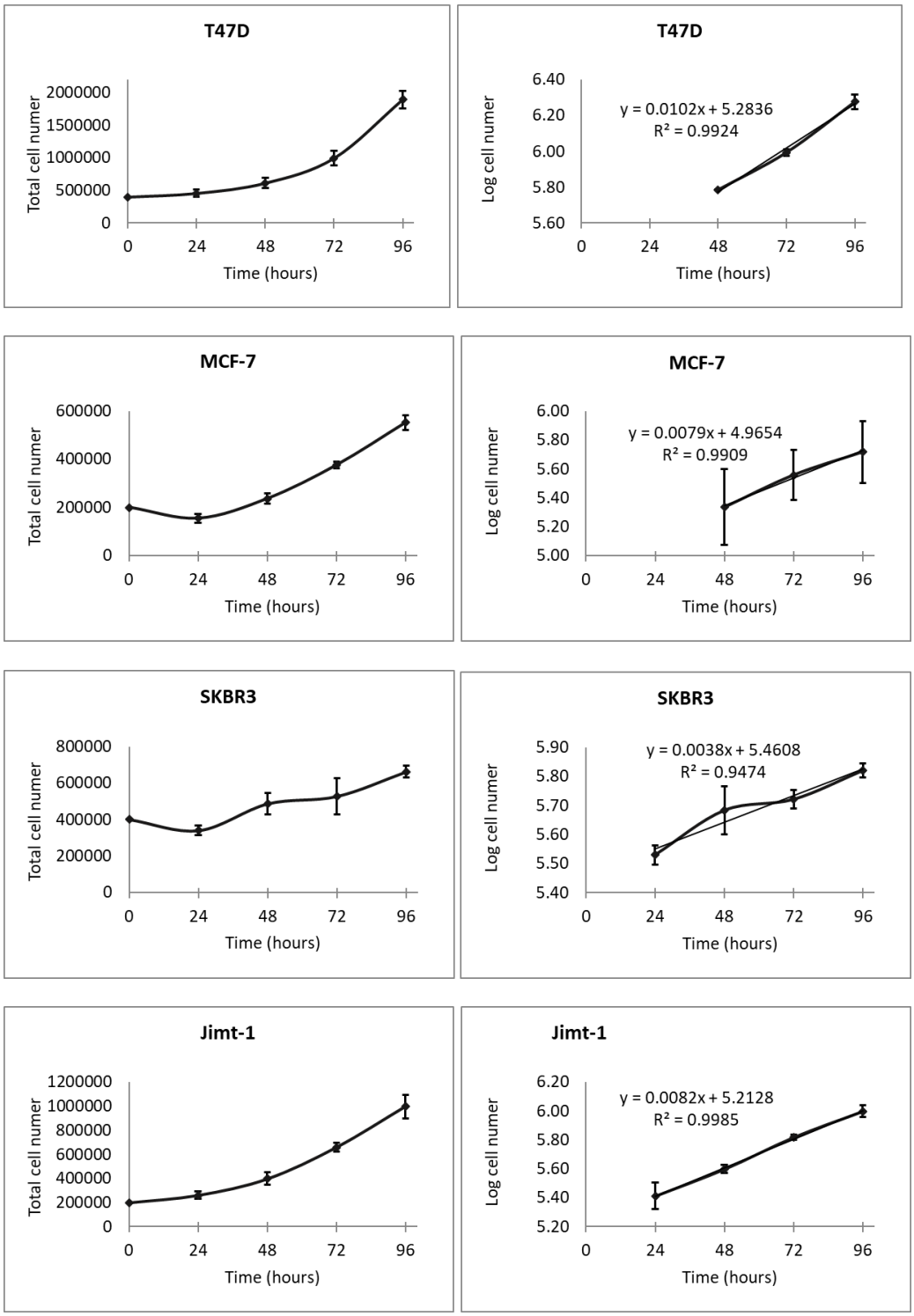


Figure C3.2 Growth curves of luminal and HER2-enriched breast cancer cell lines. Figures on the left present total cell number at each time-point while figures on the right present the log cell number at the indicated time-points chosen for population doubling time analysis. Data represent the average ± SD of three independent experiments for T47D, and of two independent experiments for MCF-7, SKBR3, and JIMT-1 cells.

Table C3.1 Summary of transfection conditions and monoclonal population selection in MDA-MB-231 cells

Clones	Transfection		Selection of monoclonal population
	Summary of transfection conditions Ratios of transfection reagent (µL) to DNA constructs (µg), incubation period & a multiple-well plate used for transfection	Optimal conditions to produce multiclonal population	
231Ctrl	1) Fugene 1.7 : 1 for 48hr in a 12-well plate	Fugene 1.7 : 1 ; 48hr in a 12-well plate Performing 1 experiment to success	Performing 1 experiment to success producing 5 monoclonal clones; clone1 was chosen.
231CAST1	1) Fugene 1.7 : 1 for 48hr in a 12-well plate 2) Lipofectamine 1.5 : 1 and 3 : 1 for 48hr in a 24-well plate 3) Viromer Red 0.4 : 1 for 48hr in a 24-well plate	Lipofectamine 1.5 : 1; 48hr in a 24-well plate (population A) Lipofectamine 3 : 1 ; 48hr in a 24-well plate (population B) Population A showed higher HA tag expression compared to the population B. Performing 2 experiments to success	Performing 5 experiment to success producing 11 monoclonal clones from the population A; 8 clones expressed HA tag; clone5 was chosen. Performing 3 experiment from the population B but unsuccessful.
231CAST2	1) Fugene 1.7 : 1 for 48hr in a 12-well plate	Fugene 1.7 : 1 ; 48hr in a 12-well plate Performing 1 experiment to success	Performing 1 experiment to success producing 5 monoclonal clones; all clones expressed HA tag; clone1 was chosen.
231CAST3	1) Fugene 1.7 : 1 for 48hr in a 12-well plate; Fugene 2.5 : 1, 3 : 1, 3.5 : 1 for 48 and 72hr in a 24-well plate; Fugene 3 : 1 for 48hr in a 12-well plate or for 72hr in a 6-well plate 2) Lipofectamine 1.5 : 1 and 3 : 1 for 48hr in a 24-well plate; Lipofectamine 1.5 : 1 for 24hr in a 24-, 12- or 6- well plate	Fugene 1.7 : 1 ; 48hr in a 12-well plate- success to produce the multi-clonal population but it was found out later that there was no HA tag expression. Performing 4 experiments but unsuccessful	Performing 1 experiment to success producing 4 monoclonal clones; none of them expressed HA tag.

Table C3.2 Summary of transfection conditions and monoclonal population selection in T47D cells

Clones	Transfection		Selection of monoclonal population
	Summary of transfection conditions Ratios of transfection reagent (µL) to DNA constructs (µg), incubation period & a multiple-well plate used for transfection	Optimal conditions to produce multiclonal population	
T47DCtrl	1) Fugene 1.7 : 1 for 48hr in a 24-well plate; Fugene 2.5 : 1 for 48hr in a 12-well plate	Fugene 2.5 : 1 ; 48hr in a 12-well plate Performing 2 experiments to success	Performing 1 experiment to success producing 3 monoclonal clones; clone2 was chosen.
T47DCAST1	1) Fugene 1.7 : 1, 2 : 1, 2.2 : 1, 2.5 : 1 and 3 : 1 for 48hr in a 24-well plate; Fugene 2:1 and 3:1 for 48 and 72hr in a 48-well plate; Fugene 2.5 : 1 for 48 and 72hr in a 48 and 12-well plate; Fugene 3 : 1 for 72hr in a 12-well plate 2) Lipofectamine 0.75 : 1, 1.5 : 1 and 3 : 1 for 48hr in a 24-well plate; Lipofectamine 1.5 : 1 for 24, 48 and 72 hr in a 48-well plate 3) Viromer Red 0.4 : 1 ; 48hr in a 24-well plate	Pooled surviving transfected cells from the conditions of the 9th experiment- Fugene 2:1, 2.5:1 and 3:1 for 48 and 72hr in a 48-well plate and Lipofectamine 1.5 : 1 for 72hr in a 48-well plate Performing 9 experiments to success	Performing 2 experiments to success producing 10 monoclonal clones; only 1 clone (clone7) expressed HA tag.
T47DCAST2	1) Fugene 1.7 : 1 for 48hr in a 24-well plate; Fugene 2.5 : 1 for 48hr in a 12-well plate; Fugene 2.5 : 1 for 24, 48 and 72hr in a 24-well plate; Fugene 2 : 1, 2.5 : 1 and 3 : 1 for 48 and 72hr in a 48-well plate; Fugene 2.5 : 1 ; 48 and 72hr in a 96-well plate (2 wells) 2) Lipofectamine 1.5 : 1 and 3 : 1 for 48hr in a 24-well plate	1) Fugene 2.5 : 1 ; 48hr in a 12-well plate- Success to produce the multi-clonal population but it was found out later that there was no HA tag expression. 2) Fugene 2.5 : 1 ; 72hr in a 96-well plate (3 wells) - success to produce 3 multi-clonal populations (populations A, B, C) from each well; population B expressed HA tag, population A had no HA tag expression; population C: N/A. Performing 5 experiments to success	1) The 1st multiclonal transfected population – performing 1 experiment to success producing 2 monoclonal clones; none of them expressed HA tag. 2) The 2nd multiclonal transfected population – performing 3 experiments to success producing 2 monoclonal clones from the population B; none of them expressed HA tag. **unfinished making monoclonal clones expressing HA tagged calpastatin from the population B
T47DCAST3	1) Fugene 1.7 : 1 ; 48hr in a 24-well plate; Fugene 2.5 : 1 for 48 and 72hr in a 12-well plate	1) Fugene 2.5 : 1 ; 72hr in a 12-well plate – successful making multiclonal population expressing HA tagged calpastatin Performing 4 experiments to success	Performing 3 experiments to success producing 5 monoclonal clones; only 1 clone (clone2) expressed HA tag.

Appendix D

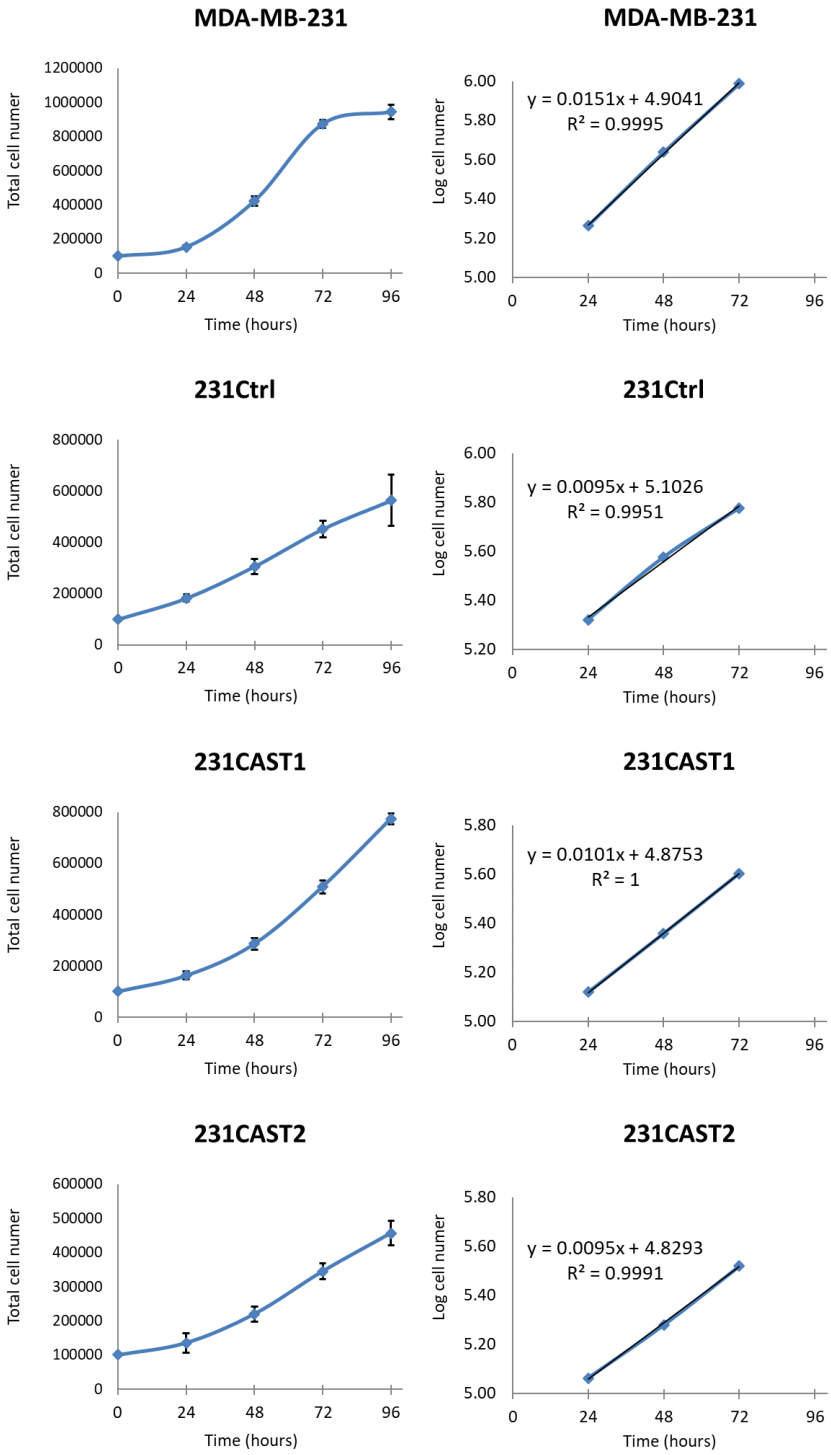


Figure D4.1 Growth curves of parental and stably transfected MDA-MB-231 cell lines. MDA-MB-231 cells and their transfected cell lines with overexpression of full-length calpastatin Type 1 (231CAST1), Type 2 (231CAST2) and the mock-transfected cells (231Ctrl) were examined growth curve analysis over 96 hours in selection medium. Figures on the left present total cell number at each time-point. Data represent the average ± SD of three independent experiments, each in triplicate. Figures on the right show the representative log phases at the indicated time-points for population doubling time analysis.

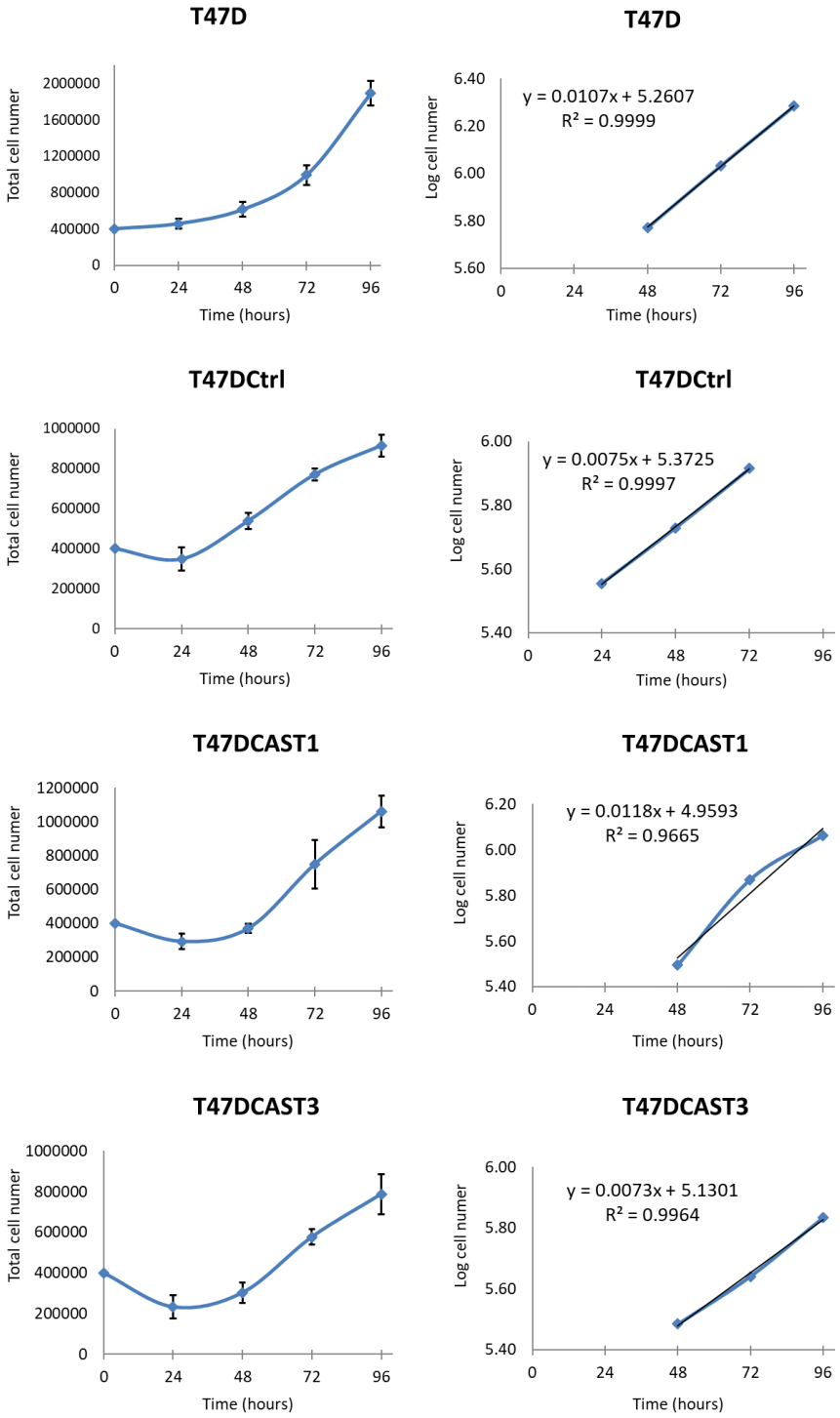


Figure D4.2 Growth curves of parental and stably transfected T47D cell lines. T47D cells and their transfected cell lines with overexpression of full-length calpastatin Type 1 (T47DCAST1), Type 3 (T47DCAST3), and the mock-transfected cell (T47DCtrl) were examined growth curve analysis over 96 hours. Figures on the left present total cell number at each time-point. Data represent the average ± SD of three independent experiments, each in triplicate. Figures on the right show the representative log phases at the indicated time-points for population doubling time analysis.